Investigating The Role Of Transient Receptor Potential Ankyrin One (TRPA1) In Cardiovascular Regulation

Bodkin, Jennifer

Awarding institution:
King's College London

Title: Investigating The Role Of Transient Receptor Potential Ankyrin One (TRPA1) In Cardiovascular Regulation

Author: Jennifer Bodkin

Investigating The Role Of Transient Receptor Potential Ankyrin One (TRPA1) In Cardiovascular Regulation

Thesis submitted for the degree of Doctor of Philosophy
Kings College London

Jennifer V. Bodkin

BHF Centre of Excellence, Kings College London, Franklin-Wilkins Building, Stamford Street, London, SE1 9NH

Abstract

TRPA1 is a member of the TRP superfamily; localised to neural and non-neuronal sites. TRPA1 is activated endogenously by products of oxidative stress, where its expression on sensory neurones leads to the release of vasoactive neuropeptides. Exogenous agonists of TRPA1, mustard oil and cinnamaldehyde, have been shown to cause concentration-dependent vasorelaxation of blood vessels via a variety of mechanisms. My PhD used TRPA1 WT and KO mice to investigate the potential for TRPA1 to alter peripheral artery tone and the implications of this on systemic blood pressure. I also studied the development of angiotensin II induced hypertension and associated pathologies.

Wire myography using murine TRPA1 WT and KO mesenteric arteries showed cinnamaldehyde to cause concentration-dependent vasorelaxation comprising a TRPA1 dependent component, which was endothelial independent and mediated by CGRP and hyperpolarisaton. Basal blood pressure monitoring by both tail cuff plethysmography and telemetry showed no overall effect of TRPA1 deletion on basal hemodynamics. However, TRPA1 KO mice displayed a previously unreported hyperactivity phenotype, measured by both telemetry and voluntary wheel running. 14 day infusion of angiotensin II by osmotic minipump induced similar hypertension in both TRPA1 WT and KO mice. Hypertrophy of the heart was seen in both genotypes, but of significantly increased magnitude in TRPA1 KO mice. Further analysis of associated inflammatory biomarkers by RT qPCR and MSD multiplex ELISA showed upregulation of pro-oxidative genes in hypertensive mice of both genotype. This was significantly greater in hypertensive TRPA1 KO mice than in hypertensive TRPA1 WT mice. These findings may partially explain the increase in hypertrophy in these mice. Angiotensin II infused mice of both genotypes showed increases in chemokine and cytokine expression. Striking, increases in IL6 and MCP-1 seen in hypertensive WT mice were significantly blunted in hypertensive KO mice, suggesting that TRPA1 may differentially modulate inflammatory responses.

Acknowledgements

Conducting this PhD has been thoroughly enjoyable, and one of the most valuable things I have done to date. However, the success of this experience would not have been possible without some very special people.

I would like to take this opportunity to recognise the hard work and constant support given to me by my primary supervisor Prof. Sue Brain. I would not have reached this point without her subtle guidance and I know she will continue to be an exemplary role model for me throughout my career. I must also show my appreciation to other members of the division who have helped me with technical aspects of this thesis; namely Manasi Nandi for her help setting up the telemetry experiments, James Clark for teaching me how to use the VEVO 770, Phil Aaronson for his guidance on myography and Mike Shattock for lending me his mouse wheeling equipment. Also, to all the BSU staff who do such a great job and play a vital role in allowing our studies to run smoothly.

I also wish to thank everyone in the Brain group for creating such an enjoyable place to work, and for their never ending technical and personal support. This also includes all of the project students I have been involved with and whose effort has contributed towards this thesis; special thanks is given to Pratish, who has been amazing during these later stages. I want to give particular recognition to Beth, Lihuan and Aisah, who have become special people in my life and whom I hope will be lifelong friends. I want to see you achieve your dreams!

Lastly, I need to acknowledge the unwavering support of my family; My Mum and Dad, my brother Phillip and my partner Tom. I wish to particularly recognise my Dad, who originally inspired a love of science within me and is always willing to help me with anything I ask of him. Thank you for your support, through which may have seemed to be a never ending education. ☺

Papers And Abstracts

Papers And Book Chapters

1. Design and pharmacological evaluation of PF-4840154, a non-electrophilic reference agonist of the TrpA1 channel., Ryckmans T, Aubdool AA, **Bodkin JV**, Cox P, Brain SD, Dupont T, Fairman E, Hashizume Y, Ishii N, Kato T, Kitching L, Newman J, Omoto K, Rawson D, Strover J., **Bioorg Med Chem Lett.** 2011 Aug 15;21(16):4857-9. Epub 2011 Jun 21 RESEARCH ARTICLE

2. The Vasoactive Potential of Kisspeptin-10 in the Peripheral Vasculature., Iain Sawyer I, Smillie SJ, **JV Bodkin**, Fernandes E, O'Byrne KT, Brain SD, **PLoS ONE**, published 09 Feb 2011, RESEARCH ARTICLE

3. Transient receptor potential ankyrin 1: emerging pharmacology and indications for cardiovascular biology., **Bodkin JV**, Brain SD. **Acta Physiol** (Oxf). 2011 Sep;203(1):87-98. doi: 10.1111/j.1748-1716.2010.02203.x. Epub 2010 Nov 9 REVIEW

4. Evidence for the pathophysiological relevance of TRPA1 receptors in the cardiovascular system *in vivo*., Pozsgai G, **Bodkin JV**, Graepel R, Bevan S, Andersson DA, Brain SD. **Cardiovasc Res**. 2010 Sep 1;87(4):760-8. Epub 2010 May 3. RESEARCH ARTICLE

5. Reactive Oxygen Species (ROS) in the sensory neurovascular component'., Graepel R, **Bodkin JV**, Brain SD, Chapter in Sauer H *et al* (Eds.), Oxidatve Stress in Applied Basic Research and Clinical Practice; **Studies on cardiovascular disorders**, Springer Science and Business Media, 2010 BOOK CHAPTER

6. Hydrogen peroxide is a novel mediator of inflammatory hyperalgesia, acting via transient receptor potential vanilloid 1-dependent and independent mechanisms., Keeble JE, **Bodkin JV**, Liang L, Wodarski R, Davies M, Fernandes ES, Coelho Cde F, Russell F, Graepel R, Muscara MN, Malcangio M, Brain SD. **Pain**. 2009 Jan;141(1-2):135-42. Epub 2008 Dec 6. RESEARCH ARTICLE

Abstracts

'Investigating the role of TRPA1 in cardiovascular regulation', NYAS meeting, "Animal Models and Their Value in Predicting Drug Efficacy and Toxicity", New York Sept 2011 POSTER

'Investigating the role of TRPA1 in cardiovascular regulation', Kings College Graduate Showcase, Kings College London, June 2011, POSTER

‘TRPA1 in the peripheral vasculature’, BHF Fellows Day, April 2011, Cambridge University, POSTER

‘TRPA1s potential to influence cardiovascular regulation’ BHF Postgraduate symposium, April 2011, Kings College London, ORAL PRESENTATION

“Applying the 3R’s to the study of Rheumatoid Arthritis”, NC3R’s Meeting, April 2011, Manchester, University, POSTER

‘Evidence of a TRPA1 component in peripheral artery vasorelaxation ’ Bristol Summer School, July 2010 POSTER

‘Evidence of a TRPA1 component in peripheral artery vasorelaxation ’ EUGeneHeart, PhD Student Exchange Meeting, July in Goettingen, July 2010, POSTER

TRPA1 activation leads to peripheral vasoreactivity, 12th Symposium on Vascular Neuroeffector Mechanisms, Odense, July 2010, POSTER

‘Transient receptor potential A1 (TRPA1)-dependent vaso-activity in murine vessels *in vitro* and *in vivo*’. Kings College symposia, June 2010 POSTER

‘Investigating the role of TRPA1 in cardiovascular regulation’ Winter BPS, December 2011, ORAL PRESENTATION

Abbreviations

α1	Alpha one adrenoceptor
α2	Alpha two adrenoceptor
β1	Beta one adrenoceptor
15-d-PGJ_2	15-d-prostaglandin D_2
2K2C	two kidney 2 clip
4-HNE	4-hydroxy-2-nonenal
4-ONE	4-Oxo-2-nonenal
5HT	5-hydroxytryptamine
AA	Arachadonic Acid
ADHD	Attention Deficit Hyperactivity Disorder
AITC	Allyl Isothiocyanate
Ang II	Ang II
ANOVA	Analysis Of Variance
ATP	Adenosine Tri-Phosphate
BIBN	BIBN 4096 BS
BK	Bradykinin Receptor
BKca	Large conductance voltage and Ca^{2+}-dependent K^+ channel
BSA	Bovine Serum Albumin
BW	Body Weight
CA	Cinnamaldehyde
cAMP	cyclic Adenosine Mono-Phosphate
cDNA	complementary DNA
CFA	Complete Freunds Adjuvant
cGMP	cyclic Guanine Mono-Phosphate
CGRP	Calcitonin Gene Related Peptide
CGRPR	Calcitionin Gene Related Peptide Receptor
CLR	Calcitonin-Like Receptor
CO	Cardiac Output ml/min
COPD	Chronic Obstructive Pulmonary Disease
DAG	Diacyl Glycerol
DMEM	Dulbecco's Modified Eagle Medium
DMSO	Dimethyl sulfoxide
DNA	Deoxyribonucleic acid
DOCA	Deoxycorticosterone acetate
DRG	Dorsal Root Ganglion
ECG	Electrocardiogram
EDHF	Endothelium Derived Hyperpolarisation Factor
5’6-EET	5’6 Epoxyeicosatrienoic acid
EF	Ejection Fraction %
ELISA	Enzyme-linked Immunosorbent Assay
eNOS	endothelial Nitric Oxide Synthase
FS	Fractional Shortening %
GAPDH	Glyceraldehyde 3-phosphate dehydrogenase
H_2O_2	Hydrogen Peroxide
H_2S	Hydrogen Sulphide
HEK	Human Embryonic Kidney 293 cells
HIF1α	Hypoxia Inducible Factor 1 alpha

HO-1	Heme-Oxygenase One
hr	Hour
HUVEC	Human Umbilical Vein Endothelial Cells
i.p.	intra-peritoneal
i.v.	intra-venous
IFNγ	Interferon Gamma
IL	Interleukin-
IP_3	Inositol trisphosphate
IR	Ischaemia Reperfusion
IVSd	Interventricular Septum at Diastole
K_{ATP}	ATP-sensitive potassium channel
KC	mouse KC/CXLC1
$Kca_{3.1}$	Calcium-activated K^+ channel KCa3.1
Kir	Inwardly Rectifying Potassium channel
KO	Knock-Out
L-NAME	L-N^G-Nitroarginine methyl ester
LTB_4	Leukotriene B_4
LV	Left Ventricle
LVAWd	Left Ventricular Anterior Wall at Diastole
LVIDd	Left Ventricular Internal Diameter at Diastole
LVPWd	Left Ventricular Posterior Wall at Diastole
MCP-1	Monocyte Chemotactic Protein One
MO	Mustard Oil
$mPLA_2$	murine Phospholipase A_2
MRI	Magnetic resonance imaging
N-	Amino terminal
NFκB	Nuclear factor Kappa-light-chain-enhancer of activated B cells
NGF	Nerve Growth Factor
NK	Neurokinin Receptor
NO	Nitric Oxide
NOS	Nitric Oxide Synthase
NOX	Nadph Oxidase
O_2	Oxygen
PCR	Polymerase Chain Reaction
PET	Positron emission tomography
PGA	Prostaglandin A
PGD_2	Prostaglandin D_2
PIP_2	Phosphatidylinositol 4,5-bisphosphate
PKA	Protein Kinase A
PKC	Protein Kinase C
PLC	Phospholipase C
PPARγ	Peroxisome Proliferator-Activated Receptor gamma
RAMP1	Receptor Activity Modifying Protein One
RAS	Renin Angiotensin System
RNA	Ribonucleic acid
ROS	Reactive Oxygen Species
Skca	Small conductance voltage and Ca^{2+}-dependent K^+ channel
SOD	Superoxide Dismutase
SP	Substance P
SPECT	Single-photon emission computed tomography

SV	Stroke Volume µl
TEA	Tetraethylammonium
THC	Tetra-hydro Cannabinol
TM	Transmembrane
TNFα	Tumour Necrosis Factor alpha
TRP	Transient Receptor Potential
TRPA1	Transient Receptor Potential Ankyrin One
TRPC	Transient Receptor Potential Canonical
TRPM	Transient Receptor Potential Melastatin
TRPML	Transient Receptor Potential Mucolipin
TRPP	Transient Receptor Potential Polycystic
TRPV	Transient Receptor Potential Vanilloid
TRPV1	Transient Receptor Potential Vanilloid One
TxA_2	Thromboxane A_2
WT	Wild-type

Contents

Chapter 1 - Introduction

Chapter 2 – Materials And Methods

Chapter 3 – Investigating The Role Of TRPA1 In Basal Hemodynamics

Chapter 5 – Investigating The Role Of TRPA1 In Experimental Hypertension

References

List Of Figures And Tables

Chapter 1

Chapter 2

Chapter 3

Chapter 4

Chapter 5

Appendix

Chapter 1 - Introduction

Transient Receptor Potential Ankyrin 1 (TRPA1) is a non selective cation channel, known to be activated by a range of exogenous noxious compounds, and endogenous products of oxidative stress. Identified just over 10 years ago, TRPA1 is classically expressed on sensory neurones and has developed a fingerprint of activity associated with neurogenic inflammation. It is now becoming the target of anti-inflammatory drug development, particularly in the field of lung inflammation. However, the contribution of TRPA1 to cardiovascular regulation is currently unclear. Several studies suggest that TRPA1 agonists can alter activity of the cardiovascular system, such as blood pressure, heart rate and vascular tone. Nevertheless, no thorough investigation has been conducted into the contribution of the TRPA1 receptor to these events. This thesis will present the data collected during my PhD, where I have investigated the role of TRPA1 in cardiovascular regulation. Present literature describing the relevant background will be summarised in this introduction. Firstly, I will discuss the role of sensory neurones and neuropeptides in the vascular system. I will then introduce the TRP channel family, first describing the classical member Transient Receptor Potential Vanilloid 1 (TRPV1), which shows many parallels with TRPA1 activity and a clearer role in cardiovascular disease. I will then discuss the TRPA1 receptor in depth, including agonists, antagonists and current evidence for a role in mediating cardiovascular regulation. The chapter will end with a summary of aims for the thesis.

Sensory Neurones And Neuropeptides

Sensory Neurones

Sensory neurones are small diameter fibres which transduce sensory information via action potentials to the central nervous system. These nerves can be sub-classified to Aβ, Aδ or C-fibres by their decreasing extent of myelination, with C-fibres being completely demyelinated and thus the

slowest of the sensory neurones. Further categorisation can be done on the basis of their mode of activation. Sensory neurone axons are predominantly derived from cell bodies lying in Dorsal Root Ganglia (DRG), originating close to the spinal cord. They innervate almost all organs of the body and have both efferent and afferent signalling roles. These nerves are grown, maintained and modulated by growth factors, such as Nerve Growth Factor (NGF) (Petruska and Mendell, 2004). Projections from the DRG into the spinal cord produce pain signalling in the brain when stimuli are strong. Afferent signals are passed into the outer lamina of the spinal cord, where synapses with spinothalamic tract neurones occur, taking the information to the brain. The passage of information is modulated by inhibitory interneurones in the spinal cord, and influenced by peripheral and central signalling (Iggo *et al.*, 1985). Further sub-types of sensory neurones exist, for example cranial nerves originating from the brain stem, which form pressure baroceptors and chemosensitive branches in the airway. Sensory neurone subtypes can express similar receptors, but with widely differing functions. This depends on their neuropeptide content and integration with other neural circuits or humoral factors (Marmigère and Ernfors, 2007). DRG derived sensory neurones are the predominant form of sensory neurones in the peripheral vasculature and will be the focus of this thesis.

Peripheral blood vessels are richly innervated by DRG derived sensory neurones, in particular by C-fibres. Fibre terminals are responsive to a wide range of stimuli and can interact with a huge range of factors in their microenvironment via expression of specialised receptors. Activation of C-fibres leads to the efferent release of neuropeptides, which can cause an acute neurogenic inflammatory response when tissue levels are elevated. Classic clinical effects include swelling, redness, heat, pain and possibly loss of function. These symptoms and associated mechanisms are well conserved among mammalian species, making the study of neurogenic inflammation highly applicable in animal models. Neuropeptides are generally considered to be small peptides, typically 4-40 amino acids, which show neural origins. To date, more than 50 neuropeptides have been characterised (Lotti *et al.*, 1995). The two best known vasoactive

neuropeptides are Substance P (SP) and Calcitonin Gene Related Peptide (CGRP), which have been well characterised.

Neuropeptides

CGRP

CGRP is a member of the calcitonin peptide family and acts on its heteromeric G-protein coupled CGRP receptor, comprised of 2 subunits; the Calcitonin Like Receptor (CLR) and Receptor Activity Modifying Protein 1 (RAMP1) (McLatchie *et al.*, 1998). It is one of the most potent vasodilators of peripheral blood vessels identified to date (Brain *et al.*, 1985). The majority of its vascular actions are via CGRP receptors expressed on arteriole smooth muscle cells and endothelium. CGRP signalling predominantly occurs via increases in cyclic Adenosine Monophosphate (cAMP) and Protein Kinase A (PKA) activation, which then goes on to phosphorylate targets and alter their function. In endothelial cells PKA activates endothelial Nitric Oxide Synthase (eNOS) and Nitric Oxide (NO) production, inducing relaxation in opposing smooth muscle. In vascular smooth muscle cells, direct CGRP receptor activation leads to PKA induced calcium desensitisation and opening of Adenosine Triphosphate (ATP) sensitive potassium channels (K_{ATP}), leading to hyperpolarisation and relaxation (Wimalawansa *et al*, 1996). CGRP has been implicated in many cardiovascular diseases, particularly those of the macrovasculature, where it has been suggested to play a protective role in diseases such as hypertension (Deng and Li, 2005) and myocardial infarction (Franco-Cereceda and Liska, 2000). However, the precise mechanisms of activity remain unclear. It also has roles in microvascular disease, such as localised acute inflammation, migraine (Brain and Grant, 2004, Edvinsson and Goadsby, 1994) and angina (Franco-Cereceda and Liska, 2000). CGRP has demonstrated both pro and anti-inflammatory actions on immune cells. These include increasing neutrophils attachment to human umbilical vein endothelial cells (HUVEC) cells (Sung *et al.*, 1992) but reducing activation of macrophages and lymphocytes (Gomes *et al.*, 2005). Therefore CGRP may also have immunomodulatory roles.

Substance P

SP is a member of the tachykinin family. It has a wide range of actions occurring via three recognised neurokinin (NK) receptors, NK_1, NK_2 and NK_3. However, most vascular activities are reported to be through NK_1 activation. SP has effects on many cell types but the most prominent include causing increased microvascular permeability by acting on venular endothelial cells to loosen their cell-cell adhesion interactions, leading to plasma extravasation. As SP and CGRP are co-released from C-fibre terminals, their combined vascular actions propagate the formation of oedema (Brain and Grant, 2004). See figure 1.1 for a schematic of the main effects of CGRP and SP in the microvasculature. While NK_1 expression in post-capillary venules is thought to mediate the majority of SP induced plasma extravasation (Saria, 1984, Palframan *et al.*, 1996). Several studies show SP-induced oedema to be heavily dependent on release of vasoactive mediators from mast cells, including serotonin and histamine, where SP induces degranulation via NK_1 dependent and independent mechanisms (Costa *et al.*, 2001, Saban *et al.*, 2002, Krumins and Broomfield, 1992). SP can also cause upregulation of adhesion molecules on microvascular endothelial cells (Steinhoff *et al.*, 2003) contributing to cell accumulation, particularly of neutrophils (Bánvölgyi *et al.*, 2004). SP induced activation of incoming and resident inflammatory cells, including neutrophils, produces further vasoactive mediators and propagates the acute inflammatory response (Holzer, 1998, Costa *et al.*, 2001). However, SP responses can differ based on the local environment. Activation of NK_1 contributes to neutrophil accumulation in inflamed but not naïve murine skin, showing it to have a potentially important immunomodulatory role in disease (Cao *et al.*, 2000). NK_1 is also expressed on arteriole endothelial cells where activation of G-protein ($Gq_{/11}$) mediated PLC activation downstream of the receptor leads to calcium increases and PKC activation. This ultimately induces NO production which also contributes to vasodilation (Maggi, 1995, Petersson *et al.*, 1995).

Sensory Neurones And Neuropeptides In Cardiovascular Regulation

It has been postulated that neurogenic inflammation plays a strong role in the formation and propagation of a variety of diseases, including asthma, chronic obstructive pulmonary disease (COPD), arthritis, inflammatory bowel disease and psoriasis. Thus gaining a better insight into the initiation of mediator release and their downstream responses is an important and relevant topic in the study of many diseases, in addition to the cardiovascular implications.

Resistance vessels are important determinants of total peripheral resistance. These vessels are also highly innervated by sensory neurones, terminating at the media/adventitia border and reaching into the smooth muscle layer; therefore being ideally placed to control vessel tone. There is reportedly a level of tonic background neuropeptide release which has been implicated in the control of basal blood pressure (Watson *et al.*, 2002). Sensory neurones have an undoubted role in cardiovascular disease. Many activating stimuli are at elevated levels in cardiovascular disease and can cause release of neuropeptides, these include mediators such as bradykinin, endothelin and also increases in wall tension (Watson *et al.*, 2002). Therefore sensory neurones may become activated in disease settings. In terms of hypertension, sensory nerve depletion is thought to increase disease susceptibility (Wang, 2005). This is likely related to a loss of neuropeptide induced vasodilatation and suppression of pressor agents.

Several studies have investigated the relationship between CGRP and hypertension. In spontaneous models of hypertension, CGRP levels commonly decrease as blood pressure increases, however, more acute models often show increases in CGRP protein or receptor expression, acting as a compensatory mechanism against overactive pressor mechanisms (Watson *et al.*, 2002, Li and Wang, 2005, Deng and Li, 2005). Similarly, angiotensin II (Ang II) has been shown to reduce the release of CGRP, and this may promote hypertension formation (Kawasaki *et al.*, 1998). These

studies also suggest that spontaneous hypertension models may form due to a lack of CGRP mediated protection. Similar relationships have been noted in patients with essential hypertension, however measurable plasma CGRP levels in patients can be both increased and reduced (Deng and Li, 2005, Smillie and Brain, 2011). These differences may reflect the diverse nature of essential hypertension pathogenesis. CGRP knock-out (KO) mice have been produced to lack αCGRP protein and characterised in many studies, some showing a hypertensive phenotype. This is thought to be due to an increase in Renin Angiotensin System (RAS) activity (Li *et al.*, 2004, Deng and Li, 2005), although this has not been found in all studies (Lu *et al.*, 1999) and may reflect differences in the method of genetic deletion. Similarly, neonatal degradation of sensory neurones through application of destructive doses of capsaicin, produces salt sensitivity characterised by insufficient suppression of the RAS and exacerbated vasoconstrictor response to salt load (Wang and Wang, 2005), which may be related to a loss of CGRP mediated vasodilatation. CGRP has been shown to reduce blood pressure when infused to both normotensive and hypertensive rats (Ando *et al.*, 1990), alters baroreflex sensitivity and sympathetic tone in the mouse (Sabharwal *et al.*, 2010) and is positively inotropic and chronotropic when given systemically in man (Franco-Cereceda *et al.*, 1987).

SP also has demonstrated roles in cardiovascular regulation. Myogenic artery constriction, a decrease in small blood vessel diameter due to increased blood pressure, is suppressed after C-fibre ablation (Scotland *et al.*, 2004). This is thought to be related to a loss of SP. Previous studies using NK_1 receptor antagonists have also demonstrated increases in blood pressure in acute experimental hypertension models, signifying that SP may be acting to counter-act blood pressure increases (Watson *et al.*, 2002).

Therefore, sensory neurones (and the neuropeptides that they contain) can have important roles in cardiovascular control and are suggested to have protective effects against the onset of cardiovascular disease, in particular hypertension.

Transient Receptor Potential channels

To date, 28 mammalian Transient Receptor Potential (TRP) channels have been identified (Yao and Garland, 2005) and divided by homology into six different subfamilies, namely Transient Receptor Potential Vanilloid (TRPV, 1-6 members), Transient Receptor Potential Melastatin (TRPM, 1-8 members), Transient Receptor Potential Canonical (TRPC, 1-7 members), Transient Receptor Potential Mucolipin (TRPML, 1-3 members), Transient Receptor Potential Polycystin (TRPP, 1-3 members) and TRPA (1 member only). Further isoforms and subfamilies can be found in lower vertebrate and invertebrates. TRP channels comprise homo or heterotetramers of six transmembrane domain (TM) subunits, with a pore-loop structure lying between TM five and six, forming a non-selective cation channel. Intracellular amino and carboxy terminals confer much of the channel regulation. TRP receptors are widely distributed and can be activated or modulated by an extensive range of local stimuli. Intensive research in the field has identified a vast array of reported physiological and pathological TRP functions, which is reflected in their low sequence homology. Faulty TRP channels, due to genetic mutations, are recognised as being directly responsible for some disease states, such as TRPP channels in polycystic kidney disease, and TRPML channels in mudocolipidosis IV, a disease involving lysosomal storage disorders.

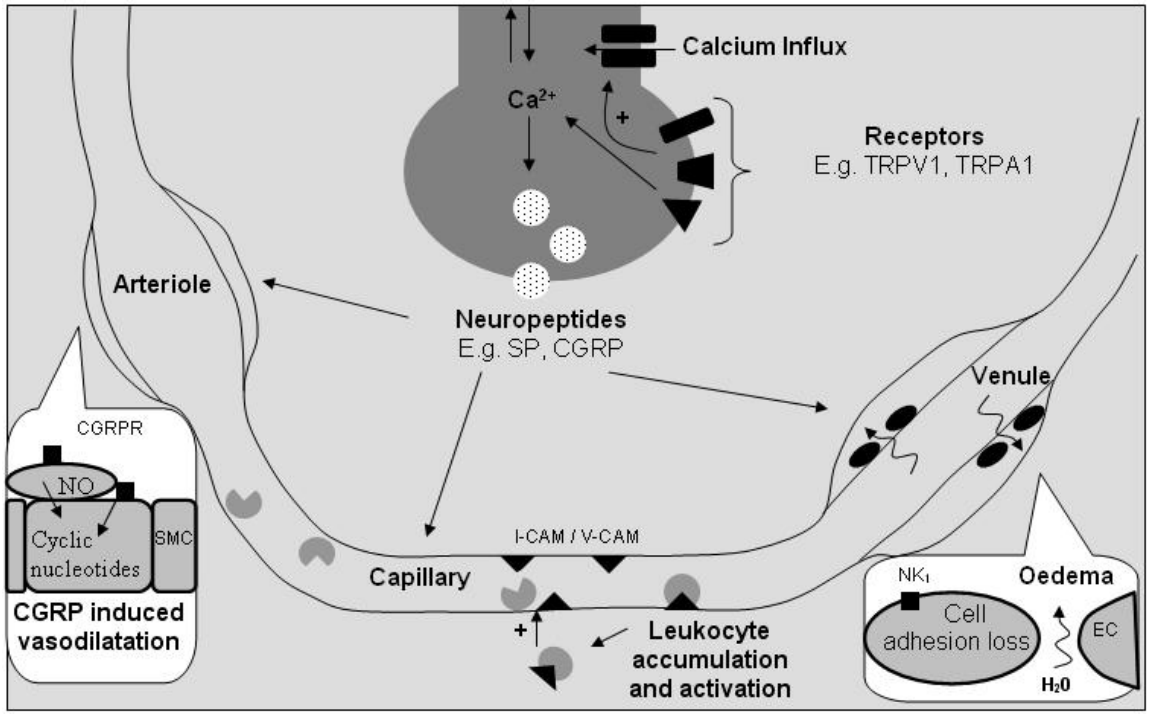

Figure 1.1; Sensory Neurone Activation In The Microvasculature. Neuronal activation by receptors leads to calcium influx and release of vasoactive neuropeptides, in particular SP and CGRP. Activation of NK_1 receptors on endothelial cells by SP causes release of cell to cell adhesions, causing oedema. NK_1 on smooth muscle cells and leukocytes causes weak vasodilatation and leukocyte accumulation respectively. CGRP receptors (CGRPR) expressed on endothelial cells cause potent vasodilatation via eNOS activation and production of NO. This diffuses in to the opposing smooth muscle to cause relaxation. CGRPR also causes direct relaxation of smooth muscle cells via cAMP production. CGRP may also cause leukocyte accumulation.

TRPV1

TRPV1 is a classical member of the TRP superfamily and has been well researched. Its' activity forms the basis of many drugs both in development and in clinical use. It is of special interest to this thesis as it shares many similarities to TRPA1, both in localisation and activity. Many of the mechanisms identified for TRPV1 may also be relevant to TRPA1. Additionally, much of this research also demonstrates the role of sensory neurones in physiology and pathology.

TRPV1 was identified by Caterina *et al* (1997) as the molecular binding site for capsaicin, an extract from hot chillies. It has since been shown to be expressed in numerous tissues, but most notably in small unmyelinated C and Aδ type sensory neurons (Caterina *et al.*, 1997). It is also expressed at lower levels in a diverse range of non-neuronal tissues, including endothelial cells, smooth muscle cells and fibroblasts of the vasculature (Gunthorpe and Szallasi, 2008). Moderate levels of capsaicin activate TRPV1 causing release of neuropeptides and inducing classic physiological signs of acute inflammation. This is accompanied by an acute burning pain followed by desensitisation or hyperalgesia depending on dose. Tachycardia, hyperthermia, sweating and a fall in metabolic rate can also occur (Szolcsányi, 2004, Caterina, 2007). Many other direct and endogenous agonists have since been demonstrated, including protons (pH<6) and heat (>43°C) (Caterina *et al.*, 2000). Additionally, TRPV1 can be sensitised by many commonly occurring tissue components, including many inflammatory mediators, acting via their G-protein receptors and leading to intracellular phosphorylation of receptor termini. This has led to the designation of TRPV1 as a polymodal receptor, where many activators and sensitisers work synergistically, reducing the activation threshold to physiological levels and ultimately causing channel activation (Szolcsányi, 2004). Studies from our group have shown that TRPV1 has an important role in pain and inflammation (Keeble *et al.*, 2009, Keeble *et al.*, 2005), particularly in arthritis (Russell *et al.*, 2009). Our group have uncovered

the importance of ROS in both the activation and downstream activities of the TRPV1 receptor, including vasodilatation (Starr *et al.*, 2008 , Keeble *et al.*, 2009). Neuropeptide release is a key component in all of these findings and continues to be a theme throughout our work.

Repeated application of the TRPV1 agonist capsaicin can be used to deplete sensory neurones of their neuropeptide store. Larger doses desensitise C-fibres in adults and causes irreversible C-fibre destruction in neonates, both forming commonly used experimental techniques for the study of sensory neurones.

Mice lacking TRPV1 have been investigated by many research groups. Caterina *et al* (2000) and Davis *et al* (2000) demonstrate that sensory neurones from TRPV1 KO mice have severe deficits in sensing vanilloids, protons and heat (>43°C), producing higher pain thresholds to capsaicin and reduced thermal hyperalgesia during *in vivo* inflammation models. TRPV1 KO neurones respond normally to non-painful mechanical stimuli (Caterina *et al.*, 2000), indicating no role for TRPV1 in physiological mechanical sensation. However, the role of TRPV1 in sensing mechanical stimuli is still controversial (Inoue *et al.*, 2009) and there is still strong evidence for a TRPV1 role in inflammatory mechanical hyperalgesia (Fernandes *et al.*, 2011).

Studies investigating the efficacy of TRPV1 antagonism in a range of disease models have shown promise (Szallasi *et al.*, 2007). Many TRPV1 antagonists are now available, with some currently in advanced clinical trials. Antagonists function through a range of distinct binding sites, however the most efficacious compounds block all modes of activation (Immke and Gavva, 2006, Szallasi *et al.*, 2006). Preclinical studies have implicated TRPV1 in numerous disease areas, including pain, inflammatory bowel disease, interstitial cystitis, urinary incontinence, airway disease, pancreatitis and migraine (Immke and Gavva, 2006). All these diseases are linked to sensory neurone dysfunction. KO studies show mice lacking TRPV1 activity to have a relatively normal phenotype,

retaining the ability to detect noxious heat and with few other side effects (Szallasi *et al.*, 2006), increasing the interest in using such antagonists clinically. However, there have been problems with changes in core body temperature in preclinical trials of TRPV1 antagonists (Kym *et al.*, 2009). TRPV1 blockade represents a novel mechanism of analgesia, preventing pain at the source instead of traditional analgesics which often aim to block or reduce pain transduction or disease resultant inflammation. Treatment of mice with a TRPV1 antagonist has been shown to reverse inflammatory thermal hyperalgesia by up to 70% (Immke and Gavva, 2006). Other studies have revealed a role for TRPV1 in chronic hyperalgesia (Bölcskei, *et al.*, 2005, Keeble *et al.*, 2005, Fernandes *et al.*, 2011). However, although acute TRPV1 activation classically leads to neurogenic inflammation, some chronic inflammation studies have suggested TRPV1 can have anti-inflammatory and analgesic actions in some settings, which has subsequently been attributed to sensory neurone release of somatostatin (Helyes *et al.*, 2004). The circumstances in which it becomes a predominant release product are not yet clear.

Although only a fraction of the currently pursued TRPV1 drugs are agonists, presumably due to the associated acute pain on administration. Their value in chronic disease states has also been undoubtedly proven (Immke and Gavva, 2006) as they provide long term desensitisation of pain neurones. TRPV1 agonists are currently in very advanced clinical trials for osteoarthritis, neuralgias, headaches, migraine, cystitis and other neurogenic pain conditions (Immke and Gavva, 2006). They are also commonly used in non-prescription medicines for muscle pain.

TRPV1 In Cardiovascular Disease

As TRPV1 is the classical receptor associated with C-fibre activation, much of the current work investigating cardiovascular disease and C-fibres has been based around it. TRPV1 KO mice have a normal hemodynamic profile at rest, apart from a specific loss of the Bezold-Jarisch reflex in response to the agonist anandamide. This response is intact in WT animals

and characterised by a brief episode of hypotension and bradycardia (Pacher *et al.*, 2004, Pozsgai *et al.*, 2010). Many other studies have identified roles for TRPV1 and C-fibres in cardiovascular disease pathogenesis and propagation.

TRPV1 has proposed renal and non-renal roles in regulation of blood pressure, both related to neuropeptide release. TRPV1 in the kidney is thought to modulate pressure or osmotic regulation of the renal system (Cohen, 2007). Activation of TRPV1 in isolated kidneys causes a decrease in renal perfusion pressures and an increased glomerular filtration rate, thought to be result of CGRP and SP release (Li and Wang, 2008). These actions can have a role in the control of blood volume and content. Exogenous application of CGRP and SP mimics this result, causing diuresis (Wang *et al.*, 2008). Ablation of C-fibres confers sensitivity to salt induced hypertension. Wang and colleagues have shown this may be due to TRPV1 becoming unregulated on a high salt diet, with its function impaired in salt sensitive animals (Wang *et al.*, 2008). They also show TRPV1 deletion exacerbates kidney damage on a high salt diet and in deoxycorticosterone acetate (DOCA) salt/uninephrectomised mice (Wang *et al.*, 2008, Wang and Wang, 2009). More recently, Yang *et al* (2010) have investigated the effects of long term capsaicin feeding (7 months) on TRPV1 WT mice and genetically hypertensive rats. They found increases in endothelial dependent vasodilation, likely meditated by an increase in eNOS activity, corresponding to decreased blood pressure in capsaicin fed hypertensive rats. This study is particularly interesting as it provides a link between sensory neurones and endothelial dysfunction, a common manifestation in cardiovascular diseases. However, basal blood pressure does not differ in TRPV1 KO mice, suggesting that TRPV1 is not necessary for the control of basal blood pressure (Pacher *et al.*, 2004).

TRPV1 and sensory neurones also have proposed protective roles during ischaemia-reperfusion (IR) injury. Neuropeptides, particularly CGRP, are thought to be important in preconditioning of the heart, a phenomenon that may confer some protection in angina (Zhong *et al.*, 2007, Li and Peng,

2002). TRPV1 derived SP also shows importance in reducing IR injury and this is supported in TRPV1 KO studies (Wang and Wang, 2005). Furthermore, Sexton *et al* (2007) show IR injury to up-regulate TRPV1, with less vasodilatation seen in TRPV1 KO than WT hearts during ischaemic events. Together, these studies support a protective role of TRPV1 and sensory neurones in cardiovascular events, likely via neuropeptide release.

Interplay Between TRPA1 And TRPV1

In depth neuronal expression studies by Kobayashi *et al* (2005) shows 96% of all TRPV1 expressing neurones are C-fibres, and within these 67% also express TRPA1. When investigated alone, the TRPA1 expressing population is nearly always found to co-express TRPV1. With such high levels of co-expression and similarities in functional mechanisms, interaction between the two receptors has been proposed and is of ongoing interest within the field. Investigations have identified many agonists to activate both receptors, though potency can vary, for example black pepper and garlic extracts (Okumura *et al.*, 2010, Koizumi *et al.*, 2009).

TRPA1 KO mice have been shown to retain their responses to capsaicin (MacPherson *et al.*, 2006). Furthermore, TRPV1 KO mice retain their responses to mustard oil (Bánvölgyi *et al.*, 2004). These studies indicate that expression of each receptor is independent of the other and that each receptor has distinct agonists and pathways of C-fibre activation. Deletion of one receptor does not lead to a general decline in nerve function, but a selective loss of agonist sensitivity. This allows us to selectively study the role of TRPA1 and its agonists. However, capsaicin desensitisation studies have shown effects on TRPA1 function, diminishing MO induced ear oedema (Inoue *et al.*, 1997). This could be occurring either by cross desensitisation or depletion of neuronal neuropeptides, suggesting that the activity of these receptors may be linked. Concentrations of capsaicin used to induce desensitisation should not induce nerve damage (Winter *et al.*, 1995). Further work supports the theory of cross-desensitisation

specifically between these two TRP channels via calcineurin and dephosphorylation mechanisms (Penuelas *et al.*, 2007). Several additional publications have described dependence on TRPV1 for normal TRPA1 currents and desensitisation patterns (Salas *et al.*, 2009, Akopian *et al.*, 2007). Other studies show a stronger effect with loss of 4-ONE contractile effect on bronchus rings (Taylor-Clark *et al.*, 2008a) and cyclopentenone prostaglandin induced release of neuropeptides (Materazzi, *et al.*, 2008) after capsaicin application. These could indicate that some agonist responses demand both TRPV1 and TRPA1 activity. Another study by Bandell *et al* (2004) show TRPV1 KO to abolish cinnamaldehyde (a TRPA1 agonist) induced hyperalgesia, indicating a stronger functional association between the receptors. This has also been suggested to be due to possible functional TRPA1/V1 heteromultimer expression (McMahon and Wood, 2006, Staruschenko *et al.*, 2010). Functional couplings have also been demonstrated in a number of studies. Pecze *et al* (2009) showed specific TRPV1 desensitisation using resiniferatoxin, a potent TRPV1 agonist, also removes TRPA1 from the membrane. Weinhold *et al* (2010) have also described synergistic relaxation of urethral muscle strips when both TRPA1 and TRPV1 agonists are applied. Bandell *et al* (2004) have also described TRPV1 activation of TRPA1 during responses to bradykinin, as both TRPV1 and TRPA1 are needed in these responses, but cation influx through the TRPA1 channel seems key.

KO of TRPA1 resembles KO of TRPV1 in response to bradykinin, additionally indicating a functional interaction between the two is needed for the full response (Bautista *et al.*, 2006). Cross sensitisation has also been suggested as topical capsaicin application caused cold sensitivity in monkeys (Kamo *et al.*, 2008). It is feasible that TRPV1 sensitisation by bradykinin could lead to influx of calcium on activation and cross sensitisation of TRPA1 and subsequent pain (Bandell *et al.*, 2004). Therefore, although TRPV1 and TRPA1 alone display interesting pharmacology and distinct functions, great potential exists for interaction with each other, as well as with other receptors on the plasma membrane. This effect is likely to be location specific.

Sensory Neurones And The Central Control of Blood Pressure

Systemic blood pressure is controlled by the balance of peripheral vasculature resistance and pressure output from the mechanical action of the heart. These factors can be altered in several ways; one of which is via neural signals from the central nervous system.

Centrally derived autonomic signals are a major determinant of blood pressure, providing fine control of the cardiopulmonary system via alterations in the sympathetic and parasympathetic efferent balance. Sympathetic efferent neurones are key to the control of blood pressure, signalling on a beat-to-beat basis in line with the cardiac cycle. They innervate key organs with control over the circulatory system, including the heart, kidney, resistance arteries and adrenal gland. A detailed review of the role of sympathetic efferent neurones in the control of systemic blood pressure is available by Guyenet (2006). A shift towards a predominantly sympathetic drive in the circulatory systems occurs physiologically, for example in exercise or following trauma, predominantly producing an increase in blood pressure via augmented cardiac output (via the beta 1 (β1) adrenoceptor) and vasoconstriction (via the alpha 1 (α1) adrenoceptor). Sympathetic outflow is largely controlled by activity of the rostal ventrolateral medulla in the brainstem, which is modulated by afferent inputs from several brain regions, including the nucleus tractus solarius, hypothalamus, and direct neural input from the spinal cord. Parasympathetic efferent signalling opposes increases in blood pressure predominantly via a decrease in heart rate, occurring via inhibition of the sino-atrial node (Moreira *et al.*, 2011, Guyenet, 2006). Numerous brain regions and humoral factors can contribute to the fine autonomic control of blood pressure, for example during mental stresses (Saha, 2005).

Several complex systems feed information to the brain, determining the appropriate level of sympathetic and parasympathetic efferent tone. Within this system, C fibre neurones can provide feedback to the central nervous

system, translating in to the ability to modulate systemic blood pressure. Three types of C-fibre efferents can provide blood pressure modulation via central signalling; baroceptor linked fibres, nociceptors and glucose sensitive fibres (Guyenet, 2006). These can operate in a feedback or feed forward mechanism, e.g. activation of baroceptor fibres can reduce sympathetic efferent function, while activation of chemosensitive and glucose sensitive fibres (by tissue metabolites and hypoglycaemia) can increase sympathetic outflow, for example during exercise. The modulation provided by each fibre type is determined by the brain regions innervated.

A key type of C-fibre which contributes to feedback control of blood pressure are baroceptor linked fibres. These originate from baroceptors in the carotid sinus, aortic arch and atria, innervating the cardiopulmonary centre of the brainstem via the vagus or glossopharageal cranial nerves. These baroceptors can also be found in this location on A fibres (type 1a), which are thicker, myelinated neurones with faster conduction and activation at lower pressures. Populations of A and C fibre baroceptors in the cat carotid nerve have been characterised by Fidone and Sato (1969), with baroceptor A fibres being of large diameter (3-5 µm diameter), myelinated and conduct faster than C-fibres (4-53m/s vs 2-3m/s). In anesthetised rabbits, A type fibres have been shown to provide beat to beat control of heart rate via inhibition of sympathetic and augmentation of vagal parasympathetic efferent neurones, while C-fibres are recruited at higher pressures, augmenting the parasympathetic response to reduce blood pressure (Kardon *et al.*, 1975). In this way, initial activation of A-fibres leads to a reduction in the sympathetic tone, predominantly redcuing systemic blood pressure via peripheral vasodilation. The C-fibre component contributes to longer term control of blood pressure via heart rate. This was confirmed in another study by Seagard *et al* (1993) using anesthetised dogs and selective inhibition of neurone populations by anodal blockade and anesthetic treatment. Anodal blockade involves application of hyperpolarising current, resulting inability to pass action potentials through a nerve area. At lower currents there is selective hyperpolarisation

of larger, myelinated fibres, but smaller C-fibres are also affected with larger currents. Anaesthetic blockade occurs in a reciprocal manner, preferentially affecting smaller C-fibres at lower levels, extending to larger myelinated A fibres at higher concentrations. This study demonstrated that selective blockade of C-fibre baroceptors in the carotid sinus caused a significant elevation in blood pressure, while blockade of A-fibre baroceptors caused a loss in baroceptor sensitivity to increased perfusion pressures. Collectively, these studies suggest that C-fibre baroceptors provide a larger magnitude and longer lasting depressor influence on blood pressure than equivalent numbers of A-fibres.

Sympathetic efferent neurones also contribute to the control of blood pressure via their extensive innervation of the kidney, an organ produceing several humoral factors with the ability to control several functions of the vasculature, renin release and ion/water excretion. In many models of hypertension there is increase renal sympathetic efferent function (Grisk and Rettig, 2004). Chemosensitive C-fibres can also contribute to the control of systemic blood pressure in the kidney via central and local mechanisms. This is demonstrated in rat studies, where neonatal degradation of chemosensitive neurones using capsaicin produces salt sensitive hypertension caused by impaired renal excretion of water and sodium (Wang *et al.*, 2008). This salt sensitivity was later shown to be prevented by sympathetic nerve depletion using guanethidine (Wang *et al.*, 2001), demonstrating the inhibitory action of chemosenstive C-fibres on renal sympathetic neurones controlling kidney function. In a reciprocal manner, activation of chemosensitive nerves by local pressor agents, such as angiotensin II and endothelin, can lead to the local release of neuropeptides including CGRP. CGRP can dilate local vasculature, increase glomerular perfusion and water/sodium excretion, but can also inhibit the production of further pressor agents. This has a diuretic effect, reducing blood volume and pressure. For a review of the role of chemosensitive neurones in the renal modulation of blood pressure, see Wang and Wang (2007).

The TRPV1 channel is now known to be the receptor for capsaicin, a compound which has been historically used to investigate the role of C-fibres in blood pressure control. In 1955, Toh *et al* showed in anesthetised cats that intra-venous capsaicin application into the carotid sinus induced reflex hypotension, bradycardia and apnoea, which they found to be vagally mediated and abolished when the sinus nerve is cut. This suggests the activation of baroceptors, which are additionally chemosensitive to capsaicin. However, intra-arterial applied capsaicin in the intestine causes a paradoxical hypertension, increases in heart rate, cardiac output and respiratory rate, which was abolished by severing of the nervous supply to the region, suggesting involvement of afferent nerves. This was later investigated again by Jones *et al* (1990), using anesthetised dogs. They additionally showed intra-arterially administered capsaicin to induce a delayed decrease of renal sympathetic nerve activity, which was shown to be reflex mediated as it was lost on baroceptor denervation or vagotomy. Renal sympathoexciation is often seen in pressor responses, causing vasoconstriction and decreases in renal blood flow, leading to a decline in glomerular filtration rate and excretory function. In combination, these studies demonstrate that baroceptor C-fibres are also chemosensitive and express receptors such as TRPV1. Activation of these nerves leads to an acute decrease in blood pressure, predominantly due to a centrally mediated increase in parasympathetic tone. However, the acute of capsaicin on chemosensitive C-fibres in muscle tissue is a transient increase in blood pressure, due to a reflex increase in sympathetic tone. This is later corrected by baroceptors. Similar reflex responses have also been shown to occur in the lung, where laryngeal instillation of capsaicin in dogs has been shown to cause a decrease in blood pressure and bradycardia via vagal neurones. Vagal afferents innervate the nucleus tractus solitaries in the brain, which influences the dorsal nucleus of the vagus and the medullary respiratory centres, causing a range of cardiorespiratory effects (Mutoh *et al.*, 1997). Similar reflex changes in blood pressure have also been described for the TRPA1 agonist cinnamaldehyde, potentially suggesting that TRPA1 may also be expressed in these neurones and be able to modulate blood pressure in response to agonists (Harada *et al.*,

1982, Pozsgai *et al.*, 2010). TRPA1 could potentially be activated in pathological conditions, such as hypertension and systemic inflammation, where high levels of reactive oxygen species may exist and activate the receptor.

Chemosensitive neurones can inhibit sympathetic efferent function at both central and peripheral terminals. This effect is also reciprocated by sympathetic signalling, where pre and post-synaptic α2 adrenoceptor activation in spinal cord and cardiopulmonary centres of the brainstem, leads to inhibition of C-fibre signalling. The physiological importance of this was demonstrated by Donnerer *et al* (1988), who showed using pharmacological tools, that the sympathetic system provides tonic feedback to the cardiopulmonary medullary centre, supressing its activity via α2 adrenoceptor activation. They also demonstrate that α2 adrenoceptor activation reduces the cardio depressor effect of capsaicin administration *in vivo*, suggesting that sympathetic stimulation depresses baroceptor induced pressure reflexes; a feature which may be important in pathophysiological pressor scenarios.

C-fibre neurones, which are known to express TRPA1 and TRPV1, have demonstrated several mechanisms of blood pressure control. This can occur locally, via the release of vasodilative peptides, but can also occur via parts of the central nervous system. C-fibres that innervate baroceptors have been shown to control long term blood pressure levels, providing feedback and initiating parasympathetic reflexes from the medulla. These neurones are also chemosensitive to compounds such as capsaicin and cinnamaldehyde, which can initiate acute reflex changes in blood pressure. Chemosensitive C-fibres in other tissues, for example skeletal muscle beds, have also been shown to induce reflex changes in blood pressure, facilitating physiological changes needed during exercise or trauma, via the central nervous system.

TRPA1

The TRPA1 receptor has undergone a rapid ascent to fame, going from a little known TRP channel to becoming a potentially valuable anti-inflammatory drug target within little more than 10 years of its discovery. First identified in 1999 as the single member of the TRPA family, it has a similar structure to the better known TRPV1 receptor, but with numerous ankyrin repeats in its amino (N) terminal (Jaquemar *et al.*, 1999). The 16 Å crystal structure of TRPA1 has been very recently published (Cvetkov *et al.*, 2011). TRPA1 activation is commonly associated with pain and localised inflammation mediated by neuropeptide release from C-fibre terminals (Andrè *et al.*, 2008, Andrade *et al.*, 2008). A recent publication has described a familial gain of function mutation in TRPA1 that is responsible for a rare human episodic pain syndrome (Kremeyer *et al.*, 2010).

TRPA1 Expression

Although initially identified as a protein poorly expressed in human fibroblasts and lost on oncogenic transformation (Jaquemar *et al.*, 1999); Story *et al* (2003) were the first to specifically characterise TRPA1 expression by northern blot, showing it to be co-expressed with TRPV1 in DRG neurones, but not found in other tissues at detectable levels. Recent expression studies, using a range of techniques, have provided evidence that TRPA1 may occur in other neuronal tissues, including trigeminal (Kobayashi *et al.*, 2005), vagal (Nassenstein *et al.*, 2008), nodose, (Nagata *et al.*, 2005) and sympathetic neurones (Andrade *et al.*, 2008), spinal cord motorneurones (Anand *et al.*, 2008), presynaptic terminals of the substantia gelatinosa (Kosugi *et al.*, 2007) and neurones of the superior cervical ganglia (Smith *et al.*, 2004). Nociceptors innervate a range of tissues including heart, lungs, bladder and intestine, and are likely to be the major source of pro-algesic and inflammatory TRPA1 actions. TRPA1 has also been identified in non-neuronal tissues including basal keratinocytes (Gratzke *et al.*, 2009, Streng *et al.*, 2008, Anand *et al.*, 2008), inner ear

(Corey *et al.*, 2004), dental pulp fibroblasts (El Karim *et al.*, 2011), basal urothelial cells (Gratzke *et al.*, 2009), olfactory epithelium (Nakashimo *et al.*, 2010), airway epithelium and smooth muscle cells (Nassini *et al.*, 2012), cerebral artery endothelial cells (Earley *et al.*, 2009) and smooth muscle cells of intestine (Dong *et al.*, 2010). The role of TRPA1 on many of these cell types is currently unknown and suggests functions in addition to noxious sensation. Although the regulation of TRPA1 expression levels is not well studied, Hatano *et al* (2012) have recently shown upregulation of TRPA1 expression in response to cytokines via nuclear factor kappa-light-chain-enhancer of activated B cells (NFκB) and Hypoxia Inducible Factor 1 alpha (HIF1α) transcription factors. TRPA1 activity has particularly been implicated in respiratory diseases, which often comprise a large C-fibre component. However, if TRPA1 antagonists are to be further developed for clinical use, it will be important to investigate the contribution of non-neuronal expression to physiological processes.

TRPA1 Activation

Method of Activation

Activation of functional TRPA1 homotetramer leads to opening of the central cation pore, allowing influx of cations into the cell. A recent study by Karashima *et al.* (2010) has used electrophysiology techniques to predict a pore diameter of at least 11 Å, with a relative basal P_{Ca}/P_{Na} of just under 5. This, in line with other publications, indicates that TRPA1 has a relatively large pore with high calcium permeability when compared to other TRP channels, including TRPV1. Cation influx is of great importance in delineating TRPA1 function, as downstream mediators are activated by intracellular calcium concentration increases. This in turn triggers events such as neuropeptide vesicle exocytosis from sensory neurones (Andrè *et al.*, 2008). Influx of cations is also important in triggering local membrane depolarisation, which activates voltage dependent sodium channels and amplifys the depolarisation. This will then form an action potential and afferent signalling to central synapses.

In vitro studies show that the majority of compounds activating TRPA1 are electrophilic and form covalent modifications of N terminal cysteines (Hinman *et al.*, 2006). The location of these residues is shown in figure 1.2. However, some non-electrophilic compounds have been shown to activate TRPA1 via a more traditional binding mechanism (Peterlin *et al.*, 2007), such as Tetrahydrocannabinol (THC). It is proposed to bind in a more classical ligand binding site. THC has been shown to not cause cross desensitisation with other agonists (Peterlin *et al.*, 2007), further indicating the mechanisms of activation are distinct. THC is a weak agonist if applied extracellularly as it is poorly diffusible into the cell, however, once inside it is reported to be one of the most potent TRPA1 agonists (Cavanaugh *et al.*, 2008), suggesting that membrane permeability is an important determinant of TRPA1 agonist potency. Activation can also occur via sensitisation of the receptor, proposed for agonists such as calcium (Cavanaugh *et al.*, 2008). This polymodal type mechanism is similar to that seen for TRPV1.

The role of bradykinin in sensitising the TRPA1 receptor has been well investigated, ultimately activating the receptor via release of intracellular messengers. *In vivo* TRPA1 KO studies have shown reduced thermal and mechanical hyperalgesia responses to intraplantar injected bradykinin, and decreased responses to bradykinin applied to trigeminal neurones from TRPA1 KO mice (Bautista *et al.*, 2006 , Kwan *et al.*, 2006). Bradykinin has also been shown to potentiate TRPA1 currents and nociception created by MO or cinnamaldehyde activation *in vitro* (Wang *et al.*, 2008a, Bandell *et al.*, 2004). Bradykinin acts on its own (BK) receptors to activate phospholipase C (PLC). This then has multiple actions that may lead to TRPA1 activation. PLC mediated degradation of phosphatidylinositol 4,5-bisphosphate (PIP_2) may have a role in receptor regulation as PIP_2 is a membrane fatty acid which has inhibitory actions on many TRP channels (Wang *et al.*, 2008a). Degradation of PIP_2 forms the second messengers diacylglycerol (DAG) and inositol 1,4,5-triphosphate (IP_3). IP_3 could sensitise TRPA1 by causing intracellular calcium release. DAG can form arachidonic acid (AA) via DAG lipase enzymes, which is the perquisite for prostaglandin agonists such as 15-d-PGJ_2 and PGA derivatives (Wang *et*

al, 2008a, Bandell *et al*, 2004). Alternatively, TRPV1 activation by bradykinin may have a role in sensitising co-expressed TRPA1 via influx of calcium ions from the extracellular space (Wang *et al.*, 2008a).

Modulation mechanisms acting on TRPA1 are being increasingly investigated, with similarities to TRPV1 being discovered. PLC and protein kinase C (PKC) coupled receptors potentiate the activity of TRPA1, demonstrating how inflammatory mediators can play a role in channel activation (Wang *et al*, 2008a), potentially bringing it into play during disease, where PLC and PKA are common signalling components downstream of G-protein coupled receptors for many inflammatory mediators. Upregulation in inflammatory and neuropathic environments is also suggested to contribute to the development of both mechanical and cold hyperalgesia during disease (Anand *et al.*, 2008, Ji *et al.*, 2008, Obata *et al.*, 2005).

TRPA1 Agonists And Their Role In Cardiovascular Regulation

The TRPA1 receptor displays sensitivity to a wide range of endogenous and exogenous reactive compounds. Many exogenous agonists are well known ingredients in traditional medicines or are known as irritants. There is evidence that TRPA1 is involved in the pathophysiology of a number of clinical diseases. The most promising areas are inflammatory diseases of the airway, such as asthma (Raemdonck *et al.*, 2011), COPD (Caceres *et al.*, 2009) and cough (Birrell *et al.*, 2009, Andre *et al.*, 2009), which appear to benefit from a reduction in TRPA1 activity and are exacerbated by environmental irritants. To date, there have been few investigations into the role of TRPA1 in the vascular system. Combined TRPA1 expression in sensory neurones terminating in the vasculature and an agonist profile showing potential activation in vascular events suggest that the receptor would be ideally placed to play a role in cardiovascular regulation. However, a common problem with TRPA1 agonists is their reactive nature and lack of specificity. The introduction of TRPA1 KO mice has improved the ability of researchers to investigate TRPA1 activities, however much

data is still derived from agonist studies. Some of the key TRPA1 agonists will be introduced in detail, along with evidence suggesting a role for the receptor in cardiovascular control.

Exogenous Agonists

Mustard Oil (MO) / Allyl Isothiocyanate (AITC)

The most commonly used experimental TRPA1 agonist is AITC, the chemical component of MO, wasabi and horseradish. For the purpose of this section, we will refer to MO only. MO has been used in cooking for thousands of years and is a large part of many traditional Asian diets and remedies. It has been investigated for a range of actions, including induction of gastrointestinal secretions and motility (Kojima *et al.*, 2009, Neutra *et al.*, 1982), blood and tissue lipid changes (Watkins *et al.*, 1995, Singh *et al.*, 1995), anti-tumor (Dwivedi *et al.*, 2003), anti-bacterial (Turgis *et al.*, 2009) and anti-fungal (Winther and Nielsen, 2006) activities, and also functions affecting the heart (Romana *et al.*, 1983, Gopalan *et al.*, 1974). More recently, Iwasaki and co-workers showed that intra-venous (i.v.) MO administration stimulates adrenaline secretion, which is dependent on sensory neurones (Iwasaki *et al.*, 2008). A diet high in MO has been correlated with a decrease in incidence of ischaemic heart disease (Rastogi *et al.*, 2004), but also increased levels of collagen deposition in various organs, including the heart (Romana *et al.*, 1983), highlighting potential cardiovascular actions of TRPA1.

MO has a significant history in neurogenic inflammation research, where it was recognised as an activator of neuronal C-fibres leading to concentration dependent release of CGRP and SP (Louis *et al.*, 1989b), well before the identification of the TRPA1 receptor. MO activation of sensory neurones via TRPA1 causes pain, inflammation, microvascular vasodilatation and thermal and mechanical hyperalgesia in mice (Jordt *et al.*, 2004, Andrade *et al.*, 2008). The role of released neuropeptides is demonstrated by the ability to reduce MO induced oedema by administration of anti-CGRP antibodies (Louis *et al.*, 1989a) and block it

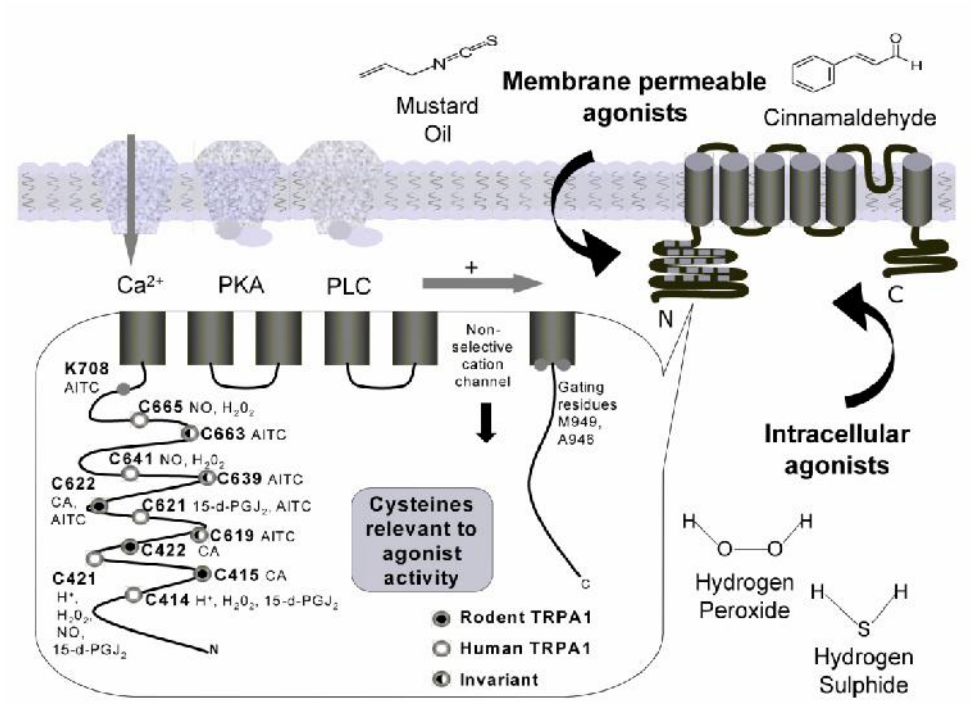

Figure 1.2; TRPA1 Reactive N Terminal Residues; showing some common agonists known to activate TRPA1 via cysteine modification. Residues which have been identified as important for receptor activation are shown for relevant species. Other mechanisms of activation have been identified, such as calcium binding to the EF hand domain and agonist binding to an unknown hydrophobic pocket motif. Sensitisation of the receptor can also occur via phosphorylation and changes in membrane lipid composition. Antagonists are available to block agonist activation of TRPA1. Residue information collected from mutagenesis studies (Hinman *et al.*, 2006, Chen *et al.*, 2008, Takahashi *et al.*, 2008 , Macpherson *et al.*, 2007a). Allyl Isothiocyante (AITC, equivalent to MO), hydrogen peroxide (H_20_2), cinnamaldehyde (CA), 15-d-prostaglandin J_2 (15-d-PGJ_2).

with NK_1 antagonism (Grant *et al.*, 2005). Mast cell derived mediators (Inoue *et al.*, 2006) and NO may also play more minor roles (Lippe *et al.*, 1993) in the inflammation. More recently, MO has become an important experimental tool in the study of TRPA1 activity. Denervation of an area or genetic deletion of TRPA1 has been shown to block the pain and inflammation caused by MO, demonstrating TRPA1 selectivity (Bautista *et al.*, 2006, Inoue *et al.*, 2006, Kwan *et al.*, 2006, Lippe *et al.*, 1993).

MO has demonstrated vasoreactivity in several *in vivo* and *ex vivo* models. However, contributing mechanisms differ greatly. Current literature investigating TRPA1 agonist induced vasoreactivity are shown in Table 1.1. MO is known to cause release of neuropeptides from sensory neurones, however this mechanism is not always seen to be of primary importance for vasorelaxation. Hikiji *et al* (2000) and Louis *et al* (1989a) show MO to cause C-fibre mediated dilation *in vivo* via neuropeptides in the cat tooth pulp and rat hind paw respectively. Hikiji *et al* (2000) demonstrated this using lidocaine, whereas Louis *et al* (1989a) used systemically administered antibodies to CGRP and SP to show neuropeptide involvement. Kunkler *et al* (2011) has more recently studied MO induced vasodilation in the rat meningeal tissue, blocking increased blood flow with the peptide CGRP receptor antagonist $CGRP_{8-37}$ or the TRPA1 antagonist HC-030031. Bautista *et al* (2005) also demonstrated MO induced vasorelaxation of rat mesenteric arteries *in vitro*, which was endothelial independent but sensory neurone and CGRP dependent.

At higher concentration of MO, as used by Lippe *et al* (1993) in the rat hind paw, NO was found to play a large role in the vasodilation, being reduced by i.v administration of the Nitric Oxide Synthase (NOS) inhibitor L-NAME. However, this was also accompanied by a decrease in overall skin blood flow and could still be a product of C-fibre activation as some neurones have been shown to produce NO (Morris *et al.*, 1992).

To date, MO has been the agonist of choice when investigating the specific role of TRPA1 in vasorelaxation. In our recent publication, the increase in

ear blood flow caused by topical MO was significantly reduced in TRPA1 KO mice (Pozsgai *et al.*, 2010). This is supported in a detailed paper by Earley *et al* (2009) using isolated rat cerebral arteries, where TRPA1 antagonist HC-030031 reduced MO induced dilation of vessels under myogenic tone. However, this study did not investigate the involvement of C-fibres or sensory neurones. TRPA1 was found to be expressed on endothelial cells, causing endothelium dependent vasodilation (Earley *et al.*, 2009). The role and location of TRPA1 were confirmed using endothelial denudation and immunohistochemistry. Using a range of pharmacological mediators, the authors of this paper were able to put together a detailed mechanism, where TRPA1 activation causes calcium influx in the endothelial cells, likely concurrently activating further calcium release from cell stores. This calcium then opens calcium activated potassium channels (small conductance calcium activated potassium channel (SK_{Ca}^{2+}) and intermediate conductance calcium activated potassium channel ($K_{Ca}^{2+}3.1$) located on endothelial projections into the smooth muscle layer, hyperpolarising the cell. The hyperpolarisation is then passed to vascular smooth muscle cells via myoendothelial gap junctions or by creating areas of elevated extracellular potassium (up to around 20 mM), which activates smooth muscle inwardly rectifying potassium channels (K_{IR}). K_{IR} channels are specialised potassium channels involved in repolarising cells following a depolarisation stimulus and preferentially carry inwardly moving positive current at the resting membrane potential, which is positive with respect to the reversal potential for potassium. As extracellular potassium is elevated, the reversal potential for potassium is made more positive, reducing the rectification of the K_{IR} channel and allowing outward flow of potassium, producing hyperpolarisation. This paper is by far the most detailed account of MO induced, TRPA1 dependant, vasodilation and may be relevant to intra-luminal sources of TRPA1 agonists. Such agonists could include oxidants released from endothelial or blood cells, or blood borne chemical agonists, including toxins.

However, as with other TRPA1 agonists, the reactive nature of MO also means there is potential for poor TRPA1 selectivity. Of particular interest, MO has been shown to activate TRPV1 (Ohta *et al.*, 2007), most recently at concentrations over 1mM (Everaerts *et al.*, 2011), and has been shown to inhibit TRPA1 activity at millimolar levels (Everaerts *et al.*, 2011). This is supported by some studies showing TRPV1 activity is needed for full MO signalling (Patil *et al.*, 2010, Staruschenko *et al.*, 2010, Salas *et al.*, 2009). See table 1.1 for a summary of concentrations used in each of the discussed studies.

Cinnamaldehyde

Cinnamaldehyde is the main component of cinnamon oil. Cinnamaldehyde has long been used in traditional Chinese medicine for treatment of circulatory and inflammatory diseases (Yanaga *et al.*, 2006, Xue *et al.*, 2011) and is well used as a food and fragrance additive. Reported physiological actions of cinnamaldehyde include anti-diabetic (Subash Babu *et al.*, 2007), anti-platelet aggregation, anti-thrombotic, (Huang *et al.*, 2007) and anti-bacterial roles (Charles *et al.*, 2008), along with anti-inflammatory activity on endothelial and inflammatory cells (Liao *et al.*, 2008, Chao *et al.*, 2008). It is one of the few well recognised TRPA1 agonists that can be easily administered *in vivo*, which is necessary for the investigation of vascular effects at both a local and systemic level.

Studies of cinnamaldehyde induced vasoreactivity are summarised in table 1.1. The mechanisms attributed differ more than that of MO. 10%, cinnamaldehyde caused significant vasodilation in the human forearm skin, measured by laser Doppler flowmetry in a study by Namer *et al* (2005). This was accompanied by hyperalgesia formation, therefore suggesting C-fibre involvement. However, in a similar study by VanderEnde and Marrow (2001) using 1% cinnamaldehyde in isopropyl alcohol water applied to the human forearm skin, vasodilation measured by reddening of area was found to be linked to high PGD_2 levels, a vasodilatory prostaglandin. This was reduced by aspirin, but not rofecoxib, a selective

cyclooxygenase 2 antagonist, suggesting the involvement of cyclooxygenase 1 enzyme. This study also suggested that the source of PGD_2 may be macrophages or Langerhans cells in the skin. These studies suggest that the concentration may be an important factor in the mechanism mediating cinnamaldehyde induced vasodilation.

Similarly, studies using aortic ring preparations have shown inherent differences in mechanisms attributed to cinnamaldehyde induced vasorelaxation, which may be related to concentration. For example, Xue *et al*, (2011) found no endothelial dependent component in the rat aorta, whereas Yanaga *et al* (2006) found a partial endothelial dependent component in the same model, which was NO-mediated and inhibited by L-NAME. Again, this may be due to the concentrations studied, as Xue *et al* (2011) used concentrations in the nanomolar range, whereas Yanaga *et al* (2006) used concentrations in the micromolar range. However, both suggest inhibition of cytoplasmic calcium increases in smooth muscle cells as the mechanism for dilation, and also find no role for potassium channels, prostaglandins and beta adrenergic receptors, as determined using the relevant antagonists. The targets bringing about the inhibition of calcium movement in smooth muscle cells are not known but could be related to the hyperpolarisation seen in other models via inhibition of voltage activated calcium channel opening. Inhibiting mechanisms which increase calcium in the cytosol alters the balance of calcium handling, favouring reuptake and extrusion mechanisms and ultimately leading to a decrease in free calcium, producing a vasodilation response.

Investigations of the systemic effects of TRPA1 activation are few, but most have utilised cinnamaldehyde as the agonist of choice due to its ability to be given i.v. In the 1970's, before the discovery of the TRPA1 receptor, Harada and colleagues published a set of five papers investigating the effects of cinnamaldehyde on various systems in the mammalian body. In publication two, Harada *et al* (1975) describe the effects of intra-arterial cinnamaldehyde application on guinea pigs. Cinnamaldehyde caused a rapid drop in blood pressure, which was attributed to peripheral blood

vessel dilation and an increase in femoral blood flow. Limited effects were seen on heart rate or respiration rate. They went on to investigate the effects on isolated hearts, showing positive chronotropic and inotropic actions, leading to arrhythmias at high doses. These effects rapidly underwent desensitisation. Similar actions were also recorded from isolated atria. In publication four, Harada and Saito (1978) show cinnamaldehydes effect on isolated hearts can be antagonised by beta adrenergic blockade and catecholamine depletion. They also show that cinnamaldehyde causes catecholamine release from isolate dog adrenal gland. This was followed up in a subsequent paper, demonstrating that the cardiac effects of TRPA1 activation are indirectly mediated by a release of catecholamines (Harada *et al.*, 1982). They showed that *in vivo* arterial, venous and dermal infusion of cinnamaldehyde to dogs, causes release of adrenaline from the adrenal gland through an unidentified mechanism (Harada *et al.*, 1982, Harada *et al.*, 1975). These findings showed parallels with more recent findings of increased sympathetic outflow following i.v. cinnamaldehyde dosing, which was dependent on sensory neurones (Iwasaki *et al.*, 2008) and is also supported by a recent study using radiotelemetered spontaneously hypertensive rats. Here, diesel exhaust fumes were inhaled by conscious animals before an arrhythmic drug was administered, increasing sympathetic mediated arrhythmias in a TRPA1 dependent manner, defined by the use of the TRPA1 antagonist HC-030031 (Hazari *et al.*, 2011).

Recently, our group has published the first evidence of TRPA1 dependence for cinnamaldehyde effects in the cardiovascular system, using cinnamaldehyde applied *in vivo* and *ex vivo* to TRPA1 WT and KO mice. We showed that cinnamaldehyde applied into the hind paw causes an increase in blood flow that was significantly reduced in TRPA1 KO mice. Furthermore, application of cinnamaldehyde to isolated mesenteric arteries caused endothelial independent vasorelaxation which was significantly reduced in TRPA1 KO vessels. When given systemically, i.v. cinnamaldehyde initiated a vaso-vagal response, similar to the Bezold-Jarisch reflex, causing an initial drop in blood pressure and heart rate,

followed by a more sustained increase in both (Pozsgai *et al.*, 2010). This response is similar to that seen on systemic TRPV1 activation, which is also lost on TRPV1 KO (Pacher *et al.*, 2004). In our study, the mechanism for cinnamaldehyde activity was found to be of vasovagal origin, lacking a contribution of CGRP and SP, defined using systemic treatment with neuropeptide antagonists. The reflex showed concentration-dependence and was significantly reduced on TRPA1 KO, and by application of antagonists to the alpha one adrenergic receptor and to cholinergic receptors (Pozsgai *et al.*, 2010). The myography data presented in this paper also features in this thesis and will be expanded upon.

Cinnamaldehyde has been shown to be metabolised *in vivo* by a number of organs, including skin and plasma, forming cinnamic acid, which is later is converted to benzoic acid and excreted in urine as hippuric acid (Cheung *et al.*, 2003, Chen *et al.*, 2009b). Therefore, consideration of cinnamaldehyde metabolites is also valuable. Previous investigation of i.v. dosing has shown cinnamaldehyde to be unstable in blood and quickly oxidised to cinnamic acid, which has a plasma half life of 1.7hrs (Yuan *et al.*, 1992). This toxicological study again showed cinnamaldehyde to cause an acute drop in blood pressure. Although not investigated in the more recent publication by Pozsgai *et al* (2010), Harada *et al* (1975) found cinnamic acid to be inactive in isolated tissues, posing questions as to the physiological relevance of findings gained from acute doses of cinnamaldehyde.

Most recently, a more chronic study has conducted 6 weeks of daily cinnamaldehyde dosing (20mg/kg/day) and shown this to be associated with reduced hyperglycaemia, inhibition of the decline in vascular reactivity and prevention of the hypertension associated with experimentally induced diabetes in rats. No investigation of TRPA1 dependency was made but this suggests that cinnamaldehyde may have actions on the vasculature and have potential as an anti-diabetic drug (El-Bassossy *et al.*, 2011).

Cinnamaldehyde has been suggested to be one of most useful experimental TRPA1 agonists. It has relatively few other known targets, shows good selectivity and potency on TRPA1 when expressed in cells *in vitro*, on *ex vivo* neurones and during *in vivo* nociception assays (Bandell *et al.*, 2004). It does not activate TRPV1 or TRPV4 at concentrations up to 0.6mM (Bandell *et al.*, 2004), however it blocks TRPM8 completely at concentrations of 5mM, and was originally identified as a TRPV3 agonist using 0.5mM (Macpherson *et al.*, 2006). Of these only TRPV1 and TRPV4 are well known to mediate vasodilation, however vasoreactivity has been shown for TRPM8 and TRPV3 (Wang *et al.*, 2006, Earley, 2011, Johnson *et al.*, 2009, Earley *et al.*, 2010). Conversely, Namer *et al* (2005) have shown TRPM8 does not mediate changes in vascular tone. It is also important to consider solvents, as ethanol is commonly used to dilute cinnamaldehyde and is known activate TRPV1 channels at 2M on tissue sections and 1ml/kg *in vivo*, stimulating the release of CGRP from trigeminal neurones and causing vasodilation (Nicoletti *et al.*, 2008). Therefore, the literature suggests that concentrations less than 500µM in minimal ethanol should provide TRPA1 selective agonism and would be appropriate for the investigation of TRPA1 dependent activities. This has been the basis of my dosing schedules, where cinnamaldehyde has been used to investigate TRPA1 induced vasorelaxation in the myograph using a concentration response curve from 3-300µM.

Despite some difficulties, cinnamaldehyde is the preferred TRPA1 agonst over MO (Bautista *et al*, 2006), as MO has shown residual effects in TRPA1 KO mice at high doses (Kwan *et al.*, 2006). However, some groups consider cinnamaldehyde to underestimate the level of TRPA1 expression, as it activates a smaller population of neurones than MO (Huang *et al.*, 2006) and does not identify all areas of TRPA1 expression shown using immunohistological methods (Bautista *et al.*, 2006).

Publication	Agonist	Species	Tissue	Comments on dilation/increase in blood flow
Xue *et al*, 2011	Cinnamaldehyde	Rat	Aortic rings	70nM-7μM causes concentration dependent relaxation from phenylephrine pre-constriction, not dependant on endothelium, NO, cGMP, prostaglandins, beta adrenergic receptors, ATP sensitive potassium channels and various other potassium channels blocked by TEA and $BaCl_2$. Reduced constriction by a range of calcium dependent agonists, indicating a calcium influx/release inhibition mechanism.
Pozsgai *et al*, 2010	Cinnamaldehyde/ Mustard Oil	Mouse	Hind Paw, Ear, Mesenteric artery	A study from our group using 1μM i.pl cinnamaldehyde on the hind paw, 1% mustard oil topical to ears, measured by laser Doppler flowmetry. 3-300μM cinnamaldehyde on mesenteric arteries in wire myograph, pre-constricted against U46619. Largely smooth muscle derived. All responses were reduced or abolished in TRPA1 KO mice, therefore authors show a TRPA1 mediated mechanism.
Yanaga *et al*, 2006	Cinnamaldehyde	Rat	Aortic rings	1μM-1mM causes concentration dependant relaxation to various preconstruction agents. Partially endothelium dependent and inhibited by L-NAME, thus endothelium dependant component is thought to be mediated by NO. Not mediated by prostaglandins, beta adrenergic receptors, activity of delayed rectifier or ATP sensitive potassium channels. May act via inhibition of cytoplasmic calcium increases and may increase cAMP, as phosphodiesterase inhibition increases dilation.
Namer *et al*, 2005	Cinnamaldehyde	Human	Forearm skin	Topical 10% cinnamaldehyde, measured by Laser Doppler Flowmetry. Show C-fibre involvement as is also linked to pain and hyperalgesia formation.
VenderEnde *et al*, 2001	Cinnamic aldehyde (Cinnamaldehyde)	Human	Forearm skin	Topical 1%, noted clinical signs of erythema, maximal at 10 minutes. Aided by plasma analysis they show PGD_2 as the main mediator, but of unknown origin. Unlikely to be from mast cells as is not accompanied by histamine release. Potentially macrophages or langerhans cells.

Morris *et al*, 1999	Acrolein	Rat	Nasal Tissue	Airbourne concentrations of 10-44µg/L, measured by acetone vapour uptake. Show accompanied oedema is reduced by capsaicin pre-treatment and NK_1 antagonist, demonstrating C-fibre and neuropeptide involvement.
Kunkler *et al*, 2011	Acrolein, Mustard oil	Rat	Meningeal Tissue	Nasal administration of 100µM mustard oil or 30µM acrolein, measured by laser Doppler flowmetry. Both blocked by CGRP antagonist, acreolin blocked by TRPA1 antagonist HC-030031 (50µM). Therefore also sight a TRPA1 and CGRP dependant mechanism.
Bautista *et al*, 2005	Allicin, Mustard oil	Rat	Mesenteric Artery	Garlic extracts (Allicin, 100nM-10µM) and mustard oil (100nM-10µM) cause concentration dependant vasorelaxation, inhibited by a non selective TRP channel antagonist and a CGRP antagonist.
Earley *et al*, 2009	Mustard oil	Rat	Cerebral Artery	Pressure myography creating myogenic tone at 70mmHg perfusion pressure, 3-100µM drug, diameter changes measured by image capture. Endothelium dependant. Reduced by TRPA1 antagonist HC-030031 (3µM), also by inhibitors of $K_{Ca}3.1$ (TRAM34), SK_{Ca} (apamin) and K_{IR} ($BaCl_2$). Not mediated by NO or prostaglandins. Sight a mechanism where TRPA1 activation leads to influx of calcium, which is perpetuated by IP_3 receptors on the endoplasmic reticulum, leading to potassium efflux through SK_{Ca} and $K_{Ca}3.1$ located on endothelium projections in to the smooth muscle layer. This is turn leads to hyperpolarisation of the vascular smooth muscle via K_{IR} channel activation by elevated potassium in the local extracellular space and also hyperpolarisation passed from endothelial cells via myoendothelial gap junctions.
Hikiji *et al*, 2000	Mustard oil	Cat	Tooth pulp	Application to second premolar tooth pulp cavity causes axon reflex dilation of the canine tooth pulp, inhibited by lidocaine. Indicates a C/Aδ fibre mechanism. Some fibres also mechanically activated.

Grant *et al*, 2005	Mustard oil	Mouse	Ear	Topical administration of 1% mustard oil, measured by laser Doppler flowmetry. Enhanced in NK1 KO mice, no effect of CGRP KO.
Lippe *et al*, 1993	Mustard oil	Rat	Hind Paw	Topical application of 5% drug, measured by in-fared emission thermography. 50% reduction by i.v L-NAME, so NO implicated. However, this was also accompanied by an increase in MAP, and decrease in skin blood flow.
Louis *et al*, 1989	Mustard oil	Rat	Hind Paw	Topical application of 0.5% drug, measured by laser Doppler flowmetry. Reduced by systemic antibodies to SP and CGRP, thus C-fibre mechanism suggested.
Graepel *et al*, 2011	4-ONE	Mouse	Hind Paw	Another paper from our group using i.pl injection of 10nmol drug, measured by laser Doppler flowmetry. Uses KO mice to demonstrate a TRPA1 and CGRP dependant mechanism, independent of TRPV1.

Table 1.1; TRPA1 Agonist Mediated Vasodilation. Table showing publications investigating vasodilation by TRPA1 agonists and mechanisms attributed. Tetraethylammonium (TEA), all other abbreviations previously used in text and available in the abbreviation list.

Other Exogenous TRPA1 Agonists

New agonists for TRPA1 have been consistently proposed since the discovery of the receptor. This has included pungent compounds including allicin from garlic (Bautista *et al.*, 2005) which has been shown to cause relaxation of *ex vivo* perfused feline mesenteric vessels (Mayeux *et al.*, 1988), isolated rat pulmonary arteries via induction of endothelial-derived NO production (Ku *et al.*, 2002) and isolated mesenteric arteries via endothelial independent relaxation mediated by sensory neurone derived CGRP (Bautista *et al.*, 2005). Garlic is also commonly used in traditional anti-hypertensive remedies and may alter blood composition and lipid levels, as defined from population studies using diets rich in allicin (Jain *et al.*, 1993, Banerjee and Maulik, 2002, Singh *et al.*, 1995, Huang *et al.*, 2007). Other TRPA1 agonists include extracts of wintergreen oil, ginger and cloves (Anand *et al.*, 2008, Bandell *et al*, 2004), extracts of perilla frutescens, a food commonly used Asian cooking (Bassoli *et al.*, 2009), extracts of Szechuan pepper (Menozzi-Smarrito *et al*, 2009), various terpenoids from natural plant sources (Iwasaki *et al*, 2009), icilin, formalin (McNamara *et al*, 2007, Macpherson *et al.*, 2007, Parada *et al*, 2001) tear gasses (Brône *et al.*, 2008), THC and various components of smoke. Cigarette smoke causes contraction of bronchial rings and plasma extravasation which can be blocked with the TRPA1 antagonist, HC030031 or in TRPA1 KO mice (Andrè *et al.*, 2008). Acreolin is a component of smoke and is also formed endogenously during inflammation and in high temperature cooking. It activates TRPA1 producing neurogenic inflammation in rodent airways, which is lost on TRPA1 KO (Michel, 2008, Andrè *et al.*, 2008). Isolated neurones also do not respond to acreolin when TRPA1 is knocked out (McNamara *et al.*, 2007). Acrolein has also been shown to cause vasodilation in the nasal and meningeal tissue of rats (Morris *et al.*, 1992, Kunkler *et al.*, 2011). In both of these studies C-fibre involvement is implicated, where Kunkler *et al* (2011), additionally show acreolin induced dilation to be blocked with a CGRP or TRPA1 receptor antagonist.

Diffusion rate into the cell is likely to be one of the most important determinants of TRPA1 agonist potency. Most of these new compounds have poor selectivity for TRPA1 but could form an important basis for further agonist or antagonist production. To date, the most potent agonists are considered to be the tear gasses (CS, CR and CN) (Brône *et al.*, 2008), however, their selectivity has yet to be tested. There is industrial interest in developing selective TRPA1 agonists to aid research in the field. We have recently been part of a study characterising a new, selective, non electrophilic and potent TRPA1 agonist called PF-4840154 (Ryckmans *et al.*, 2011).

TRPA1 has been located in auditory hair cells (Corey *et al.*, 2004). It is expressed at the onset of mechanical responsiveness where TRPA1 knockdown studies in mice virtually abolished hair cell transduction (Corey *et al.*, 2004). TRPA1 KO studies have since shown no loss of hearing, and TRPA1 antagonism does not affect basal mechanical thresholds in the paw (Eid *et al.*, 2008). However, interest in a role for TRPA1 in mechanosensation still exists. TRPA1 KO mice show deficits in detecting punctate mechanical stimuli (Kwan *et al.*, 2006) and exhibit reduced mechanical hyperalgesia formation in a Complete Freund's Adjuvant (CFA) induced arthritis model (Eid *et al.*, 2008). Kerstein *et al* (2009) have recently showed antagonism of TRPA1 to reduce mechanical perception and Zhang *et al* (Zhang *et al.*, 2008) have shown hypertonic solution to activate TRPA1 in HEK cell lines, possibly linked to mechanosensation. Recent reports from TRPA1 antagonists studies also suggest a role in noxious mechanosensation in normal tissue (McGaraughty *et al.*, 2010). Additionally, studies from our group have shown TRPA1 to have a critical role in Tumour Necrosis Factor α (TNFα) mediated and CFA induced joint hyperalgesia, both mimicing aspects of arthritis (Fernandes *et al.*, 2011). These findings suggest potential for TRPA1 channels to participate in systemic blood pressure control via its proposed action as a mechanosensor, particularly as the mechanism by which vascular cells sense pressure is currently unclear.

TRPA1 is also an important receptor in the field of cold sensation. Story *et al* (2003) originally characterised TRPA1 as a channel activated at temperatures <17°C, where TRPA1 knockdown reduces cold induced hyperalgesia formation. Although many other KO and antagonist treatment studies have now been carried out, the role for TRPA1 in temperature sensation is not yet clear. Results from TRPA1 receptor knockout studies in mice are conflicting, with Bautista *et al* (2006) showing neurones from TRPA1 WT and KO mice to have similar activity profiles when cooled down to 6°C; whilst Kwan *et al* (2006) show TRPA1 KO mice to possess behavioural deficits in cold plate tests undertaken at 0°C. The mice used in my research are derived from those derived by Kwan *et al.* Other studies question the role of TRPA1 in cold sensation, showing many cold sensing neurones do not express TRPA1 (Munns *et al*, 2007), while Ji *et al* (2008) show cold hypersensitivity to correspond to upregulation of TRPA1, an increased MO response and a lowered mechanical threshold. However, Jordt *et al* (2004) show neurones activated by cold are not responsive to MO, indicating TRPA1 may not be involved. More recently, further *in vitro* and *in vivo* evidence to support the role of TRPA1 in cold sensation has been recently published (Karashima *et al.*, 2009) along with several reviews of the topic, including Caspani and Heppenstall (2009), Kwan *et al* (2009) and Wetsel (2011). Despite the contradicting roles of TRPA1 in physiological mechanical sensation, a role in cold hyperalgesia seems better established, where several studies show inhibition using the TRPA1 antagonist HC-030031 (del Camino *et al.*, 2010, da Costa *et al.*, 2010). Therefore TRPA1 mediated cold activation may be more relevant in inflammatory conditions and could potentially play a role in the associated cold hyperalgesia.

Endogenous TRPA1 Agonists

Identifying potent and selective endogenous ligands for TRPA1 has been challenging, with an increasing number of compounds proposed over the last few years. To properly define the functional roles of TRPA1 *in vivo*, it

will be important to identify the relevant endogenous agonists. As reviewed by Chen and Kym (2009) and Bianchi *et al.,* (2012), the TRPA1 protein has some notable protein, functional and pharmacological differences between species. However, studies show that the sensory function of TRPA1 is evolutionarily conserved, with several common ligands and activating mechanisms being identified across species. This suggestion is well supported by the positive identification of agonists using cells transfected with human TRPA1, which has translated into animal models, for example nitrooleic acid (Taylor-Clark *et al.,* 2009) and ozone (Taylor-Clark and Undem, 2010). Therefore current evidence suggests that although caution should be exercised when interpreting functional effects, many commonly used TRPA1 agonists that are well characterised in rodent models will also be functional in humans.

Oxidative Stress

Oxidative stress produces two families of TRPA1 agonists; the first is reactive oxygen species (ROS) themselves, the other is lipid peroxidation products.

ROS, in particular H_20_2, are proposed activators of TRPA1. ROS occur naturally at low levels and participate in basal cell signalling. However, their levels are greatly increased in inflammation and they have proven role in the pathogenesis and symptoms of disease (Bochkov, 2007). Intraplantar injection of H_20_2 causes pain which is reduced in TRPA1 KO mice (Andersson *et al.*, 2008, Keeble *et al.*, 2009). Additionally, respiratory and pain responses associated with inhaled H_20_2 are severely reduced in TRPA1 KO mice (Bessac *et al.*, 2008). High levels of ROS are found in cigarette smoke, therefore potentially explaining some of its inflammatory nature (Bessac *et al.*, 2008). TRPA1 is also associated with sensitivity to hydroxyl radicals (Hill and Schaefer, 2009).

ROS are important for the formation of compounds such as acreolin and electrophilic alkenals as products of membrane peroxidation (Kondo *et al.*,

2001). 4-hydroxynonenal (4-HNE) is an electrophilic alkenal formed by membrane peroxidation during oxidative stress and tissue injury. It has been shown to activate TRPA1 *in vitro* at concentrations similar to those found in human blood during disease states (Macpherson *et al.*, 2007b, Trevisani *et al*, 2007). This causes release of CGRP and SP *in vivo* which is lost in TRPA1 KO mice (Trevisani *et al.*, 2007). 4-Oxo-2-nonenal (4-ONE) is a similar compound to 4-HNE, but has a more electrophilic structure and thus is 10 times more potent at activating TRPA1 (Andersson *et al.*, 2008, Taylor-Clark *et al.*, 2008a). Taylor-Clark *et al* (2008a) showed 4-ONE to cause neuropeptide release from isolated C-fibres, an effect lost in TRPA1 KO neurones. Activation of TRPA1 was additionally shown in human embryonic kidney cells (HEK) cells, also activating TRPV1 at concentrations over 100 μM. Our group has recently investigated the activity of 4-ONE in TRPA1 WT and KO mice, showing it to cause TRPA1 mediated vasodilation and nociception, while also displaying some TRPA1 independent oedema (Graepel *et al.*, 2011).

Studies looking at oxidative stress levels in hypertensive patients show increased levels compared to normotensive patients. There are also several polymorphisms in ROS producing genes associated with increased risk of hypertension (Touyz and Briones, 2011). Lipid peroxidation product levels increase during inflammation, including cardiovascular diseases, and have shown links to pathogenesis (Bochkov, 2007). However, their full clinical relevance has not been determined. 4-HNE is the best characterised TRPA1 activating lipid peroxidation product, shown to be present in plasma at concentrations of around 0.07μM in early adulthood, increasing with age to around 0.1μM in octogenerians (Poli *et al.*, 2008, Kim *et al.*, 2006), this also co-insides with the age related increase in cardiovascular risk. It has also been shown to increase in the blood during several neurological and cardiovascular diseases, such as myocardial infarction, atherosclerosis and rheumatoid arthritis, where lipid peroxidation products are potential markers of cardiovascular risk (Poli *et al.*, 2008).

Other Endogenous Agonists

Other endogenous agonists have also been described, however their poor selectivity and potency means that there are relatively few relevant studies available. Other proposed activators include Hydrogen Sulphide (H_2S) (Streng *et al.*, 2008), 5'6-epoxyeicosatrienoic acid (5'6-EET) (Sisigano *et al*, 2012), a potential EDHF, calcium (Cavanaugh *et al.*, 2008), which may act via sensitisation rather than direct activation (Jordt *et al*, 2004) and pH changes, where alkalisation has been shown to cause pain that is lost in TRPA1 KO mice (Fujita *et al.*, 2008 , Peterlin *et al.*, 2007). These pose possible links to disease where changes in localised pH commonly occur.

Another family of proposed TRPA1 agonists are cyclopentenone prostaglandins and isoprostones. 15-d-PGJ_2 is a cyclopentenone prostaglandin produced from non-enzymatic degradation of PGD_2, the most common tissue prostaglandin. It has weak effects at prostaglandin DP receptors and is thought to modulate NFkB signalling, but is largely known as an activator of peroxisome proliferator-activated receptor gamma (PPARγ). Its levels are increased in disease and inflammation, where it has largely anti-inflammatory actions (Taylor-Clark *et al.*, 2008b, Kondo *et al.*, 2001, Scher and Pillinger, 2005, Jackson *et al.*, 1999, Takahashi *et al.*, 2008). 15-d-PGJ_2 has also demonstrated nociceptive activity, causing acute pain. This is blocked by the TRPA1 antagonist HC030031 and in TRPA1 KO mice (Cruz-Orengo *et al.*, 2008, Taylor-Clark *et al.*, 2008b). There are also no changes in blood pressure when 15-d-PGJ_2 is i.v infused, or general correlations between oxidised phospholipids and systolic blood pressure (Collin *et al.*, 2004, Ragino *et al.*, 2005). Other cyclopentenone prostaglandins such as isoprostones and derivatives of prostaglandin A (PGA) also activate C-fibres, causing neuropeptide release and pain, an effect lost on KO of TRPA1 (Materazzi *et al.*, 2008).

Another interesting TRPA1 agonist is NO, which has been shown to cause nociceptive responses in mice via TRPA1 and TRPV1 at endogenous levels (Miyamoto *et al.*, 2009). NO can sensitise pain pathways, however

the settings in which it becomes painful are not yet clear. Nitrated fatty acids, formed under oxidative or nitrative stress, also potently activate TRPA1 (Taylor-Clark *et al.*, 2009). Activity was shown to be specific to MO activated bronchopulmonary neurones and lost on TRPA1 KO or antagonist treatment (Taylor-Clark *et al.*, 2009). They are stable in human plasma and commonly found at active concentrations during inflammation e.g. asthma, COPD, IR injury, arthritis and in pollution. However, they are also known to activate many other pathways due to their chemical reactivity (Taylor-Clark *et al.*, 2009).

TRPA1 Antagonists And KO mice

The various uses of TRPA1 antagonists and KO mouse strains have been detailed above. These tools have been vital in determining the TRPA1 dependent effect of agonists in physiological and pathophysiological processes. There are currently only few available antagonists, and two KO mouse strains. Development of further methods to highlight TRPA1 activity would be welcomed, particularly in light of the poor selectivity of TRPA1 agonists. While much information can be gained from agonist studies, there is a need to identify the mechanisms at work. In particular, a lack of good quality and specific TRPA1 antibodies currently means that localisation of TRPA1 expression is challenging. A brief summary of TRPA1 agonists is shown in figure 1.3. Other tools to inhibit TRPA1 activity are available, including siRNA treatment, but these are infrequently used and thus not discussed.

TRPA1 Antagonists

The possibility that TRPA1 is involved in pain and inflammatory syndromes has led to TRPA1 antagonist development. Some of these are shown in table 1.2. At present, commonly available antagonists are limited to HC-030031 (McNamara *et al.*, 2007) or AP18 (Petrus *et al.*, 2007). HC-030031, based on a xanthine core structure, has proven to be effective after oral dosage, reducing inflammatory and neuropathic pain in animal models (Eid *et al.*, 2008). Originally from Hydra Biosciences, it has shown good

potency and selectivity to TRPA1 and has reportedly entered preclinical investigations (Baraldi *et al.*, 2010). Newer compounds are now being released, based on the HC030031 structure and with increased potency.

Most recently this has been demonstrated by publications using systemic applications of Chembridge-5861528 from ChemBridge Corporation, which was used to attenuate diabetic and MO induced mechanical hypersensitivity (Wei *et al.*, 2010, Wei *et al.*, 2009). This antagonist has now been reproduced by Tocris, under the name TCS5861528 and is commercially available. Studies undertaken in this thesis will use both HC-030031 and TCS5861528.

AP-18 represents an alternative TRPA1 antagonist, with an oxime derived structure. It was identified by Petrus *et al* (2007), where it blocked cinnamaldehyde induced pain when co-injected in to murine hind paws. Limitations of AP-18 have proved to be its localised action and a short length of activity, however in some experimental designs these features may be beneficial. There are current attempts to improve on AP-18, some of which have been published in a recent letter (DeFalco *et al.*, 2010). A recent publication using systemic doses of A-967079, one of the new compounds from Abbott laboratories based on the AP-18 core structure, demonstrates a reduction in noxious mechanosensation in both normal and inflamed (CFA-treated) rat hind limbs (McGaraughty *et al.*, 2010).

The success of antagonists in animal studies has demonstrated the potential for oral TRPA1 antagonists to be clinically useful. A number of pharmaceutical companies have filed patents and are known to be increasing their profiles of potential TRPA1 antagonists, with many entering clinical trials for treatment of inflammatory conditions. See Baraldi *et al* (2010) for a recent review.

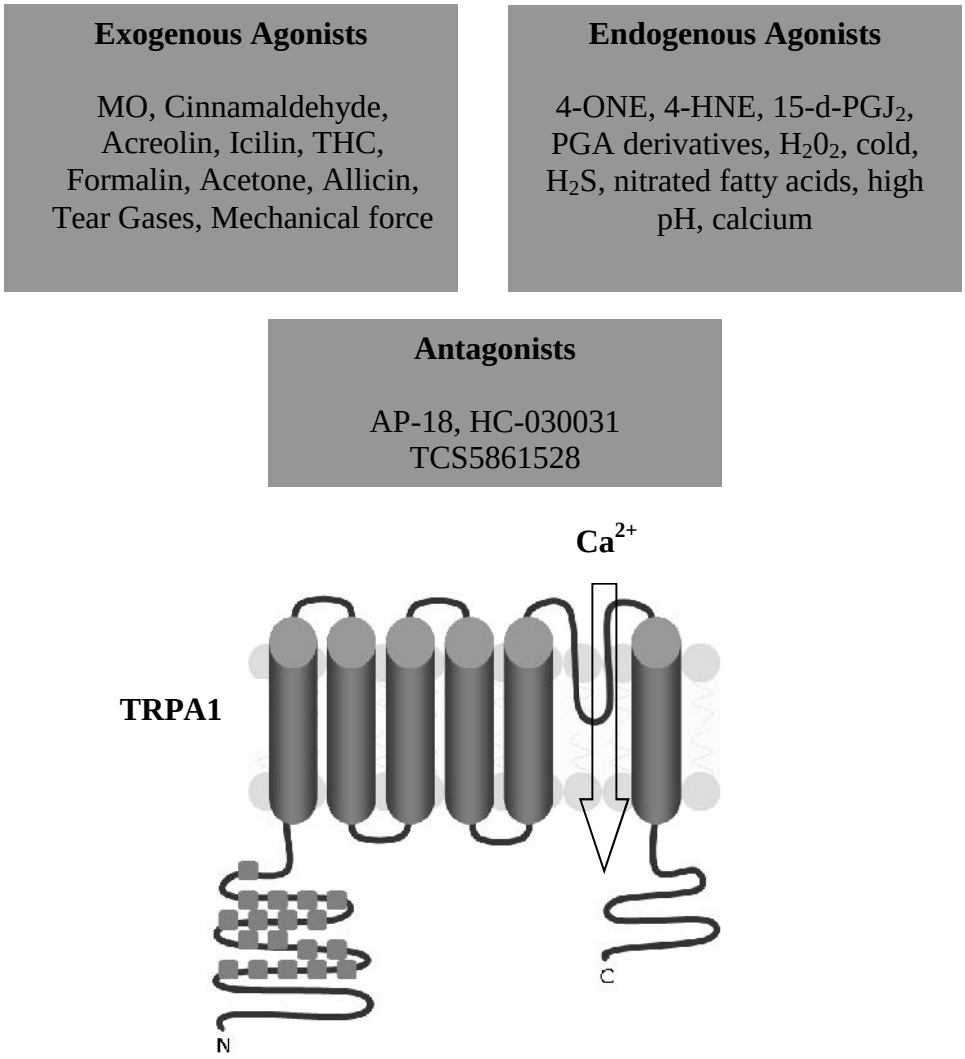

Figure 1.3; TRPA1 Receptor Agonists, TRPA1 is activated by many exogenous and endogenous agonists, leading to influx of calcium into the sensory neurone terminal and release of stored neuropeptide containing vesicles. The majority of these agonists are electrophilic and bind to the receptors N-terminal via covalent interactions. THC and icilin are proposed to have a more traditional binding pocket mechanism located on the intracellular side of the receptor body. Sensitisation pathways act on the termini.

Antagonist	Structure	IC50
Ruthenium Red	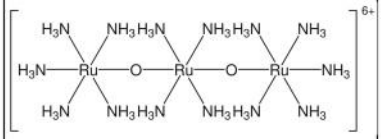	3μM / Mustard Oil (Nagata et al, 2005)
Camphor	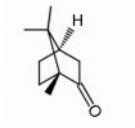	68μM / Mustard Oil (MacPherson et al, 2006)
HC-030031	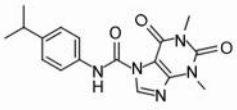	6 μM / Mustard Oil (McNamara et al,2007)
Chembridge-5861528	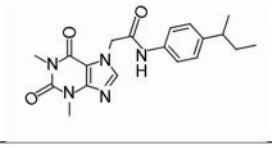	14μM / Mustard Oil (Wei et al, 2009)
AP-18	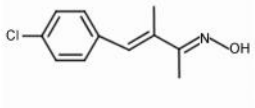	10 μM / Mustard Oil (Chen et al, 2009)
A-967079	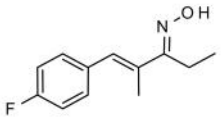	67nM / Mustard Oil (McGaraughty et al, 2010)

Table 1.2; TRPA1 Antagonists. Table of TRPA1 antagonists, showing their structure and determined IC_{50} (Nagata *et al.*, 2005, Macpherson *et al.*, 2006, McNamara *et al.*, 2007, Wei *et al.*, 2009, Chen *et al.*, 2009a, McGaraughty *et al.*, 2010).

TRPA1 KO Mice

A growing number of research groups now have access to TRPA1 KO mouse strains, developed originally by Kwan *et al* (2006) and Bautista *et al* (2006) groups respectively. Differences in the method of TRPA1 gene deletion occur between these strains (Story and Gereau Iv, 2006), but both produce clear loss of functional TRPA1. However, both are commonly also on mixed genetic backgrounds, representing problems for researchers when extrapolating data to and from other mouse models. Despite this, TRPA1 KO mice are currently the best tool for investigating the role of endogenous TRPA1 *in vivo*.

TRPA1 KO mice derived by Kwan *et al* (2006) were created by replacement of the exons encoding the S5 and S6 pore forming domains, with a cassette containing an internal ribosome entry site, a human placental alkaline phosphatase gene and a polyadenylation sequence. Endoplasmic reticulum retention and stop signals were also placed before the cassette. The product of this was a TRPA1 transcript that cannot form a functional channel, and if produced, is retained in the endoplasmic reticulum. These mice are now available to us, and studies in our group are undertaken using this TRPA1 KO maintained on a mixed C57Bl/6J and B6129PF2/J background. They have also been used in various publications from other groups and their genotype confirmed independently.

TRPA1 KO mice from Bautista *et al* (2006) were created by a similar mechanism, deleting not only the pore loop but also much of the sixth transmembrane domain. These mice are available on a C57/BL6 background and are used by many experimental groups, with a proven genotype. Similar to those from Kwan *et al* (2006), these KO mice show clear deficits in sensing TRPA1 agonists when compared to WT littermates. TRPA1 KO mice from Bautista *et al* (2006) are also reported to show haplosufficiency, as heterozygous mice have an agonist sensitivity lying between that of the WT and KO.

The Role Of TRPA1 In Systemic Inflammatory Diseases

There is evidence that TRPA1 is involved in the pathophysiology of a number of clinical diseases. Many TRPA1 agonists have potential roles in the formation and propagation of inflammatory diseases, for example ROS (Bessac *et al.*, 2008). Expression of TRPA1 has also been shown to increase in response to inflammation (Hatano *et al.*, 2012). TRPA1's sensitivity to oxidants also suggests it may play a role in pathogenesis of inflammatory diseases involving high oxidative stress, such as ischemia, diabetes and arthritis, many of which have vascular components. There are a number of disease areas where TRPA1 has gained particular attention, and I propose that the background information presented in this introduction suggests there may be undiscovered roles for TRPA1 in cardiovascular regulation.

The most promising disease areas showing TRPA1 involvement are inflammatory conditions of the airway, such as asthma, COPD (Caceres *et al.*, 2009) and cough (Birrell *et al.*, 2009, Andre *et al.*, 2009), which appear to benefit from a reduction in TRPA1 activity and are exacerbated by environmental irritants which can activate the receptor. Neuropeptide release in the lung following TRPA1 activation causes bronchial contraction and tracheal plasma extravasation (Andrè *et al.*, 2008). TRPA1 antagonists and TRPA1 KO mice show protection during lung disease models including asthma, where Caceres *et al* (2009) have shown TRPA1 KO and administration of TRPA1 antagonist HC030331 to dramatically reduce inflammatory processes and symptoms in a mouse model of allergic asthma. Additionally, Raemdonck *et al.*, (2011) have recently shown TRPA1 activation on sensory neurones to initiate a central reflex, causing bronchoconstriction in the late asthmatic response via parasympathetic nerves.

Cigarette smoke inhalation is a major cause of COPD, inducing sensory neurone derived, SP mediated, oedema in guinea pig bronchi models, which can be blocked by TRPA1 KO and instillation of HC-030031 (Andrè

et al., 2008). Many TRPA1 agonists have also been identified as pro-tussive agents, including cinnamaldehyde, MO and acreolin (Andre *et al.*, 2009, Birrell *et al.*, 2009), thus antagonists may also have a place as future cough remedies and be particularly valuable in treatment against irritant exposure, including tear gases exposures and industrial disasters. A recent review of the role of TRPA1 in cough is available by Grace and Belvisi (2011).

Success has also been demonstrated using TRPA1 antagonists and KO mice to reduce pain and hyperalgesia in inflammatory disease models originating in other areas of the body, including the CFA model of arthritis and TNFα induced hyperalgesia (Eid *et al.*, 2008, Fernandes *et al.*, 2011). Another potential therapeutic areas linked to TRPA1 activity is bladder overactvity (Andersson *et al.*, 2010), where activation of TRPA1 on sensory neurones may be responsible for pain and inflammation of haemorrhagic cystitis. TRPA1 therapies may also be useful in the treatment of bladder pain following some cancer chemotherapies, as acreolin can be formed as a metabolite of drugs and can concentrate in urine (Bautista *et al*, 2006). Oxaliplatin is another anticancer drug which has shown TRPA1 induced mechanical and cold hyperalgesia, also causing CGRP mediated vasodilation of pulmonary arteries (Nassini *et al.*, 2011). Additionally, recent studies are now focussing on the role of TRPA1 in dental pain due to injury and bleaching (Markowitz, 2010), as the mouth is densely innervated with sensory neurones.

All current disease areas associated with TRPA1 activity are related to the activation of sensory neurones, where there is release of vasoactive neuropeptides and pain signalling. As described in section 1, sensory neurones also have important roles in cardiovascular regulation, in particular the neuropeptides CGRP and SP which oppose the onset of vascular disease. Several lines of evidence described in this introduction demonstrate that sensory neurones and neuropeptides are activated by TRPA1 agonists, many of which are increase in inflammatory vascular disease and cause changes in vascular regulation to occur. This is

particularly clear at the vascular level, where several TRPA1 agonists cause vasodilation, often found to be mediated by CGRP. Several systemic effects of TRPA1 agonist administration have also been shown, particularly using cinnamaldehyde. The cardiovascular roles of TRPA1 has also been the subject of my recent review (Bodkin and Brain, 2010). I now have access to a range of experimental tools, including TRPA1 KO mice, which allow me to conduct this novel study of the effects of TRPA1 in cardiovascular regulation.

Hypothesis And Aims Of The Thesis

In the light of the highlighted evidence, I have formed a hypothesis that TRPA1 is involved in the control of resistance vessel tone *in vivo*. There, it contributes to the control of blood pressure by keeping peripheral resistance low and will resist the onset of hypertension by releasing neuropeptides when it is activated by elevated levels of endogenous agonists. Genetic deletion of TRPA1 will lead to a loss of this process, increasing basal blood pressure and resulting in susceptibility to hypertension, resulting in increased systemic inflammation and worsened hypertensive endpoints.

I have a number of experimental aims for this thesis;

- Investigate the basal cardiovascular phenotype of TRPA1 KO mice compared to matched WT mice. I wish to particularly focus on basal blood pressure control and will measure this in conscious animals by both tail cuff plethysmography and telemetry.
- Analyse the role of TRPA1 in the vasorelaxant response to cinnamaldehyde. I will use isolated mesenteric arteries in a wire myograph to study the nature of TRPA1 involvement in this process and attempt to dissect the contributing signalling.
- Study the onset and endpoints of experimental hypertension in TRPA1 WT and KO mice, investigating the potential roles of TRPA1. This will be done in terms of blood pressure, hypertrophy and endpoint inflammation measures in matched TRPA1 WT and

KO mice following implantation of an osmotic minipump infusing Ang II subcutaneously over a 14 day experimental period.

Chapter 2 - Materials and Methods

Animal Procedures

All animals were housed in a climatically controlled environment, on a 12 hour light (7am-7pm) /dark (7pm-7am) cycle, with free access to a normal food diet and water. Experiments were carried out in accordance with the Animals (Scientific Procedures) Act 1986. Both genders of mice (20-35g) were used in these experiments. C57BL/6-B6129P1/F2J mixed genetic background TRPA1 KO and WT mice were a gift from Prof. S Bevan and have been bred both homozygously and heterozygously in-house. Each litter was genotyped and has been previously confirmed by both Prof. S Bevan and Kwan *et al.* (Kwan *et al.*, 2006). CD1 mice (18-30g) were purchased from Charles River, UK. C57BL/6 αCGRP KO and WT mice were a gift from Dr. A-M Salmon, Institute Pasteur, Paris, France who have confirmed the genotype (Salmon *et al.*, 1999), and have been homozygously bred in-house and genotyped regularly. Male Wistar rats (300-400g) were purchased from Harlan, UK.

Anaesthesia

For the majority of studies, no anaesthesia was necessary. However, where it was used, this was as brief as possible. For surgical procedures, a deep level of anaesthesia was maintained. This was assessed by the loss of paw or tail pinch reflex. For recovery procedures, inhalation isoflurane (Abbott Laboratories, UK), 3% in O_2 carrier gas at 4L/minute was used. Induction was carried out in a chamber with the animal then transferred to a nose cone. Recovery was monitored in a clean home cage, under infra-red light. For Laser Doppler flowmetry, anaesthesia was induced using i.p administration of a ketamine (75mg/kg, NMDA receptor antagonist, an anaesthetic and analgesic) and medetomidine (1mg/kg, alpha2-andrenoceptro agonist, a sedative and analgesic) mix (Vetlar and Domitor, Pfizer), made in fresh saline each occasion.

Genotyping Of TRPA1 WT And KO mice

Genotyping of the mice was carried out using endpoint polymerase chain reaction (PCR). Genomic DNA was extracted from ear punches or tail tips, collected using the appropriate tools. PCR was carried out for the TRPA1 gene or neomycin cassette using primers (Sigma, UK or Eurofins DE); WT (5'-TCCTGCAAGGGTGATTGCGTTGTCTA-3' and 5'-TCATCTGGGCAACAATGTCACCTGCT-3') and KO (5'-CCTCGAATCGTGGATCCACTAGTTCTAGAT-3' and 5'-TCATCTGGGCAACAATGTCACCTGCT-3'). Both the extraction solutions and PCR mix were provided in a commercially available kit (ExtractRED-N-Amp tissue PCR kit, Sigma, UK). A thermal cycler (Techne, Cambridge UK) was used to denature the DNA and activate the Taq for 2 minutes at 94°C, then 34 cycles of 94°C for 30 seconds, 64°C for 30 seconds, 68°C for 30 seconds were used to amplify the gene of interest. The product was then held at 4°C and analysed by agarose gel (1.8% w/v) electrophoresis in TBE buffer (0.5% Tris-borate-EDTA buffer, BioRad) with images taken under a UV camera (Syngene, G-Box). WT band appeared at 310 bp, mutant KO band appeared at 200 bp. Both were apparent in heterozygous animals.

Mouse Activity Wheels

The protocol for these measurements was developed in-house, based on suggestions and guidance of Prof. M. Shattock. Litters of heterozygous mice (2 months of age) had plastic wheels (13 cm diameter) added to their home cage. This was to acclimatise them to running on the wheels. After 3 weeks, mice were separated into pairs of the same genotype and moved to a quiet room. Mice were kept in littermate pairs to avoid social stress affecting the running response. In most published studies mice are housed singly for running experiments. Pairs of mice were chosen for this study to reduce potential stress from social separation and to reduce variation between results. Initial trials of paired mice suggested this was a preferable adaptation to the model. Daily running was measured using a rotational counter on loan from M. Shattock, which uses a Powerlab and Chart 5 to

present the data. One side of the wheel circumference is painted dark. Using this each turn of the wheel can be picked up by the powerlab as a change in voltage change (approx 8V). The intervals between these peaks can be used to calculate wheel turning speed, whilst the number of revolutions gives a measure of distance ran by the mice. Most running took place overnight and totals for each 24 hour period were collected over a period of 7 days/6 nights. Similar measurements are made of voluntary exercise using other measurement systems, for example Ajojola *et al* (2009), who studied the effect of exercise in a mouse atherosclerosis model. My data was also analysed for preferred speed of wheel revolutions, showing running speed. In nearly all current models use mice that are single housed for running. This was avoided in my study due to the potential for stress responses, where I additionally found inter-cage variability to be reduced when mice ran as pairs.

Measurement Of Blood Flow Using Laser Doppler Flowmetry

Cutaneous blood flow in the mouse was assessed using a non-invasive two-channel laser Doppler flowmeter (Moor Instruments, UK) connected to a PowerLab data acquisition system, which measures blood flow in a single blood vessel (ADInstruments, UK) (Grant *et al.*, 2005). A probe was placed directly on the surface skin of each ear. Baseline blood flow was obtained from the laser Doppler flowmeter for 5 min. Cinnamaldehyde (1-10% in 20µl) was applied topically on the ipsilateral ear and the contralateral ear received vehicle (10% DMSO in ethanol) topically, and blood flow responses were then recorded for 30 min. A dose of 10% of cinnamaldehyde was found to produce the most significant reliable increase in blood flow. Blood flow data were recorded in arbitrary flux units, which are proportional to blood flowing through the vessel. Results are expressed as the integral of the recorded flux vs. time trace ($\times 10^3$ flux units).

Measurement Of Blood Pressure

Tail Cuff Plethysmography

Blood pressure was measured by mouse tail cuff using the CODA 6 system (Kent Scientific, USA). This is a non-invasive computerised system of blood pressure acquisition, based on the principle of volume pressure recordings. This method has been shown to give a good correlation to indwelling catheters and telemetry, and has been successfully used in previous publications, including from this group (Feng *et al.*, 2008, Bunag, 1973, Mahoney and Brody, 1978, Liang *et al.*, 2009). Several studies have shown this method to be particularly suited to measurement of systolic blood pressure in the physiological range (Bunag and Riley, 1974, Mahoney and Brody, 1978).

This system has been well validated by the company against telemetered animals, the gold standard technique for measuring rodent blood pressure. The method of measurement is very similar to that used for humans, where an occlusion cuff obstructs the flow of blood to the tail. As this is slowly deflated, a second cuff measures the characteristics of the returning blood. Systolic blood pressure is measured as the appearance of swelling following release of occlusion, diastolic pressure is calculated at ceasing of swelling. Twenty seconds of deflation time was recorded each cycle. When using this technique, animals were trained on the machine for at least 7 consecutive days, until measurements were consistent. In practice, training data was collected daily for 2-3 weeks, at a similar time each day. The protocol consisted of acclimatisation to a warmed (25°C) room for at least an hour, then placing the animals in warmed tube restraints before conducting five acclimatisation cycles and fifteen measurement cycles of data acquisition. For some studies, an additional warmed platform was used under the restraints. Cycles were discounted if the animal moved during the measurement. Average blood pressure readings (Systolic/Mean/Diastolic) are expressed for each animal per day, and a group average calculated from this, over many days where possible. Three

or more daily cycles must have been successfully collected for the animal's data to be used.

Telemetry

Blood pressure was also measured using implantable telemetry devices (PA-C10, DSI, Netherlands). This is the current gold standard of rodent monitoring. The advantages of this method over tail cuff plethysmography include that it measures parameters in a more clinical setting, with free running, undisturbed animals in their home cage. It is considered a more humane method and improves attainment of 3R's principles. Due to reduced data variability, fewer mice are needed to provide statistical significance. Additionally, the animals involved are considered to undergo less stress over the course of the experiment compared to serial tail cuff measurements. Restraint needed to undertake tail cuff plethysmography has been shown to induce physiological signs of stress, including increases in blood pressure, heart rate and plasma catecholamines (Kramer *et al.*, 2001), although actual pressure readings obtained can be similar with good training (Krege *et al.*, 1995). With these benefits in mind, telemetry is now well used for cardiovascular studies, in both academia and industry. However, there are some disadvantages to keep in mind. The telemetry equipment is expensive to set up, with limited battery life in each probe. It also requires an initial surgery which is usually well tolerated, but requires micro surgery which is invasive and can potentially lead to infection, immune reaction or catheterised vessel remodelling (Mills *et al.*, 2000). In my protocol, this will also be followed by a second smaller surgery, for subcutaneous implantation of the osmotic minipump. This occurs 14 days after the telemetry probe surgery. The transmitter itself is relatively bulky for a mouse to carry and has been shown to reduce wheel running activity (Mills *et al.*, 2000), indicating it may affect the animals ability to exercise. A good comparative review on telemetry is available from Van Viliet *et al* (2006).

During implantation, proper aseptic technique was observed and sterile tool and drape packs were used (SLS, UK). Items needed for the surgery were autoclaved in batch packs, one for each animal. The skin covering the throat was shaved and treated with iodine tincture before and after the surgery. Mice >20g underwent surgery to cannulate the left common carotid artery, with the probe tip inserted till it enters the aortic arch. During the surgery, mouse eyes were protected from drying using eye gel (Viscotears, Novartis) and analgesia was given in the form of intra-musclar buprenorphine (50µg.kg, Vetergesic, Alstoe animal health). The catheter was secured using sterilised surgical braided silk (5.0, waxed, Pearsalls sutures) and the transmitter body inserted into a sub-cutaneous pocket on the animals right flank. The pocket was irrigated with sterile saline to reduce irritation and provide fluid resuscitation. Outer skin was closed with absorbable sutures (4.0, Ethicon, Johnson and Johnson, USA) in a discontinuous pattern. Animals were singly housed and monitored daily for signs of pain or infection. Telemetry probe recordings were collected after implantation to check positioning, but baseline data was not collected until 10 days post-surgery, when recovery had occurred. Where probes were re-used, they underwent cleaning and sterilisation by Tergazyme (Alconox, USA) and Cidex (Cidex-OPA, Johnson and Johnson, USA), following the guidelines provided by DSI. Data was collected and calculated by the DSI software (DSI Dataquest A.R.T.™ System, DSI, Netherlands)

The PAC-10 telemetry probe measures a number of parameters, averaged over the length of the reading;

Systolic Blood Pressure; Measured from peak of cardiac cycle as an indication of the hearts ability to create force but, also reflects inherent pressure in the system.

Mean Blood Pressure; Calculated from the systolic and diastolic blood pressures by the Dataquest software. Reflects average pressure seen by the major vessels of the vascular system.

Diastolic Blood Pressure; Measured from the base of the cardiac cycle, showing the inherent pressure in the system caused a combination of vessel tone, heart volume and blood volume factors.

Heart Rate; Measured as the number of cardiac pressure cycles per minute. Controlled largely by autonomic influences.

Pulse Pressure; Measured as the difference between systolic and diastolic blood pressures. Shows the pressure developed by the heart, indicating contractile characteristics.

Activity counts; An arbitary number to represent movement measured by the accelerometer. Indicative of mouse spontaneous activity levels.

Experimental Hypertension

Implantation Of Ang II Filled Osmotic Minipumps

Ang II (Sigma, UK) was infused into mice at a rate of 0.23µl/hr (the flow rate is batch specific and specified by the manufacturer upon purchase) in a saline vehicle via a subcutaneously implanted Alzet minipump (Charles River UK) in the mid-scalpular region. Mice were aged 2.5-3 months and weighed >20g. Surgical procedures were conducted in line with those previously described for telemetry surgery,;i.e.aspetic technique. This model is widely used and very reproducible. Our group has previously published data successfully gained from this model using the same pressor doses of Ang II (Liang *et al.*, 2009). The concentration of Ang II was adjusted so that each mouse received a dose of 1.1mg/kg/day. Control mice received an empty pump, known from previous studies to act similarly to saline filled control pumps. However, I recognise that saline filled controls would have been preferable. Blood pressure data was measured by tail cuff plethysmography or telemetry, collected at least three days ahead of mini-pump implantation and on the morning of the implantation, but not for three days after the operation in the case of tail cuff. Telemetered animals were monitored immediately. Implantation was conducted under isoflurane anaesthesia and using surgical aseptic technique. Pain relief was administered before the short procedure in the

form of intra-musclar buprenorphine (50µg.kg, Vetergesic, Alstoe animal health). The small wound needed was sutured up with absorbable sutures in a discontinuous pattern or closed with tissue glue (Vetbond tissue adhesive, 3M). Animals were singly housed after the operation and monitored daily for signs of pain or infection.

Termination Of Experimental Hypertension

Two weeks after implantation, the final blood pressure measurements were taken and the mice sequentially terminated. Blood was collected by cardiac puncture and centrifuged at 2000 rpm for 15 minutes. 100µl aliquots of plasma were snap frozen and stored at -80°C. Final body weight was recorded and mice dissected so that the heart, aorta, mesentery, brain and DRG could be stored for future work. Brains were grossly dissected to dissociate brainstem, cortex and striatum structures. Weights of the overall heart, left ventricle free wall and right ventricle free wall were recorded, along with that of the osmotic minipump to ensure it had properly functioned. Brain, DRG, heart, mesenteric vessels and lower aorta portion were individually stored in *RNA later* (Sigma), left overnight at 4°C, then stored at -80°C.

Echocardiography

Cardiac echocardiography was performed on a VEVO 770 with a mouse scanhead (RMV 707B, 30HZ, VisualSonics, Inc., Toronto, Canada). Other available methods include Magnetic Resonance Imaging (MRI), Single-photon emission computed tomography (SPECT) or Positron emission tomography (PET), however these are expensive and not widely available. They also often demand the use of radioactivity or long scanning times. A review of these techniques is available in Lahoutte (2007). Measurements of left ventricular (LV) mass taken during echocardiography have been shown to correlate closely to those collected at necropsy, although absolute values vary (Stypmann *et al.*, 2006). Echocardiography is now a relatively common technique for the assessment of genetically modified mouse phenotypes, and for the serial tracking of disease progression.

Echocardiography is carried out as described in the materials and methods of the published online video (Respress and Wehrens, 2010). When designing the experiment, there are a number of important considerations raised in the literature. Many of these considerations surround choice on anaesthesia. All anaesthetics depress cardiovascular responses and cause reduction in heart rate and body temperature. All of these will impact on the functional measurements gained from echocardiography. For these reasons, use of light isoflurane anaesthesia was considered best practice (Collins *et al.*, 2003). It has also been reported that examinations can be performed on awake animals with training, see Collins *et al* (2003), however this was not deemed suitable in this project. Heart rate in a conscious mouse is 500-700 bpm at rest. Altering this rate will in turn affect left ventricle function and fractional shortening in particular, therefore it is important to maintain a physiological heart rate where possible (Rottman *et al.*, 2007). In my study, mice were maintained at an anaesthetic level that produced heart rates between 400-500 bpm, with the whole examination lasting less than 20 minutes. These parameters have previously been shown to give good levels of data reproducibility (Wu *et al.*, 2010). In line with best practice, mice were maintained in the supine position, with limited pressure on the chest and core body temperature maintained at 37.4°C using a homeothermic heated platform and rectal probe. Protective eye gel was used to prevent drying damage (Vicscotears, Novartis). The chest hair was removed of hair using hair removal cream (Veet, Reckitt Benckiser, UK). Heart and respiration rate were recorded, along with electrocardiogram (ECG). Heart images were taken with warmed ultrasound gel. These controls are necessary to give optimum conditions for physiologically relevant measures.

Three main images were collected for analysis. 1) A parasternal long axis, where the LV apex is at its maximum length and the aortic root is in full view. M-mode is collected at the level of the papillary muscle for consistently comparable cross-sections. 2) A clockwise, 90° rotation of the transducer then also produced a short axis view, with another M-mode taken between the two papillary muscles. M-mode images were then

analysed using the leading edge to leading edge method over 5 sinus beats, and calculations made by the onboard software. 3) Each examination also included an aortic pressure wave Doppler, giving an indication of systolic function. Mouse weight was collected at the start of the procedure and measurements expressed as a ratio. Previous studies have shown that there are no statistical differences in heart size and function between genders of CD1 mice (Stypmann *et al.*, 2006). However, this study did show that heart size was not consistent until 12 weeks of age. Therefore, to avoid potential weight phenotype and age artefacts, all my data was expressed as a ratio to body weight. A full cardiac examination was collected on all mice, producing a range of morphology and functional measures. See figure 2.1 and 2.2. The meaning of each one is described below;

Morphological measures

LV mass: Measures overall calculated mass of the left ventricle. This is the ultimate measure of heart tissue size used for the study of hypertrophy.

Left Ventricular Internal Diameter at diastole (LVIDd): Measures diameter of the left ventricle when relaxed. This gives a measure of volume and is an indication of the hearts capacity to relax. Hearts with much hypertrophy may be bigger in mass but with less volume and relaxation capacity due to fibrosis.

Left Ventricular Anterior Wall thickness at diastole (LVAWd): Shows the measured thickness of the left ventricle anterior wall when relaxed.

Left Ventricular Posterior Wall thickness at diastole (LVPWd): Shows the measured thickness of the left ventricle posterior wall when relaxed.

Interventricular Septum thickness at diastole (IVSd): Shows the measured thickness of septal wall when relaxed.

Functional Measures

Fractional shortening (FS%); Fractional shortening describes the amount of diastolic space that is lost during systole. It is therefore a direct measure of heart contractility. It is the most common indice of left ventricle function. As it is heart rate dependent, it is important to control anaesthesia well.

Stroke Volume (SV µl); Stroke volume is a measure of the amount of blood ejected from the heart each beat. It is measured from the change in left ventricle volume from diastole to systole. It is a functional measure of heart output.

Ejection Fraction (EF %); This indicates the percentage of blood of blood ejected from the left ventricle, it is related to stroke volume and fractional shortening.

Cardiac Output (CO ml/min); This is the most commonly used measure of heart output, combining the stroke volume with the heart rate.

Peak Aortic Flow (mm/s); Peak outflow into the aortic arch is measured by Doppler. The echocardiograph does not measure pressure but the speed out outflow is an indicator of systolic function and/or valve function.

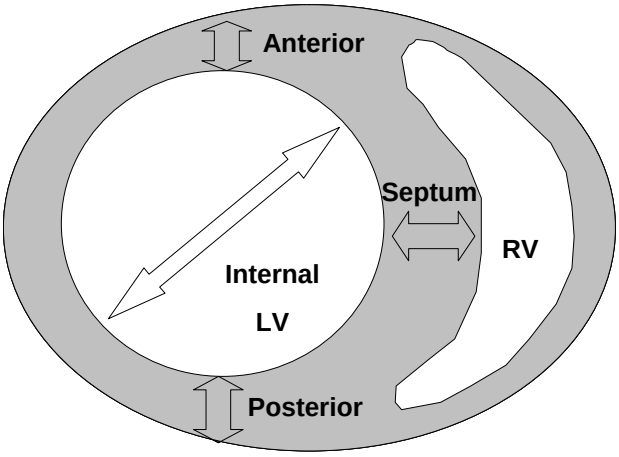

Figure 2.1; Relevant positions of cross sectional measurements of heart size. These dimensions will be referred to in the description of echocardiography data. Diagram for representation only and is not to scale.

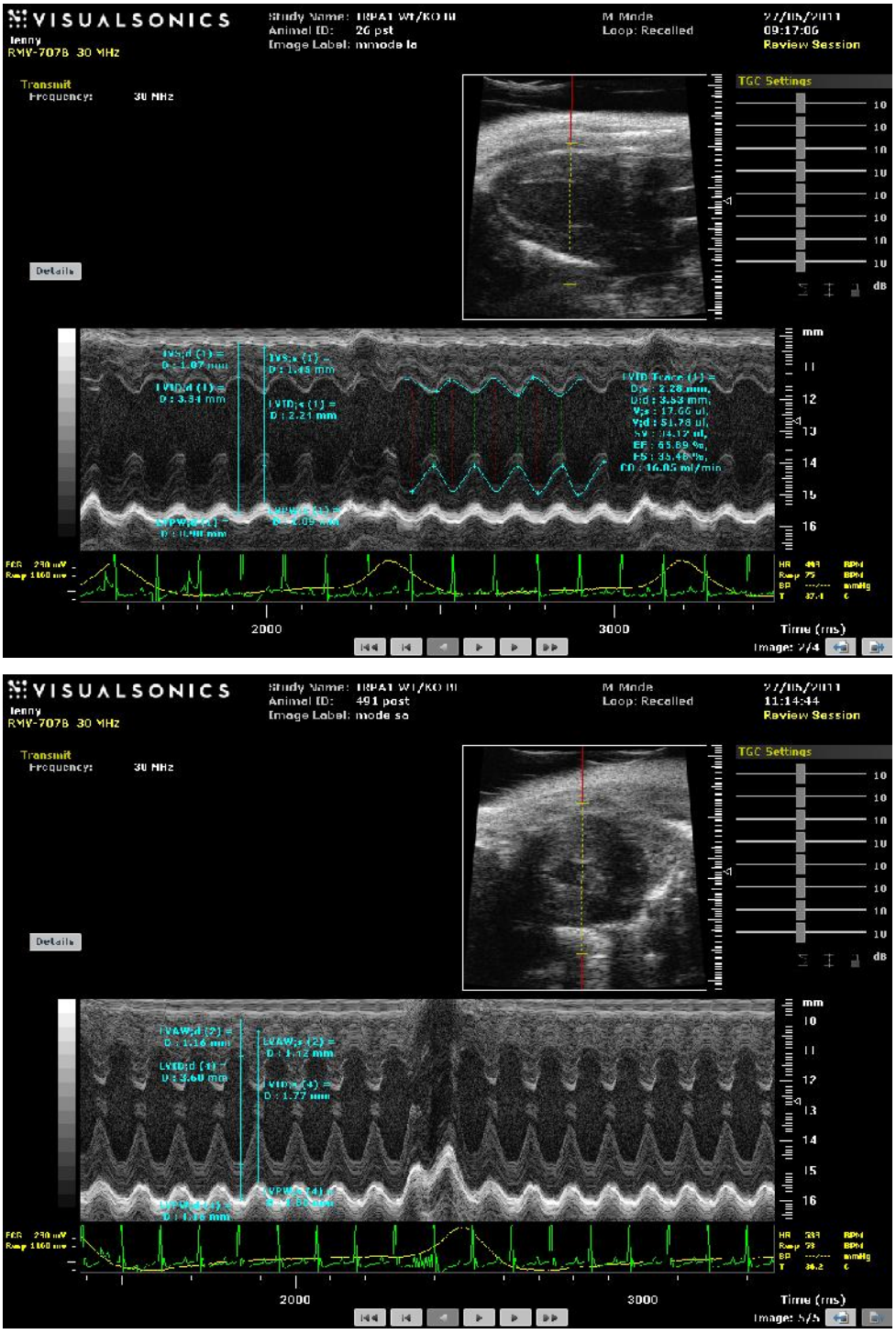

Figure 2.2; Sample m-mode measurements from long axis (top) and short axis (bottom) views. M-modes are collected from the level of the papillary muscle where the heart can be seen at its fullest. For the long axis, this is where the aortic root and heart apex can be seen; the short axis this is at 90˚ to this. Views are representative and depict measurement collection from the movement of the ventricle wall. ECG and breathing rate is also shown along the base of the image, and experiences minimal variation through the collection period.

Cytokine MSD Multiplex ELISA

Plasma and culture medium cytokines were measured using a seven spot multi-plex mouse pro-inflammatory assay kit (Meso-Scale Discovery, Gaithersburg, MD, USA): Levels of IL-6 and KC (the murine analogue of IL-8) were measured from one sample well. Standard manufacturer's instructions were followed and reagents supplied. Results were expressed as pg cytokine per ml of sample, calculated against a supplied standard curve. This assay employs a sandwich immunoassay format, where specific cytokine capture antibodies are pre-fixed on the specific spots on the base of the well. Cytokine levels can be quantified using a cytokine-specific detection antibody labelled with a tag that emits light upon electrochemical stimulation. All detection antibodies exhibit less than 1% cross-reactivity with other analytes.

Plasma CGRP ELISA

Plasma CGRP levels were measured using an ELISA kit (Rat/Mouse, Pheonix Pharmaceuticals Inc, USA). This kit detects 0.16-100ng/ml CGRP. Plasma peptides were extracted using SEP-COLUMN's (Pheonix Pharmeaceuticals Inc, USA) before use in the ELISA kit. All additional reagents were purchased from Pheonic Pharmaceuticals. In this assay, a pre coated plate contained secondary antibodies to a CGRP primary antibody. This antibody was competitively bound by CGRP in the sample/standard or by biotinylated peptides. Where biotinylated peptides were bound, interaction with streptavidin-horseradish peroxidise allowed production of a yellow product from substrate. This yellow colour was directly proportional to the amount of CGRP bound to the primary antibody and thus the concentration found in the extracted plasma sample. Cross-reactivity occurs with all CGRP forms and to some degree with CGRP from other species, but not to closely related peptides such as amylin, calcitonin or somatostatin.

Reverse Transcription Quantitative PCR

Total ribonucleic acid (RNA) was extracted from tissues stored in *RNA later* using a commercial kit (Qiagen® RNeasy Microarray tissue mini Kit). 20-50mg pieces of tissue were used, as per manufacturer's suggestion. This kit extracts RNA of >200 nucleotides using spin columns and their patented phenol-guandine-based *QIAzol* Lysis Reagent. Tissues were homogenised at 300Hz for 2 minutes using 5mm stainless steel beads (Qiagen®) and Qiagen's TissueLyser® LT. The homogenate was then treated with chloroform and the precipitated RNA sequentially purified and eluted using the supplied reagents and spin columns. RNA was eluted in nucleotide free water and stored at -80°C.

RNA quality was assessed using a Nanodrop Spectrophotometer. 1µl of sample was analysed for RNA quantity (ng/µl) and also for contamination, with blank values removed. 260/280 and 260/230 values of around 2 are considered to show pure RNA, a lower value indicates protein contamination or ethanol contamination respectively. Samples with values unusually far from those expected were removed from the population. 500ng of RNA was used for the reverse transcription to cDNA. This was done using a High capacity RNA to cDNA, Reverse Transcription enzyme kit with RNAase inhibitor (Applied Biosciences) and thermal cycler (Applied Biosystems) set to temperatures recommended in the manufacturer's guidelines (37°C 60 minutes., 95°C 5 minutes, cool and hold at 4°C >5minutes). Stock cDNA was then diluted 1:40 for further experiments.

A SYBR-green based PCR mix (Sensi-Mix®, SYBR-green No ROX, Bioline) was made up to halve volumes of manufacturers specification, resulting in 10µl reactions containing 2µl cDNA, 5µl SYBR-green, 1µl of 25µM forward and reverse primers with 2µl RNAse free water. This was prepared and added to 100 well gene discs (Qiagen®) by an automated robot (CAS1200, Corbett Robotics®). These discs then underwent PCR (hold: 10 min at 95^{o}C; cycling: 45 cycles: 10 s at 95^{o}C, 15 s at 57^{o}C and 5 s

at 72°C; melt: 68-90°C) in a Corbett Rotorgene, which monitors copy numbers via fluorescence. SYBR-green is a dye which intercalates with double stranded DNA, absorbing blue light and emitting fluorescent green light during the amplification as an index of copy numbers. Raw data was analysed using the rotorgene 6000 series software and collected as an output of copies/µl. It was then standardised against three housekeeping genes using GeNorm software (Vandesompele *et al.*, 2002). These were murine Phospholipase A_2 ($mPLA_2$), Actin and Glyceraldehyde 3-phosphate dehydrogenase (GAPDH). The GeNorm program calculates a normalisation factor from the geometric mean of the three housekeeping genes. Housekeeping gene expression stability is ensured by a calculated M value. All genes showed M values in the usable range (<1.5), showing they were not altered by experimental conditions, therefore represent good housekeeping genes.

RT qPCR Primers

RT qPCR primers were desalted and unmodified, purchased from Sigma, UK. The sequences are shown in table 2.1. They were re-suspended in nucleotide free water for use. These oligos were used with a pool of septic and hypertensive mouse cDNA to create a standard curve.

	Accession Number	Forward Sequence	Reverse Sequence	Amplicon Size
TRPV1	NM_001001445.1	CAACAAGAAGGGGCTTACACC	TCTGGAGAATGTAGGCCAAGAC	83
TRPA1	NM_177781.4	AGGTGATTTTTAAAACATTGCTGAG	CTCGATAATTGATGTCTCCTAGCAT	168
MCP-1	NM_011333.3	ACTGAAGCCAGCTCTCTCTTCCTC	TTCCTTCTTGGGGTCAGCACAGAC	274
SOD	NC_000082.5	CTGGACAAACCTGAGCCCTA	GATAGCCTCCAGCAACTCTCC	61
HO-1	NC_000074.5	GGTCAGGTGTCCAGAGAAGG	CTTCCAGGGCCGTGTAGATA	70
NOX-2	NM_007807.2	TGCCAACTTCCTCAGCTACA	GTGCACAGCAAAGTGATTGG	73
NOX-4	NM_015760.2	GAACCCAAGTTCCAAGCTCA	AAGGCACAAAGGTCCAGAAA	63
IL-6	NM_031168.1	GCTACCAAACTGGATATAATCAGGA	CCAGGTAGCTATGGTACTCCAGAA	78
mPLA$_2$	NC_000070.5	TGGATATAAACCATCTACCA	GGGAAGGGATACCTATGTTCAGA	77
Actin	NM_007393.3	CACAGCTTCTTTGCAGCTCCTT	TCAGGATACCTCTCTTGCTCT	250
GAPDH	NM_008084.2	GGTCATCCCAGAGCTGAACG	TTGCTGTTGAAGTCGCAGGA	210

Table 2.1; Table Of Primer Sequences, Shows forward and reverse primer sequences, in the 5’ to 3’ direction, the accession number and amplicon size.

Mesenteric Artery Wire Myography

First and second-order mesenteric artery branches (approx. 30-40µm diameter at rest, approx. 100µm under tension) were isolated from mixed gender TRPA1 WT and KO mice or CD1 mice, in ice cold Krebs (118mM NaCl, 24mM $NaHCO_3$, 1mM $MgSO_4$, 4mM KCl, 0.5mM NaH_2PO_4, 5.5mM glucose, and 2.5mM $CaCl_2$). They were cleaned of fatty tissue, mounted and normalized to normal peripheral artery tension (13.3kPa) on a wire myograph (DMT 610M or 620) using 0.025 mm tungsten wire, under a light microscope. Vessels were maintained throughout the experiment in 37°C Krebs solution gassed with air/5% CO_2. This gas mixture was chosen to produce a more physiological oxygen tension than obtained when using oxygen only. All salts were bought in their anhydrous forms from Sigma UK, with the exception of NaCl from MP Biomedicals, UK. Tissue viability was tested and peak contraction assessed using 2 minute incubations in 'high K' solution (38mM NaCl, 24mM $NaHCO_3$, 1mM $MgSO_4$, 80mM KCl, 0.5mM NaH_2PO_4, 5.5mM glucose, and 2.5mM $CaCl_2$). Endothelial function was assessed using carbachol (10µM diluted in water, Sigma, UK), where a relaxation of >60% over 2 minutes was used as a positive threshold. This concentration of carbachol was selected as it is commonly used to produce endothelial dependent relaxations of mesenteric arteries, and particularly used for the determination of endothelial function, for instance in Johns *et al* (2007) who similarly use mouse mesenteric arteries in a wire myograph. Average responses to carbachol are included in figure 4.1, demonstrating clear differences in responsiveness, consistent with their classification of holding functional or non-functional endothelium. Tissues were sub-maximally pre-constricted with U46619 (10nM in 5µl water, Biomol, UK). This is a stable agonist of the thromboxane A_2 receptor. Activation of this receptor on smooth muscle cells leads to activation of Gq signalling, producing IP_3 and DAG, both of which lead to intracellular calcium concentration increases from a combination of store release and extracellular influx (Dorn and Becker, 1993). Relaxation to cinnamaldehyde (trans-cinnamaldehyde >95%, Sigma, 3–300 µM in 5µl ethanol) was assessed from single concentrations,

measured after 5 minutes, or from cumulative additions, measured for 3 minutes per concentration. All drugs supplied as <100% purity had their concentration adjusted accordingly. Data was expressed as percentage relaxation of pre-constriction.

For some experiments, additional pharmacological mediators were used. These included further dilutions of U46619 (0.1-300nM in water), phenylephrine (Sigma UK, 0.03-30µM in water), KCl (Sigma UK, producing 10-300mM K^+ in water), SP (Sigma UK, 10nM-1µM in 0.01% BSA/water), CGRP (Sigma UK, 1-100nM in 0.01% BSA/water), the peptide CGRP antagonists $CGRP_{8-37}$ (Sigma, 3µM in 0.01% BSA/water) and BIBN 4096 BS (Gift from Dr H Doods (See Doods *et al.*, 2000), Boehringer, 10µM in 5µl DMSO added 15 minutes before pre-constriction), the larger conductance calcium activated potassium channel (BK_{Ca}) blocker Paxilline (1µM in 5µl DMSO, added to bath 15 minutes before pre-constriction), the TRPA1 antagonists HC-030031 (Pfizer UK, 30µM in 5µl or 10µM in 1.67µl DMSO) and TCS5861528 (Tocris, 30µM in 5µl DMSO), both added 15 minutes before pre-constriction, and a 30mM potassium Krebs (90mM NaCl, 24mM $NaHCO_3$, 1mM $MgSO_4$, 30mM KCl, 0.5mM NaH_2PO_4, 5.5mM glucose, and 2.5mM $CaCl_2$) used as a 3 minute pre-constriction which blocks hyperpolarisation. Vehicle controls were used for each vessel. Rational behind each concentration choice are explained in the text.

Bronchial Ring Wire Myography

Major bronchi were dissected from the airway of CD1 mice under ice cold Krebs solution (composition previously listed). Rings of approximately 2mm were cut and mounted on the wire myograph, using the procedure used for mesenteric arteries. Following a 60 minute rest, baseline tension was set to around 2mN (Manzini, 1992). Several concentrations of carbachol were investigated for contractile ability, with 1µM (in 5ul water) giving a sub-maximal but strong and consistent pre-constriction. This pre-constriction is similar to that used by Manzini (1992) who also investigated

neurogenic dilation of murine bronchi. Cinnamaldehyde shows selectivity to the TRPA1 receptor at low to mid µM concentrations (Bandell *et al*, 2004), therefore several concentrations from 3-300µM were tested, with 60µM showing a sub-maximal but reproducible relaxation of bronchi rings (about 40% over 3 minutes). No previous studies have investigated the dilation effect of cinnamaldehyde on isolated mouse bronchi. In fact, Andre *et al.*, (2008) have previously shown 30µM cinnamaldehyde to induce contraction of the guinea pig bronchi; however in the mouse model I see no evidence of contractile effects. To further demonstrate the presence of epithelium, 1µM SP (5ul in 0.01% BSA in water) was applied for a 3 minutes following cinnamaldehyde application. Similar to that of carbachol, this concentration is commonly found in similar studies in published literature e.g. Szarek *et al.*, (1998), where a relaxation response indicates the presence of intact, functional epithelium. In between each contraction peak, tissues were washed three times with Krebs and allowed to rest for at least 10 minutes.

For some experiments additional pharmacological antagonists were added to the bath 15 minutes before pre-constriction. These included HC-030031 (50 and 100µM in 0.05% DMSO in Krebs), AP-18 (100µM in 0.1% DMSO in Krebs) and SR140333 (1µM in 5ul water). These antagonists are used at similar concentrations to published studies (Zhou *et al* (2011), Yu and Ouyang (2008), Andre *et al* (2008) Cao *et al*, (2012), Nassini *et al* (2012) Taylor-Clark *et al* (2008)), with 100µM HC-030031 being double the concentration reported to inhibit TRPA1 induced bronchi contractions (Andre *et al*, 2008).

Cerebral And Pulmonary Artery Wire Myography

Middle cerebral, cerebellar and pulmonary arteries were dissected from male Wistar rats (300-400g) under ice cold Krebs solution (composition previously listed). Sections were mounted on the wire myograph using the procedure used for mesenteric arteries. Following a 60 minute rest, baseline tension was set using the normalisation module of the LabChart

software so that it was similar to the pressure experienced *in vivo* (9 kPa for cerebral arteries, 2 kPa for pulmonary arteries). Tissue viability and peak contraction were assessed using three sets of 2 minute incubations in 'high K' solution (previously defined composition). Cumulative concentration curves to the contractile agents U46619 (0.1-1µM in 1-5µl water) and phenylephrine (0.03-10nM in 1-5µl water) were than collected with additions every 2 minutes, to establish optimal pre-constriction. Change in tension was recorded as raw values (mN) or normalised to maximal tension obtained during 2 minute incubations with 80mM potassium Krebs. Subsequently, 30nM and 100nM U46619 (for 5 minutes) were used to pre-constrict cerebral and pulmonary arteries respectively. Endothelial function was assessed using carbachol (10µM in 5µl water, Sigma, UK), where a relaxation from pre-constriction of >60% over 2 minutes was used as a positive threshold.

Following U46619 pre-constriction, cumulative concentration curves to cinnamaldehyde (3-300µM) and MO (1-100µM), with additions every 3 minutes, were used to reveal the effect of TRPA1 on these tissues. Relaxation is presented as % of U46619 pre-constriction tension. In some studies, pre-constriction was followed by a single application of 300µM cinnamaldehyde or vehicle (5µl ethanol), added for 3 minutes. This was also completed in the presence of HC-030031 (10-100µM in 0.05% DMSO in Krebs) or vehicle, added 15 minutes before pre-constriction. The concentrations of HC-030031 selected are in-keeping or above those using similar tissues in published studies (Taylor-Clark *et al* (2008), Earley *et al* (2009)).

Macrophage Cultures

Peritonitis was elicited by 1ml i.p injection of 1% oysterglycogen (Sigma, UK) in TRPA1 WT and KO mice under isoflurane. After 18 hours, mice were terminated by careful cervical dislocation. Cells were collected by peritoneal lavage using a 22G needle (BD Biosciences) into cold D-PBS (No Ca^{2+}/Mg^{2+}, Invitrogen). Live cells diluted 1/5 in Trypan Blue (Sigma,

UK) were counted using a Neubauer chamber at 20x magnification on a microscope. The remaining cells were centrifuged to a pellet (15min, 4°C, 2000 rpm) and re-suspended in culture medium in a culture hood, at a concentration of 2 x 10^6 cells per ml. Medium was Dulbecco's Modified Eagle Medium (DMEM, No glutamine, PAA, Austria) with added 10% fetal bovine serum, glutamine (2mM), 1x pencillin and streptomycin (all PAA, Austria). 0.6 x 10^6 cells in 300µl of medium was plated in to 8 well culture slides (BD Biosciences) and incubated in a cell culture incubator for 2 hours to allow cells to adhere. Finally, the culture slide was washed twice with 300µl medium, leaving 100µl covering the slide and adherent cells.

Wells were then treated with Ang II (1µM final bath concentration with medium vehicle) or control vehicle addition, and left for 8,12,18 or 24 hours in the incubator. At the end of this time, culture medium was collected for cytokine analysis and the adherent cells stained on the slide using QuickDiff (Gamidor, UK) a form of Romanowski stain. Macrophage phenotype was defined by imaging under oil immersion microscopy (100x).

Data Analysis

Data was analysed in Microsoft Excel and Graphpad Prism 5, expressed as mean +/- the standard error of the mean where N>2. In the case of small N numbers (3-5), the error of the mean is a predictive value to illustrate data variation only. All data sets were tested for normality using the Shapiro-Wilks test. Where they conformed to a Gaussian distribution, data was subsequently analysed with parametric tests. For two group data sets, analysis by paired or unpaired t-test was used. This was paired where both data sets were collected from the same mouse. One-tailed analysis was used where the hypothesis was to test for changes in a single direction. Two-tailed analysis was used where potential for changes in either direction existed. For data with multiple sets, one-way ANOVA with Bonferroni's post-test was chosen. For time courses, two-way ANOVA with Bonferroni's post test was used. Statistical significance was assumed

where $p<0.05$. In some graphs with multiple data sets, clear trends were not significant in ANOVA tests. This was generally due to low N numbers in one or more of the groups. Where comparisons were important for data interpretation, a single unpaired t-test was additionally used. This was generally in conditions of low numbers of control animals, comparing two treated groups of higher N.

Where data showed divergence from Gaussian distribution, non-parametric tests were used. 'SEM' is shown for these groups to allow illustration of data variability in a similar manner throughout the thesis. For graphs of two data sets the Mann-Whitney U test was used, for multiple data sets the Kruskall-Wallis test with Dunn's post test was used. Similarly, statistical significance was assumed where $p<0.05$. In practice, non-Gaussian data was seen for measures of activity and the cytokines IL-6 and mIL-8 only.

Chapter 3 – Investigating the role of TRPA1 in basal cardiovascular hemodynamics

Introduction

The TRPA1 receptor was first identified and characterised over 10 years ago (Jaquemar *et al.*, 1999, Story *et al.*, 2003). It was quickly identified as a potentially interesting cation channel, with publications linking it to several sensory functions. In 2006, two sets of KO mice were created and published simultaneously. One of these mice were from the Bautista group (Bautista *et al.*, 2006), the other by the Kwan group (Kwan *et al.*, 2006). Many groups have now used these mice to show an important role for TRPA1 in pain and inflammation. Few have investigated vascular implications of TRPA1 activation. Our group maintain a colony of TRPA1 WT and KO mice derived from those by Kwan KO (Kwan *et al.*, 2006). This is our preferred KO strain as expression of the remaining receptor portion is limited by addition of an endoplasmic reticulum retention signal. No fundamental differences between the KO strains have been reported, however using these mice removes the unlikely possibility that a portion of the receptor may remain to be expressed on the cell surface. Although this protein is unlikely to show signalling activity itself, it could still potentially interact and modulate the activity of other membrane receptors and components. I aim to use these mice to characterise the cardiovascular phenotype associated with global TRPA1 deletion *in vivo*. Further discussion of TRPA1 KO strains is provided in the introduction.

TRPA1 KO mouse lines and commercially developed antagonists clearly demonstrate that TRPA1 is important for sensing noxious and potentially noxious compounds. Many noxious compounds have cardiovascular effects. TRPA1 is primarily expressed on sensory neurones, but has also been found in other neuronal and non-neuronal locations, some of which may be relevant to cardiovascular regulation control, for example vagal neurones (Nassenstein *et al.*, 2008) and endothelial cells (Earley *et al.*, 2009). There is also evidence that TRPA1 is involved in the

pathophysiology of a number of clinical diseases, particularly of the airway, bladder and joint. All of the identified diseases are linked to sensory neurone activity, largely in relation to pain and inflammation. If TRPA1 antagonists are to be further developed for clinical use, it will be important to investigate the role of TRPA1 in the cardiovascular system and investigate the contribution of non-neuronal expression to physiological processes.

Currently, several studies have investigated the vasodilatory properties of proposed TRPA1 agonists. These have been introduced in chapter 1 and will be discussed further in chapter 4, however the mechanisms attributed are often based upon neuropeptide release (see table 1.1). The studies support a role for TRPA1 in regulating local vascular tone, which could lead to changes in blood pressure via a change in peripheral resistance.

Although very few studies have investigated the systemic cardiovascular effects of TRPA1 activation, cinnamaldehyde is the most well used TRPA1 agonist *in vivo*. Similarly to the actions of intra-vascular capsaicin acting on TRPV1 receptors; intra-luminally applied TRPA1 agonists can also trigger central reflexes and alter blood pressure. Although these responses have not been characterised to the degree of those to capsaicin, intra-arterial cinnamaldehyde application to rats (Yuan *et al.*, 1992) and guinea pigs causes a drop in blood pressure via increases in peripheral blood vessel diameter (Harada *et al.*, 1975). This was shown to have a central reflex component in a recent publication from our group, where i.v. cinnamaldehyde caused a drop in blood pressure and heart rate, followed by a pressor response and tachycardia, both of which were reduced in TRPA1 KO mice. Use of the pharmacological agents prazosin and atropine, which are adrenergic and cholinergic antagonists respectively, revealed that the TRPA1 mediated response to cinnamaldehyde comprised an autonomic mediated vaso-vagal mechanism (Pozsgai *et al.*, 2010). Additionally, in isolated hearts cinnamaldehyde has shown positive chronotropic and inotropic actions, leading to arrhythmias at high concentrations (Harada *et al.*, 1975). This was shown to be mediated by

catecholamine release acting on beta adrenergic receptors (Harada and Saito, 1978). The source of catecholamine release is thought to be the adrenal gland (Harada and Saito, 1978). Evidence of increased sympathetic outflow following TRPA1 activation is also supported by a recent study using genetically hypertensive rats, where sympathetic mediated arrhythmias were observed on inhalation of diesel fumes, and shown to be TRPA1 dependent (Hazari *et al.*, 2011).

Summary Of The Background

TRPA1 KO mice have provided a valuable research tool to investigate TRPA1 mediated responses. To date, they have proven the importance of neuronally expressed TRPA1 in inflammatory diseases linked to neurogenic inflammation. However, the role of non-neuronally expressed TRPA1 has yet to be investigated. Previous studies have shown the ability of the TRPA1 agonist cinnamaldehyde, which is well characterised and can be dosed *in vivo*, to influence the heart and alter cardiovascular regulatory systems. More recently, there have been an increasing number of papers describing the vasodilatory nature of various TRPA1 agonists. As there is growing industrial interest in developing TRPA1 antagonists for clinical use, it is now timely to investigate the potential role for TRPA1 to influence cardiovascular regulation. Therefore I have used WT and KO mice to investigate the phenotype created when TRPA1 has been globally deleted.

Aims

- To confirm the genotype of the TRPA1 WT and KO mouse colony
- To investigate basal characteristics of TRPA1 WT and KO mice in terms of body weight, activity, heart weight, left ventricle size, heart function and blood pressure; also considering the effect of gender.

Results

Confirming The Genotype Of The TRPA1 Mice

TRPA1 WT and KO mice were genotyped by ear punching before weaning. This was done according to the method stated in the materials and methods section, using primers recommended in Kwan *et al* (2006). Figure 3.1 shows a representative image, created using tail tip tissue, showing how the genotype of mice can be determined. In most cases, the mice were bred from heterozygous matings, leading to litters containing a range of genotypes. This allowed littermate pairings to be created for the majority of studies.

Investigating The Basal Characteristics Of TRPA1 WT And KO Mouse Hearts Using Echocardiography

Mice aged 2.5 to 3 months were assessed for their body weight and left ventricular size under light isoflurane anaesthesia. Body weight was similar between WT and KO mice, and did not vary significantly between genders (WT F 22.5g, M 29g, KO F 26.6g, M 27.5g). However there was a tendency for males to be of larger mass. They are presented as pooled data in figure 3.2, with an average of 24-25g. This graph provides a snapshot of comparable animals, thus does not preclude against weight differences at other ages. However, it is important when comparing heart sizes that the mice are as similar in size as possible. With this in mind, all echocardiographical measures are presented as a ratio to body weight, eliminating it as a confounding variable.

Echocardiography is one of the most accurate methods of obtaining *in vivo* left ventricular morphology and functional data from mice. Method of collection and parameters measured are explained in chapter 2. A complete examination was performed on 27 TRPA1 WT and 29 TRPA1 KO mice of 2.5-3 months of age. Many of these mice were littermate pairs. Figure 3.3 shows average morphological characteristics of the left

ventricle. No differences were seen in any of the left ventricle wall thicknesses, or in total left ventricle mass of either group. These mice were later used in a hypertrophy study (Chapter 5), therefore these measures could not be confirmed by necropsy at this point. However, previous publications have demonstrated good correlations between necropsy heart weight and left ventricle size calculated by echocardiography (Stypmann *et al.*, 2006). Table 3.1 is a table showing the average values separated by gender.

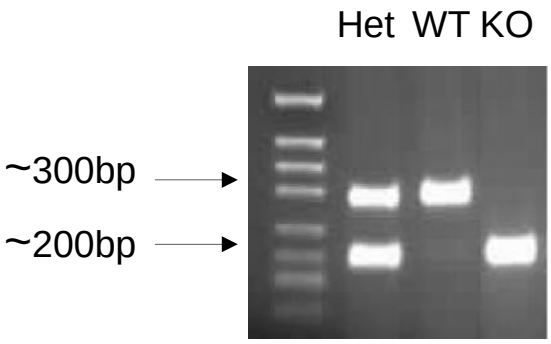

Figure 3.1 Genotype Determination Of TRPA1 Colony Mice By Endpoint PCR. Results show products of endpoint PCR from tail tip samples extracted using the Sigma ExtractRED-N-Amp tissue PCR kit, run on a 1.8% agarose gel with pBS/Hpa II ladder. Image is taken under UV light. The WT band runs at ~310 bp, whereas the KO band runs at about ~200bp. Heterozygous mice show both the WT and KO band.

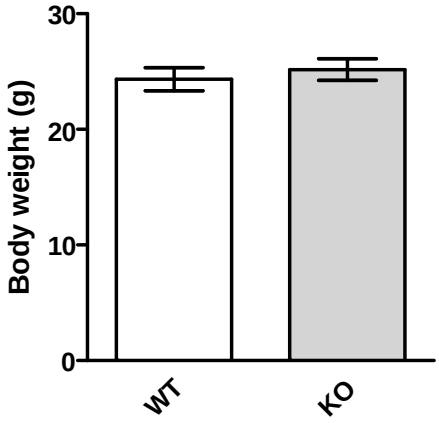

Figure 3.2 Body Weight Of Paired, Littermate, TRPA1 WT And KO Mice. Results show naive male and female pairs of mice, weighed at 2.5-3 months of age. N=27 pairs, 16 Female, 11 Male. Not significantly different in a unpaired, two way t-test.

Although there are no statistical differences between mice of the same gender, but different genotypes; there are consistent differences seen between same genotype mice of different genders. Female mice of both genotypes showed significantly larger hearts, with thicker walls, for all measures, except for LVPW width, which did not reach significance. This may be due to slight differences in body weight between genders, as given above.

Figure 3.4 shows heart function measured in the same WT and KO mice as the morphological data. As described in the materials and methods section, fractional shortening is the most commonly used measure of left ventricular contractility, and is related to both ejection fraction and stroke volume. All measures of left ventricular emptying showed similar heart function in both genotypes. Cardiac output is based on calculations of heart ejection volume and heart rate, simultaneously measured by ECG. In this experiment, heart rates are controlled between 400 and 500 beats per minute to provide comparable measurements of heart function. Aortic peak flow shows the velocity of blood leaving the aortic root, and is therefore an indicator of systolic function. In line with the previously presented data, heart contractility and output were similar in mixed gender groups of paired TRPA1 WT and KO mice.

A table containing averages split by gender is shown in table 3.2. No statistical differences were seen between WT and KO averages collected from mice of the same gender. However, significant differences were seen in measures of stroke volume, cardiac output and peak aortic flow between male and female groups of the same genotype. These may all be due to the significant differences in stroke volume, which will in turn affect cardiac output and peak aortic flow. The data shows smaller stroke volume in females, but as heart rate was controlled during the experiment, cardiac output is also lower. The reasons for this are not related to left ventricle size differences, where my data shows females to have larger heart mass, likely due to thicker heart walls, contradicting most data from humans and animal models where male hearts are bigger with thicker walls (Baumann

et al., 2008, Huxley, 2007). Larger hearts would be expected to produce larger stroke volumes. These findings also differs from those of Stypmann *et al* (2006), who show left ventricle size and left ventricle function do not change significantly with gender in CD1 mice. These partially agree with data presented in a review by Huxley (2007), showing human females to have smaller stroke volume, but similar cardiac output due to a higher heart rate. However, female hearts were also of smaller mass.

Summary 1; Body Weight, Heart Size And Function In TRPA1 WT And KO Mice.

- Age matched TRPA1 WT and KO mice do not differ significantly in terms of body weight.
- TRPA1 WT and KO mice do not significantly differ in terms of heart size or function.
- Female mice displayed significantly bigger hearts with thicker walls than male mice. However, this corresponded with decreased stroke volume, cardiac output and peak aortic flow.

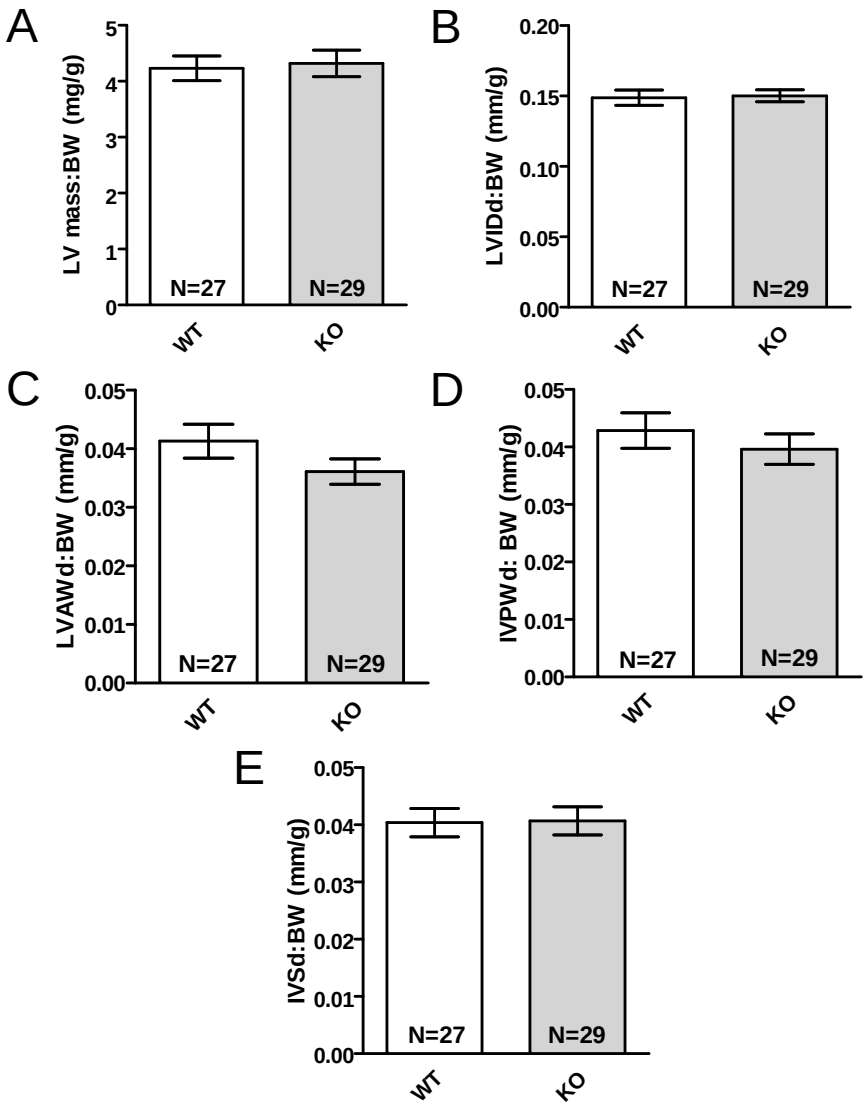

Figure 3.3 Baseline Left Ventricle Physical Parameters In TRPA1 WT And KO Mice Measured By Echocardiography. Result show A. calculated left ventricle mass as a ratio to body weight (BW). B. left ventricular internal diameter at diastole as a ratio to BW (LVIDd:BW). C. left ventricular anterior wall thickness at diastole, as a ratio to BW (LVAWd:BW). D. left ventricular posterior wall thickness at diastole, as a ratio to BW (LVPWd:BW) E. interventricular septum thickness at diastole, as a ratio to BW (IVSd:BW). All graphs show mixed gender mice. No significance in an unpaired, two tailed t-test.

	Mixed		Male		Female	
	WT	KO	WT	KO	WT	KO
LV mass:BW (mg/g)	4.23 +/- 0.22	4.32 +/- 0.24	3.37 +/- 0.20 ****	3.74 +/- 0.31 *	4.83 +/- 0.26	4.78 +/- 0.31
LVIDd:BW (mm/g)	0.15 +/- 0.005	0.15 +/- 0.004	0.13 +/- 0.006 **	0.14 +/- 0.006 *	0.16 +/- 0.007	0.16 +/- 0.005
LVAWd:BW (mm/g)	0.04 +/- 0.003	0.04 +/- 0.002	0.03 +/- 0.002 ****	0.03 +/- 0.002 *	0.05 +/- 0.003	0.04 +/- 0.003
LVPWd:BW (mm/g)	0.04 +/- 0.003	0.04 +/- 0.003	0.03 +/- 0.001 ***	0.03 +/- 0.003	0.05 +/- 0.004	0.04 +/- 0.004
IVSd:BW (mm/g)	0.04 +/- 0.002	0.04 +/- 0.002	0.03 +/- 0.003 ****	0.03 +/- 0.003 ***	0.05 +/- 0.002	0.05 +/- 0.003

Table 3.1 Baseline Left Ventricle Physical Parameters In TRPA1 WT And KO Mice, Measured By Echocardiography and split by gender. Results show A. calculated left ventricle mass as a ratio to body weight (BW). B. left ventricular internal diameter at diastole as a ratio to BW (LVIDd:BW). C. left ventricular anterior wall thickness at diastole, as a ratio to BW (LVAWd:BW). D. left ventricular posterior wall thickness at diastole, as a ratio to BW (LVPWd:BW) E. interventricular septum thickness at diastole, as a ratio to BW (IVSd:BW). Table shows average values from 11 male WT and 11 male KO mice, 16 WT female mice and 18 KO female mice. Statistics are compared to female equivalent in an unpaired, two tailed t-test. *$p<0.05$, **$p<0.01$, ***$p<0.001$, ****$p<0.0001$.

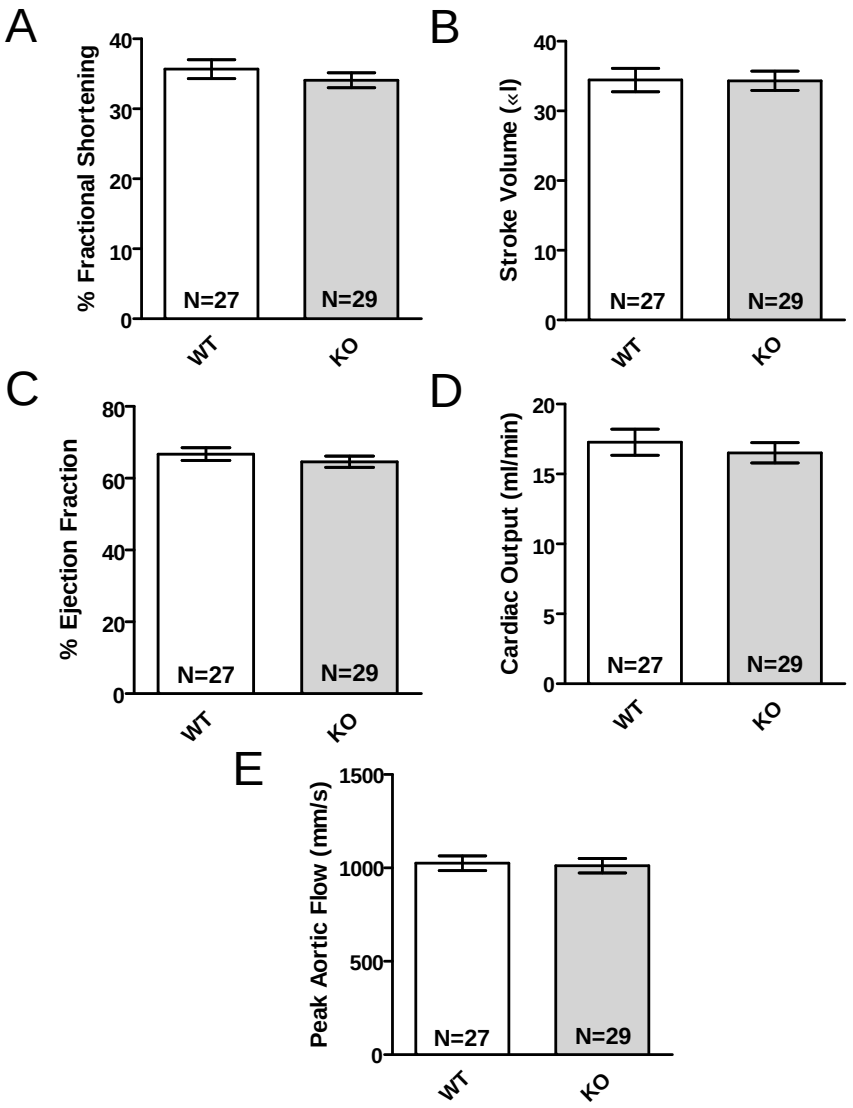

Figure 3.4 Baseline Heart Function In TRPA1 WT And KO Mice Measured By Echocardiography And Aortic Arch Doppler. Results show A. percentage fractional shortening. B. stroke volume in microlitres. C. percentage ejection fraction. D. cardiac output in millilitres per minute. E. peak aortic flow rate in mm/seconds. All graphs show male and female mice. Not significantly different in an unpaired, two tailed t-test.

	Mixed		Male		Female	
	WT	KO	WT	KO	WT	KO
Fractional shortening (%)	35.7 +/- 1.36	34.1 +/- 1.07	38.7 +/- 1.93	35.4 +/- 1.45	35.3 +/- 1.98	34.7 +/- 1.63
Stroke Volume (µl)	34.4 +/- 1.68	34.3 +/- 1.38	40.4 +/- 1.96 **	41.0 +/- 2.11 **	30.4 +/- 1.95	31.7 +/- 1.79
Ejection Fraction (%)	66.7 +/- 1.76	64.6 +/- 1.57	69.3 +/- 2.38	65.1 +/- 2.04	65.0 +/- 2.43	64.3 +/- 2.25
Cardiac Output (ml/min)	17.3 +/- 0.93	16.5 +/- 0.72	19.9 +/- 1.30 *	20.7 +/- 1.49 **	15.5 +/- 1.10	15.0 +/- 0.88
Peak Aortic Flow (mm/s)	1025 +/- 39.6	1012 +/- 38.7	1101 +/- 53.6	1200 +/- 70.0 **	970 +/- 53.3	936 +/- 47.8

Table 3.2 Baseline Heart Function In TRPA1 WT And KO Mice Measured By Echocardiography And Aortic Arch Doppler, Split By Gender. Results show A. percentage fractional shortening. B. stroke volume in microlitres. C. percentage ejection fraction. D. cardiac output in millilitres per minute. E. peak aortic flow rate in mm/seconds. Table shows average of 11 WT and 11 KO male mice and 16 WT and 18 KO female mice. Statistics are compared to female equivalent in an unpaired, two tailed t-test. *p,0.05, **p<0.01.

Investigating The Basal Blood Pressure Of TRPA1 WT And KO Mice Using Tail Cuff Plethysmography And Radiotelemetry

The basal blood pressure of WT and KO mice was initially established using tail cuff plethysmography. Several batches of mice were needed to collect a large enough data set, however the process was kept as similar as possible for each, as described in the materials and methods section. Figure 3.5 shows average systolic, mean and diastolic for TRPA1 WT and KO mice. This figure also contains the data split by gender (3.5B/C). Statistical analysis showed that KO mice had a significantly lower blood pressure, in terms of all parameters, compared to WT mice. This significance remained in the female group when the data was split, however the difference in the male group was smaller and did not reach statistical significance. Figure 3.6 shows the average mean blood pressure, measured by tail cuff in young mice at different ages (8-14 weeks). This data is taken from daily training readings and shows that the KO mice displayed a consistently hypotensive phenotype from a young age, suggesting that it is an inherent part of their phenotype and not developed with age. The consistency of the reading over time also suggests that the mice quickly became well trained using the method and gave reproducible measurements.

Different sets of mice were fitted with radiotelemetry devices, measuring central blood pressure and heart rate from the aortic arch. These have been introduced in chapter 2. Use of telemetry devices in cardiovascular research has been widely validated, particularly in reviews by Kramer (Kramer *et al.*, 2000, Kramer and Kinter, 2003, Kramer *et al.*, 2001).

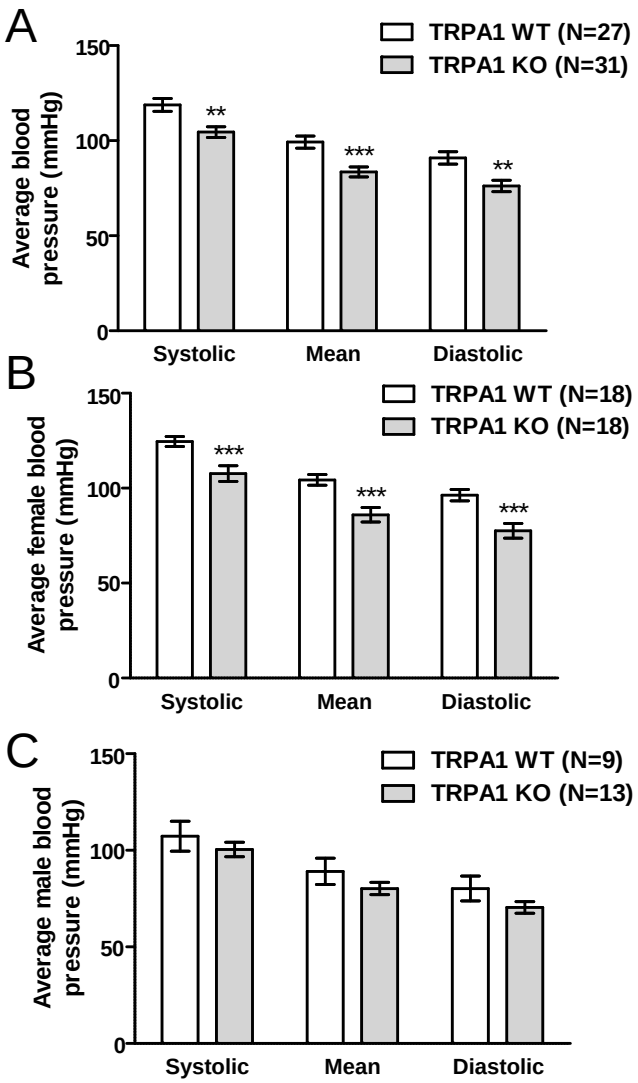

Figure 3.5 Average Baseline Blood Pressures In TRPA1 WT And KO Mice Measured By Tail Cuff Plethysmography. Results show A. average blood pressure in mixed gender mice. B. female only. C. male only. N= number of mice. Statistics are from an unpaired, two tailed t-test compared to WT, **p<0.01, ***p<0.001.

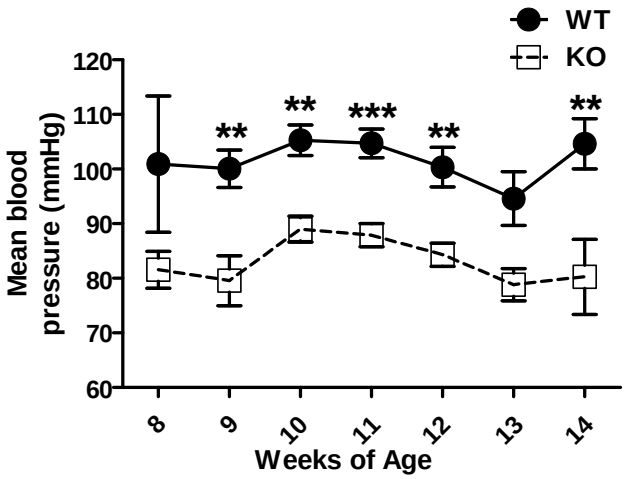

Figure 3.6 Baseline Mean Blood Pressure Measured By Tail Cuff Plethysmography Between 8 And 14 Weeks Of Age In TRPA1 WT And KO Mice. Results show mixed gender mice. N=27 WT and 31 KO mice. Data presented as an average from N= 4-72 readings per week. (N from from week 8 to 14, WT: 5, 41, 63, 56, 45, 22, 14, KO: 4, 25, 46, 72, 62, 35, 35). Average of all readings from the same mouse shown as N=1 on previous graph. Statistics are two way ANOVA with Bonferroni's post-test, **p<0.01, ***p<0.001.

Figure 3.7 shows basal blood pressure, heart rate and activity levels for mixed gender TRPA1 WT and KO mice, measured by telemetry and plotted at half hourly intervals over one day. This data was collected over days' 10-13 post implantation, and averaged to give a more accurate 24 hour profile. Recovery from the procedure was measured by lack of pain behaviours, good healing and increasing daily body mass measurements. Seven to ten days post surgery is generally considered an adequate recovery time from the experiences of other groups who do similar telemetry surgery and is often used in publications. TRPA1 WT and KO mice displayed similar profiles of blood pressure. This also applied to heart rate and pulse pressure. Through all these graphs, TRPA1 KO mice appeared to have consistently higher readings. These were never statistically different at any time interval, but when the whole profile is compared with a two-tailed unpaired t-test, TRPA1 WT and KO profiles were significantly different in terms of systolic and mean blood pressure, and pulse pressure.

Figure 3.9 F shows activity levels. Again, the profile is similar between the TRPA1 WT and KO mice; however there is a higher nocturnal activity peak in KO mice. This was not significant at any half hourly interval, but showed significance in a Mann-Whitney U test, a non parametric form of t-test comparing the whole 24 profile. A non-parametric test was chosen as TRPA1 KO data did not fit a Gaussian distribution. Overall, there was a general trend of increased activity in the KO mice.

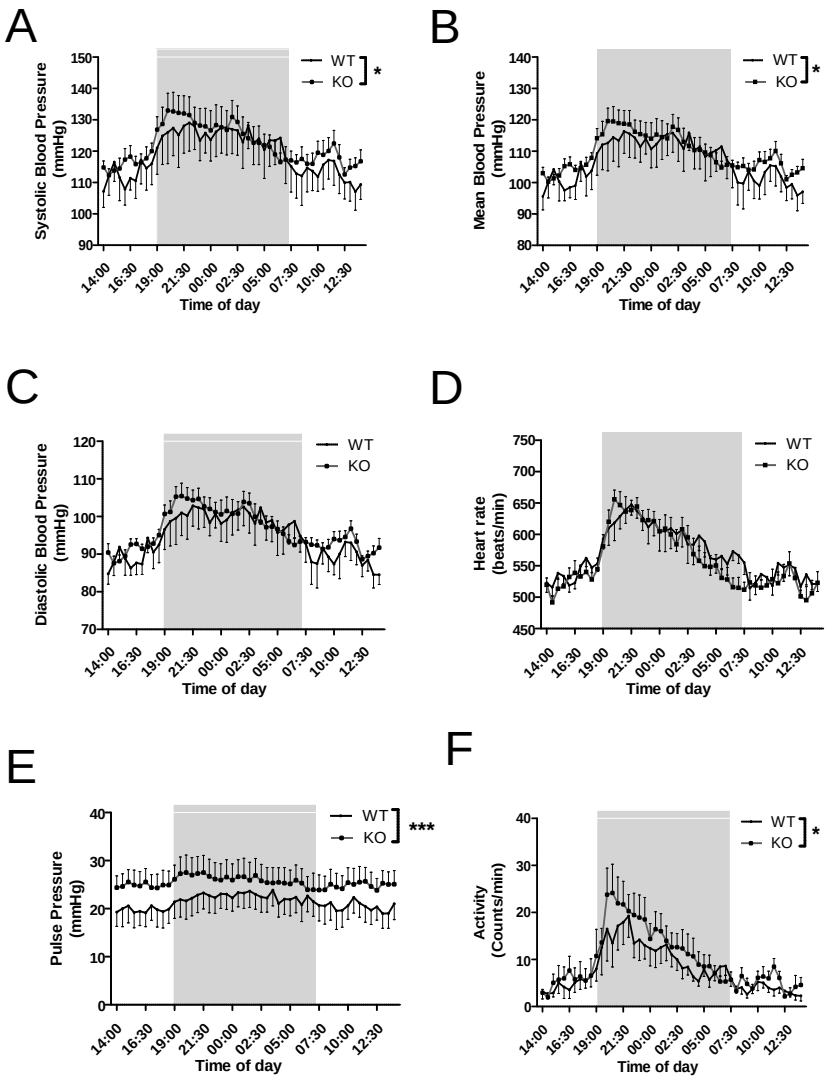

Figure 3.7 Baseline 24 Hour Hemodynamic And Activity Profiles Of Mixed Gender TRPA1 WT And KO Mice, Measured By Telemetry. Results show average profile of weekend days 10-13 after implantation of telemetry probe PA-C10 with aortic arch placed catheter. Mice experience a 12/12hr light/dark cycle, with the dark cycle shown in the shaded area. Data shown as half hourly averages. A. Systolic blood pressure. B. Mean blood pressure. C. Diastolic blood pressure. D. Heart rate. E. Pulse pressure. F. Spontaneous activity. Graphs show data from mixed gender mice. N=7 WT and 10 KO mice in A-D, N=9 WT and 10 KO for E-F. Statistics in graphs A-E are from a two tailed unpaired t-test of the whole profile, WT compared with KO. *$p<0.05$, ***$p<0.001$, or in the case of activity (F), which has a non-Gaussian distribution, a two tailed Mann-Whitney U test *$P<0.05$.

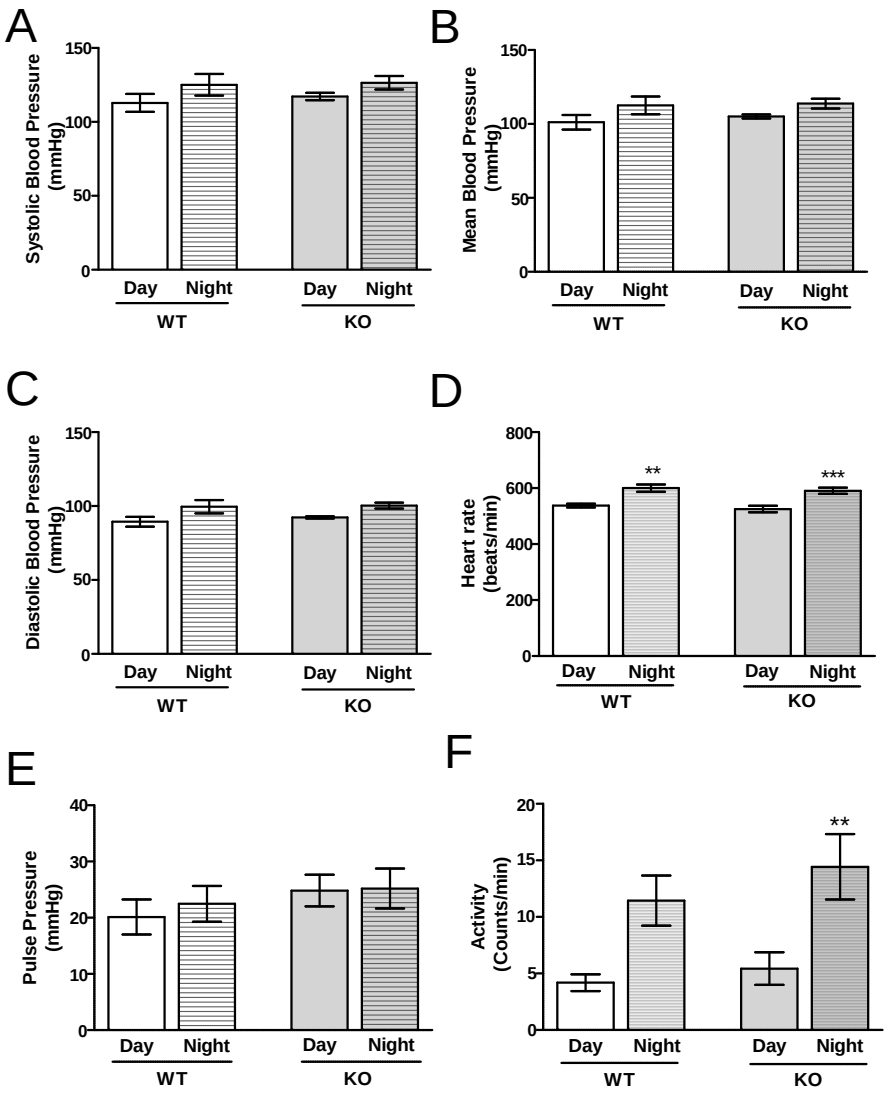

Figure 3.8 Baseline Day/Night Hemodynamic And Activity Averages From Mixed Gender TRPA1 WT And KO Mice, Measured By Telemetry. Results show averages of 12 hour day time and 12 hour night time readings taken during weekend days 10-13 after implantation of telemetry probe PA-C10, with aortic arch placed catheter. 24 hour profiles shown on previous graph. A. Systolic blood pressure. B. Mean blood pressure. C. Diastolic blood pressure. D. Heart rate. E. Pulse pressure. F. Spontaneous activity. Graphs show data from mixed gender mice. N=7 WT and 10 KO mice in A-D, N=9 WT and 10 KO for E-F. One way ANOVA with Bonferroni's post test completed on A-E, day time compared with daytime **p<0.01, ***p<0.001. Activity has a non Gaussian distribution, so statistics are from a non parametric test, the Kruskall-Wallis test with Dunn's post test, **p<0.01 compared to daytime.

The 24 hour profiles clearly show both sets of mice to express diurnal variations in all parameters. Mice were more active, with higher blood pressures and heart rate during the night, consistent with them being nocturnal mammals. Figure 3.8 shows day time and night time averages from each of the profiles shown in figure 3.7. These graphs show the magnitude of the diurnal variations is similar between WT and KO animals. Increased nocturnal blood pressures and pulse pressures were seen, mirroring that seen in the profiles, however these were not significant in an ANOVA analysis. On the other hand, both TRPA1 WT and KO mice showed significant increases in heart rate during the night time. This was in line with an increase in activity.

Activity levels were analysed with a non-parametric test, namely the Kruskall-Wallis test with Dunn's post-test, a non-parametric form of ANOVA. Increased nocturnal activity counts were seen in both groups, increasing to 3-4 times daytime averages, which was significant in KO mice.

As there is potential for differences to occur between gender, the baseline telemetry profiles were also split to show females and males separately. This is shown in figure 3.9 and 3.10 respectively. Profiles accurately reflect diurnal patterns seen when the data sets are combined. Female mice also reflected the outcome of mixed gender profiles, showing KO mice to give significantly higher systolic and mean blood pressures, pulse pressures and activity readings over the 24 hours, being statistically different in a two-tailed unpaired t-test, or Mann-Whitney U test in the case of activity. Again, these values were not statistically significant at any half hourly interval when tested by ANOVA. When plotted alone, male mice gave an opposing pattern, with WT mice giving significantly higher systolic, mean and diastolic blood pressure readings, heart rate and pulse pressure, when profiles are compared by two-tailed unpaired t-test. This may indicate sex specific characteristics, however, conclusions drawn from this separated data should be considered with care due to low mice numbers.

Summary 2; Blood Pressure And Heart Rate Phenotype Of TRPA1 WT And KO Mice Using Tail Cuff Plethysmography And Telemetry.

- Tail cuff plethysmography gave consistent blood pressure readings after mouse training. Using this technique, TRPA1 KO mice displayed a significant hypotensive phenotype compared to WT mice, which was apparent from our first measurements at 8 weeks of age and appeared consistently over the experimental period.
- Telemetered TRPA1 WT and KO mice produced similar diurnal rhythms, but blood pressure parameters were significantly higher in TRPA1 KO mice over 24 hours. These were not significantly different when averaged into daily and nightly readings.

Voluntary Wheel Running In TRPA1 WT And KO Mice

Telemetry data suggested a hyperactivity phenotype in telemetered TRPA1 KO mice. Therefore, I compared daily wheel running distance in pairs of TRPA1 WT and KO mice. See chapter 2 for measurement method. This is shown in figure 3.11 where mice were trained for three weeks with a wheel in their home cage, then measured in pairs for one week. Adding wheels is common for cage enrichment, but has also been used by several studies to investigate the physiological and psychological effects of exercise. For example, a 4 week wheel placement is used by Eisele *et al* (2008) to show that exercise increases mitochondria content in cardiomyocytes, but does not alter left ventricle morphology. This change may be beneficial for the performance of the heart. In my study, mice were naïve and were not used for other measures in this thesis, therefore I did not measure their heart size. Results from wheel running measurements mirrored the findings from telemetry, where KO mice ran significantly further each night than WT pairs. These findings were consistent as there was a similar magnitude increase (around 60%), from single and combined 7 day readings. Further analysis of the data is presented in figure 3.12, showing speed of wheel

turning as an index of preferred running speeds. The average turning speeds from each pair is taken over the course of the 7 days. Panel A shows a histogram of the frequency that specific turning speeds were measured from each pair of mice. Analysis of the mode of this data, to indicate most preferred speed, and area under the curve, to show distance ran, is shown in panel B and C respectively. Together, these graphs show that in addition to KO pairs running significantly more distance than WT pairs, they also show a preference for running faster. The distance is shown by a significantly bigger histogram, analysed by area under the curve (3.12C). The increased speed is shown by significant preferences for faster running speeds in TRPA1 KO pairs, compared to WT pairs (3.12A/B). This narrowly missed significance when compared by modes (3.12B).

Summary 3; TRPA1 KO Mice Are More Active And Conduct More Voluntary Nocturnal Running

- Telemetered TRPA1 KO mice showed significantly higher nocturnal spontaneous activity levels compared to WT mice.
- When given voluntary running wheels, TRPA1 KO mouse pairs ran further each night and in total over 6 nights, compared to WT mice.
- This was shown to be due to both increased running speed preferences and increased wheel distance ran. Indicating a increased preference for exercise in KO mice, compared to WT mice.

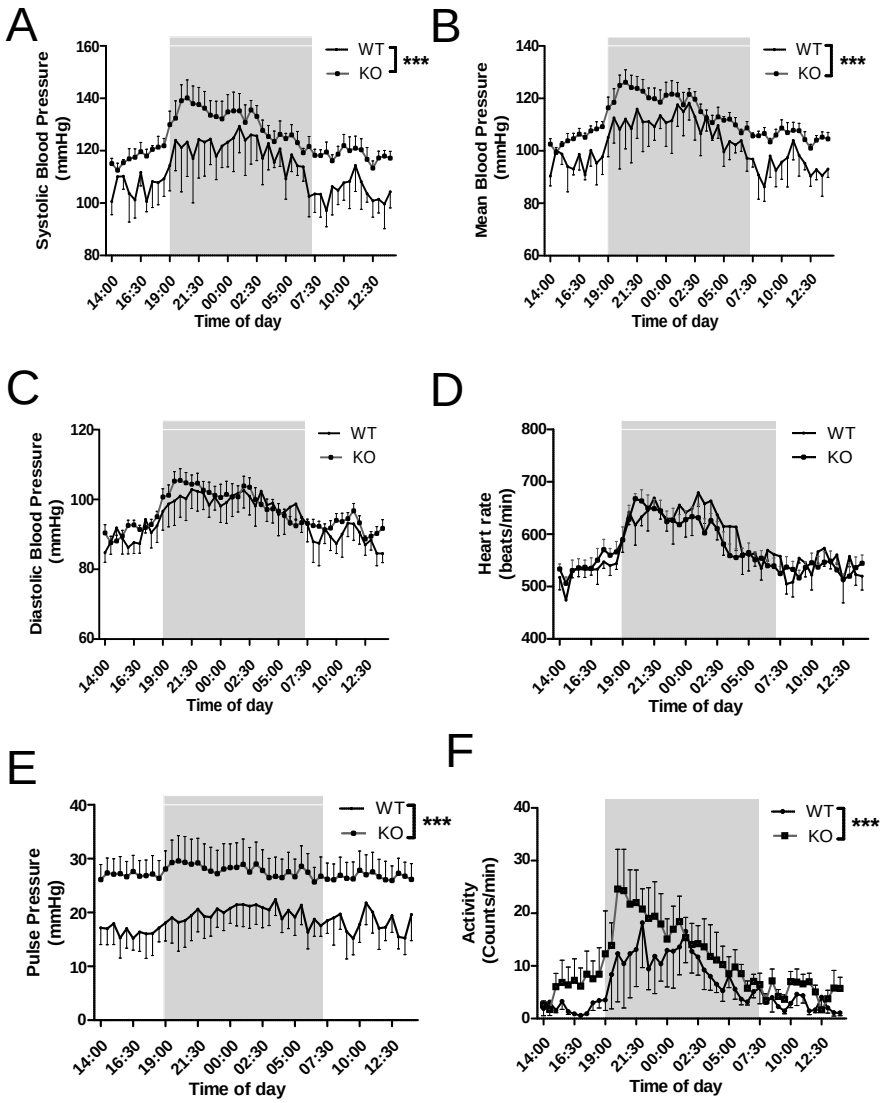

Figure 3.9 Baseline 24 Hour Hemodynamic And Activity Profiles From Female TRPA1 WT And KO Mice, Measured By Telemetry. Results show average profile of weekend days 10-13 after implantation of telemetry probe PA-C10 with aortic arch placed catheter. Mice experience a 12/12hr light/dark cycle, with the dark cycle shown in the shaded area. Data shown as half hourly averages. A. Systolic blood pressure. B. Mean blood pressure. C. Diastolic blood pressure. D. Heart rate. E. Pulse pressure. F. Spontaneous activity. N=3 WT and 7 KO mice in A-D, N=4 WT and 7 KO for E-F. Statistics in graphs A-E are from a two tailed unpaired t-test of the whole profile, WT compared with KO. ***$p<0.001$, or in the case of activity (F), which has a non-Gaussian distribution, a two tailed Mann-Whitney U test ***$P<0.05$.

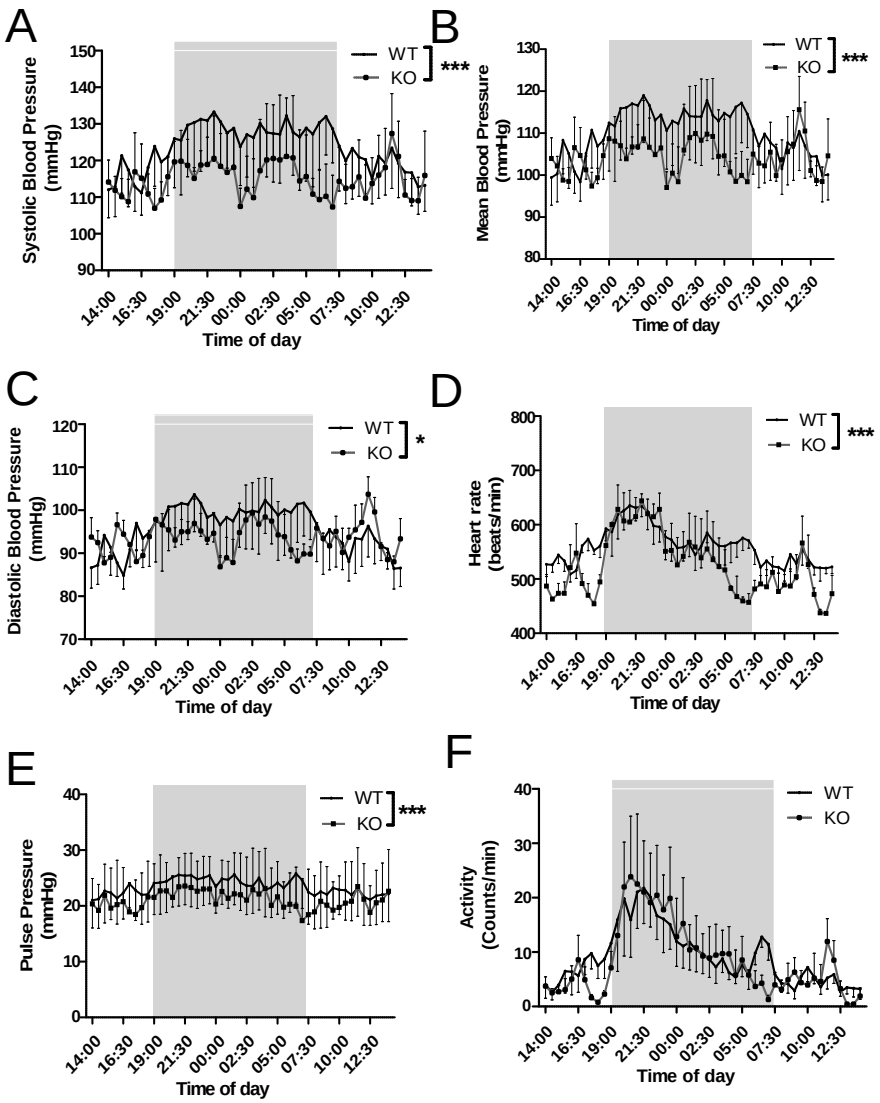

Figure 3.10 Baseline 24 Hour Hemodynamic And Activity Profiles From Male TRPA1 WT And KO Mice, Measured By Telemetry. Results show average profile of weekend days 10-13 after implantation of telemetry probe PA-C10 with aortic arch placed catheter. Mice experience a 12/12hr light/dark cycle, with the dark cycle shown in the shaded area. Data shown as half hourly averages. A. Systolic blood pressure. B. Mean blood pressure. C. Diastolic blood pressure. D. Heart rate. E. Pulse pressure. F. Spontaneous activity. N=5 WT and 3 KO mice in A-D, N=5 WT and 3 KO for E-F. Statistics in graphs A-E are from a two tailed unpaired t-test of the whole profile, WT compared with KO. *$p<0.05$, ***$p<0.001$, or in the case of activity (F), which has a non-Gaussian distribution, a two tailed Mann-Whitney U test.

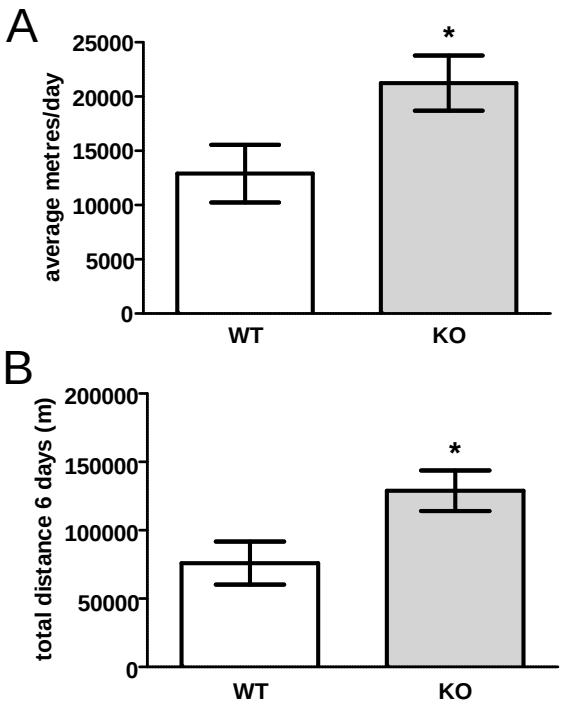

Figure 3.11 Voluntary Wheel Running Distance In Mixed Gender TRPA1 WT And KO Mice. A. daily averages. B. Total over 6 nights/7days, measured in metres from pairs of mice with cage mounted wheels. N= 6 WT pairs, 3 female, 3 male, 4 KO pairs, 2 female, 2 male. Statistics are from a one tailed, unpaired t-test, WT compared with KO. *$p<0.05$.

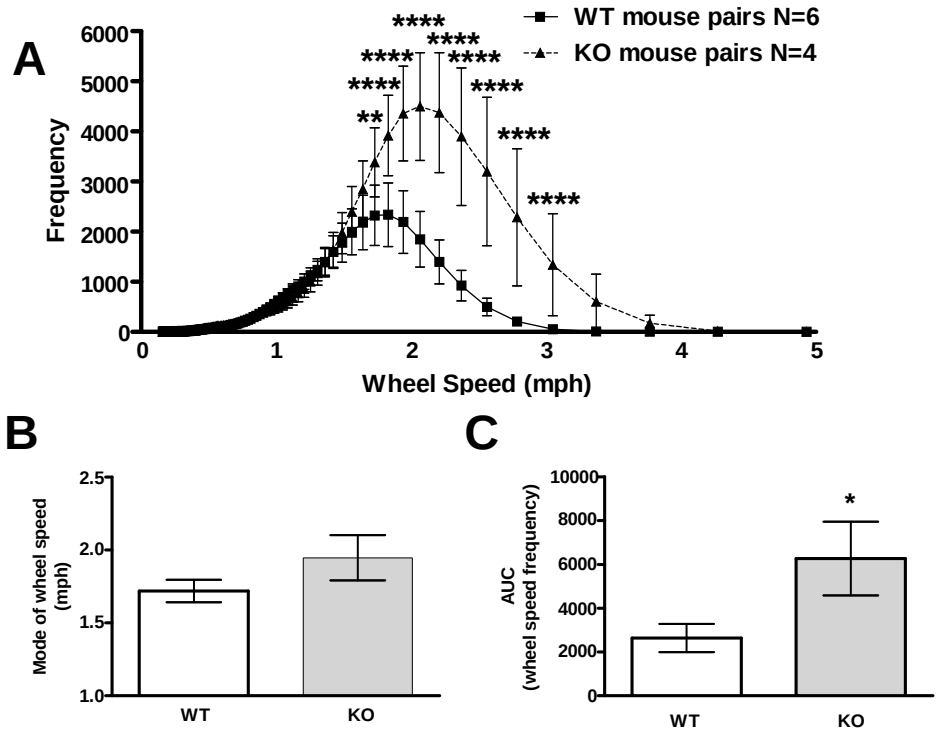

Figure 3.12 Preferred Wheel Speeds Of Voluntary Exercising TRPA1 WT And KO Mice. Graph uses the same data as presented in 3.13. A. Histogram of the frequency of average wheel speeds measured from each pair of mice over 7 days. B. Mode of data in A. C. AUC of data in A. Statistics are from a two-way ANOVA in A, **** $p<0.0001$, ** $p<0.01$ compared to WT. One tailed, unpaired t-test in C, compared with WT. *$p<0.05$. N= 6 WT and 4 KO mixed gender pairs for all graphs.

Discussion

This study has approached characterisation of TRPA1 WT and KO mice from a novel angle, focusing on cardiovascular parameters. In this chapter, I show that TRPA1 WT and KO littermates can be accurately genotyped using small sections of tissue, and that they display similar characteristics in terms of appearance, weight, heart morphology, heart function and basal hemodynamic. Small differences were displayed in some of the data collected, for instance between methods of data collection, and when data is split by gender. However, the conflicting nature and mild magnitude of these changes suggests that TRPA1 KO mice display only a mild cardiovascular phenotype when compared to WT mice. In contrast, TRPA1 KO mice displayed a striking increase in both spontaneous activity and voluntary exercise compared to TRPA1 WT mice.

TRPA1 Littermates Show Similar Physical Characteristics

TRPA1 WT and KO mice bred in-house, display indistinguishable physical characteristics and have similar weights at 2.5-3 months of age. Data presented here is for mixed gender mice, where at this time point mice did not significantly vary in weight depending on gender. However, as expected, there were trends for increased body mass in males emerging. As mice age, gender based differences in body weight occur in all strains (See growth charts available from JAX mice http://jaxmice.jax.org/support/weight/index.html). Mice used in this study were relatively young, therefore the lack of significant body weight differences seen in the data is not entirely unexpected. Longer term tracking of body weight in TRPA1 WT and KO mice would be a desirable addition to the study; however no TRPA1 dependent basal body weight differences have been reported by other groups. TRPA1 has not been directly linked to metabolism or body weight, however many of the identified agonists do possess such links. For example, MO and cinnamaldehyde have been shown to delay gastric emptying (Doihara *et al.*, 2009), cinnamaldehyde reduces blood glucose and cholesterol levels

(Subash Babu *et al.*, 2007), and has insulinotropic effects (Anand *et al.*, 2010). A potential improvement to this data would be a time course, following the weight of a large cohort of TRPA1 WT and KO littermates. To approach the problem of weight and gender differences in subsequently presented data, heart morphology is shown as a ratio to body weight, and results are also presented for separate genders.

TRPA1 WT And KO Mice Show Similar Heart Morphology And Function, Measured By Echocardiography

Echocardiography was used to measure the dimensions of the left ventricle in paired TRPA1 WT and KO mice. Many studies have investigated gender related differences in heart size and function in humans, using echocardiography. A review by Huxley (2007) describes human females to have smaller hearts, and thus stroke volume, but similar cardiac output due to a higher heart rate. The response to stress is also different between genders, with males predominantly increasing TPR, whereas females increase heart rate, to achieve higher cardiac output. Stypmann *et al* (2006) has provided echocardiographical reference values for 12 and 52 week old CD1 mice. They show no significant differences in heart morphological and functional parameters between different genders or over time points, suggesting that heart size stays stable in these mice over time. Conversely, Baumann *et al* (2008) have investigated gender differences in echocardiographical heart measurements from two mouse strains. They show similarities to data from human studies, where female mice have small left ventricular dimensions, thinner heart walls, but similar overall functional measurements. Differences were more prominent in C57/BL6 than in BalbC mice, again suggesting strain influences. However, female mice were also smaller in body weight, and significant gender differences were lost when the results were normalised to body mass. Therefore, to eliminate weight related errors, my data is expressed as a ratio to body weight, both as mixed and split gender. Trends are similar between genders, however absolute values differ. Many of these observed differences are in line with the publications presented above, showing

female mice to have smaller stroke volume. However, I also found female mice to have thicker heart walls and overall larger heart mass, which conflicts with reported data from humans and animal models. The explanation for this is not clear, but may represent a problem from processing mice in single sex experimental groups where housing conditions are not identical i.e. Groups of mice per cage. These factors could affect feeding and body weight. Although gender body weight differences were not significant, there were small differences apparent at this time point. It may also be a result of small differences in heart rate during the measurements, but this was not recorded.

When mixed gender groups are analysed, left ventricle mass as a ratio to body weight is similar between TRPA1 WT and KO mice, as were the internal dimensions and wall thicknesses. This data suggests that TRPA1 deletion does not influence heart morphology. Similar results are seen when data is split by gender, suggesting that genders were similarly affected by TRPA1 deletion. Left ventricular function was assessed using echocardiographical measurements and Doppler readings. Mixed gender TRPA1 WT and KO mice show similar left ventricular volumes, contractility and systolic functioning. Again, the data remained similar when split by gender, suggesting that TRPA1 KO does not influence cardiac function.

There are some differences in the absolute values of echocardiographical data collected from males and females in disease models (Leinwand, 2003), thus many studies are conducted using one gender only. My data reflects potential differences in absolute values between genders. However, most relevant clinical findings and strong phenotypes appear in a non-gender specific manner, therefore it is potentially more relevant to study mixed gender populations, best reflecting the patient population. This is particularly important in this study, as it is a novel investigation of the cardiovascular phenotype of TRPA1 KO mice. Excluding a gender from this study would potentially overlook valuable data. Using power analysis to determine group sizes, I examined a relatively high number of

mixed gender mice, enabling splitting of the data. Although variability was more than expected, enough mice were used to get accurate measures and there were no observations of a strong phenotype, either gender or TRPA1 dependent. TRPA1 has been suggested to be directly activated by ROS, including H_2O_2 and products of oxidative stress (Bessac *et al.*, 2008, Andersson *et al.*, 2008, Trevisani *et al.*, 2007). These ROS are thought to contribute to protein damage and onset of age related diseases, including those of the vasculature (Stadtman, 2001). Therefore a longer term study may be warranted, due to the potential for age related differences to occur. This could be a topic for future study, measuring heart characteristics serially, over the lifetime of the mice.

TRPA1 KO Mice Present A Hypotensive Phenotype When Measured By Tail Cuff Plethysmography

Average blood pressures in mice are similar to that of humans; namely around 120mmHg systolic pressure, 100mmHg mean pressure and 80mmHg diastolic pressure. Significant deviations above or below these levels indicate hypertensive or hypotensive phenotypes, respectively. Tail cuff plethysmography is a well validated method to collect serial measurements of blood pressure from trained, conscious mice. It has been previously used in our group to characterise three different genotypes of mice. In my study, mixed gender TRPA1 WT mice produced stable and reproducible blood pressures, around 120/80mmHg, similar to that expected. However, paired TRPA1 KO mice presented with significantly lower blood pressures than WT mice, around 110/75 mmHg. This is not hypotension using clinical definitions (<90/60mmHg), but shows a significantly lower blood pressure than TRPA1 WT mice. Significant efforts were made to ensure reproducibility of this data, using multiple blinded sets of mice, and employing independent investigators. This has included several undergraduate students, trained under my supervision, and another PhD student. In total, similar measurements have been taken from around 7 distinct sets of mice, by 4 investigators, with similar data patterns in all cases. When data was split by gender, similar trends occurred in both male and female mice. However, a generally lower blood pressure and

increased variability was seen in male mice and prevented significance. These factors may have been due to behavioural differences between genders of mice, where male mice are harder to obtain measurements from due to increased movement and vasoconstriction. This results in lower measurable values. It is known that androgens are important mediators of aggression, along with changes in 5-hydroxytryptamine (5HT) signalling (Nelson and Chiavegatto, 2001). Aggression and stress responses are strongly linked. Therefore, further investigation of these responses may be interesting, particularly as sensory neurones and TRPA1 have recently been linked to aggression via pheromone receptors in drosophilia (Liu *et al.*, 2011). The neuropeptide SP is also consistently linked to the formation of aggressive behaviours, acting via NK receptors in the brain (Katsouni *et al.*, 2009). Various blood borne markers and behavioural tests for stress and aggression are available.

The literature describes various mechanisms of TRPA1 mediated vasodilation *in vivo* (Bodkin and Brain, 2010). Evidence thus far suggests that TRPA1 deletion would remove a valuable peripheral artery dilation mechanism, which may lead to an increased blood pressure via an increase in total peripheral resistance. This suggestion is supported by my data presented in chapter 4, showing the TRPA1 agonist cinnamaldehyde to cause peripheral artery vasodilation. My findings of hypotension in TRPA1 KO mice opposes these suggestions, but may suggest TRPA1 has other activities relevant to blood pressure control. However, there are some potential methodological considerations which may have contributed to these findings. Firstly, the generation of KO mice has potential side effects. Many KO strains, particularly global KO's, show some evidence of compensatory expression. To date, TRPA1 KO mice have been well studied and have had no reported compensations. However, this is the first study to investigate systemic cardiovascular regulation in these mice, therefore it is possible that deletion of TRPA1 and removal of its dilatory signalling has been over-compensated in the KO mice, leading to a hypotensive phenotype. Another consideration is of the tail cuff method, as it is associated with increased animal stress due to restraint, which could

increase blood pressure and heart rate (Kramer and Kinter, 2003). In this study, extensive training was used to habitualise animals to the procedure, in an effort to reduce the effects of stress. The mice are also likely to be warmed above ambient temperatures when inside the restraint tube. Warming is an essential part of the technique, where the tail artery must be dilated to gain good quality tail swelling measurements, which are used to determine the blood pressure. Therefore the effect of heat stress and tail dilation may also have a role in my findings. However, results from WT mice show the expected blood pressure, indicating the training efforts were successful and that confounding factors were avoided. Additionally, there are also considerations of the effect of TRPA1 deletion on stress responses in mice. Lower blood pressure recordings could potentially be caused by either a decrease or increase in stress responses, preventing acquisition of accurate measurements.

Tail cuff plethysmography measures mainly systolic pressure (Mahoney and Brody, 1978), from the tail large artery. Although this has been shown to give good correlation to central blood pressure, there are differences in absolute measured pressures (Bunag and Riley, 1974). At physiological pressures (100-120mmHg) tail cuff plethysmography gives very similar readings to telemetry probes, however at lower and higher pressures there are slight under and over valuations, respectively (Mahoney and Brody, 1978). These differences were only of a few mmHg but differences at the extremities of normal blood pressure were also seen by Bunag and Riley, (Bunag and Riley, 1974) who simultaneously measured blood pressure by both methods in rats treated with hypertensive and hypotensive agents.

There are also considerations of pressure wave reflections in vessels downstream of the aorta, which may alter measurements. Differences in blood pressure measurements and the effect of antihypertensive drugs have been reported (McEniery, 2009) and the level of pressure wave deflection can vary in disease settings, where measurement of this deflection correlates with cardiovascular risk (Safar and Jankowski, 2009). Therefore

both peripheral and central measurements of blood pressure can have value as disease predictors.

A finding that TRPA1 is involved in the regulation of blood pressure would be hugely influential, both in terms of drug development and physiological understanding. For all of the reasons outlined above, there was therefore a great need to validate the findings using the gold standard method of conscious mouse blood pressure recordings, which is radiotelemetry.

TRPA1 WT And KO Mice Have A Similar Blood Pressure Phenotype When Measured By Radiotelemetry

Radiotelemetry probes are an important and powerful tool for phenotyping mouse blood pressure (Van Vliet *et al.*, 2006). Telemetry probes measuring central blood pressure from the aortic arch, showed TRPA1 WT and KO mice to have similar hemodynamic profiles and diurnal variations at room temperature (around 21°C), unrestrained in their home cage. Mixed gender mice showed clear daily patterns of blood pressure, heart rate and activity; increasing sharply at the beginning of the night time and coming down as the night progressed. These profiles are also seen when data is split by gender. Day time pressures and activity were low and relatively stable. Measurements of home cage circadian rhythms are one of the major advantages of using telemetry. This is particularly important in mice, as they are nocturnal and differences in blood pressure will be most pronounced during times of activity. My results showed an average blood pressure of around 120/80mmHg during the day time, when mice were resting and had low activity levels. Blood pressure increased during spontaneous nocturnal activity, rising to an average around 130/100mmHg. Day time and night time averages were significantly different in terms of heart rate and activity, with clear trends in other parameters. Such increases are consistent with those reported in Van Vleit *et al* (2006), who worked on characterising the use of telemetry probes, suggest the value of 24 hour diurnal recordings and averaging these values to produce a more

consistent blood pressure average. Diurnal changes are likely to be as a result of physical and thus sympathetic activity (Shepherd, 1987).

The most interesting and novel findings from the telemetered mice concerned the increase in spontaneous activity counts during the night time in TRPA1 KO mice, when compared to the WT mice. This increase in activity may partially explain the trends of increased blood pressure in the female KO mice. Activity is measured by an accelerometer feature of the telemetry transmitter, fitted to the right flank of the animal. This gives an arbitrary number of activity counts. The accuracy of these counts has been questioned, with suggestions that the sensitivity of the count can be affected by telemeter orientation and receiver position (Van Vliet *et al.*, 2006). There is also no measure of the type of activity undertaken by the telemetered mice, which would demand use of specialised activity cages or night time video recordings. Therefore, I cannot be certain that increased counts truly demonstrate increased spontaneous activity, or the type of movements. For this reason, further studies were undertaken measuring voluntary wheel running in pairs of littermate TRPA1 WT and KO mice. These were collected from a separate group of animals with running wheels in their home cage and support the telemetry findings, showing that TRPA1 KO mice participate in more voluntary exercise, consistently running significantly further and faster than WT mice. Future work will be needed to investigate the reasons for the observed activity differences in TRPA1 WT and KO mice.

The effect of activity in this study are in line with findings from Adlam *et al* (2011) showing telemetered mice undergoing exercise to predominantly increase their heart rate, not blood pressure, to reach the increase in cardiac demand. There are many investigations using wheel running training in the literature, looking at a variety of adaptive changes. My findings are similar to those of Koteja *et al* (1999), who selectively bred for higher running distance and show that this is due to an increased speed, not time spent running. However, in their study, running distance was not correlated with overall activity levels in the mice, using specialised activity measuring

cages. Therefore wheel running may represent an independent measure of activity to that of telemetry. Together, the wheel running and telemetry activity data strongly suggest a hyperactivity phenotype in TRPA1 KO mice. Long distance running is reported to be a heritable trait in many studies (Swallow *et al.*, 1998), although the exact genes responsible are not clear. Therefor genetic manipulation has the potential to result in changes in activity. Additionally, high running mice have been shown to have similar neurobiology to sufferers of Attention deficit hyperactivity disorder (ADHD) (Rhodes *et al.*, 2005).

Increased blood pressure variability over 24 hours, and from day to day, is emerging as an important indicator of cardiovascular event risk as it is suggested to be the cause of much end organ damage (Rothwell, 2011). Heart rate variability is also a factor that could be extrapolated from the data, giving a measure of autonomic function, with reduced variability also linked to cardiovascular events and can be increased by exercise (Routledge *et al.*, 2010). Alterations in activity level mean that analysis of the data for blood pressure variability is not appropriate. Therefore these parameters were not measured in this study.

Findings from tail cuff plethysmography, showing hypotension in TRPA1 KO mice, were not confirmed using telemetry. Earley *et al*, (2009) have recently described intraluminal administration of the TRPA1 antagonist HC-030031 in pressurised cerebral arteries to cause an increase in myogenic tone *in vivo*. This could potentially lead to increased blood pressure through an increase in peripheral resistance, and suggests that TRPA1 could potentially provide a tonic dilatory influence on vessel tone. Based on this evidence, TRPA1 KO mice may be expected to show increased blood pressure. In my study, telemetry data from mixed gender profiles showed a trend for consistently higher systolic and mean blood pressures in TRPA1 KO mice. This pattern of increased blood pressure was retained in female data analysis, but was reversed in male analysis. However, split gender data must be interpreted with caution due to the increase in activity in TRPA1 KO mice and lower N numbers. The small

magnitude of blood pressure differences and incompatibility of this data between measurement methods, suggests that there is no clear blood pressure phenotype associated with TRPA1 deletion. The differences between measurement methods could be further investigated in this study by concomitantly measuring blood pressure by tail cuff and telemetry. This has been done in many other validation studies and shows good correlations, particularly of basal systolic pressures (Feng *et al.*, 2008, Whitesall *et al.*, 2004), but was logistically impossible to complete during the time frame of this PhD. These measurements would also allow us to investigate the effects of wheel running exercise in the TRPA1 WT and KO mice. Such dramatic differences between tail cuff and telemetry findings may be due to a physiological response to the tail cuff procedure, which may differ in TRPA1 WT and KO mice. This opens many potential avenues of investigation, relating to stress responses and the TRPA1 receptor.

Conclusion

In this chapter, I have shown that TRPA1 KO mice do not display any strong physical or hemodynamic phenotypes when compared to TRPA1 WT mice. They share similar weights, heart morphology, heart function, heart rate and blood pressure. Measurements of blood pressure were collected by both tail cuff plethysmography and telemetry, with differing results. However, this is likely to be due to methodological considerations. Telemetry is the gold standard approach to mouse blood pressure phenotyping and this data suggests there are no clear differences between TRPA1 WT and KO mice. The telemetry data also suggests hyperactivity characteristics may be expressed in KO mice. This data was backed up by significant increases in voluntary wheel running distances and speeds, an independent measure of activity. Therefore, I show the potential for TRPA1 KO mice to display increased levels of physical activity which warrant further investigation.

Chapter 4 – Characterising Cinnamaldehyde Induced Vasoreactivity In The Mouse Mesenteric Artery, Using The Wire Myograph

Introduction

Mechanisms attributed to local blood flow control vary depending on tissue type and can be modulated *in vivo* by central control mechanisms. This is often linked to the cell types involved and the tissue innervation. Blood pressure can be altered by changing the total peripheral resistance of the vascular system; where increasing the resistance increases the pressure of the system. Therefore, the vascular tone experienced in large vascular beds, such as mesenteric beds, can easily influence systemic blood pressure. Many antihypertensive drugs work by reducing peripheral resistance.

An increasing number of studies are demonstrating that proposed TRPA1 agonists can modulate vascular tone in isolated arteries, causing vasorelaxation (See table 1.1). This leads to the hypothesis that TRPA1 can have a role in peripheral resistance control both via both local and central signalling. The main TRPA1 experimental agonists are currently MO and cinnamaldehyde. We have recently used cinnamaldehyde to investigate central reflexes initiated by intra-vascular TRPA1 agonism, demonstrating induction of a vaso-vagal reflex. We are now interested in characterising the locally mediated component of TRPA1 induced vasorelaxation, as this may play an important role in the response to locally produced TRPA1 agonists. Several studies have used topically applied cinnamaldehyde on the human forearm, showing it to cause physiologically relevant increases in local blood flow (Namer *et al.*, 2005, VanderEnde and Morrow, 2001). Additionally, unpublished data from our group collected by Aisah Aubdool, has shown topical application of cinnamaldehyde to the mouse ear causes a robust increase in local blood flow which does not alter flow in the vehicle treated contralateral ear. Furthermore, this response is almost completely lost in TRPA1 KO mice and in WT mice following

treatment with TRPA1 antagonists. Some of this data will be presented later in this chapter. Together, these studies suggest that topical application of cinnamaldehyde induces TRPA1 mediated vasodilation of the local vasculature, but does not allow enough agonist to reach the circulation to activate reflex mechanisms, and does not release enough vasodilator agents to leak in to the circulation and induce systemic changes in blood pressure. When investigating the signalling pathways responsible, studies have utilised a range of techniques to show the effect of TRPA1 agonist application to localised vascular beds, including using various species and techniques to propose a range of different mechanisms. These varying findings may be due to methodological differences, as human and animal *in vivo* studies demonstrate C-fibre and neuropeptide components, whereas isolated animal vessels often show changes in calcium handling and hyperpolarisation of the smooth muscle. These mechanisms are not incompatible but this suggests that non-neuronal tissues may react to the agonists, modulating the vasorelaxant response, potentially via TRPA1.

Several studies suggest that sensory neurone derived peptides, such as CGRP, may be important in TRPA1 mediated vasorelaxation. Hikiji *et al* (2000) and Louis *et al* (1989a) show MO in the cat tooth pulp and rat hind paw respectively, causes C-fibre mediated dilation via neuropeptides. Using Laser Doppler flowmetry, MO induced blood flow increases have been shown to be modulated by SP and CGRP in the mouse ear (Grant *et al.*, 2005) and in our recently published study we also found that topically applied cinnamaldehyde causes vasodilation that is TRPA1 mediated (Pozsgai *et al.*, 2010).

Several TRP channels have been shown to be expressed on endothelial cells and cause endothelial dependent vasodilation (Yao and Garland, 2005). Earley *et al* (2009) recently used isolated rat cerebral arteries treated with the TRPA1 antagonist HC-030031 (3μM) in the pressurised myograph, to show MO induced vasorelaxation was dependent on TRPA1 expressed on endothelial cells. They proposed a tissue specific mechanism in which TRPA1 activation causes calcium activated calcium release from

stores, opening calcium activated potassium channels (SK_{Ca} and $K_{Ca}3.1$) and hyperpolarising the cell. The hyperpolarisation is then passed to vascular smooth muscle cells via myoendothelial gap junctions or by creating areas of high extracellular potassium, which activates smooth muscle K_{IR} channels. This study used a range of antagonists for the potassium channels investigated, including apamin (for SK_{Ca}), TRAM34 (for $K_{Ca}3.1$) and $BaCl_2$ (for K_{IR}), and is currently one of the most highly cited accounts of TRPA1 induced relaxation. However, it is likely to be specific to the cerebral artery, as similar arrangements of TRPA1 receptors with potassium activated calcium channels has not been reported in other vascular beds. Earley *et al* did not investigate the role of neuropeptides or sensory neurones in their model. The mechanism in the cerebral arteries also differs from those identified in other tissues, which do not show endothelial dependence, but do provide evidence of sensory neurone/neuropeptide involvement. For example, when using similar concentrations of cinnamaldehyde on rat aortic rings, Xue *et al*, (2011) find no effect of endothelial removal, L-NAME, ODQ or indomethacin addition (inhibitors of NO, soluble guanylyl cyclase and prostaglandin production respectively), whereas Yanaga *et al* (2006), using the same model, find a partial endothelium dependent component which is NO mediated and blocked by L-NAME. Neither of these studies investigated dependence on TRPA1. Consequently, there is a need to characterise a complete pathway in a tissue, before investigating how this differs between tissues, and in different scenarios, using similar methodology. I am particularly interested in tissues relevant to blood pressure control. We were the first group to investigate *in vivo* blood flow changes in TRPA1 KO mice, showing local application of cinnamaldehyde to the paw induces significant blood flow increases in TRPA1 WT mice only (Pozsgai *et al.*, 2010). In this publication we also showed that i.v. cinnamaldehyde application initiated a TRPA1 mediated, neuropeptide independent vaso-vagal response, causing an initial drop in blood pressure and heart rate followed by a more sustained increase in both. These findings suggest that TRPA1 activity is relevant to the regulation of the cardiovascular system; however the mechanisms at play are still unclear. The tone of small blood vessels in

large vascular beds is important for total peripheral resistance and thus blood pressure. Determining the contribution of TRPA1 to local vascular tone is therefore of value in investigating its potential role in blood pressure control.

Aims

- To investigate cinnamaldehyde induced vasorelaxation in isolated resistance vessels of the mesenteric vascular bed.
- To investigate the TRPA1 dependency of this relaxation
- To demonstrate that this is relevant in vivo by studying skin blood flow in the anaesthetised mouse ear.
- To study the mechanism mediating TRPA1 induced vasorelaxation.

Results

Cinnamaldehyde Induced Vasorelaxation And Vasodilation

First order mesenteric arteries isolated from TRPA1 WT and KO mice were investigated using a wire myograph. These mice had been genotyped as previously described. In all experiments, arteries were rested before use, allowing the tissue to stabilise. The vessels were challenged three times with high potassium solution (80mM), establishing maximum tissue contraction, before endothelium function was assessed by the extent of relaxation to carbachol (10μM, added for 2 minutes) after pre-constriction using U46619 (10nM, 5 minutes), a TxA_2 mimetic. Representative traces of raw data collected from TRPA1 WT mesenteric arteries during high K^+ challenges and carbachol treatment are shown in appendix figure 1. U46619 was chosen as a pre-constriction agent due its long and consistent contraction of the mesenteric arteries. Other pre-constriction agents were investigated, in particular phenylephrine, however this did not produce a stable constriction over the test period. A carbachol relaxation response of more than 60% was used to define positive endothelium function. In initial studies, WT mouse mesenteric arteries were used to assess the

concentration related effect of cinnamaldehyde, using single a concentration treatment on each U46619 pre-constriction Representative traces of raw data collected from TRPA1 WT and KO mesenteric arteries treated with a single concentration of cinnamaldehyde following pre-constriction are shown in appendix figure 2. Average percentage relaxation is calculated and plotted on figure 4.1. This figure also shows the effect of vehicle addition (0.01% ethanol, final bath concentration), with the total relaxation shown as 'vehicle or 0μM cinnamaldehyde'. The relaxation to vehicle provides a useful control, showing the effect of both time and vehicle on the level of pre-constriction. Panel A and B of figure 4.1 show data split for vessels with and without functional endothelium respectively. This is combined in panel C. These vessels were from animals of both gender, and graphs showing data split by sex are shown in figure 4.2. These graphs show similar response patterns to the combined data, suggesting that gender is not an important modulator of the response to cinnamaldehyde. By grouping the data into mixed gender groups, I was able to increase N and strengthen my statistical analysis.

In both TRPA1 WT and KO vessels, cinnamaldehyde causes a concentration dependent vasorelaxation. This suggests that cinnamaldehyde has both TRPA1 dependent and independent vasodilatory actions. In the mouse mesenteric artery, with and without functioning endothelium, TRPA1 KO mice displayed a concentration response curve shifted to the right in comparison to WT mice, which was significant at 30μM cinnamaldehyde for vessels with and without functional endothelium, demonstrating reduced potency. This provides evidence that TRPA1 is an important mediator of the cinnamaldehyde response, but is not the exclusive mediator in this tissue.

Panel C of figure 4.1 shows combined data from vessels with and without endothelial function. This graph can be used to compare responses within genotype, where differences show the extent of endothelial dependence in the response. In figure 4.1, both WT and KO vessels show a very small rightward shift in cinnamaldehyde concentration response when endothelial

function is absent. This shows that cinnamaldehyde does have some vasodilatory action occurring via the endothelium. This is of bigger magnitude in KO vessels compared to WT vessels, indicating that the TRPA1 component is likely to be endothelium independent. Moreover, these changes cannot be attributed to differing levels of endothelium function, as groups with and without functional endothelium in both genotypes, show similar positive and negative responses to carbachol.

Figure 4.3 shows the EC_{50} calculated as an average for each treatment group using each animal's individual concentration response curve. This graph illustrates the decrease in the potency of cinnamaldehyde in TRPA1 KO vessels, increasing the EC_{50} value. This reached significance only between WT and KO vessels where functional endothelium was absent. Additionally, data shows little endothelium dependency in WT mice. Only in KO mice does removal of the endothelium cause a significant decrease in the potency of cinnamaldehyde. Together with the previous figure, these results suggest that cinnamaldehyde has TRPA1 dependent and independent relaxation mechanisms in the mesentery, and that TRPA1 is involved in the portion mediated by vascular smooth muscle cells, as only the KO vessel response was affected by loss of endothelial function.

There have been no previous studies investigating differences in mesenteric artery vasorelaxation between TRPA1 WT and KO mice. If TRPA1 KO vessels were to have a different sensitivity to pre-constriction agents, this may impact on their vasorelaxant ability. Here, data shows that TRPA1 WT and KO mesenteric arteries without functional endothelium are able to produce similar levels of raw tension (mN) and % constriction compared to the maximal tension produced by 80mM potassium Krebs, in response to cumulative concentrations of the physiologically relevant contractile agonist phenylephrine (mimicking sympathetic tone), depolarising levels of KCl and U46619, the pre-constriction agent commonly used in this chapter. This data is shown in figure 4.4. I therefore conclude that the ability to produce tone is not influenced by a TRPA1 dependent component.

My data suggests that *ex vivo* cinnamaldehyde induced vasorelaxation is likely to be partially dependent on the TRPA1 receptor. Data produced by my colleague Aisah Aubdool also shows the *in vivo* consequences of topical cinnamaldehyde application by measuring cutaneous blood flow. In figure 4.5, donated by Aisah, topical application of 10% cinnamaldehyde to TRPA1 WT mouse ear causes a significant increase in blood flow. In TRPA1 KO mice, this response is significantly attenuated (Figure 4.4A). Similarly, an attenuation of the response occurs in CD1 mice, after i.p. pre-treatment with the TRPA1 antagonist TCS5861528 (10mg/kg) (Figure 4.4B). This concentration has previously been used to reduce mechanical hypersensitivity in diabetic rats when given i.p. by Wei *et al* (2009).

Several studies, including that of Earley *et al* (2009), have previously investigated TRPA1 induced vasodilation using MO. I have also used MO on the mesenteric vessels from TRPA1 WT and KO mice, with and without functional endothelium, presented in figure 4.6. A representative trace of raw data collected during a cumulative concentration response curve to MO in a TRPA1 WT mesenteric artery, is shown in appendix figure 3. The effects of MO vehicle additions are also shown. In my hands, MO caused a concentration dependent vasoconstriction, which was not influenced by endothelium or TRPA1 presence.

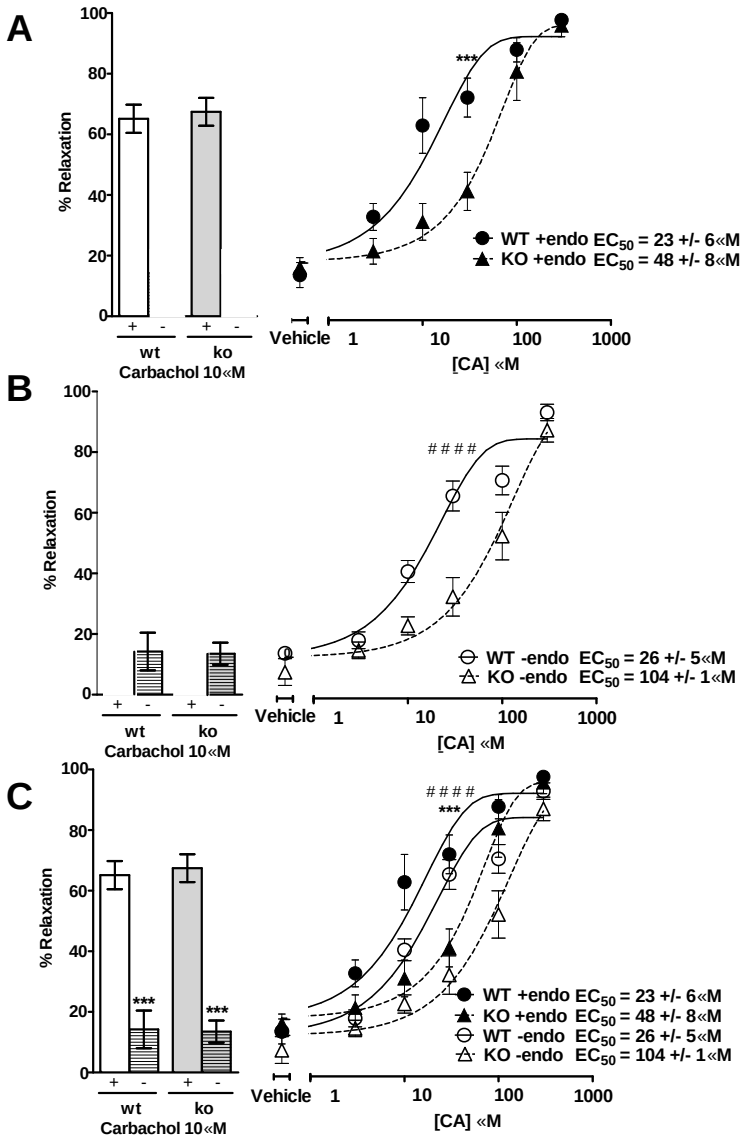

Figure 4.1 The Effect Of Cinnamaldehyde On TRPA1 WT And KO Mouse Mesenteric Arteries With And Without Functional Endothelium. Results are from vessels on a wire myograph pre-constricted to U46619 (10nM, 5 minutes). The effect of single concentrations of cinnamaldehyde are shown (CA, 3-300μM) and % relaxation at 5 minutes measured. Endothelium function is assessed using carbachol (10μM) added for 2 minutes. The EC50 is calculated per animal and expressed as group averages. Graph shows combined data from mixed gender mice. A. endothelial intact only N=10-11. B. No functional endothelial N=14-15. C. Data from A and B combined. Statistics are one way ANOVA with Bonferroni for carbachol, or two-way ANOVA with Bonferroni for cinnamaldehyde additions ***$p<0.001$, compared to intact endothelium, ***$p<0.001$ vs +endo WT, # # # #$p<0.0001$ vs –endo WT.

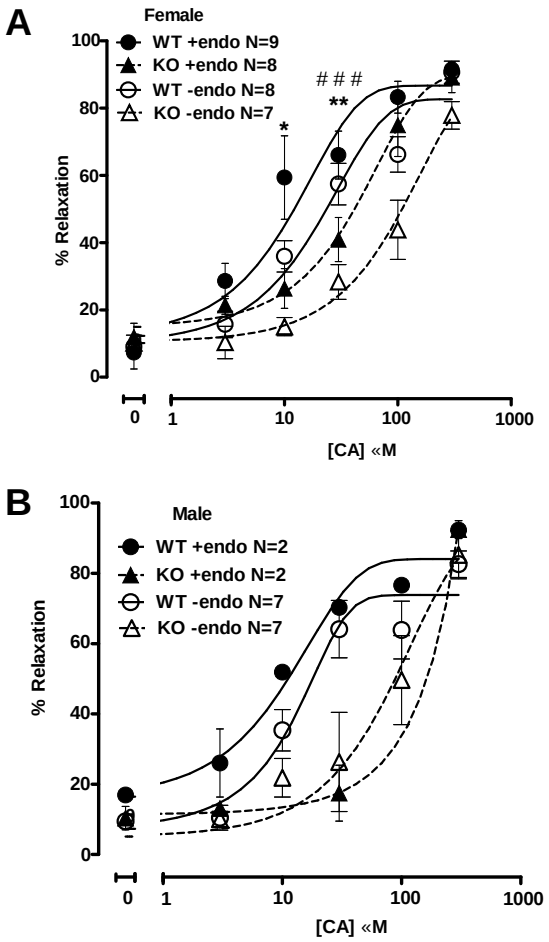

Figure 4.2 The Effect Of Cinnamaldehyde On TRPA1 WT And KO Mouse Mesenteric Arteries With And Without Functional Endothelium, Split By Gender. Results are from vessels on a wire myograph pre-constricted to U46619 (10nM, 5 minutes). The effect of single concentrations of cinnamaldehyde are shown (CA, 3-300μM) and % relaxation at 5 minutes is measured. A) Female B) Male mesenteric arteries. N numbers are as indicated. Statistics are from a two-way ANOVA with Bonferroni's post test, *p<0.05, **p<0.01 comparing WT +endo with KO +endo, # # #p<0.001, comparing WT –endo with KO –endo.

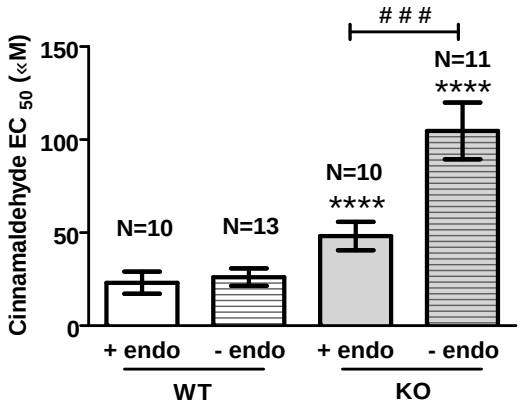

Figure 4.3 Potency Of Cinnamaldehyde Induced Vasorelaxation In TRPA1 WT And KO Mouse Mesenteric arteries. Results show vessels pre-constricted to U46619 (10nM, 5 minutes). EC_{50} is calculated per animal and presented as an average. Graph shows pooled data from male and female paired mice. Statistics are from one way ANOVA with Bonferroni's post-test, ****p<0.0001, compared to WT without functional endothelium (-endo). ###p<0.001 KO endothelium (+endo) compared to KO without endothelial function (-endo). N numbers are as indicated

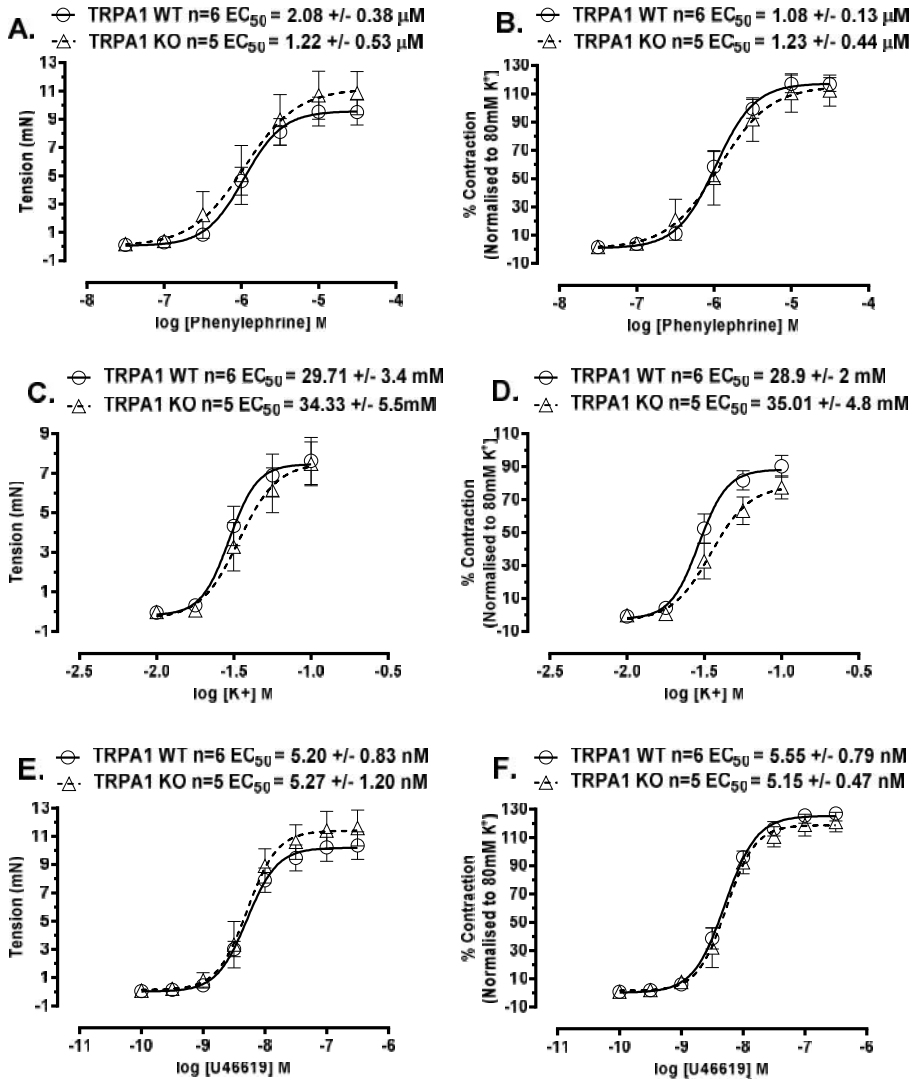

Figure 4.4 The contractile ability of mesenteric arteries from TRPA1 WT and KO mice in response to phenylephrine, KCl and U46619. Results show vessels without functional endothelium, pre-constricted with cumulative concentrations of phenylephrine (0.03-30µM A-B), KCl (K^+ 10-300mM C and D) or U46619 (0.1-300nM E-F) at 3 minute intervals. Panel A, C and E show raw tension, whereas panels B,D and F show tension as a % of the maximal tension recorded in response to 3, 2 minute challenges with 80mM K+ Krebs. EC_{50} is calculated per animal and presented as an average. Graph shows pooled data from male and female paired mice.

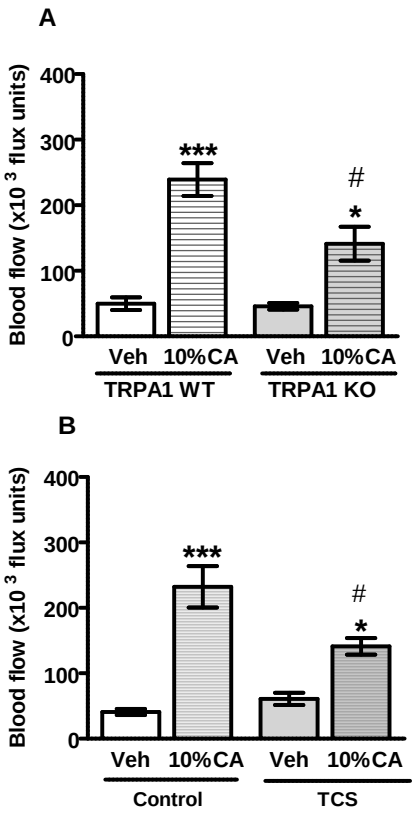

Figure 4.5 The Effect Of Cinnamaldehyde On Blood Flow In The Anaesthetised TRPA1 WT And KO Mouse Ear, Measured By Laser Doppler Flowmetry. Results show blood flow measured for 30 minutes after topically applied cinnamaldehyde (CA, 10% in ethanol) or vehicle, total flow is calculated as area under the curve. A. TRPA1 WT and KO female mice. N=4 B. Male CD1 mice pre-treated for 30 minutes with TRPA1 antagonist (TCS5861528 (TCS), 10mg/kg i.p.) or vehicle (20% DMSO in saline). N=5. Statistics are from a one way ANOVA with Bonferroni's post test, *$p<0.05$, ***$p<0.001$ compared to respective vehicle, #$p<0.05$ compared to control CA treated ear. Graph is of unpublished data by Aisah Aubdool.

Effect of TRPA1 antagonists on cinnamaldehyde induced vasorelaxation

To further confirm the TRPA1 component of cinnamaldehyde induced vasorelaxation, I pre-treated tissues from CD1 mice (TRPA1 WT) with two concentrations of the TRPA1 antagonist HC-030031, 10 and 30μM. This concentration range is used in other publications, with both 10 and 30μM significantly reducing cinnamaldehyde (300μM) induced contraction on isolated bladder smooth muscle (Andrade *et al.*, 2011). The peak of my cinnamaldehyde concentration response curve is also 300 μM. Figure 4.7 shows that neither concentration of HC-030031 had an effect on cumulative cinnamaldehyde concentration response curves in vessels with and without functional endothelium. In panel C, where all data is overlaid, the graph shows a small non-significant difference between vessel with and without functional endothelium. A representative trace showing the effect of vehicle (ethanol) additions rather than cinnamaldehyde, over the same time course of a cumulative concentration curve is shown in appendix figure 4, where no effects of vehicle are seen. Representative traces of the raw data collected from a cumulative concentration curve to cinnamaldehyde, conducted in a CD1 mouse mesenteric artery, pre-treated with HC-030031 (30μM) or its vehicle (0.01% DMSO) are shown in appendix figure 5.

Studies presented in this chapter commonly use mesenteric arteries from CD1 mice, which are WT with respect to the TRPA1 receptor. These mice hold a different genetic strain background from that of TRPA1 WT and KO mice, which have a mixed C57/BL6 and B6129P1/F2J background. In order to address the possibility that strain differences may account for my inability to block cinnamaldehyde responses with HC-030031, a separate series of studies used mesenteric arteries from CD1 and C57/BL6 mice pre-treated with either vehicle (0.05% DMSO in Krebs), or 10, 30, 50 or 100μM HC-033031, prior to application of cumulative cinnamaldehyde concentrations. None of these antagonist concentrations reduced the

vasorelaxation response to cinnamaldehyde, although higher concentrations were conversely associated with an increased relaxation response (figure 4.8), which may be due to detrimental effects on tissue viability. In figure 4.9, these findings are built upon using mesenteric arteries from TRPA1 WT mice pre-treated with 50µM HC-030031 or its vehicle (0.05% DMSO in Krebs), before accumulating concentrations of cinnamaldehyde. 50µM HC-030031 was chosen as the highest concentration which did not show detrimental effects on tissue viability in previous figures. As seen in arteries from CD1 and C57/BL6 mice, HC-033031 was ineffective at inhibiting vasorelaxation to cinnamaldehyde in TRPA1 WT arteries. Figure 4.9 also shows raw tension from TRPA1 WT arteries where 50µM HC-030031 pre-treatment results in a reduction in arterial tone throughout the cinnamaldehyde concentration response curve. The experiments presented in figure 4.8 and 4.9 were collected over several months and a difference in cinnamaldehyde EC_{50} values is observed compared to some previously and subsequently presented data. As previously presented data showed similar contractile ability in TRPA1 WT and KO mesenteric vessels, it is likely that high concentrations of HC-030031 act to inhibit smooth muscle contraction. This is similar to the finding of Capasso *et al* (2011) who showed 10µM HC-030031 to be ineffective at blocking MO induced contraction of the murine intestine in an organ bath, but that higher concentrations of antagonist are anti-spasmodic, inhibiting contraction to acetylcholine.

The contractile abilities of mesenteric vessels from the different strain backgrounds I have used in this chapter was also characterised, in a similar manner to that previous described for TRPA1 WT and KO mice. This is presented in figure 4.10, where contractile responses to phenylephrine and U46619 were indistinguishable in CD1, C57/BL6 and TRPA1 WT mesenteric arteries. These findings suggest that strain is not a key factor influencing the response to cinnamaldehyde, therefore CD1 vessels are commonly used as WT vessels in further work for enhanced economic ease and availability, along with vessels from genetically modified C57/BL6 mice. This allowed further investigation of mechanistic elements.

Preliminary studies conducted in mesenteric arteries from CD1 mice utilised another TRPA1 receptor antagonist, TCS5861528, which is an analogue of HC-030031, but reportedly with increased solubility. Similarly to HC-030031, a representative trace of the raw data is shown in appendix figure 6. A concentration of 30μM shows no significant effect on cinnamaldehyde induced vasorelaxation in vessels without functional endothelium (figure 4.11). This concentration has previously been shown to completely inhibit inward current from rat TRPA1 expressed in HEK cells (Wei *et al.*, 2010). In this chapter, TCS5861528 has previously been shown to inhibit topical cinnamaldehyde induced vasodilation (figure 4.5) suggesting it does block TRPA1 responses at higher concentrations. For both antagonists, higher concentrations of antagonist were attempted but were found unsuitable due to solubility problems. Therefore, although vessels from our TRPA1 KO mice suggest partial dependence of cinnamaldehyde induced vasoreactivity on TRPA1 activity, these findings cannot be confirmed using the selected TRPA1 antagonists.

Summary 1; The TRPA1 Component In Cinnamaldehyde Induced Vasorelaxation.

- Cinnamaldehyde causes concentration dependent vasorelaxation of mouse mesenteric arteries.
- This occurs in both TRPA1 WT and KO vessels, with and without functional endothelium. However, in TRPA1 KO vessel there a decrease in potency, shown by a significant increase in EC_{50}. This demonstrates a TRPA1 dependent component in the response.
- This response is relevant *in vivo*, where topical cinnamaldehyde causes an increase in blood flow which is significantly reduced in TRPA1 KO and mice pre-treated with a TRPA1 antagonist.
- TRPA1 WT and KO mice do not differ in their ability to produce contractile tone. Additionally, contractile abilities do not differ between TRPA1 WT, CD1 or C57/BL6 mesenteric vessels.

- MO causes concentration dependent vasoconstriction of mesenteric arteries; a response which did not show TRPA1 dependence.
- TRPA1 antagonists are unable to alter the cinnamaldehyde response at a range of concentrations, up to a level where they interfere with tissue contraction. This occurs similarly in CD1, C57/BL6 and TRPA1 WT arteries.

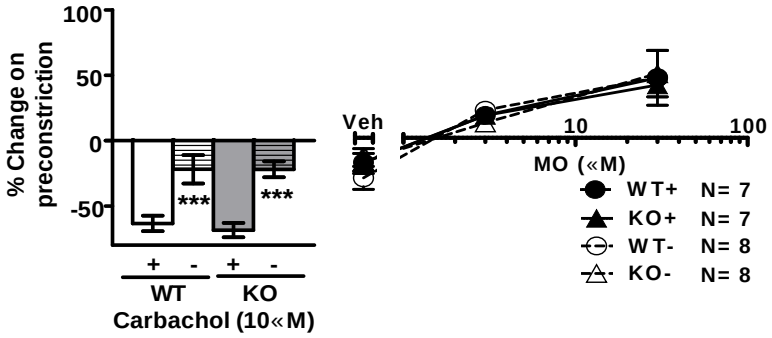

Figure 4.6 The Effect Of MO On Vascular Tone Of TRPA1 WT And KO Mesenteric Arteries. Results show vessels mounted on a wire myograph, pre-constricted to U46619 (10nM, 5 minutes). The effect of single concentrations of MO are shown (MO, 3-30μM) and % change in tension at 5 minutes measured. Endothelium function is assessed by % response to carbachol (10μM) added for 2 minutes. Average relaxation is shown, for vessels with functional endothelium (+) and without (-). Graph shows mixed gender mice. Statistics are from a one way ANOVA with Bonferroni's post test, comparing vessels with and without endothelium from the same genotype. ***$p<0.001$. N numbers are as indicated. No significant differences are seen in a two way ANOVA.

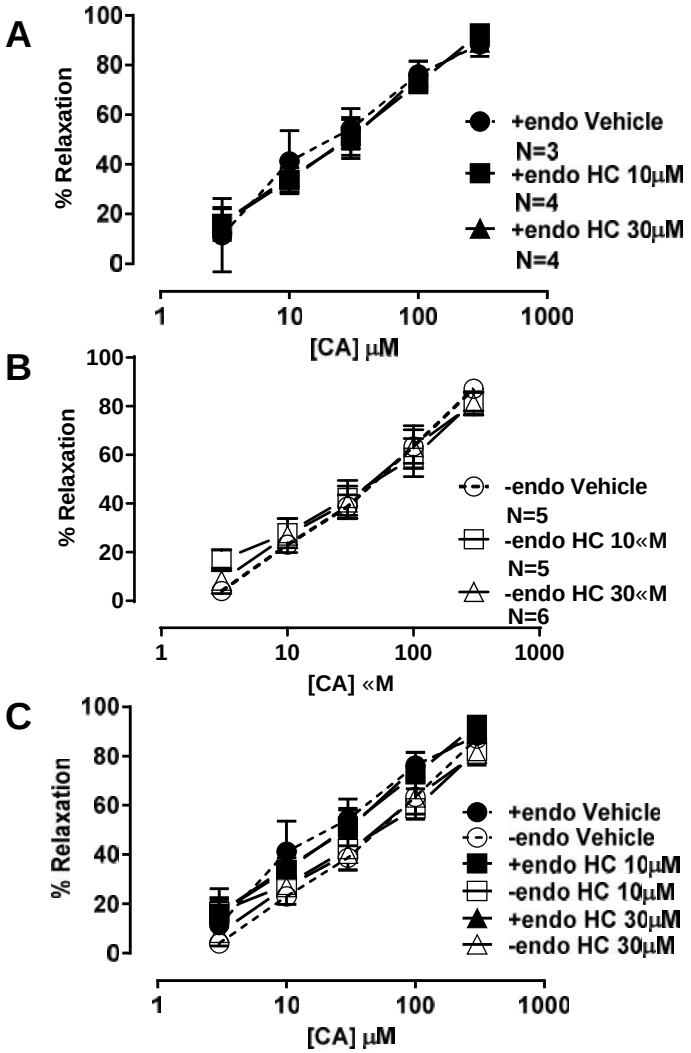

Figure 4.7 The Effect Of Cinnamaldehyde On Vascular Tone In CD1 Mouse Mesenteric Arteries, With And Without Functional Endothelium And Addition Of The TRPA1 Antagonist HC-030031. Results show vessels on a wire myograph, pre-constricted to U46619 (10nM, 5 minutes). The effect of cumulative concentrations of cinnamaldehyde are shown (CA, 3-300µM in ethanol), using % change in tension at 3 minutes. HC-030031 (HC, 10 or 30µM in DMSO vehicle), a TRPA1 receptor antagonist, was added to the bath 15 minutes before pre-constriction. Graph shows mixed gender mice. A. Vessels with functional endothelium (+endo) B and without (-endo). C. Combined. N numbers are as indicated. No significance is seen in a two way ANOVA.

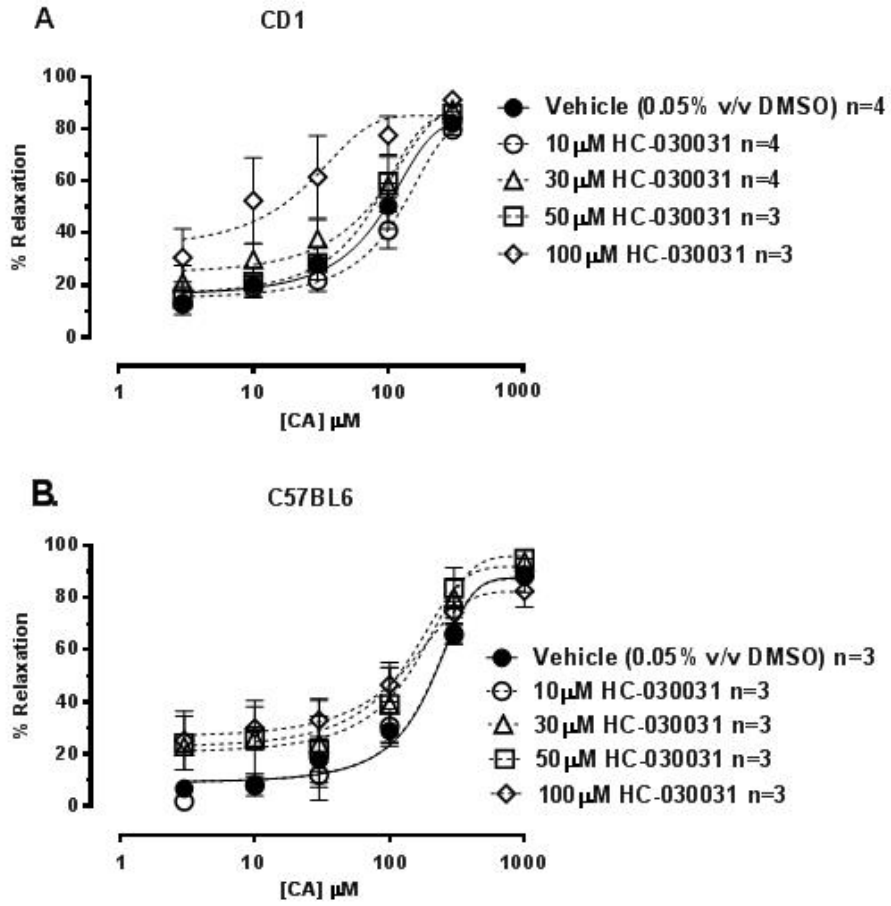

Figure 4.8 The Effect Of Cinnamaldehyde On Vascular Tone In CD1 And C57/BL6 Mouse Mesenteric Arteries Without Functional Endothelium, With And Without Addition Of Increasing Concentrations Of The TRPA1 Antagonist HC-030031. Results show vessels from CD1 (A) or C57/BL6 (B) mice on a wire myograph, pre-constricted to U46619 (10nM, 5 minutes). The effect of cumulative concentrations of cinnamaldehyde are shown (CA, 3-300 or 1000µM in ethanol) as % change in tension at 3 minutes. HC-030031 (HC, 10, 30, 50 or 100µM in DMSO vehicle), a TRPA1 receptor antagonist, was added to the bath 15 minutes before pre-constriction. Graph shows mixed gender mice. N numbers are as indicated.

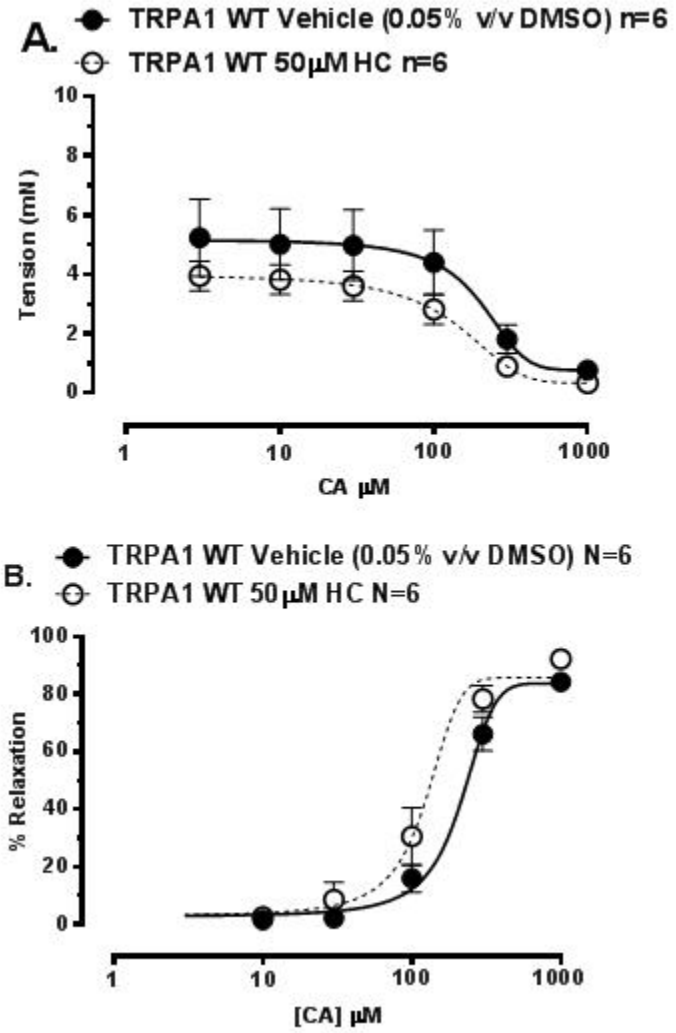

Figure 4.9 The Effect Of Cinnamaldehyde On Vascular Tone In TRPA1 WT Mouse Mesenteric Arteries Without Functional Endothelium, With And Without Addition Of The TRPA1 Antagonist HC-030031. Results show vessels from TRPA1 WT mice on a wire myograph, pre-constricted to U46619 (10nM, 5 minutes). The effect of cumulative concentrations of cinnamaldehyde are shown (CA, 3-1000µM in ethanol), using raw tension (A) or % change in tension at 3 minutes (B). HC-030031 (HC, 10 or 30µM in 0.05% DMSO vehicle), a TRPA1 receptor antagonist, was added to the bath 15 minutes before pre-constriction. Graph shows mixed gender mice. N numbers are as indicated.

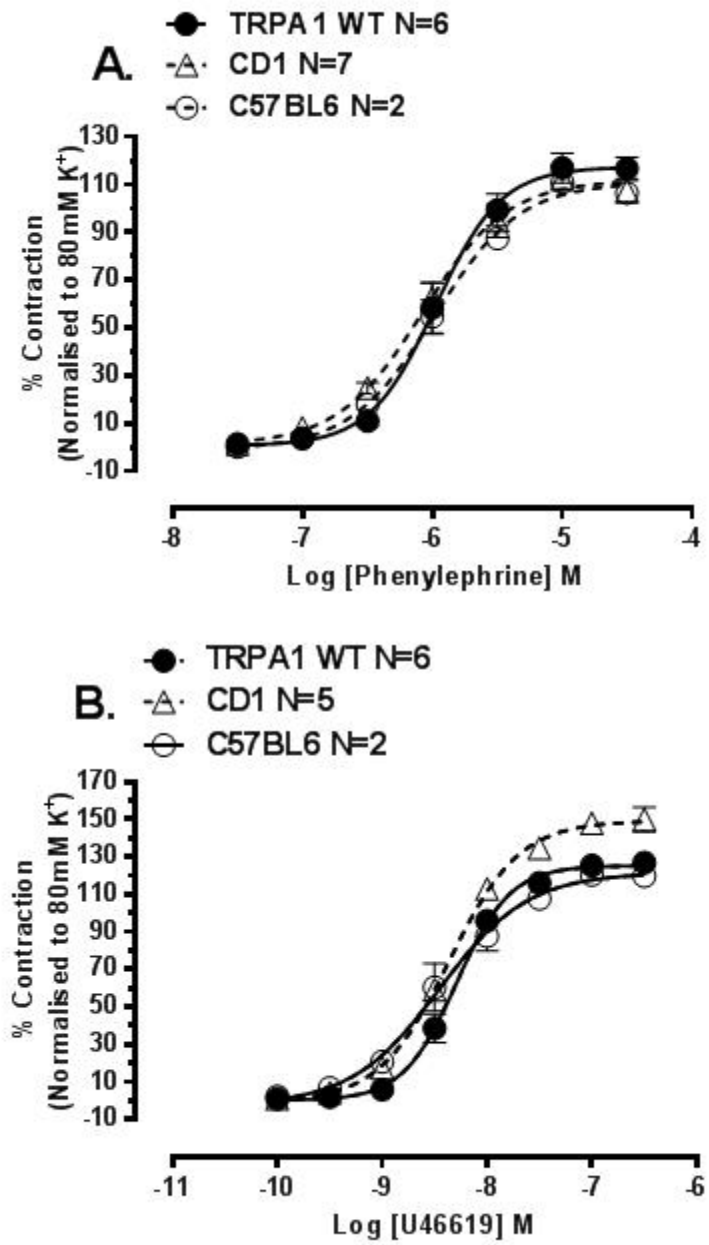

Figure 4.10 The contractile ability of mesenteric arteries from TRPA1 WT, CD1 and C57/BL6 mice in response to phenylephrine and U46619. Results show vessels without functional endothelium, pre-constricted with cumulative concentrations of phenylephrine (0.03-30µM A) or U46619 (0.1-300nM B) at 3 minute intervals. Data shown as a % of the maximal tension recorded in response to 3, 2 minute challenges with 80mM K+ Krebs. Graph shows pooled data from male and female paired mice. Statistically, potency of phenylephrine and U46619 are not different in TRPA1 WT and KO vessels.

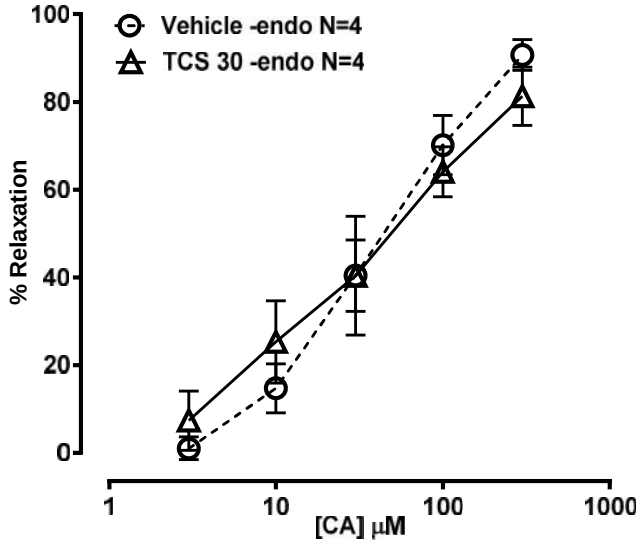

Figure 4.11 The Effect Of Cinnamaldehyde On Vascular Tone In CD1 Mouse Mesenteric Arteries Without Functional Endothelium, With And Without Addition Of The TRPA1 Antagonist TCS5861528. Results show vessels on a wire myograph, pre-constricted to U46619 (10nM, 5 minutes). The effect of cumulative concentrations of cinnamaldehyde are shown (CA, 3-300µM in ethanol) using % relaxation at 3 minutes. TCS5861528 (30µM in DMSO vehicle (TCS 30)), a TRPA1 receptor antagonist, was added to the bath 15 minutes before pre-constriction. Graph shows equal numbers of mixed gender mice. N numbers are as indicated. No significant differences seen in a two way ANOVA.

Investigating the effect of TRPA1 antagonist HC-030031 in rodent tissues

In this chapter I have shown cinnamaldehyde to cause concentration dependent relaxation of murine mesenteric arteries, in a manner that is significantly inhibited by genetic deletion of TRPA1 but not by addition of the TRPA1 antagonist HC-033031, or structurally related antagonist TCS5861528. I have also shown that cinnamaldehyde induces vasodilation *in vivo*, which can be significantly inhibited by TCS5861528. Several other studies have utilised HC-030031 to investigate the role of TRPA1 in isolated tissues, although none have demonstrated activity in wire myograph or on the mouse mesenteric artery. A summary of previous findings using HC-030031 in isolated tissues is shown in table 4.1. To investigate the activity of HC-030031 in whole tissue preparations in the wire myograph, several of the tissues used in this table were revisited.

The rodent airway has been used in several studies investigating TRPA1 function. Zhou *et al* (2011) and Yu and Ouyang (2008) used preparations of rat and guinea pig respiratory system in an organ bath. In both studies, neurones expressing TRPA1 were isolated from the tissue for the direct recording of neural activity. Neural responses to TRPA1 agonists could be inhibited by pre-incubation with HC-030031 at a concentration of 30µM and 10µM respectively. In another study, isolated bronchial rings from guinea pigs were maintained in an organ bath and contracted in response to the TRPA1 agonist's acreolin, crotonaldehyde, cinnamaldehyde (30µM) and those within cigarette smoke (Andre *et al.*, 2008). These responses were significantly inhibited by 50µM HC-030031. Contraction and relaxation of murine bronchi rings can be measured in the wire myograph and this formed the basis of the first preliminary investigation. Bronchi rings (2mm thickness) from one CD1 mouse were mounted on the wire myograph and held under approximately 2mN tension. The protocol was similar to that described by Manzini (1992) to investigate capsaicin induced relaxation of murine bronchi rings and the protocol was devised in collaboration with Dr Dom Spina. Rings contracted in response to 1µM

carbachol and relaxed to further addition of 1µM SP, an indication of the presence of the NK_1 receptor on the epithelium. This was later confirmed by use of an NK_1 receptor antagonist. After initial concentration response trials, 60µM cinnamaldehyde was chosen as a concentration producing submaximal relaxation of bronchi rings from carbachol pre-constriction (average 5.71 mN following 5 minute pre-constriction, dropping to 4.69mN after 3 minute cinnamaldehyde application). This is in contrast to the contraction response to 30µM cinnamaldehyde seen by Andre *et al* (2008) in isolated guinea pig bronchi rings. Upon further addition of SP (1µM), tension returned to baseline (average of 1.64mN). To investigate the role of TRPA1 in this response, bronchi were incubated with 50 and 100µM HC-030031 for 15 minutes before pre-constriction. This did not significantly influence the relaxation to cinnamaldehyde (figure 4.12) or later applied SP. The effect of the structurally distinct TRPA1 antagonist AP-18 (100µM) was also investigated in similar manner, however it failed to inhibit the response to cinnamaldehyde and SP, despite this concentration being identical to that recently used to inhibit TRPA1 dependent insulin secretion from whole pancreatic islets (Cao *et al*, 2012) and ten times higher than that recently used in a recent study investigating TRPA1 activities in the mouse airway (Nassini *et al.*, 2012). Representative traces of the raw data can be found in appendix figure 7.

Inability to block cinnamaldehyde induced vasorelaxation of the murine airway with TRPA1 antagonists indicates that TRPA1 may not be involved in the response. I also present preliminary data investigating the role of SP in cinnamaldehyde induced bronchi relaxation, as this is likely to represent a neuropeptide mediating relaxation following sensory neuron activation. Application of SR140333, a NK_1 antagonist, blocked the relaxation response to both cinnamaldehyde and exogenous SP. This data is included in figure 4.12 and in representative traces of the raw data in appendix figure 8. This concentration of NK_1 antagonist was previously used by Taylor-Clark *et al* (2008) to block substance P dependent contraction of the guinea pig bronchus in response to TRPA1 activation by 4-ONE. Together, this data presents a complex picture where SP appears to be

mediating the cinnamaldehyde response in the airway, suggesting a neurogenic mechanism, but where the role of TRPA1 cannot be confirmed by blockade using either HC-030031 or AP-18.

Preliminary findings suggested that bronchi rings would not yield a positive confirmation of HC-030031 antagonist ability. Further studies moved to a new tissue; namely the cerebral artery. Due to the size of this vessel, this could not be conducted using mice, therefore arteries were collected from albino Wistar rats. Earley *et al* (2009) have previously shown rat cerebral arteries to dilate in response to MO in the pressure myograph; a response which is blocked by just 3µM HC-030031. Therefore I attempted to reproduce this data in the wire myograph. Figure 4.13 shows the contractile ability of cerebral arteries challenged with cumulative concentrations of U46619 (0.1nM-1µM, additions every 2 minutes) or phenylephrine (0.03nM – 0.1µM additions every 2 minutes). Cerebral arteries contracted in response to U46619 with an EC_{50} of 1.7µM when calculated from raw tension data and 40.5nM when data is normalised to maximal response to high potassium depolarisation. Cerebral arteries were insensitive to phenylephrine. Representative traces of a cerebral artery cumulative concentration curve to U46619 are shown in appendix figure 9. Subsequently, 30nM U46619 (5 minutes) was used as a pre-constriction agent to investigate the effect of TRPA1 agonists. This concentration produced consistent and clear sub-maximal contractions which can be seen in the raw data trace in appendix figure 10, also showing the cumulative concentration curve in response to cinnamaldehyde (3-300µM, A). Results from the complete data-set are presented in figure 4.14., which also shows the observed relaxation response to MO (1-30µM, B). Both of these plots would benefit from further extension of the concentration response curve, but clearly demonstrate a concentration related relaxation response to TRPA1 agonists can be achieved in the rat cerebral artery. To investigate the TRPA1 dependency of this response, a single application of 300µM cinnamaldehyde was given following U46619 pre-constriction, producing an average relaxation of 80% over 3 minutes. Pre-treatment of the same vessels with HC-030031 (10µM, 15 minutes

before pre-constriction), at a concentration three times that used to block MO-induced vasodilation in the cerebral artery by Earley *et al* (2009), did not significantly alter this response (88% relaxation from pre-constriction). Addition of vehicle (0.05% DMSO in Krebs) in place of HC-030031 and vehicle (5ul ethanol) in place of cinnamaldehyde resulted in an average constriction over 3 minutes of 8%. A representative trace of the raw data can be seen in appendix figure 11. Therefore I conclude that HC-030031 is ineffective at blocking cinnamaldehyde induced vasorelaxation in rat cerebral arteries.

Nassini *et al* (2011) have recently described MO-induced vasorelaxation of guinea pig pulmonary arteries, which can be blocked with HC-030031 (10µM) or the CGRP receptor antagonist BIBN 4096 BS (BIBN) (10µM). Using a similar approach to that used for cerebral arteries, I investigated cinnamaldehyde induced vasorelaxation of rat pulmonary arteries. Figure 4.15 shows contraction of arterial rings to cumulative concentrations of U46619 (0.1nM-0.3µM) and phenylephrine (0.03-10nM), as previously described for cerebral arteries. Concentration dependent contraction to both stimuli was observed, however the response to phenylephrine was biphasic, with contraction turning to dilation at higher concentrations. U46619 application produced consistent contractions, with an EC_{50} of 47nM based on raw tension data and 46nM when tension is normalised to maximal depolarisation induced contraction. 100nM was selected as an appropriate concentration for pre-constriction, producing clear and consistent sub-maximal tension over 5 minutes. Representative tension traces showing cumulative concentration curves to U46619 in pulmonary arteries is presented in appendix figure 12. Cumulative concentration response curves to cinnamaldehyde (10-300µM) and MO (1-100µM) were conducted from U46619 pre-constriction. As shown in figure 4.16 A and B, concentration dependent relaxation was seen in response to cinnamaldehyde, however MO produced an incremental contraction on top of pre-constriction tone. Representative raw data traces of the dose dependent response to cinnamaldehyde can be seen in appendix figure 13. Similar to experiments previously presented in the cerebral artery, a single

cinnamaldehyde concentration was used to test the ability of HC-030031 (10µM) to inhibit the relaxation response to cinnamaldehyde. 300µM cinnamaldehyde produced an average vasorelaxation from U46619 pre-constriction of 72%. Following pre-treatment with HC-030031, at the concentration shown by Nassini *et al* (2011) to inhibit MO induced relaxation (10µM), a similar average relaxation was seen (74%). This demonstrates that HC-030031 does not inhibit cinnamaldehyde induced relaxation in the pulmonary artery (panel C). Additions of vehicle in place of HC-030031 (0.05% DMSO in Krebs) and in place of cinnamaldehyde (5ul ethanol), resulted in an average contraction of 9% over 3 minutes. A representative trace of the raw data can be seen in appendix figure 14.

Andrade *et al* (2011) have recently shown contraction in rat bladder strips treated with cinnamaldehyde. Contraction induced by 300µM cinnamaldehyde could be blocked with 60 and 100µM HC-030031, suggesting a TRPA1 dependent mechanism. Therefore I attempted to demonstrate the antagonistic ability of HC-030031 against cinnamaldehyde actions in the mouse bladder, using rings of tissue mounted in the wire myograph. Clear contraction was produced in response to 1µM carbachol, but no response was seen upon application of up to 600µM cinnamaldehyde. Tension in response to carbachol was not maintained sufficiently enough to study any potential relaxation effects of cinnamaldehyde. Therefore this data is not included.

My previously presented findings show cinnamaldehyde induced vasorelaxation of the mouse mesenteric artery to be slightly but significantly reduced in TRPA1 KO mice. No differences in the contractile ability of TRPA1 WT and KO mesenteric were found, suggesting a role for TRPA1 in this vasodilative response. I then attempted to confirm these findings using pharmacological antagonists of the TRPA1 receptor. HC-030031 is the most commonly used TRPA1 agonist to date, often used in isolated cell and neurone studies. HC-030031 was ineffective at reducing the relaxation response induced by cinnamaldehyde at several concentrations, in WT mesenteric arteries from several strains. This was

also the case for the related antagonist TCS5861528. Several attempts were made to ascertain if HC-030031 could block cinnamaldehyde responses in isolated tissues mounted in the wire myograph, which is important as a positive control. As described in Table 4.1, several tissues have been used to study TRPA1 and utilised HC-030031. In the rodent bronchi, cerebral artery and pulmonary artery I was able to demonstrate cinnamaldehyde induced relaxation responses. However none of these responses were affected by HC-030031 at concentrations similar and above those used in similar published studies. My findings are summarised in summary 2. It is hard to conclude whether this data demonstrates a lack of function of this antagonist in the wire myograph preparation, or if the response in not mediated by TRPA1. Several extensions to this data are possible, including collection of full cinnamaldehyde concentration response curves under a range of HC-030031 concentrations and the testing of HC-030031's ability to block other TRPA1 agonist responses in these tissues. Despite this, several lines of evidence suggest that the mechanism of cinnamaldehyde induced relaxation may be sensory neurone and TRPA1 mediated, and there is little evidence to eliminate this option. The remainder of this chapter discusses the investigation of the mechanism driving cinnamaldehyde induced vasorelaxation of the mouse mesenteric artery.

Summary 2; Investigating the effect of TRPA1 antagonist HC-030031 in rodent tissues

- Cinnamaldehyde causes relaxation responses in rodent bronchi rings, cerebral arteries and pulmonary arteries.
- In murine bronchi this response is not affected by the TRPA1 antagonists HC-030031 or AP-18, but is almost abolished by NK_1 antagonism, suggesting a SP mediated mechanism.
- HC-030031 also does not alter this response in rat cerebral and pulmonary arteries. Rat cerebral arteries also relax in response to MO.

- A positive confirmation of HC-030031 activity in the wire myography tissue mount was not obtained. This does not allow us to conclude if our previous results suggest a lack of TRPA1 activity in the cinnamaldehyde response, or a loss of antagonist binding.

	Concentration of HC-030031	Tissue and Species	Experimental Set-up	Findings
Capasso *et al*, 2011	10µM dissolved in DMSO	Ileum and Colon, Mice	Measurement of longitudinal contractions from ileum/colon segments in an organ bath.	No reduction in tissue contraction to mustard oil (10^{-4}-10^{-7}M). They find that higher concentrations of HC-030031 are antispasmodic, inhibiting contraction to acetylcholine (Data not shown).
Zhou *et al*, 2011	30µM dissolved in DMSO	Lung and bronchi, Rat	Isolated lung and bronchi in an organ bath, with vagal nerve trunk isolated and activity of fine branches recorded by suction electrode.	Inhibition of cinnamaldehyde (1mM) induced afferent vagal nerve activity. No reduction in cold (8°C saline) induced afferent nerve activity.
Andrade *et al,* 2011	10, 30, 60, 100µM dissolved in DMSO and Tween 80.	Bladder strips, Rat	Contraction of bladder strips (10mm by 4mm) from sham mice or following spinal cord injury in an organ bath.	Estimated IC50 values against cinnamaldehyde (300µM) was 46.3µM in sham treated mice and 31.2µM in bladder strips following spinal cord injury. In sham mice, only 60 and 100µM HC-030031 significantly inhibited bladder contraction.
Krueger *et al,* 2010	10µM dissolved in DMSO	Colon segments, Guinea pig and human patients	Measured secretory responses to H2S (0.2-1mM) using an Ussing chamber.	No significant alterations.
Earley *et al*, 2009	3µM dissolved in DMSO	Cerebral artery, Rat	Mounted in a pressure myograph.	Luminally applied HC-030031 significantly inhibits vasodilation to 100µM mustard oil.
Yu and Ouyang, 2008	10µM dissolved in DMSO	Oesophagus/ Trachea, Guinea Pig	Vagal nerves (Jugular and nodose) are isolated within tissue maintained in an organ bath. Neural activity is recorded during oesophageal pressure distension.	HC-030031 prevents mechanical hypersensitivity following bradykinin treatment.

	Concentration of HC-030031	Tissue and Species	Experimental Set-up	Findings
Andre *et al*, 2008	50µM	Bronchi, Guinea Pigs	Measurement of bronchial ring (2mm) contractions in an organ bath.	HC-030031 significantly inhibits contraction to cigarette smoke extract, crotonaldehyde, cinnamaldehyde (30µM) and acreolin.
Nassini *et al*, 2011	10µM	Pulmonary artery, Guinea Pigs	Measurement of arterial contraction in an organ bath	HC-030031, BIBN and capsaicin desensitisation significantly reduces arterial relaxation in response to MO (10µM).

Table 4.1 The use of HC-030031 as a TRPA1 antagonist in isolated tissue studies. Describing the concentration, solvent, tissue and species, experimental set-up and findings from a range of published studies using the TRPA1 antagonist HC-030031.

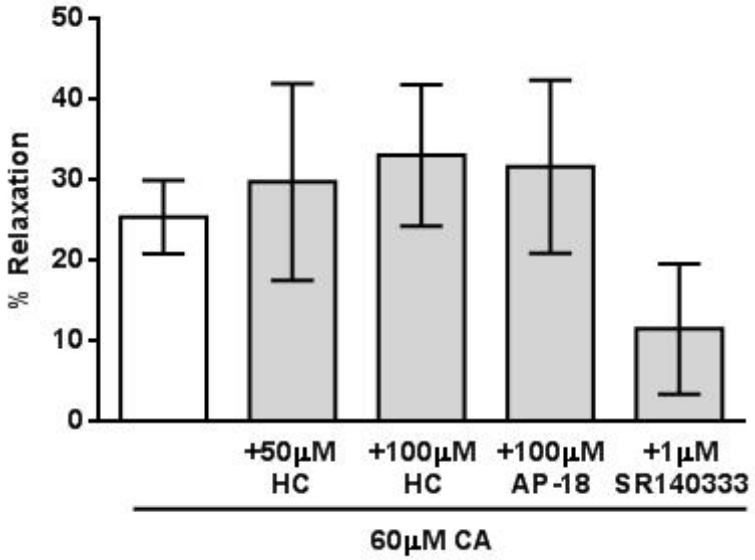

Figure 4.12 The Effect Of Cinnamaldehyde On CD1 Mouse Bronchi Rings Arteries Treated with TRPA1 Or SP Antagonists. Results show using % relaxation at 3 minutes of bronchi mounted on a wire myograph, pre-constricted to carbachol (1µM, 5 minutes). The effect of 60µM cinnamaldehyde (CA in 5µl ethanol) is shown in the open bar, with shaded bars showing the effect of 15 minute pre-treatment with HC-030031 (50 or 100µM in 0.05% DMSO in Krebs), AP-18 (100µM in 5ul DMSO) or SR140333 (1µM in 0.01% BSA in water). Graph shows bronchi with intact epithelium from one male mouse, N for bronchi rings is 3 for CA alone, plus pretreatments of AP-18 and SR140333. N is two rings for other treatments. As N is low and from one animal only, SEM is indicative of variation only.

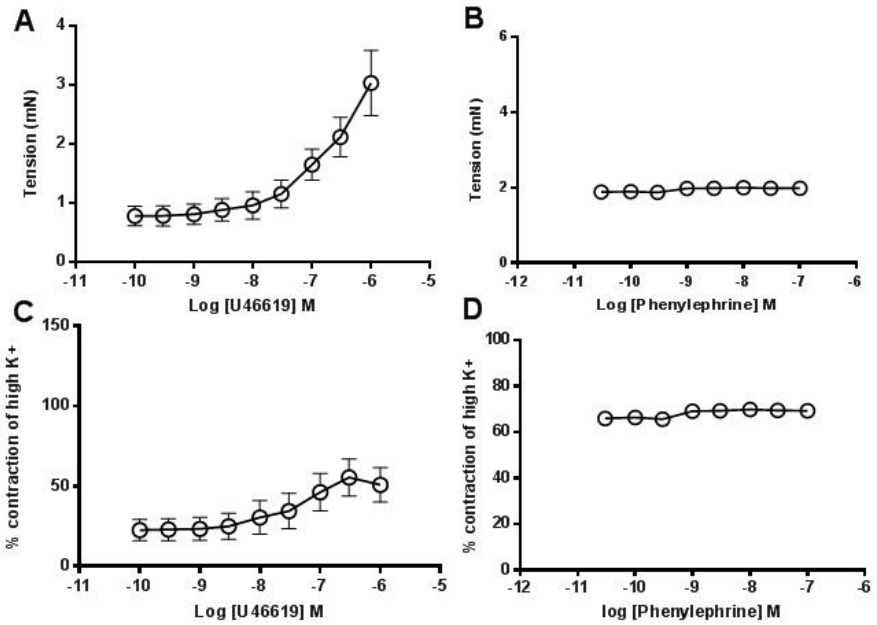

Figure 4.13 The Contractile Response Of Rat Cerebral Arteries To U46619 And Phenylephrine. Results show raw tension measurements (A/B) and tension as a % of maximal response to Krebs containing 80mM potassium (C/D) in response to U46619 (0.1nM-1µM in water A/C) and phenylephrine (0.03nM-0.1µM in water B/D). Cumulative concentration curves were constructed with additions every 2 minutes to segments of rat cerebral artery mounted on a wire myograph. Graph shows a total of 4 rats with 9 vessels in A, 1 in B, 8 in C and 1 in D, with and without intact endothelium.

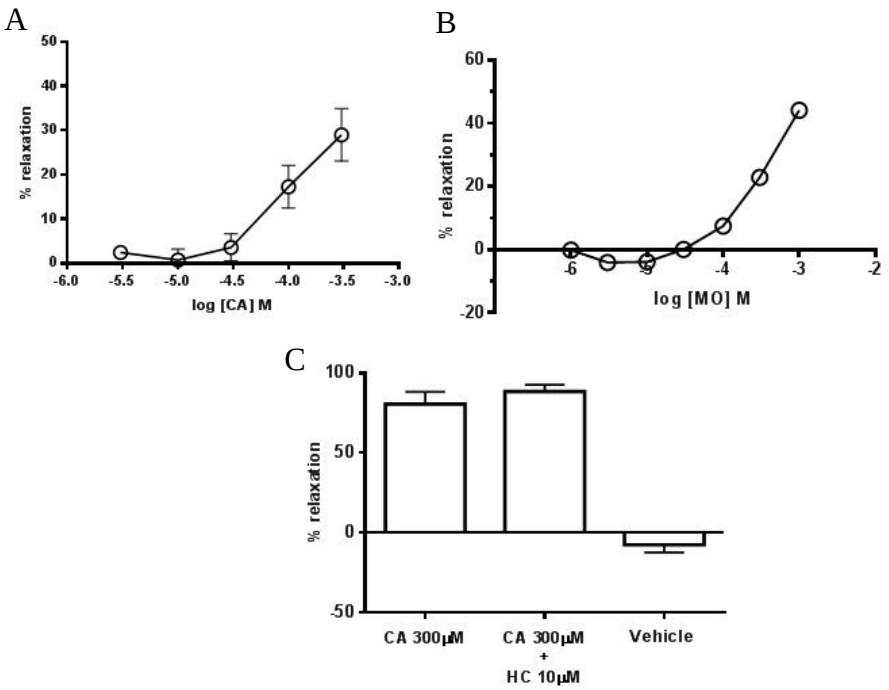

Figure 4.14 The Effect of TRPA1 Agonists On Rat Cerebral Arteries With and Without Treatment With TRPA1 Antagonists. Results show % relaxation from U46619 (30nM, 5 minutes) pre-constriction of rat cerebral arteries subject to cumulative concentration additions of cinnamaldehyde (CA 3-300µM every 3 minutes, A) or MO (1-30µM every 3 minutes, B). The effect of a single concentration of cinnamaldehyde (300µM in 5ul ethanol) or vehicle following pre-constriction is shown in C, where 15 minute pre-treatment with HC-030031 (10µM in 0.05% DMSO in Krebs) does not affect % relaxation. Graph shows a total of 4 rats with 7 vessels in A, 1 in B and 7 in each bar in C, all with and without intact endothelium.

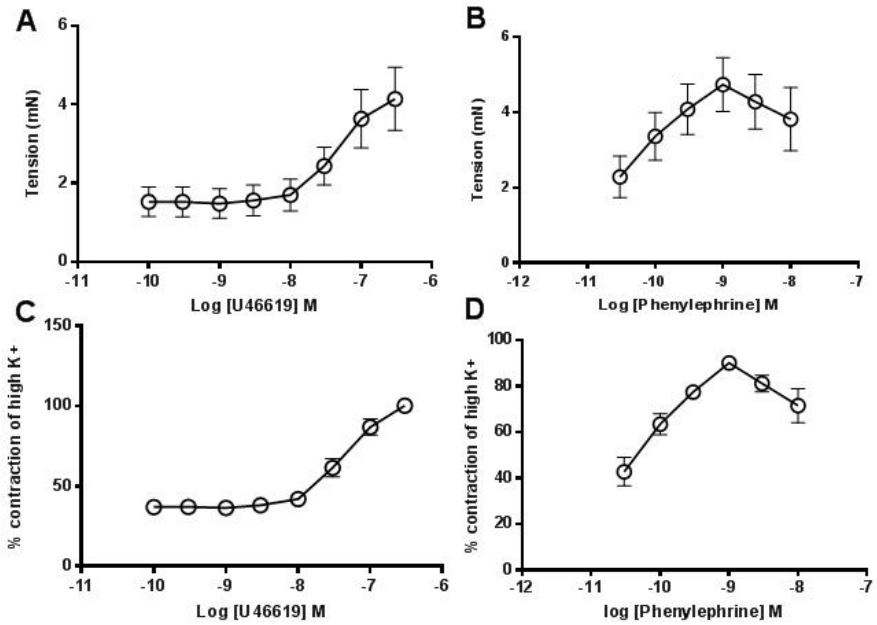

Figure 4.15 The Contractile Response Of Rat Pulmonary Arteries To U46619 And Phenylephrine. Results show raw tension measurements (A/B) and tension as a % of maximal response to Krebs containing 80mM potassium (C/D) in response to U46619 (0.1nM-0.3µM in water A/C) and phenylephrine (0.03nM-10nM in water B/D). Cumulative concentration curves were constructed with additions every 2 minutes to segments of rat pulmonary artery mounted on a wire myograph. Graph shows a total of 4 rats with 12 vessels in A, 3 in B, 9 in C and 3 in D, with and without intact endothelium.

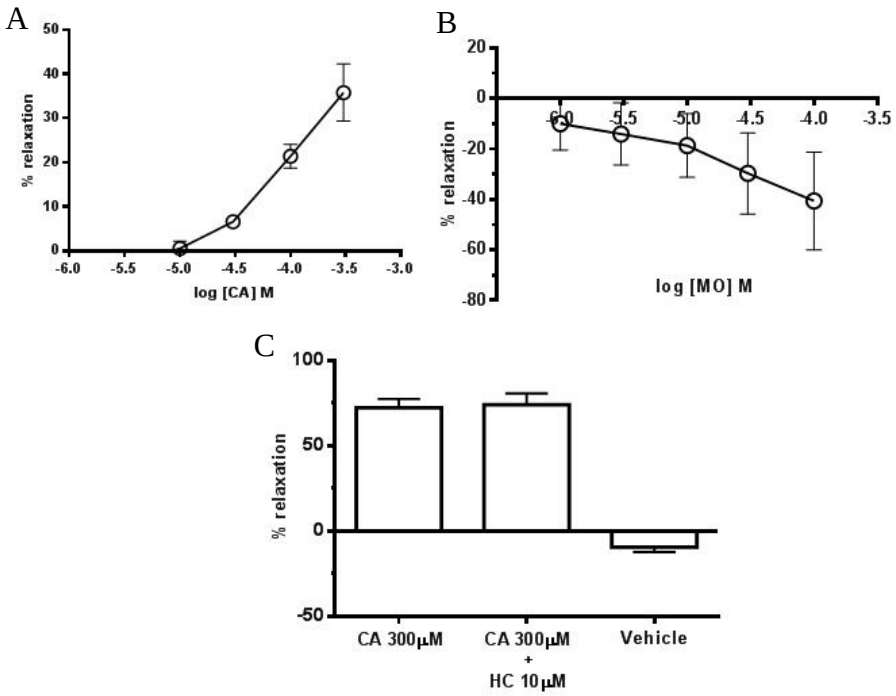

Figure 4.16 The Effect of TRPA1 Agonists On Rat Pulmonary Arteries With and Without Treatment With TRPA1 Antagonists. Results show % relaxation from U46619 (100nM, 5 minutes) pre-constriction of rat pulmonary arteries subject to cumulative concentration additions of cinnamaldehyde (CA 10-300µM every 3 minutes, A) or MO (1-100µM every 3 minutes, B). The effect of a single concentration of cinnamaldehyde (300µM in 5ul ethanol) or vehicle following pre-constriction is shown in C, where 15 minute pre-treatment with HC-030031 (10µM in 0.05% DMSO in Krebs) does not affect % relaxation. Graph shows a total of 4 rats with 6 vessels in A, 3 in B and 7-8 in each bar in C, all with and without intact endothelium.

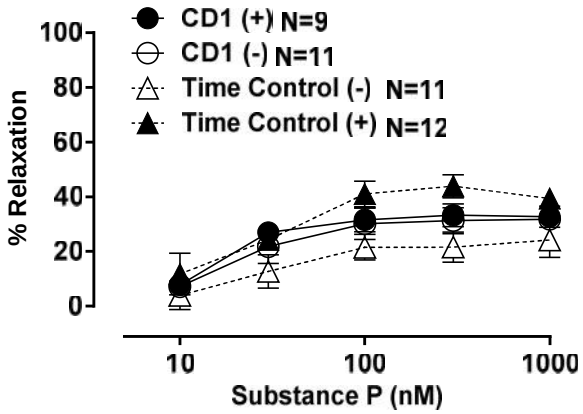

Figure 4.17 The Effect Of SP On Vascular Tone In CD1 Mouse Mesenteric Arteries. Results show vessels mounted on a wire myograph, pre-constricted to U46619 (10nM, 5 minutes). The effects of cumulative concentrations of substance P are shown (10-1000nM in 0.01% BSA in water) using % relaxation at 3 minutes. Time controls show natural relaxation of the tissue over the same time of pre-constriction. Graph shows mixed gender mice. N numbers are as indicated. Not significantly different in a two-way ANOVA.

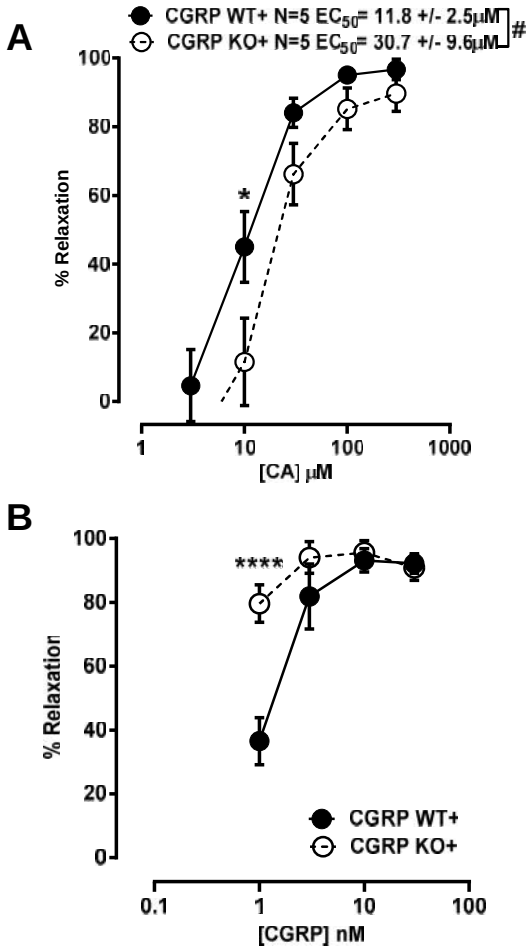

Figure 4.18 The Effect Of Cinnamaldehyde And αCGRP On Vascular Tone Of αCGRP WT And KO Mesenteric Arteries. Results show endothelial intact vessels mounted on a wire myograph, pre-constricted to U46619 (10nM, 5 minutes). A) The effect of cumulative concentrations of cinnamaldehyde (CA, 3-300µM in ethanol) or B) cumulative concentrations of αCGRP (1-30nM), measured as % relaxation at 3 minutes is shown. Graph shows female vessels with functional endothelium. Statistics are from two way ANOVA with Bonferroni's post test. *$p<0.05$, ****$p<0.0001$ WT+ compared to KO+. EC_{50} shown for cinnamaldehyde only, statistics are from a two-way unpaired t-test, #$p<0.05$. N numbers as indicated.

Investigating The Mechanism Of Cinnamaldehyde Induced Vasorelaxation

Several investigations of TRPA1 agonist induced vasorelaxation have demonstrated C-fibre and neuropeptide involvement. Therefore I examined the contribution of the neuropeptides substance P and CGRP to the cinnamaldehyde vasorelaxation response. Figure 4.17, shows cumulative concentration response curves to substance P (1-1000nM), in CD1 WT mice, with and without functional endothelium. CD1 mice were used in these experiments as a substitute for TRPA1 WT mice, which were the ideal choice but not available at the time these studies were conducted. CD1 mice have a different genetic background to that of TRPA1 WT and KO mice, but show similar responses to contractile agents and cinnamaldehyde application, suggesting that the effect of TRPA1 activation may be similar. Time control relaxation from pre-constriction is also shown. Representative traces of raw data collected from cumulative concentration response curves to CGRP and SP, in vessels without functional endothelium, are shown in appendix figure 15. The concentration range was similar to that used by Ahluwalia and Vallance (1997), who constricted rat mesenteric veins to 1-10000nM substance P. In my model, substance P treated vessels relaxed to a maximum of about 30% from pre-constriction. This is in line with that of the natural relaxation of the tissue over time and shows no significant differences from time controls. These differences suggest that substance P does not relax small diameter mesenteric arteries of the mouse. A similar lack of effect was seen by Berthiaume *et al* (1997), who saw no effect of 0.5nM substance P applied to the mouse mesenteric circuit (arteries and veins) pre-constricted with U46619.

CGRP is one of the most potent microvasculature vasodilators identified to date (Brain and Grant, 2004). It is released from sensory neurones and is implicated in TRPA1 induced vasodilation through studies that use a range of agonists, as discussed previously. Here, I used αCGRP KO mice to investigate its contribution to cinnamaldehyde induced vasorelaxation

(Figure 4.18). These mice have a C57/BL6 background, something partially shared with TRPA1 WT and KO mice, and display identical pharmacological responses to contractile agents. Cinnamaldehyde caused a concentration dependent relaxation of both αCGRP WT and KO arteries (Figure 4.18A). Cinnamaldehyde displayed significantly decreased potency in αCGRP KO vessels, shown by a significantly increased EC_{50}. Additionally, there was significantly less relaxation of U46619 pre-constricted vessels to 10μM cinnamaldehyde where αCGRP was deleted. Therefore, this suggests that αCGRP plays an important role in cinnamaldehyde induced vasorelaxation. I additionally investigated the ability of αCGRP to relax pre-constricted αCGRP WT and KO mesenteric arteries. I found vessels from both genotypes to be very sensitive to αCGRP; however αCGRP KO arteries were significantly more reactive to 1nM αCGRP than αCGRP WT vessels. This is expected from previous studies using αCGRP KO mice, showing them to be more responsive to exogenously applied αCGRP than αCGRP WT mice (Gangula *et al.*, 2000). This is likely to be via an increase in receptor mediated sensitivity when endogenous αCGRP is removed (Smillie and Brain, 2011). Representative traces of raw data collected from CGRP WT and KO mesenteric arteries treated with cumulative concentrations of cinnamaldehyde and αCGRP are shown in appendix figure 16.

I aimed to confirm my findings using $CGRP_{8-37}$, a peptide antagonist of the CGRP receptor. A range of concentrations are used in studies that involve mesenteric vessels (generally ranging from 1μM to 10μM). However, this compound is expensive and thus I aimed to find the lowest effective concentration. I have characterised my chosen concentration. In figure 4.19 I illustrate the effect of $CGRP_{8-37}$ (3μM), on αCGRP cumulative concentration response curves (1-100nM). This concentration of antagonist is well within its expected activity range as seen in other publications. Similarly, αCGRP is a potent vasodilator and has previously been used at these concentrations and below, to relax mesenteric arteries in a wire myograph (Meens *et al.*, 2009). Panel A and B, shows that αCGRP causes a concentration dependent vasorelaxation in vessels with and

without functional endothelium. In both cases, the concentration response curve is shifted to the right on pre-incubation with 3μM $CGRP_{8-37}$, which is significant in places, indicating decreased αCGRP potency (For EC_{50}, see later). This confirms that the antagonist is effective. When all of the data is overlaid in panel C, vehicle treated vessels with and without functional endothelial cells showed comparable reductions in αCGRP mediated relaxation. However, in both groups, addition of the CGRP receptor antagonist causes a statistically significant reduction in αCGRP induced relaxation. The EC_{50} for αCGRP on each animals' mesenteric arteries are calculated, in the presence and absence of $CGRP_{8-37}$. The results of this are shown in more detail in figure 4.20. Reflecting conclusions from the concentration response curves, the potency of αCGRP on vessels with and without functional endothelium is similar. Incubation with $CGRP_{8-37}$ increases the EC_{50} in both groups, however the increase is only significant in vessels with functioning endothelium suggesting that the endothelium may play a role in αCGRP induced vasorelaxation. Endothelium dependent and independent vasodilatory roles of CGRP have been shown in the literature (Brain and Grant, 2004).

Having established an effective concentration of peptide CGRP receptor antagonist, I used it to further investigate the involvement of CGRP in the cinnamaldehyde response. The concentration chosen was effective at a range of tissue relevant concentrations of exogenous αCGRP, thus I was confident it would be appropriate for antagonism of stimulus released endogenous αCGRP. Figure 4.21 shows cumulative cinnamaldehyde concentration response curves in CD1 TRPA1 WT vessels, with and without functional endothelium and with and without application of peptide CGRP receptor antagonist. Results show no significant changes in cinnamaldehyde responses with addition of the peptide CGRP antagonist. Representative traces of the raw data are shown in appendix figure 17. Panel A shows the antagonistic effect of $CGRP_{8-37}$ on the cumulative concentration response to αCGRP, whereas panel B shows no effect of $CGRP_{8-37}$ on the cumulative concentration response to cinnamaldehyde. These findings conflict with data from αCGRP KO mice and may represent

an inability for this concentration of $CGRP_{8-37}$ to effectively access and block the CGRP receptor in these tissues. Despite efforts to validate this concentration of $CGRP_{8-37,}$ higher concentrations may be needed to be to block the endogenously released CGRP. Again, there was a small and non significant decrease in relaxation to cinnamaldehyde was seen when endothelium was removed.

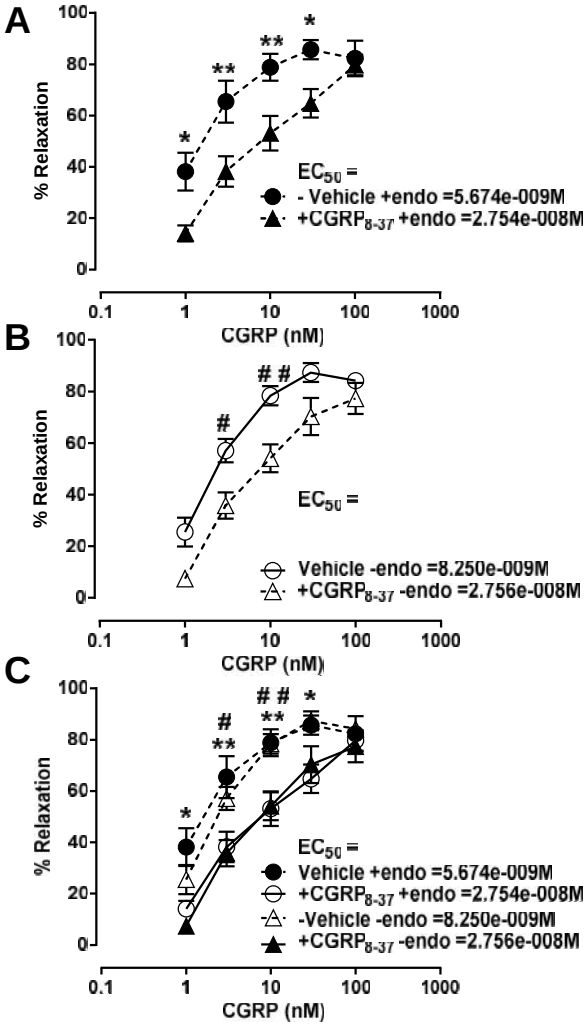

Figure 4.19 The Effect Of Peptide CGRP Receptor Antagonist On αCGRP Induced Vasorelaxation Of CD1 Mouse Mesenteric Arteries With And Without Functional Endothelium. Results show vessels on a wire myograph, pre-constricted to U46619 (10nM, 5 minutes). The effect of cumulative concentrations of αCGRP are shown (1-100nM) as % change in tension at 3 minutes. $CGRP_{8-37}$ (3μM), a CGRP receptor antagonist, was added to the bath 15 minutes before pre-constriction. Graph shows mixed gender mice. A. Without functional endothelium N=12 for points 1-30nM, N=5-9 100nM. Statistics are from two way ANOVA with Bonferroni's post test, **$p<0.01$, *$p<0.05$ comparing $CGRP_{8-37}$ and vehicle. B. With functional endothelium N=13-15 for 1-30nM, N=5-9 for 100nM. # #$p<0.01$, #$p<0.05$ comparing $CGRP_{8-37}$ and vehicle. C. Combined.

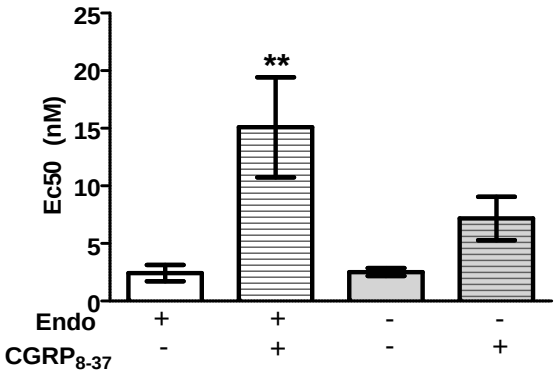

Figure 4.20 Potency Of αCGRP Induced Vasorelaxation In CD1 Mouse Mesenteric Arteries, With And Without Functional Endothelium And With And Without Addition Of Peptide CGRP Receptor Antagonist. Results show vessels on a wire myograph, pre-constricted to U46619 (10nM, 5 minutes). EC_{50} calculated from αCGRP cumulative concentration response, as seen in previous figures. $CGRP_{8-37}$ (3μM), a CGRP receptor antagonist, was added to the bath 15 minutes before pre-constriction. Graph shows mixed gender mice. N=11-12. Statistics are from one way ANOVA with Bonferroni's post test. **p<0.01 compared to same vessels without $CGRP_{8-37}$.

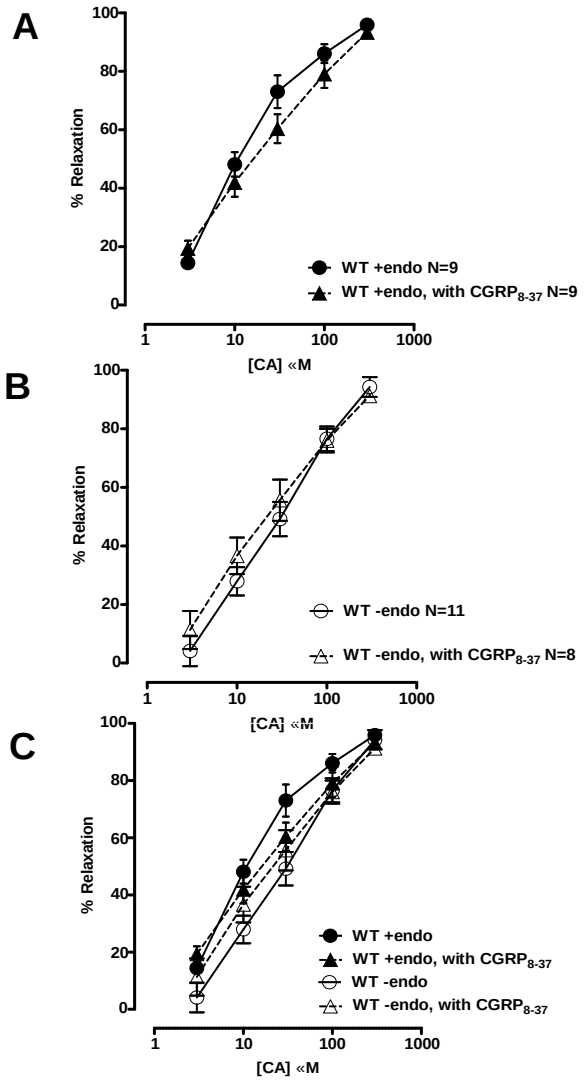

Figure 4.21 The Effect Of Cinnamaldehyde Induced Vasorelaxation In CD1 Mouse Mesenteric Arteries, With And Without Addition Of Peptide CGRP Receptor Antagonist. Results show vessels mounted on a wire myograph and pre-constricted to U46619 (10nM for 5 minutes). The effect of cumulative concentrations of cinnamaldehyde are shown (CA, 3-300μM in ethanol) using % change in tension at 3 minutes. $CGRP_{8-37}$ (3μM in 0.01% BSA in water) a CGRP receptor antagonist, is added to the bath 15 minutes before pre-constriction. A) Vessels with functional endothelium (+endo) B) Vessels without functional endothelium (-endo), C) combined data. Graph shows mixed gender mice. N numbers are as indicated. No significant differences in a two way ANOVA.

The previously presented data using αCGRP KO mice suggested a CGRP component was present in the vasorelaxation model. This was not supported by the use of the peptide CGRP receptor antagonist $CGRP_{8-37}$. To clarify the findings, I used another CGRP receptor antagonist BIBN. This is a well characterised non-peptide antagonist, developed by Boehringer for use in migraine and first characterised by Doods *et al* (2000). This molecular antagonist is more stable and 200x more potent than $CGRP_{8-37}$ at the human CGRP receptor, being 150x less potent at the rat CGRP receptor (Doods *et al.*, 2000, Verheggen *et al.*, 2002). I used a concentration of 10μM, as this has been previously used effectively in mouse aortic ring relaxation within this group, where it blocked the action of up to 10nM αCGRP (Grant *et al.*, 2004). Use of multiple concentrations of this antagonist would have been preferable in this study, however this drug is not commercial available and the company is not currently providing it for academic studies. Therefore, I chose a concentration of this compound previously validated in our laboratory. At this concentration, the slow kinetics of the antagonist mean that receptor block is almost insurmountable, resembling that of a non-competitive antagonist (Hay and Poyner, 2005). In figure 4.22, BIBN is shown to significantly inhibit cinnamaldehyde induced vasorelaxation in vessels with functional endothelium. Representative raw data traces showing cumulative concentrations curves to cinnamaldehyde in the presence of BIBN or its vehicle, are shown in appendix figure 18.

The data collected using BIBN and vessels from αCGRP KO mice suggest a strong involvement of CGRP in the cinnamaldehyde response. This conflicts with data using the peptide antagonist $CGRP_{8-37}$, likely due to the concentration selected only producing a small inhibition of endogenous CGRP vasorelaxation. The effect of BIBN seems to be more pronounced than that observed in the αCGRP KO mice. The reasons for this are not clear, but may be related to the different mechanisms of CGRP antagonism. In αCGRP KO mice, the αCGRP protein is lost, which may cause compensation from other dilator peptides such as β-CGRP. αCGRP KO mice were additionally shown to be more sensitive to CGRP receptor

agonism. Together, this data shows that the CGRP receptor and the αCGRP protein are both involved in the vasorelaxation response to cinnamaldehyde.

Recent investigations using MO and cinnamaldehyde have identified hyperpolarisation of the vascular smooth muscle as a potential mechanism of action (Earley *et al.*, 2009)(See table 1.1). The results presented in this chapter have shown cinnamaldehyde induced vasorelaxation *ex vivo*, to be partially TRPA1 dependent and largely endothelial independent (Figure 4.1/4.3). Data collected using αCGRP KO mice and the non peptide CGRP receptor antagonist BIBN, have also suggested that there is a CGRP mediated component to cinnamaldehyde induced vasorelaxation. To investigate the mechanism further, I used vessels without functional endothelium pre-constricted with 30mM K^+ Kreb's. Normal Kreb's has only 4mM K^+. Increases in extracellular potassium can hyperpolarise smooth muscle cells via several mechanisms. At low levels such as 10mM, increases in Na^+/K^+ and K_{IR} channel activation cause hyperpolarisation of the tissue due to increased K^+ permeability, pushing the membrane potential towards the K^+ equilibrium potential, as described by the Nernst equation. At concentrations such as the 30mM used in my Krebs, there is a diminished transmembrane K^+ gradient, along with additional Na^+/K^+ and K_{IR} channel activation, increasing the resting potential and causing a small amount of depolarisation of the membrane, whilst blocking further K^+ efflux and hyperpolarisation. Therefore, pre-constriction using 30mM K^+ Kreb's is often used as a method of pre-constriction which can also determine if a dilatory response is being mediated by hyperpolarisation. Depolarisation by increasing extracellular K^+ has previously been used in the priming stages of the experiment, where I use an 80mM K^+ Kreb's solution to fully depolarise the tissue and gain an understanding of the maximum constriction that can be achieved for each vessel. This concentration greatly reduces the potassium gradient across the membrane and opens K_{IR} channels by releasing their rectification, allowing the membrane potential to depolarise to the new resting membrane potential which is much more positive than that in normal extracellular conditions,

which increases the opening probability of voltage operated sodium channels. Resultant further depolarisation due to sodium entry will activate voltage operated calcium channels, leading to calcium influx and tissue contraction. However, high levels of K^+ such as 80mM, are damaging to tissues over a period of more than a few minutes due to cell swelling and the depletion of ATP by saturation of the sodium potassium exchanger. Figure 4.23 shows that cumulative applications of cinnamaldehyde are unable to fully relax vessels which are constricted with 30mM K^+ Kreb's. This is likely to be due to the inability of the tissue to hyperpolarise, therefore blocking cinnamaldehyde signalling and vasorelaxation via this mechanism. The potency and efficacy of cinnamaldehyde is greatly decreased in comparison to vessels in normal Kreb's (see previous graphs), with relaxation in 30mM K^+ Kreb's not reaching 50% even at the peak of the concentration response curve. However, these higher concentrations of cinnamaldehyde, did significantly relax the vessels compared to that of the time relaxed control. This suggests that mechanisms other than hyperpolarisation are also occurring in the cinnamaldehyde induced vasorelaxation response. Representative traces of the raw data in appendix figure 19 show the cumulative concentration curve to cinnamaldehyde is strongly inhibited during pre-constriction using 30nM K^+.

TRPA1 is a non-selective cation channel, with a preference for calcium and sodium permeation. In rat mesenteric artery smooth muscle, the BK_{Ca} channel is highly expressed (Hilgers *et al.*, 2006) and activated by calcium influx. Therefore, calcium influx from the opened TRPA1 channel could potentially activate BK_{Ca} channels in the mouse mesenteric artery, causing vessel relaxation. To investigate this as a potential link between TRPA1 and hyperpolarisation, vessels without functional endothelium were treated with the BK_{Ca} channel blocker paxilline (1μM). This concentration is widely used and has been shown by Tammaro *et al* (2004) to greatly reduce channel activity. Figure 4.24 shows no significant shifts in the cinnamaldehyde cumulative concentration response curve when vessels are incubated with paxilline, compared to vehicle incubated control. This suggests TRPA1 is not causing vasorelaxation via a direct activation of

receptors expressed on vascular smooth muscle cells. Representative raw data traces showing the cumulative concentration response curve to cinnamaldehyde in the presence of paxilline or its vehicle are shown in appendix figure 20.

Summary 3; The Mechanism Of Cinnamaldehyde Induced Vasorelaxation

- Cinnamaldehyde induced vasorelaxation was significantly reduced in αCGRP KO vessels, along with those treated with the non-peptide CGRP receptor antagonist BIBN. However, it was not affected by a concentration of the peptide CGRP antagonist $CGRP_{8-37}$ that reduced exogenous CGRP induced vasorelaxation.
- SP does not cause vasorelaxation of mesenteric arteries, therefore is not involved in the cinnamaldehyde response.
- Blocking hyperpolarisation significantly blunts cinnamaldehyde induced vasorelaxation, therefore is likely to be a key mediator. However, this is not occurring via the BK_{Ca} channel, strengthening conclusions of a CGRP and sensory neurone dependent mechanism.

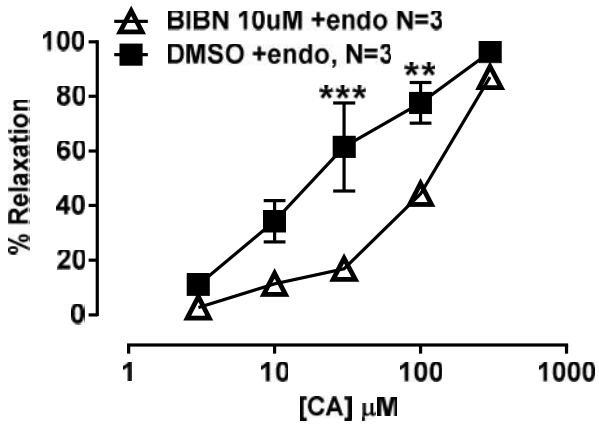

Figure 4.22; The Effect Of Cinnamaldehyde Induced Vasorelaxation In CD1 Mouse Mesenteric Arteries, With And Without Addition Of Non-Peptide CGRP Receptor Antagonist

Results show endothelial intact vessels mounted on a wire myograph, pre-constricted to U46619 (10nM, 5 minutes). 10µM BIBN4096BS (BIBN) was added 15 minutes before pre-constriction and cumulative concentrations of cinnamaldehyde (CA, 3-300µM in ethanol). Graph shows male mice. Statistics are from two-way ANOVA with Bonferroni's post test. **$p<0.01$, ***$p<0.001$ compared to DMSO control. N numbers as indicated.

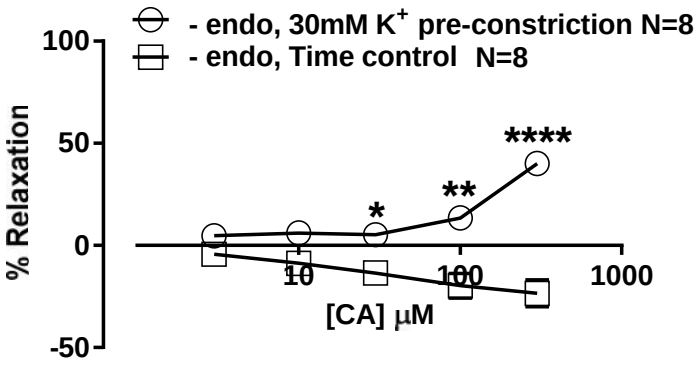

Figure 4.23 The Effect Of Cinnamaldehyde On The Vascular Tone Of CD1 Mesenteric Arteries, Pre-constricted With 30mM K^+ Kreb's. Results show vessels without functional endothelium mounted on a wire myograph, pre-constricted to 30mM K^+ Kreb's for 3 minutes, preventing hyperpolarisation of the smooth muscle. The effect of cumulative concentrations of cinnamaldehyde are shown (CA, 3-300μM) using % change in tension at 3 minutes. Time control line shows natural relaxation of the tissue over the time of the pre-constriction. Graph shows data from mixed gender mice. Statistics are from two-way ANOVA with Bonferroni's post test. ****$p<0.0001$, **$p<0.01$, *$p<0.05$, comparing CA treated vessels to time control. N numbers are as indicated.

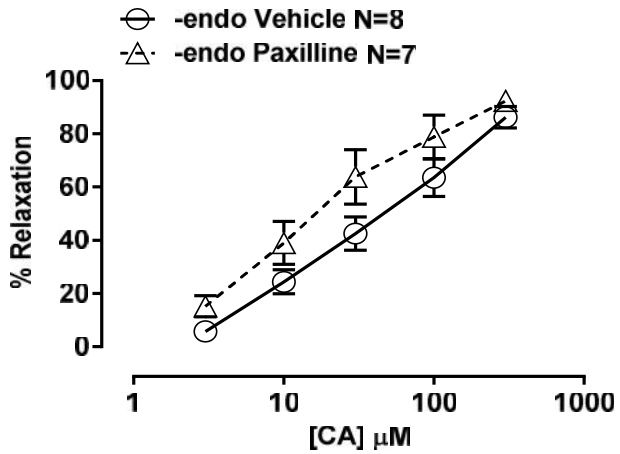

Figure 4.24 The Effect Of Cinnamaldehyde On Vascular Tone Of CD1 Mesenteric Arteries, With And Without Antagonism Of The BkCa Channel. Results show vessels without functional endothelium mounted on a wire myograph, pre-constricted to U46619 (10nM, 5 minutes). Paxilline (BK_{Ca} channel antagonist, 1µM in DMSO) or vehicle was added 15 minutes before pre-constriction. The effect of cumulative concentrations of cinnamaldehyde are shown (CA, 3-300µM) as % change in tension at 3 minutes. Graph shows data from mixed gender mice. N numbers are as indicated. No significant differences are seen in a two-way ANOVA.

Discussion

In this chapter, I have demonstrated that the TRPA1 agonist cinnamaldehyde, but not MO, causes concentration dependent vasorelaxation of murine mesenteric arteries. This was found to be largely endothelial independent, thus vascular smooth muscle derived, with a TRPA1 component defined by genetic but not pharmacological interventions. I also show data demonstrating that the ability of mesenteric arteries to constrict in the presence of the contractile agents phenylephrine and U46619, is not affected by genetic TRPA1 deletion and is not significantly altered in mice from different strain backgrounds. Data from my colleague Aisah Aubdool was shown, demonstrating that this is dilation is relevant *in vivo* at a peripheral site, where increases in blood flow following topical application of cinnamaldehyde to the mouse ear were reduced in mice pre-treated with TRPA1 antagonist and in TRPA1 KO mice. I also show data from several rodent tissue types where inhibitory activity of the TRPA1 antagonist HC-030031 against cinnamaldehyde relaxation could not be demonstrated in the wire myograph. Investigations into the underlying mechanism used CD1 WT mice with pharmacological inhibitors and genetically altered C57/BL6 mice. The results demonstrate that there is no involvement of the neuropeptide SP, but that αCGRP peptide, the CGRP receptor and hyperpolarisation of the smooth muscle are all important parts of the vasodilation mechanism. Together, the identified mechanisms support a conclusion of cinnamaldehyde induced activation of sensory neurones, causing CGRP release and hyperpolarisation of the smooth muscle cells, leading to vasorelaxation.

Cinnamaldehyde Causes Concentration Dependent Vasorelaxation Which Is Partially TRPA1 Mediated And Largely Endothelium Independent.

Several published studies have investigated TRPA1 agonists for vasoreactivity. The most commonly used agonist are cinnamaldehyde and MO, which induce relaxation and vasodilation. Methodology and findings differ greatly among published papers (See table 1.1), suggesting that there

are concentration and tissue specific effects. While others have shown dependence on TRPA1 using receptor antagonists (Earley *et al.*, 2009, Kunkler *et al.*, 2011), we were the first to do this using vessels from TRPA1 KO mice (Pozsgai *et al.*, 2010). Data presented in this chapter has shown that TRPA1 KO mouse vessels have reduced vasorelaxation responses to cinnamaldehyde. The tissue is still able to respond to cinnamaldehyde but with reduced potency, suggesting the presence of TRPA1 dependent and independent mechanisms. The contribution of the endothelium to this response was investigated using arteries without functional endothelial responses. These showed only a very small reduction in relaxation in WT vessels, with slightly more in the KO vessels, suggesting that the endothelium has only a minor role in the TRPA1 mediated component of cinnamaldehyde induced vasorelaxation. Indeed, the finding that endothelial loss has a significant effect on the EC_{50} only in KO mice, potentially suggests that the endothelium has taken on a stronger relaxant role when TRPA1 is genetically deleted. This implies that some compensatory changes may have occurred in the TRPA1 KO vessels. Further investigation is warranted, as these compensations could impact on our findings and others who use this mouse strain. This is particularly important as the TRPA1 KO colony is maintained on a mixed strain background, which may mean that results cannot be extrapolated easily to other mouse strains. Compensatory changes in relaxation mechanisms are common in many research settings and would not be unexpected if TRPA1 was part of a physiologically relevant dilation pathway.

In order to examine whether TRPA1 WT and KO mesenteric arteries responded differently to contractile agents, their contraction in response to phenylephrine, depolarising concentrations of potassium (via KCl additions) and U46619 was characterised. This was presented in terms of raw vessel tension and also normalised to maximal tension produced in response to a depolarising solution (80mM K^+ Krebs). Phenylephrine and KCl were used in addition to U46619, which is used commonly for pre-constriction in this chapter, to demonstrate that our findings are not stimulus specific. Phenylephrine is chosen as it mimics the *in vivo* setting,

where sympathetic nervous activation plays a role in vascular tone via receptor signalling. Additions of KCl demonstrate the ability of depolarisation to induce vascular contraction. No significant differences were seen in the contractile ability of mesenteric arteries from TRPA1 WT or KO mice to any stimuli. These valuable findings suggest that differences in contractile responses do not contribute towards the significantly blunted vasodilation response to cinnamaldehyde in TRPA1 KO vessels. Additionally, data in this chapter shows that contractile abilities to these stimuli does not differ between TRPA1 WT, CD1 and C57/BL6 mouse mesenteric arteries, which is important where later studies have utilised CD1 vessels for pharmacological studies and C57/BL6 vessels from genetically modified mice.

I further investigated cinnamaldehyde induced vasorelaxation using the TRPA1 antagonists HC-030031 and TCS5861528. These are related antagonists, based on a common core structure. TCS5861528 is a new derivative of HC-030031, suggested to be more potent and soluble (Wei *et al.*, 2009). However, neither of these antagonists were able to reduce cinnamaldehyde induced vasorelaxation. This data conflicts with my findings from TRPA1 KO mice, suggesting that the receptor may not be involved in the cinnamaldehyde response. However, the *in vivo* studies by Aisah Aubdool show TCS5861528 was able to reduce cinnamaldehyde induced increases in blood flow in an *in vivo* situation. Significant efforts were presented in this chapter to demonstrate the activity of TRPA1 antagonists in the wire myograph preparation. This particularly focussed on HC-030031 as it is the most commonly used TRPA1 antagonist, however inhibition of cinnamaldehyde-induced relaxation could not be achieved using several relevant antagonist concentrations in rodent bronchi, cerebral artery and pulmonary artery. The bronchi did show evidence of neurogenic activation as cinnamaldehyde induced relaxation was almost abolished by a NK_1 antagonist. Further investigations of TRPA1 antagonists could be made, using structurally different alternatives or by investigating inhibition of responses induced by other TRPA1 agonists; MO responses for example. However responses to MO were

inconsistent in the rodent tissues studied, producing a mixture of relaxation and contractile responses which do not align with those expected following sensory neurone activation. Therefore this study has concentrated on cinnamaldehyde, which produces consistent relaxation responses in a range of rodent tissues. However, TRPA1 activity on non-neuronal cells and TRPA1 independent actions of cinnamaldehyde are likely to also contributing towards the observed relaxations, as shown by the remaining relaxation response seen in TRPA1 KO mice.

The use of indomethacin and L-NAME as inhibitors of endothelial mediated vasorelaxation was not utilised in this study. These would be potentially valuable additions to the investigation of TRPA1 WT and KO vessel vasorelaxation as this would remove the main endothelial derived mediators whilst leaving the myoendothelial gap junctions intact and allowing electrical coupling. However, there are also a number of disadvantages with this approach. For example, the use of these inhibitors also removes the potential contribution of smooth muscle or sensory neurone derived NO and COX products. Also, retaining electrical coupling of endothelial and smooth muscle cells does not allow us to completely dissect the roles of the endothelium vs. the smooth muscle layer in the vasodilating response. Although in this experiment I cannot prove that the endothelial cell layer has been completely removed using carbachol responses, I assume that endothelium removal has occurred as I have not inhibited its action and vessels respond similarly to smooth muscle and nerve stimuli, suggesting vessels are in good condition, while having lost their responses to carbachol, an endothelial specific vasodilator.

My findings show only a small role for the endothelium in mediating cinnamaldehyde induced vasorelaxation. This agrees with investigations using rat aortic rings from Yanaga *et al* (2006), who show partial endothelial dependence, and Xue *et al* (2011) who find no role for the endothelium in the same model. However, Earley *et al* (2009) have found the MO induced dilation mechanism in rat cerebral arteries to be dependent on TRPA1 mediated endothelial hyperpolarisation. Mechanisms may

therefore be location specific, with differences arising from vessel components. Species and regional differences in the reactivity of arteries to both extracellular potassium and hyperosmolarity have been described, particularly in relation to cerebral and mesenteric arteries (Ryman *et al.*, 1989).

Cinnamaldehyde Induced Vasorelaxation Is Relevant *In Vivo*

Our group has previously published studies showing cinnamaldehyde injected into the mouse hind paw to cause vasodilation and increases in blood flow (Pozsgai *et al.*, 2010). In this chapter, I additionally present unpublished data showing topically applied cinnamaldehyde causes an increase in blood flow in the mouse ear which is TRPA1 mediated. In this chapter, data from Aisah Aubdool, shows 10% cinnamaldehyde to induce an increase in cutaneous blood flow measured by Laser Doppler. This shows similarities to studies on human forearm skin by Namer *et al* (2005) and VanderEnde at al (2001), who have measured increased blood flow and erythema respectively, in response to topically applied cinnamaldehyde. Together, these studies show that cinnamaldehyde reliably causes increased blood flow *in vivo*. However, my colleague Aisah Aubdool built on these findings in the literature by using genetic and pharmacological alterations to show reduction of the cinnamaldehyde response in TRPA1 KO and TRPA1 antagonist treated mice, demonstrating a heavy dependence on TRPA1 activity. We have further evidence to support an endothelial independent mechanism in the mouse ear, as pre-treatment with indomethacin and L-NAME have no effect on the responses. As the response is not completely blocked in TRPA1 KO mice, this data mirrors the findings from isolated vessels, where some of the relaxation induced by cinnamaldehyde is TRPA1 independent.

In the previous chapter I investigated whether TRPA1 KO mice had altered basal characteristics in terms of blood pressure. No striking phenotype was observed in the TRPA1 KO mouse. Similarly, when using Laser Doppler we can compare basal levels of blood flow in peripheral tissues,

investigating whether TRPA1 mediated vasodilation is an important mediator of tissue perfusion. In figure 4.4 there were no differences in basal blood flow, indicating that TRPA1 is not needed to control basal tissue perfusion. However, it has the clear potential to be involved in reactive changes in perfusion.

Evaluating the potential role of TRPA1 in myogenic constriction

The myogenic response, also termed the Bayliss effect, is particularly important for the control of blood flow through peripheral arterioles. Increases blood pressure cause additional stretch of the smooth muscle cells lining the arterioles. This activates the release of intracellular calcium stores and surface channels, inducing a contractile response. This process does not require external signals, occurring on a cell by cell basis. However the collective result will be a constriction of the arteriole and a normalisation of blood flow. The myogenic response has a role in essential hypertension, where the response is enhanced. Mixed conclusions have been draw as to whether this represents a protective function against organ damage or part of the pathophysiology of hypertension (See Review by Hughes and Bund, 2002).

Scotland *et al.,* (2004) have described a role for C-fibres and TRPV1 induced SP release in the rat mesenteric artery myogenic response. In the pressure myograph, spontaneous myogenic constriction was seen from around 60-100mmHg, in line with the pressure these vessels would experience *in vivo*. This constriction was endothelium independent but dependent on calcium influx and could be virtually abolished by ablation of sensory neurones or by antagonism of the TRPV1 receptor. Similar reductions were seen with NK_1 receptor antagonism or in vessels from mice which lacked the NK_1 receptor, suggesting a SP dependent mechanism. 20-HETE is an eicosanoid produced by vascular smooth muscle cells under luminal stretch, with a clearly defined role in the myogenic response (Miyata and Roman, 2005). Scotland *et al.,* also demonstrated that 20-HETE can activate TRPV1 expressed in CHO cells.

Therefore they suggest that 20-HETE produced under stretch activates C-fibre TRPV1, leading to SP release and arteriole constriction via NK_1. However, 20-HETE can also directly depolarise smooth muscle cells (Miyata and Roman, 2005). Potentially supporting these findings, Kannan and Seip (1986) show SP inhibits relaxations induced by field stimulation in rat mesenteric arteries under myogenic tone, but does not cause contraction of the tissue. The latter of these findings are similar to my own data presented within this chapter, showing no changes in mouse mesenteric artery tone on SP application. My vessels are subject to physiological tension and produce myogenic tone, although this is distinctly different to the type of pressure experienced *in vivo* or in a pressurised myograph. Despite these findings, several reports concerning NK_1 activation on the vasculature demonstrate a dilation response, suggesting anatomically distinct vessel beds may utilise different mechanisms. In humans, infusion of SP in to the brachial artery or superficial vein of the hand induces an increase in blood flow (McEwan *et al*, 1988), indicative of a dilation response.

In my study the mechanisms controlling myogenic tone were not directly investigated. Similar contractile abilities to a range of agents were observed in both TRPA1 WT and KO vessels (See figure 4.4), suggesting that sensitivity to contraction is not altered by genetic deletion of TRPA1. In a recent study by Earley *et al* (2009) using cerebral arteries in a pressure myograph, application of the TRPA1 antagonist HC-030031 was associated with a small increase in myogenic tone, suggesting that tonic activation of TRPA1 was associated with a vasodilatory influence. In this study TRPA1 expression is shown to occur on the endothelial cells. This study contrasts with the findings of Scotland *et al* (2004), where tonic TRPV1 activity on C-fibres exerts a constricting influence via SP release. This data suggests TRPA1 does not show a similar relationship with myogenic tone as TRPV1.

MO Mediates Vasoconstriction In Mesenteric Arteries

One of the most commonly used experimental TRPA1 agonists is MO. It has been used by several groups, including ours, to demonstrate TRPA1 mediated vasorelaxation both *in vivo* and *ex vivo*. We have previously shown that topically applied MO increases cutaneous blood flow, which is greatly reduced in TRPA1 KO mice (Pozsgai *et al.*, 2010). Earley *et al* (2009) have shown relaxation of isolated cerebral arteries in the perfusion myograph induced by MO (3-100μM) is reduced by 3μM of the TRPA1 antagonist HC-030031. Therefore, I applied similar concentrations of MO to the mesenteric arteries (3-30μM). These concentrations are below those reported to activate TRPV1 (1mM) (Everaerts *et al.*, 2011). I found that instead of relaxing the vessels, MO caused concentration dependent vasoconstriction, which occurred at a similar magnitude irrespective of tissue genotype or endothelial function. TRPA1 activity has previously been shown to cause smooth muscle contraction in other locations, such as the airway (Andrè *et al.*, 2008) and bladder (Andrade *et al.*, 2006). However, the action applies to all agonists of the receptor and does not explain why differential effects are found with cinnamaldehyde and MO in our model. As MO is less selective than cinnamaldehyde, and shows similar effects in TRPA1 WT and KO mice, I assume that this constriction is occurring independently of TRPA1 activity in our model. I have therefore not investigated this agonist further and suggest caution to other groups where MO is used as a TRPA1 agonist. Where our group has previously shown TRPA1 dependent vasodilation induced by MO applied topically to mouse skin (Pozsgai *et al.*, 2010), we may need to investigate the contribution of TRPA1 expression in cell types outside the vessel wall, in particular sensory neurones and keratinocytes which may be involved.

CGRP, But Not SP, May Mediate Cinnamaldehyde Induced Vasorelaxation

Several studies using TRPA1 agonists suggest a mechanism where C-fibres are activated, causing release of vasodilator neuropeptides such as CGRP

and SP. Most studies that have investigated this with pharmacological or genetic manipulations use MO (See figure 1.6). In the mesenteric vessels used in this study, SP does not cause vasorelaxation. Therefore, it cannot be contributing to the cinnamaldehyde induced vasorelaxation. I used αCGRP KO mice to show that cinnamaldehyde induced vasorelaxation is partially dependent on CGRP release. I then attempted to use two CGRP receptor antagonists to strengthen the findings.

I validated a concentration of the peptide CGRP antagonist $CGRP_{8-37}$ against exogenous αCGRP, showing it to significantly reduce the magnitude of vasorelaxation. However, at this concentration it showed no inhibition of cinnamaldehyde induced vasorelaxation. Although the concentration of CGRP antagonist was validated, it is possible that receptor blockade was not strong enough to significantly alter the vasorelaxation of endogenously released CGRP following cinnamaldehyde application. This study would benefit from increasing the concentration of antagonist.

The non peptide CGRP receptor antagonist BIBN was also used in this study. A similar concentration (3μM) has previously been used within our group to significantly reduce vasorelaxation of up 30nM exogenous CGRP (Tam *et al.*, 2006), and the 10μM concentration I have used in this chapter was previously published by Grant *et al* (2004), both in isolated mouse aortic rings. This antagonist is more potent and binds with more affinity than $CGRP_{8-37}$, likely producing a non-surmountable receptor block at the concentration used (Hay and Poyner, 2005). This antagonist revealed a strong role for the CGRP receptor in the vasorelaxation induced by cinnamaldehyde.

Although the strength of the conclusions would be enhanced with consistent results from genetic and pharmacological manipulations, it is likely that the αCGRP KO mice give us the best idea of αCGRP peptide involvement, whilst BIBN gives the best idea about CGRP receptor involvement. Together, they provide strong evidence for the involvement of CGRP release and signalling in cinnamaldehyde induced vasorelaxation.

The endogenous CGRP in our model is likely to be held in sensory neurones, released when they are stimulated with cinnamaldehyde, via TRPA1 receptor activation. The sensory neurones in our mesenteric vessel tissues are severed and could potentially become depleted in the model. To test this, I applied sequential and varying concentrations of capsaicin to our endothelium intact and denuded vessels. Capsaicin application to mesenteric arteries has previously been shown to induce CGRP release and cause vasodilation (Fujimori *et al.*, 1990). At a concentration of 10μM, relaxation of around 60% is obtained in WT vessels and is repeatable in four sequential capsaicin additions. This suggests that sensory neurones are present in the vessels, and are not easily neuropeptide depleted. This could be further tested by using repeated capsaicin dosing *in vivo* to deplete the sensory neurones of neuropeptides. Consequently, this data supports the previous conclusions that cinnamaldehyde induced vasorelaxation of the mouse mesenteric artery is partially mediated by CGRP.

Cinnamaldehyde Induced Vasorelaxation Is Largely Hyperpolarisation Mediated

A previous study using MO, published by Earley *et al* (2009), has shown TRPA1 dependent vasodilation to be mediated by endothelial hyperpolarisation, which is then passed to the underlying smooth muscle by myo-endothelial gap junctions and increases in local extracellular potassium. This particular mechanism shows specificity to the cerebral vasculature; however other studies have also suggested hyperpolarisation to be an important mediator of cinnamaldehyde induced vasorelaxation (See table 1.1). To investigate the role of hyperpolarisation in the response to cinnamaldehyde, I have used arteries without functional endothelium, as previous findings have not shown endothelial cells to be important in the TRPA1 dependent portion of the relaxation. This also allows isolation of the smooth muscle mediated mechanisms. Vessels were bathed in raised extracellular potassium, constricting the smooth muscle and preventing hyperpolarisation. In this setting, cinnamaldehyde induced vasorelaxation was strikingly blunted, more than seen in TRPA1 KO mice. Therefore I

can conclude that hyperpolarisation is important in the TRPA1 dependent and independent portions of the cinnamaldehyde response. This could ideally be confirmed in parallel studies where the smooth muscle membrane potential is measured with an electrode. However this is a challenging technique for which we lack the equipment and expertise necessary.

CGRP receptors are known to be expressed on vascular smooth muscle cells and CGRP itself causes smooth muscle hyperpolarisation via the activation of K_{ATP} channels and endothelial derived NO (Wimalawansa, 1996). TRPA1 expression itself has not been previously described in vascular smooth muscle tissue. Data presented in the next chapter show TRPA1 expression to be very low in all levels of the vasculature, but at higher levels in DRG. This strengthens conclusions that TRPA1 expressed on sensory neurones is mediating the CGRP release, which in turn causes vasorelaxation via hyperpolarisation of the vascular smooth muscle layer. Sensory neurones also contain a number of neuropeptides other than CGRP and SP. Therefore, these could also play a role in the vascular consequences of TRPA1 activation.

TRPA1 is a non-selective cation channel and if it was directly expressed on smooth muscle cells, it has the potential to activate calcium dependent mechanisms without the need for further mediators. This mechanism may also be involved in cinnamaldehyde induced vasorelaxation. The major calcium activated potassium channel in smooth muscle cells is the BK_{Ca} channel. This channel is activated by calcium, such as that potentially entering the cell following TRPA1 activation, causing a large efflux of potassium from the smooth muscle cell and causing hyperpolarisation. In smooth muscle cells this will lead to relaxation. Endothelial derived epoxyeicosatrienoic acids (Zhang *et al.*, 2001) have been shown to dilate vessels via BK_{Ca} channels, and are thought to be a potential EDHF mechanism in some tissues. I tested the potential for the BK_{Ca} channel to mediate cinnamaldehyde induced vasodilation by using a channel blocker called paxilline, in vessels without functional endothelium. This

compound has been used extensively by other groups at a concentration of 1μM, which I have replicated. Fountain *et al* (2010) have previously shown mouse mesenteric arteries to express BK_{Ca}, and the channel has been shown to be blocked by with 1μM paxilline in mouse cutaneous sensory neurones (Zhang *et al.*, 2010). Paxilline works by binding to the alpha subunit of the BK_{Ca} channel, common to all isoforms. In this study, blocking BK_{Ca} had no effect on cinnamaldehyde induced vasorelaxation, thus it has proven not to be a key channel in this response.

This study suggests that TRPA1 activity can lead to hyperpolarisation mediated vasorelaxation. Data has further suggested a role for CGRP induced hyperpolarisation in cinnamaldehyde induced vasorelaxation, without the need for functional endothelium. CGRP can act directly on vascular smooth muscle cells to increase cAMP levels. This leads to several mechanisms of vasodilation, including activation of potassium channels and hyperpolarisation of the cell. These channels are not BK_{Ca}, but via ATP sensitive potassium channels (K_{ATP}) (Nelson *et al.*, 1990). This has been demonstrated in rabbit mesenteric arteries (Nelson *et al.*, 1990), human placental blood vessels by Dong *et al* (2004) and is discussed in Brain and Grant (2004). However, as recently described for Gs signalling downstream of beta-adrenergic receptors in the rat mesenteric artery, K_{ATP} activity is not required for PKA mediated vasodilation, but facilitates the spreading of this dilation response through the artery (Garland *et al.*, 2011). In my study, pre-constriction is gained using U46619. I thought to use the K_{ATP} channel antagonist glibenclamide to investigate the component mediated by K_{ATP} channels in the relaxation to cinnamaldehyde. However, it has been reported that glibenclamide itself antagonises U46619 induced constriction with some evidence of tissue and species specificity (Cocks *et al*, 1990, Kemp and McPherson, 1998) Within our group we have preliminary evidence to demonstrate this is also the case in mesenteric arteries. CGRP also causes relaxation of smooth muscle cells via hyperpolarisation independent mechanisms, such as PKA stimulated increase in sarco/endoplasmic reticulum Ca^{2+}-ATPase (SERCA) activity. These alternative pathways may account for the hyperpolarisation

independent relaxation observed at higher concentrations of cinnamaldehyde in our experiments; however these are unlikely to be TRPA1 dependent. An alternative method of studying signalling downstream of CGRP receptors is to pharmacologically block cAMP increases or PKA activity, however it must be remembered that these signalling components are common to many pathways. CGRP can also cause endothelial dependent vasorelaxation, via the stimulation of NO production and hyperpolarisation of underlying smooth muscle via activation of BK_{Ca}, downstream of PKA and PKG. In this study, I have shown cinnamaldehyde to cause largely endothelial independent vasorelaxation and suggest sensory neurones mediate this action. This conclusion is in line with the data showing lack of BK_{Ca} involvement in cinnamaldehyde induced vasorelaxation when endothelial cells are removed. The exact contribution of each potassium channel involved in TRPA1 agonist induced vasorelaxation has not yet been investigated, thus the evidence is novel and is of value to the field. In my model, further use of potassium channel inhibitors or other signalling manipulations will be needed to elucidate a clear mechanism. These could include alternative K_{ATP} blockers or inhibitors of PKA to investigate the links with CGRP. The dependence of this on TRPA1 activity can then be assessed using TRPA1 WT and KO mice.

A recent study by Xue *et al* (2011), using lower concentrations of cinnamaldehyde in rat aortic rings, did not show direct involvement of potassium channels. They instead suggest relaxation is due to effects on calcium handling, reducing smooth muscle calcium influx and store release. A similar mechanism, at concentrations of cinnamaldehyde similar to mine, was identified by Yanaga *et al* (2006), also in rat aortic rings. However, hyperpolarisation could be playing a role in these findings as it inhibits voltage operated calcium channels, the main channel responsible for calcium influx. Inhibition of calcium influx and store release was not investigated in this chapter. Several remaining questions could be better answered if the hyperpolarisation study was repeated in TRPA1 WT and KO mice. Additionally, as in Xue *et al* (2011), I could apply

cinnamaldehyde before the pre-constriction, or measure cytoplasmic calcium levels, assessing its ability to block calcium increases.

Yanaga *et al* (2006) also identified an endothelial dependent component in cinnamaldehyde induced vasorelaxation in rat aortic tissue which was NO mediated. These concentrations are similar to those used in this chapter, which also shows a TRPA1 independent endothelial component, suggesting that this portion could be NO mediated.

Differences in mechanism between studies may be due to location as differential expression of potassium channels has been demonstrated across the vascular system. For example, lower messenger RNA (mRNA) copy numbers of BK_{Ca} channel components are found in aortic tissue compared to mesenteric tissue (Fountain *et al.*, 2004). Also, K_{IR} channels, which are important for amplifying smooth muscle hyperpolarisation, are poorly expressed in mesenteric arteries when compared with coronary and cerebral arteries (Smith *et al.*, 2008). Therefore, the mechanism operating in each tissue may differ. Differences may also be found with agonist concentration. In this study, I did not measure the potassium channel components in the tissue. However this would be a valuable addition to the data.

In my model, cinnamaldehyde induces both TRPA1 dependent and independent relaxation processes, the later becoming predominant at high concentrations. As our interests are not in cinnamaldehyde per se, but of TRPA1 induced vasorelaxation, it will be important for future studies to identify a more selective agonist. This could include a recently identified non electrophilic TRPA1 agonist that our group have played a role in characterising (Ryckmans *et al.*, 2011). This will eliminate many of the problems experienced in this research field, where agonist activity cannot always be fully attributed to the receptor of study.

Conclusion

In this chapter, I have investigated the vasodilation induced by the TRPA1 agonist cinnamaldehyde. Several other groups have shown that TRPA1 agonists can cause vasorelaxation of isolated vessels, and cause increases in blood flow *in vivo*, but clear mechanisms have not been established. We were the first group to use TRPA1 KO mice to demonstrate TRPA1 dependent components in cinnamaldehyde induced vascular responses both *ex vivo* and *in vivo* (Pozsgai *et al.*, 2010). I have now studied a range of channels and mediators, using both genetic and pharmacological interventions, to identify the pathway involved in this response in murine mesenteric arteries. This is important in the context of the investigation into the role of TRPA1 in cardiovascular regulation. In isolated mesenteric arteries, cinnamaldehyde induces vasorelaxation which is largely endothelium independent, with a TRPA1 component likely to be originating from expression on sensory neurones. The potency of cinnamaldehyde was reduced in TRPA1 KO mice; however the presence of a TRPA1 component could not be confirmed using TRPA1 antagonists, which also did not block cinnamaldehyde responses in a number of rodent tissues. These studies did not rule out a neurogenic mechanism and I further hypothesised that activation of TRPA1 may lead to CGRP release. The response to cinnamaldehyde was found to be reduced in αCGRP KO mice and with the use of a non peptide CGRP receptor antagonist. I have additionally used pharmacological manipulations to show the neuropeptide SP is not involved in the response of the mesenteric artery. CGRP release is thought to lead to hyperpolarisation of the vascular smooth muscle layer. In my model, blocking hyperpolarisation in the tissue significantly blunted cinnamaldehyde induced smooth muscle dilation. I also investigated the involvement of the BK_{Ca} channel, the most likely candidate channel to be mediating a direct TRPA1 induced relaxation of vascular smooth muscle. Use of an antagonist of the BK_{Ca} channel did not affect the cinnamaldehyde response. This conclusion strengthens the findings that CGRP is mediating the TRPA1 dependent component via sensory neurone activation. Further work will be needed to investigate other mediators of

cinnamaldehyde induced smooth muscle hyperpolarisation and to investigate the calcium handling changes suggested in other publications. However, future studies should look to use more selective TRPA1 agonists and antagonists when isolating the receptor dependent pathways.

Chapter 5 – Investigating The Role Of TRPA1 In Experimental Hypertension

Introduction

In the previous chapter, I showed a TRPA1 agonist to cause vasorelaxation of the murine mesenteric artery, an example of a resistance vessel. Resistance vessels are small arteries and arterioles, important in the control of total peripheral resistance in the vascular system. They are highly innervated by sensory neurones, terminating at the media/adventitia border and reaching into the smooth muscle layer. Several neuropeptides can be released from these nerves and have been suggested to inhibit increases in blood pressure (Watson *et al.*, 2002). Neuropeptides have several suggested roles in hypertension. SP acts on its major vascular receptor, NK_1. Previous studies using NK_1 receptor antagonists have demonstrated increases in blood pressure in acute experimental hypertension models. These findings suggest that SP may be able to counter-act blood pressure increases (Watson *et al.*, 2002). However, in the previous chapter I have shown that SP does not mediate mesenteric artery relaxation. Furthermore, CGRP is a potent vasodilator acting via endothelial dependent and independent mechanisms. Blood pressure in CGRP KO mice has been characterised by several groups, some showing spontaneous hypertension (Li *et al.*, 2004, Deng and Li, 2005), whilst others could not find any changes (Lu *et al.*, 1999). This may be due to the method used to create the KO strain, as Li *et al* have also removed the calcitonin gene. Both groups measured central blood pressure. CGRP release has also been described as a key compensatory mechanism against rising blood pressure (Watson *et al.*, 2002, Li and Wang, 2005, Deng and Li, 2005, Smillie and Brain, 2011). In our group, there are ongoing investigations showing that CGRP is protective against the onset of Ang II induced hypertension, and reduces the emergence of hypertensive markers (Smillie, Unpublished data). In chapter 4, data is presented suggesting that TRPA1 activation in the vasculature leads to vasorelaxation via CGRP release. This is highly indicative of a protective role for TRPA1 in hypertension.

Ang II is a key modulator of basal blood pressure in humans and has a role in the development of essential hypertension. It has various actions on many cell types, causing vasoconstriction, increasing blood volume, oxidative stress and inflammatory mediator transcription (Rosendorff, 1996, Gavras and Gavras, 2002, Mehta and Griendling, 2007). The mouse Ang II infusion model of hypertension, originally used by Byrne *et al* (Byrne *et al.*, 2003), is well characterised in our laboratory. An osmotic minipump containing Ang II is implanted subcutaneously in to the mouse, infusing the drug over 14 days and creating significant hypertension (Liang *et al.*, 2009). This model produces quick onset, moderately severity hypertension and mimics some of the pathology found in human hypertension but occurs over a shorter time span than that found clinically. This includes hypertrophy of large blood vessels and heart, along with induction of associated inflammatory biomarkers (Monassier *et al.*, 2006).

In normal conditions, ROS producing enzymes have important intracellular signalling roles, contributing to cellular activities such as growth, differentiation, migration and apoptosis. The likely signalling molecular is H_2O_2. In pathological conditions, the redox homeostasis is shifted in favour of oxidative stress by an increase in the production of ROS and a depletion of antioxidant defences. Many of the changes seen in the Ang II model are linked to the induction of oxidative stress (Hitomi, *et al.*, 2007), showing clear parallels with the clinical situation, where ROS are closely associated with essential hypertension and the resultant hypertrophy (Zalba *et al.*, 2001). The resultant oxidative stress leads to activation of inflammatory gene transcription, such as Interleukin-6 (IL-6) and Monocyte chemotactic protein 1 (MCP-1). This systemic inflammation has destructive effects; in terms of hypertension this can lead to vasoconstriction, endothelial dysfunction and vascular remodelling.

There are currently no studies which investigate the pathophysiological relevance of TRPA1 in cardiovascular disease, but the likeliness of such a role has been suggested (Bodkin and Brain, 2010). As the TRPA1 receptor

has been shown to be activated by oxidative stress (Andersson *et al.*, 2008, Trevisani *et al.*, 2007) and upregulated by inflammatory mediators (Hatano *et al,* 2012), there is potential for *in vivo* activation during hypertension. Therefore use of the Ang II infusion, which is associated with oxidative stress production (Hitomi *et al.*, 2007), is an appropriate model for investigating our hypothesis of TRPA1 mediated vascular protection. In line with my hypothesis, I have conducted this novel study investigating the development and endpoints of experimental hypertension in TRPA1 WT and KO mice. Blood pressure and hypertension endpoints are evaluated, including measures of hypertrophy and inflammatory mediators. ROS are produced by a range of enzymes, including the NADPH oxidase (NOX) family. Several, differentially regulated isoforms of NADPH oxidase are expressed in vascular tissues, in different cellular locations. NOX2 and NOX4 are both associated with ROS production, and show increases in activity on Ang II stimulation in the rat (Wang *et al.*, 2007). NOX2 is particularly implicated in hypertension, where its over-expression in mouse endothelial cells worsens oxidative stress and hypertension (Bendall *et al.*, 2007) during Ang II infusion, and NOX2 KO mice are protected against hypertrophy in a similar model (Johar *et al.*, 2006). The role of NOX4 is currently less clear, likely due to its intracellular location, however it has also been implicated in Ang II receptor dependent hypertension and hypertrophy (Wang *et al.*, 2007). Both NOX2 and NOX4 are measured in this chapter as pro-oxidative markers.

The tissue ROS level is balanced by the scavenging activity of antioxidant systems, such as superoxide dismutase (SOD). SOD is an antioxidant gene which converts superoxide to hydrogen peroxide, in order for its degradation. ROS induce additional anti-oxidative genes, such as heme-oxygenase (HO-1), which can be used as both an indicator of ROS production and as a level of mounted anti-oxidant defence. The protective effects of HO-1 activity are multifold, producing both vasodilator and anti-oxidant compounds (Turkseven *et al.*, 2005). The levels of SOD and HO-1 are measured as antioxidant defence genes. Their expression has also been

shown to increase during Ang II infusion, reducing pathology (Chen *et al.*, 2003, Peterson *et al.*, 2009, Gongora *et al.*, 2006).

Hypertension is a disease of systemic inflammation, associated with the expression of cytokines and chemokines. The levels of some of these are investigated during this chapter as a measure of inflammation severity (Yao *et al.*, 2006). This will include MCP-1, IL-6 and KC (the murine analogue of IL-8), which are all associated with Ang II stimulation and cellular inflammation, an important step in the progression of cardiovascular disease towards vascular events (Fisman and Tenenbaum, 2010). In particular, these biomarkers are positively associated with hypertensive remodelling and poor disease outcome (Behr *et al.*, 2004, Kolattukudy *et al.*, 1998, Manhiani *et al.*, 2007, Collier *et al.*, 2011).

The results of this thesis so far indicate that TRPA1 is involved in a dilatory pathway *ex vivo*, with more complex effects *in vivo*, I hypothesise that TRPA1 is activated *in vivo* during Ang II induced hypertension, leading to the release of CGRP which compensates against blood pressure rises and pathological changes. The loss of these pathways in global genetic TRPA1 deletion, although not important basally, might therefore be damaging in a disease setting associated with vasoconstriction and oxidative stress.

Aims;

- Use tail cuff plethysmography to initially characterise the profile of hypertension onset in TRPA1 WT and KO mice using the Ang II infusion model.
- Collect in depth pressure, heart rate and activity readings over the infusion period using telemetered TRPA1 WT and KO mice, ascertaining if TRPA1 has a role in the hypertension induced in this model.

- Investigate the influence of TRPA1 on cardiac remodelling. Use echocardiography to assess cardiac hypertrophy, confirming these findings at necropsy.
- Study the expression of TRPA1 in the vasculature and on DRG neurones, comparing this with TRPV1 and CGRP expression or release.
- Investigate the influence of TRPA1 on the markers and mediators of inflammation associated with Ang II induced hypertension. Use quantitative RTPCR and multiplex ELISA to measure the levels of transcribed and circulating biomarkers as described above.

Results

Ang II Induced Hypertension Is Evaluated In TRPA1 WT And KO Mice Using Tail Cuff Plethysmography

In chapter 3, TRPA1 WT and KO mice were trained for blood pressure measurement by tail cuff plethysmography. After ascertaining their basal blood pressure, they underwent mild surgery to implant an osmotic minipump subcutaneously. Ang II was delivered at a rate of 1.1mg/kg/day under the skin of the animal for 14 days. Control mice were also used, carrying an empty pump. After the first 3 days, blood pressure was measured daily using tail cuff plethysmography. This model was previously used effectively in our group (Liang *et al.*, 2009). Figure 5.1 A, shows the mean blood pressure of mixed gender mice for days 3-14 post implantation. As seen in previously presented data, TRPA1 KO mice have a lower blood pressure than WT mice. This difference is reflected over the 14 day period, in both control and Ang II treated mice. Control mice of both genotypes maintain a stable blood pressure throughout the experimental period. This can be seen more clearly in figure 5.3, which additionally shows readings collected during the training period. Ang II treated mice of both genotypes display a steady increase in blood pressure. Blood pressure was never statistically different between WT and KO mice in either treatment groups, however, WT mice showed earlier significant

blood pressure increases in Ang II treated animals, when compared to their respective controls. By day 11, Ang II treated mice of both genotypes showed significantly elevated blood pressure compared to their control groups.

As blood pressure can vary depending on gender, panels B and C of figure 5.1 show the data split into female and male mice respectively. Although the sample size is relatively small, and shows large variations, slight differences in onset profile between genders may be apparent. However, this is not significant and is likely to be due to variability between males in particular. In further analysis it is assumed that gender does not have a large influence on basal blood pressure, or the response to experimental hypertension model, in keeping with previously presented data. Further data is presented from mixed gender groups.

Figure 5.2 shows alternative analysis of blood pressure during the experimental period, as shown as a profile in figure 5.1. Analysis by area under the curve, as shown in figure 5.2A, illustrates the increase in blood pressure over the 14 day treatment period. Percent change between day 0 and day 14 (5.2B), describes the magnitude of change from the beginning of the experimental protocol, as a measure of hypertension severity. This measure takes into account the differences in basal blood pressure. Similarly, average blood pressure from the final 3 days (12-14) (5.2C) describes the average absolute hypertensive pressures experienced by each group. All measures demonstrated that the Ang II infusion robustly causes hypertension. Significant hypertension was gained by analysis using percentage change and average of final 3 days blood pressure. No significant changes in blood pressure were seen in control mice, as shown in figure 5.3. Ang II treated TRPA1 WT and KO mice both became significantly hypertensive, showing an average mean blood pressure of 150-180 mmHg (figure 5.2C. As systolic blood pressure is always higher, this demonstrates that the model induces a quick onset, severe hypertension. None of the panels suggest significant differences in the

magnitude of Ang II response between TRPA1 WT and KO mice, considering the difference in baseline blood pressure.

In figure 5.3, additionally showing the extended training period for control mice, there are significant differences in the blood pressure of TRPA1 WT and KO control mice at training days -3 to implantation day (day 0). This reflects previously presented data in chapter 1, where KO mice appear to have a hypotensive phenotype when blood pressure is measured by tail cuff plethysmography.

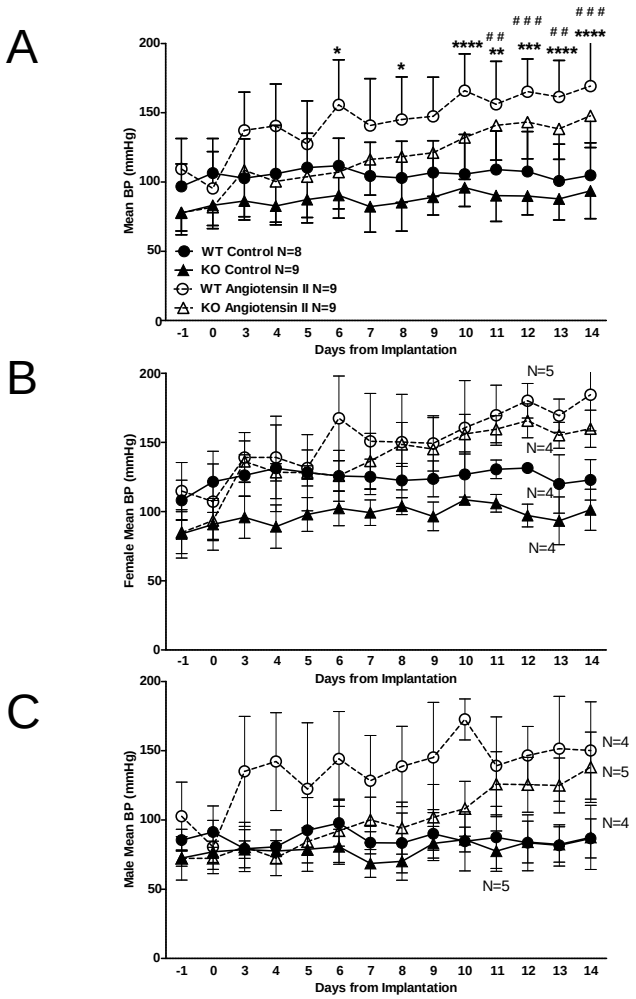

Figure 5.1 Blood Pressure Measured By Tail Cuff Plethysmography During 14 Days Of Ang II Infusion Or Following Operation Control, In TRPA1 WT And KO mice. Mean blood pressure measured daily (around 4pm) in Ang II infused (1.1mg/kg/day) or control operated animals. Averaged readings are taken from each mouse, then given as a group average. N=8-9. A. Shows mixed gender mice B. Shows only female mice N=4-5. C. Shows only male mice. N=4-5. Statistics are from two way ANOVA with Bonferroni's post-test. *p<0.05, **p<0.01, ***p<0.001, ****p<0.0001 comparing WT control to WT Ang II treated animals. # #p<0.01, # # #p<0.001, comparing KO Control to KO Ang II treated animals. N numbers as indicated.

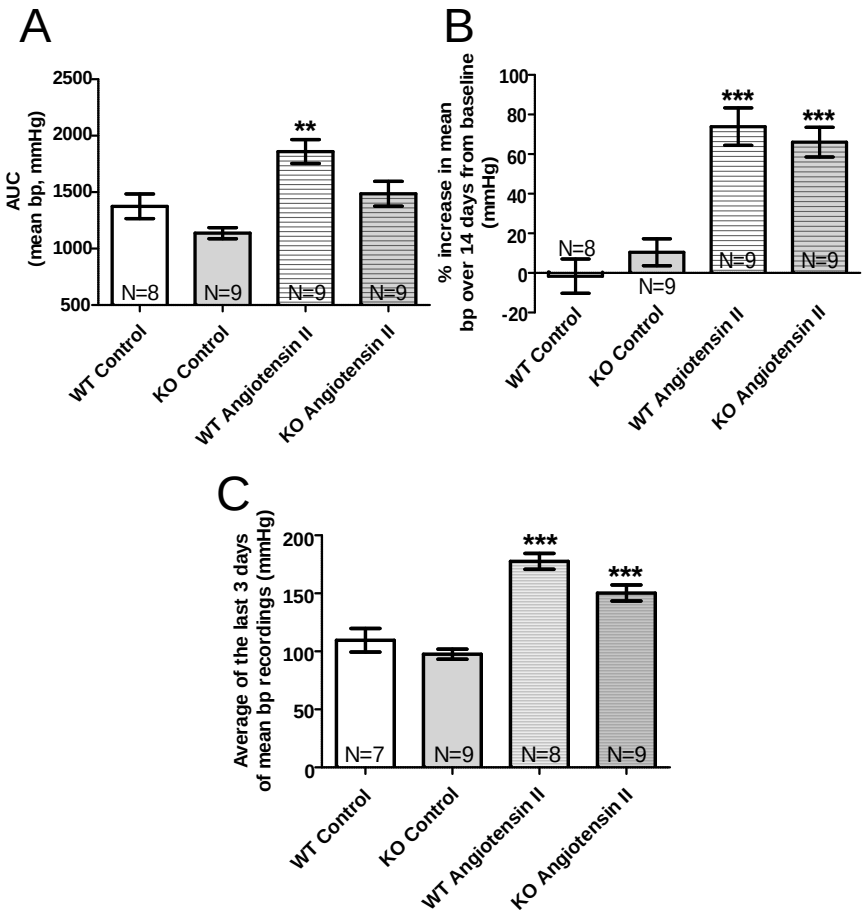

Figure 5.2 Change In Blood Pressure Over 14 days Of Ang II Infusion Or Control Operation, In TRPA1 WT And KO Mice, Measured By Tail Cuff Plethysmography. Mean blood pressure readings are taken from mixed gender mice, then given as a group average. A. Area under the 14 day mean blood pressure curve for mixed gender mice. Profile in previous graph. B. Percentage increase in mean blood pressure from day 0 to day 14 average reading. C. Average mean blood pressure during day 12, 13 and 14 of the infusion. Statistics are from one way ANOVA with Bonferroni's post-test. ***$p<0.001$, compared to respective control operated animals. N numbers are as indicated.

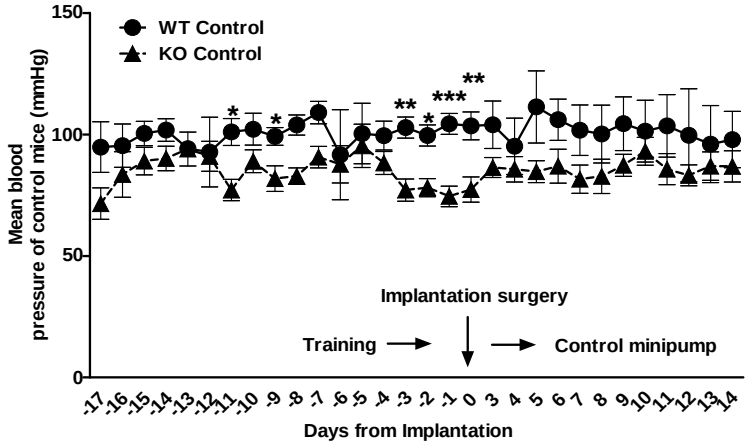

Figure 5.3 Serial Blood Pressure Readings Obtained By Tail Cuff Plethysmography From Control TRPA1 WT And KO Mice. Averaged readings are taken from each mouse, then given as a group average. N=2-27 mice per day. (from -17 to 14 in order; WT; 3,5,21,17,2,6,19,18,23,22,18,3,5,18,22,24,23,20,6,6,6,6,6,6,6,6,6,6,6,4,4, 4, KO; 4,4,19,19,2,6,21,20,25,27,20,4,5,21,24,24,25,21,8,8,8,8,8,8,8,8,8,8, 8,6,6,6). Statistics are from two way ANOVA with Bonferroni's post-test. *p<0.05, **p<0.01, ***p<0.001, WT Control to KO Control animals.

Effect Of Ang II Induced Hypertension Measured By Telemetry In TRPA1 WT And KO mice

Using telemetry allows us to collect the best quality of data from conscious and unstressed animals. Although the tail cuff plethysmography study did not suggest striking differences between TRPA1 WT and KO mice, previous data presented in chapter 1 showed that outcomes may differ between data collection methods. In the telemetry study, baseline data was collected before treatment with Ang II, therefore each mouse is able to serve as its own control, reducing the numbers of mice needed for this experiment. This also allows data to be analysed more robustly for statistical evaluation.

Figure 5.4 shows blood pressure parameters measured from Ang II infused TRPA1 WT and KO mice, presented as 4 hour averages. These graphs comprise mice which completed the entire experimental period. A summary of the hypertension results are described in figure 5.5. In both genotypes, Ang II infusion causes significant and severe hypertension by day 13, the final complete measurement day. Severe hypertension is clinically defined as a systolic blood pressure above 180mmHg or a diastolic blood pressure above 110mmHg (Carretero and Oparil, 2000). No statistical significance is seen between genotypes for average daytime and night time blood pressures; however these are significantly elevated from daytime measures, in line with increased activity. TRPA1 WT and KO mice treated with Ang II show similar levels of blood pressure increase both nocturnally and during amgiotensin II induced hypertension. The combination of telemetry and Ang II induced hypertension is associated with approximately 25% premature deaths (KO, 2x Females day 5, 1x Male day 10, WT 2x Male day 6). This affected the original power calculations for this study and meant that for many experiments, a lower N number was collected than had been originally planned, reducing the ability to achieve statistical significance. These losses were not associated with the telemetry surgery itself, as the few deaths that occurred this way were replaced before the start of the experimental period. Loss also seems

not to be gender related and slightly higher than the 10% associated with tail cuff measurements, suggesting a negative effect of having two implants. The reason for the death of these animals is not clear, as all occurred at night. However they occurred several days after the minipump surgery, after the blood pressure had risen, suggesting a relationship with the establishing hypertension. Data including that from mice which were lost during the protocol is presented later. Strikingly, and in contrast with data collected by tail cuff plethysmography (figure 5.1), the hypertension measured by telemetry is of very rapid onset. Hypertension is established within the first day, levelling off to a mean blood pressure of around 150mmHg at day 2 in Ang II treated TRPA1 KO mice and day 5 in Ang II treated WT mice (figure 5.4). This pattern is again in contrast with that seen in tail cuff plethysmography data, where WT mice established the hypertension more rapidly and increases continue until day 11. Hypertension is maintained in both genotypes of mice over the rest of the experimental period when measured by telemetry, with no significant blood pressure differences seen between groups for any parameter.

The telemetry probe also allows us to collect measurements of other parameters such as heart rate, pulse pressure and activity levels of the TRPA1 WT and KO mice. This data is presented as 4 hour averages in figure 5.6, and summarised in figure 5.7. Heart rate and pulse pressure are similar between TRPA1 WT and KO mice and are stable over the 14 days infusion (figure 5.6). Heart rate shows clear diurnal rhythms, being increased at night time, in line with increased activity levels. There are no differences in heart rate or pulse pressure seen after 13 days of Ang II treatment, the last full day of recording, compared to baseline measurements (5.7 A/B).

Previous data presented in chapter 1 indicates that TRPA1 KO mice display a basal hyperactivity phenotype. In figure 5.6C, this is clearly exacerbated during the Ang II infusion period. Each subsequent day the mice show an increased nocturnal activity peak, returning to an elevated baseline level during the day. Figure 5.7C shows average daytime and

night time activity, again reflecting the suggested hyperactivity phenotype of TRPA1 KO mice, which is exacerbated during Ang II infusion albeit with some individual variation. The trend is further analysed in figure 5.8, investigating activity counts at 4 hour intervals at baseline and on the last day of Ang II infusion. Statistical differences between genotype are not found, despite a clear increase in activity in KO mice (figure 5.8 A and B). The data is also analysed as activity counts over days 1-7 and 8-14 by area under the curve (Figure 5.8 C). This allows comparison of the first half of the experiment (1-7), where mice are less active, with that of the later half (8-14), where mice were most active The activity data is routinely tested for normality using the Shapiro-Wilk normality test but does not fit a Gaussian distribution, thus is analysed using non-parametric tests. In the case of figure 5.8C, I am most interested in if there are significantly higher activity levels in TRPA1 KO mice, compared to TRPA1 WT mice, at the end of the Ang II infusion period. Therefore a Mann-Whitney U test is used to compare these two data sets. Interestingly, Ang II infused TRPA1 WT mice show a similar level of nocturnal activity throughout the 14 day infusion, whereas TRPA1 KO mice show increasing levels of activity as the infusion progresses. Analysed in this way, there is a statistical increase in activity in Ang II treated TRPA1 KO mice, compared to the comparable WT group, during the later stages of Ang II infusion (days 8-14). As activity levels vary greatly between individuals, the measures proposed here may need more animals to reach further significance.

Figures 5.9 and 5.10 show the same data as presented in figures 5.4 and 5.6, additionally including data from mice that died before the end of the protocol. Although increasing the sample size increases the statistical power of the data, it also causes the results to show skewed trends in later stages where more hypertensive mice may have died, leading to a drop in average blood pressure readings around day 6-9 of recording. This could represent some compensation in the remaining mice. The time of first death is shown on each graph as a black dashed line. Almost all deaths occurred around day 5/6, corresponding to the peak of developing hypertension. This is several days after mini-pump implantation, and some

time since the telemetry surgery (approx. 2 weeks). Therefore the formation of hypertension is likely to have played a role in these deaths, perhaps via increased risk of thrombosis. They did not show signs of discomfort during daily inspections (activity, alertness, posture etc.) prior to death, therefore I believe they suffered an acute event. Inclusion of this data has little effect on patterns of heart rate, pulse pressure and activity, compared to those previously described (figure 5.10). However, differences in blood pressure are seen. This further suggests an acute event as a result of hypertension, as longer term discomfort would have resulted in reduced night time activity scores. When data from mice which prematurely died are included, the onset of hypertension occurs similarly in both TRPA1 WT and KO mice. I believe this to be a true representation of the pathophysiological situation. Both groups steadily increase their mean blood pressure to around 150mmHg at day 6. This is the point where the first death occurred; further suggesting cardiovascular events were causative.

Summary 1 – Hemodynamic Parameters And Activity Levels In Ang II Infused TRPA1 WT And KO Mice.

- Ang II infusion causes severe hypertension measured by tail cuff plethysmography and telemetry. This was of faster onset when measured by telemetry, occurring directly after initation of infusion.
- There were no significant differences between the magnitude of hypertension in TRPA1 WT and KO mice when measured by tail cuff plethysmography, both groups of mice showed an approximate 70mmHg increase in mean blood pressure. However, significant hypertension became established earlier in TRPA1 WT mice, occurring from day 6, whereas TRPA1 KO mice showed significant hypertension from day 11.
- There were no significant differences between the magnitude of hypertension in TRPA1 WT and KO mice when measured by telemetry from the aortic arch, where both genotypes demonstrated around 160mmHg systolic blood pressure at the end of the infusion period. Onset patterns were similar between genotypes.
- In line with previous findings, TRPA1 KO mice were more active throughout the protocol. Their activity levels increased with each day of Ang II infusion, which did not occur in WT mice. By the end of the infusion period, TRPA1 KO mice showed around twice the average peak activity count of that seen in the WT group. Significantly increased levels of activity were recorded from KO mice, compared to WT mice, during days 8-14 of the Ang II infusion, when hypertension was established.

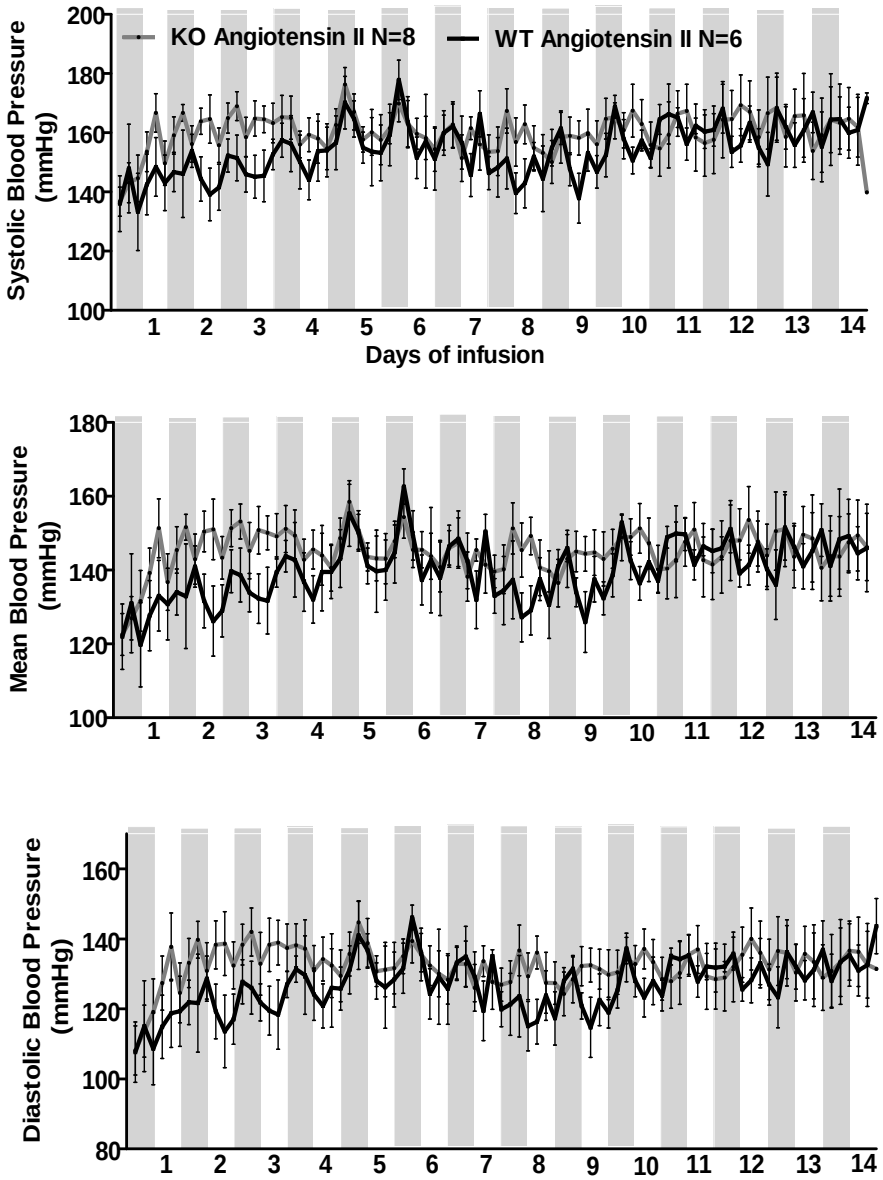

Figure 5.4 Blood Pressure Measurements In Ang II Treated TRPA1 WT And KO Mice Which Completed The Protocol, Collected By Telemetry. Results show measurements taken every 15 minutes from the aortic arch during 14 day Ang II infusion (1.1mg/kg.day) expressed as 4 hour averages. Data is from mixed gender mice. Dark stripes indicate nocturnal period. Graph includes only mice that completed the whole 14 day treatment. No significant differences are seen in a two-way ANOVA with Bonferroni's post-test.

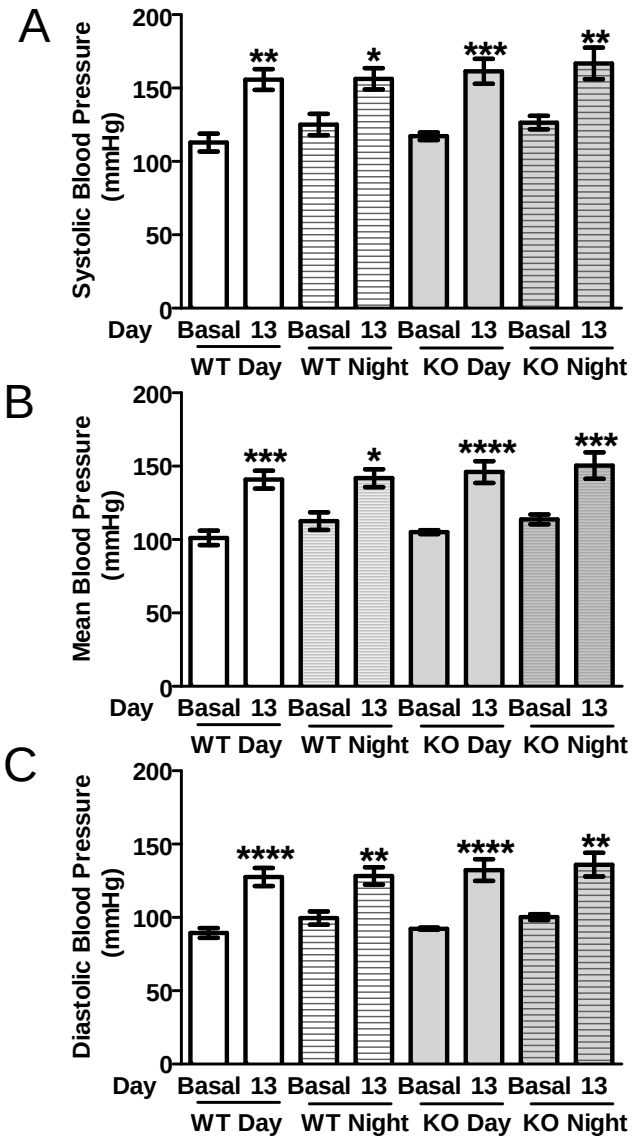

Figure 5.5 Changes In Blood Pressure In TRPA1 WT And KO Mice Which Completed The Protocol, Measured By Telemetry At Baseline And Day 13 Of Ang II Infusion. Results include basal data previously analysed separately in chapter 3. Ang II infused at a rate of 1.1mg/kg/day by osmotic minipump, blood pressure measured from aortic arch. Daytime readings are average from 7am-7pm. Night time is average of 7pm-7am readings. All graphs show mixed gender mice, paired baseline and day 13 readings N=6-10. Statistics are from a one-way ANOVA with Bonferroni's post-test. *p<0.05, **p<0.01, ***p<0.001.

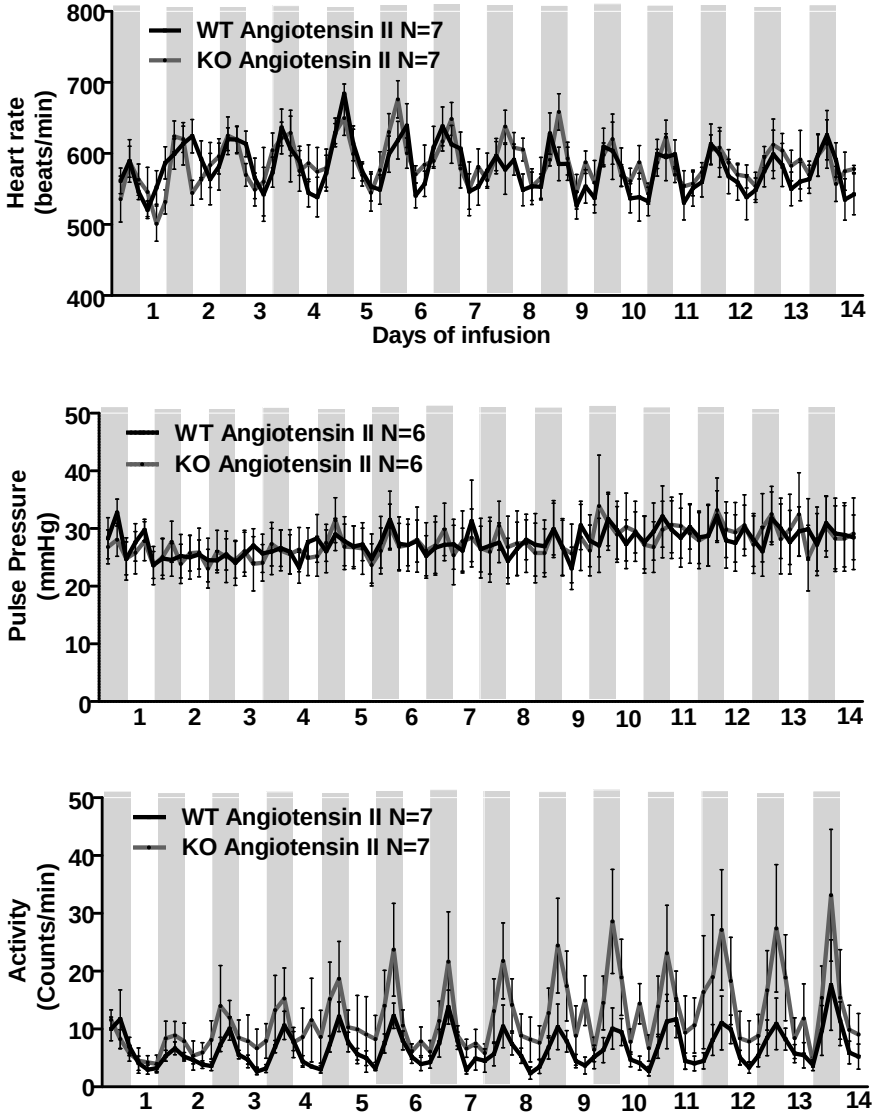

Figure 5.6 Heart Rate, Pulse Pressure And Activity Measurements In Ang II Treated TRPA1 WT And KO Mice Completing The Protocol, Collected By Telemetry. Results show measurements taken every 15 minutes from the aortic arch during 14 day Ang II infusion (1.1mg/kg.day) expressed as 4 hour averages. Data includes mixed gender mice. Dark stripes indicate nocturnal period. Graph includes only mice which completed the whole 14 day treatment. No significance is seen in a two way ANOVA with Bonferroni's post-test.

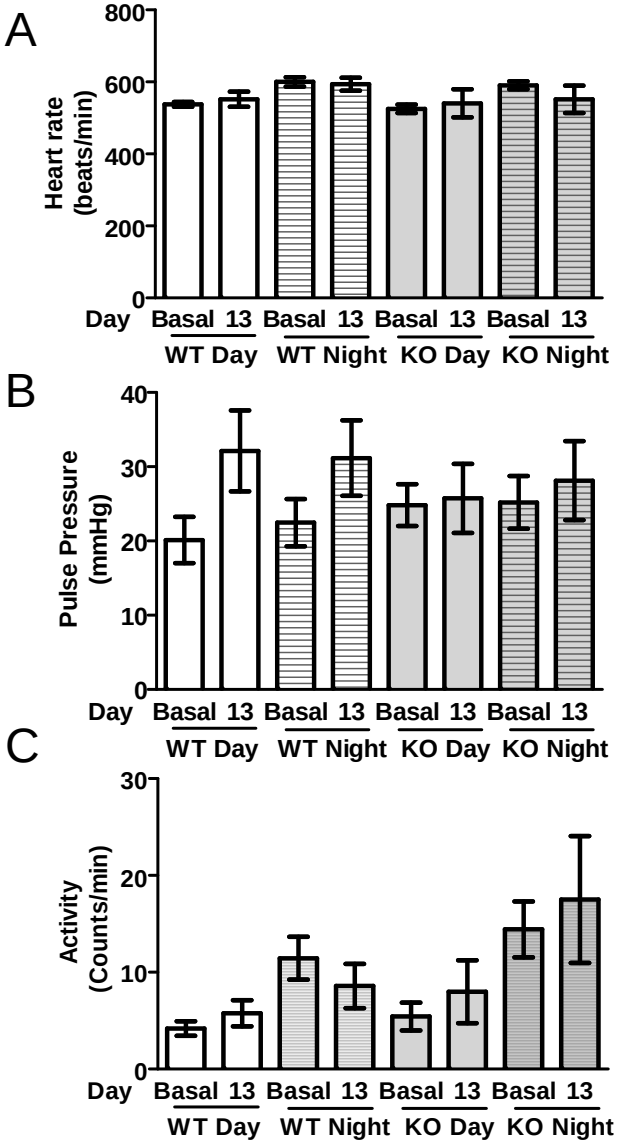

Figure 5.7 Changes In Heart Rate, Pulse Pressure And Activity In TRPA1 WT And KO Mice Completing The Protocol, Measured Using Telemetry At Baseline And Day 13 Of Ang II Infusion. Results include basal data previously analysed separately in chapter 3. Ang II infused (1.1mg/kg/day) by osmotic minipump, pressures measured from aortic arch. Daytime readings are average from 7am-7pm, Night time is average of 7pm-7am readings. All graphs show mixed gender mice, paired baseline and day 13 readings N=6-10. No significance seen in a one way ANOVA for heart rate and pulse pressure, or Kruskall-Wallis test in the case of activity, which does not show a Gaussian distribution.

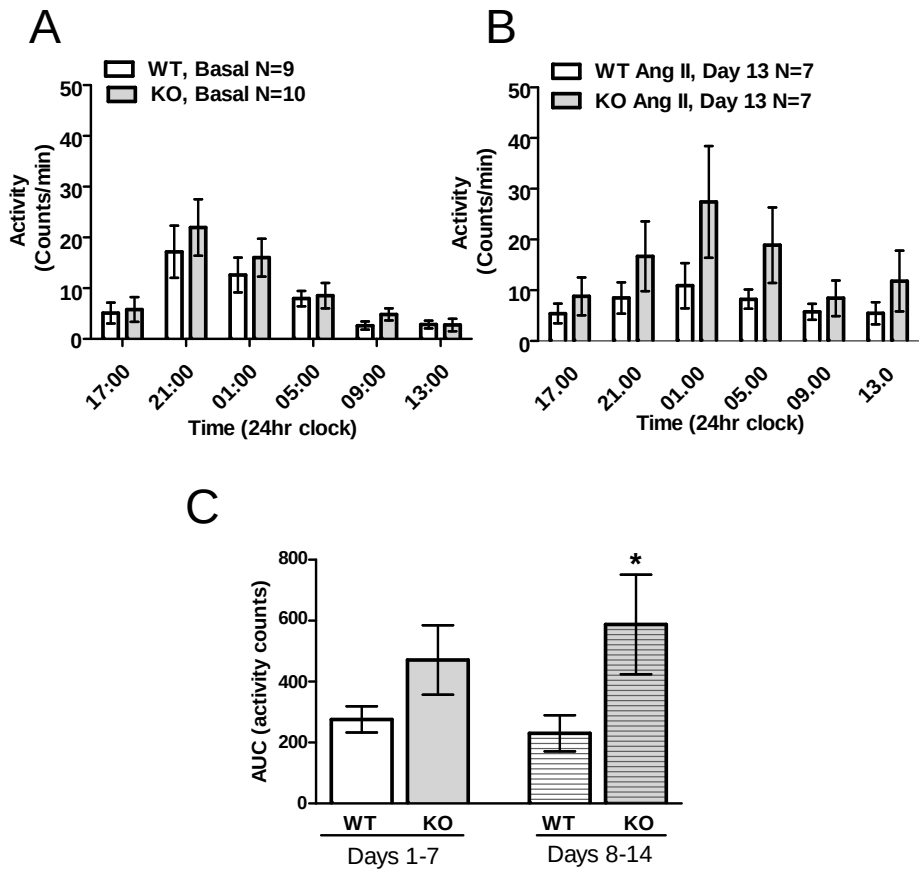

Figure 5.8 Activity Levels In TRPA1 WT And KO Mice Measured Using Telemetry At Baseline And After Ang II Infusion. Results show A) baseline data plotted at 4 hourly intervals. Basal data previously analysed separately in chapter 3. B) Day 13 of Ang II infusion at a rate of 1.1mg/kg/day by osmotic minipump. C) Activity counts over days 1-7 or 8-14 of Ang II infusion measured by area under the curve, grouped by genotype. N=9 for WT, 7 for KO. Statistics are from a one tailed, Mann-Whitney U test comparing WT and KO days 8-14, * $p<0.05$. All graphs show mixed gender mice.

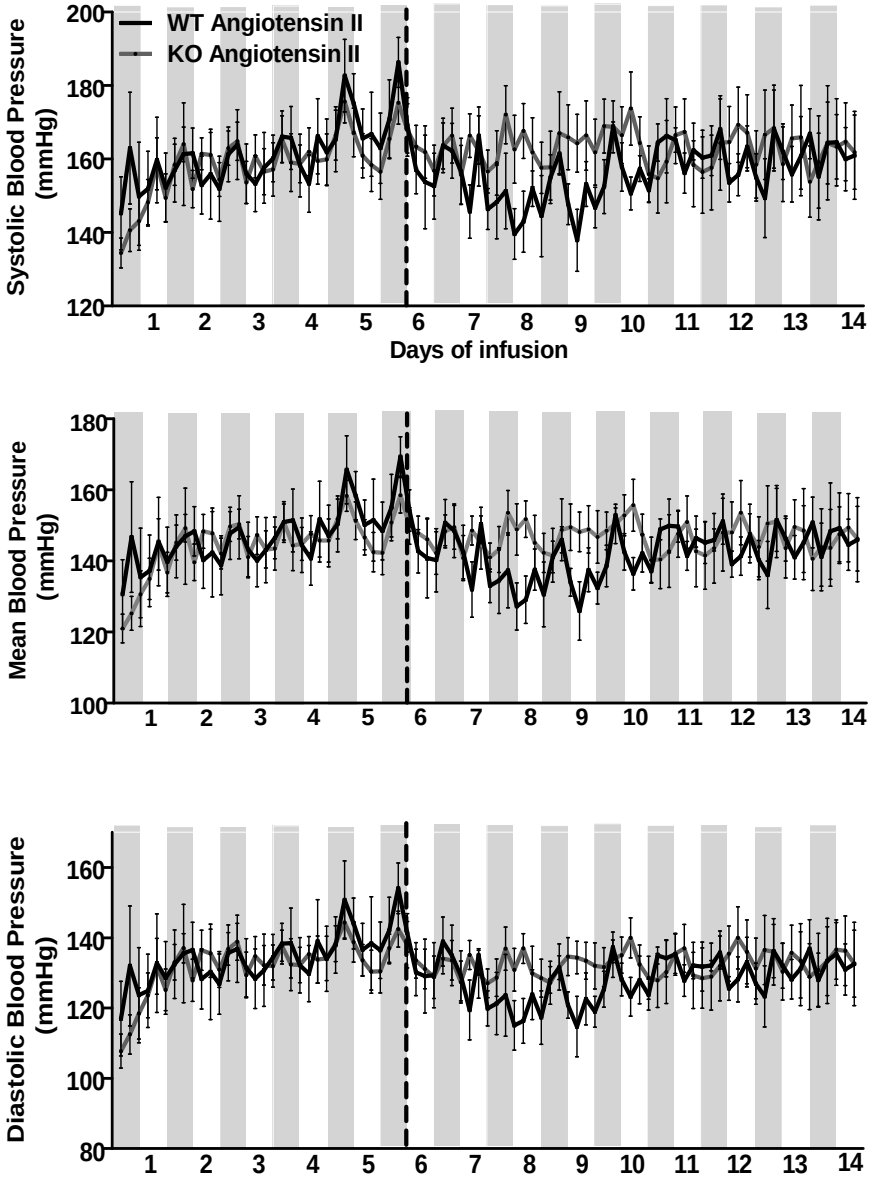

Figure 5.9 Blood Pressure Measurements From All Ang II Treated TRPA1 WT And KO Mice Entering The Protocol, Collected By Telemetry. Results show measurements taken every 15 minutes from the aortic arch during 14 day Ang II infusion (1.1mg/kg.day) expressed as 4 hours averages. Data includes mixed gender mice. Dark stripes indicate nocturnal period. Graph includes all mice entering the protocol, including those who died prematurely. Time of first death is shown as dashed line, WT loss 2x day 5, 1x day 10, KO loss 2x day 6). N=8-11. No significance seen in a two-way ANOVA.

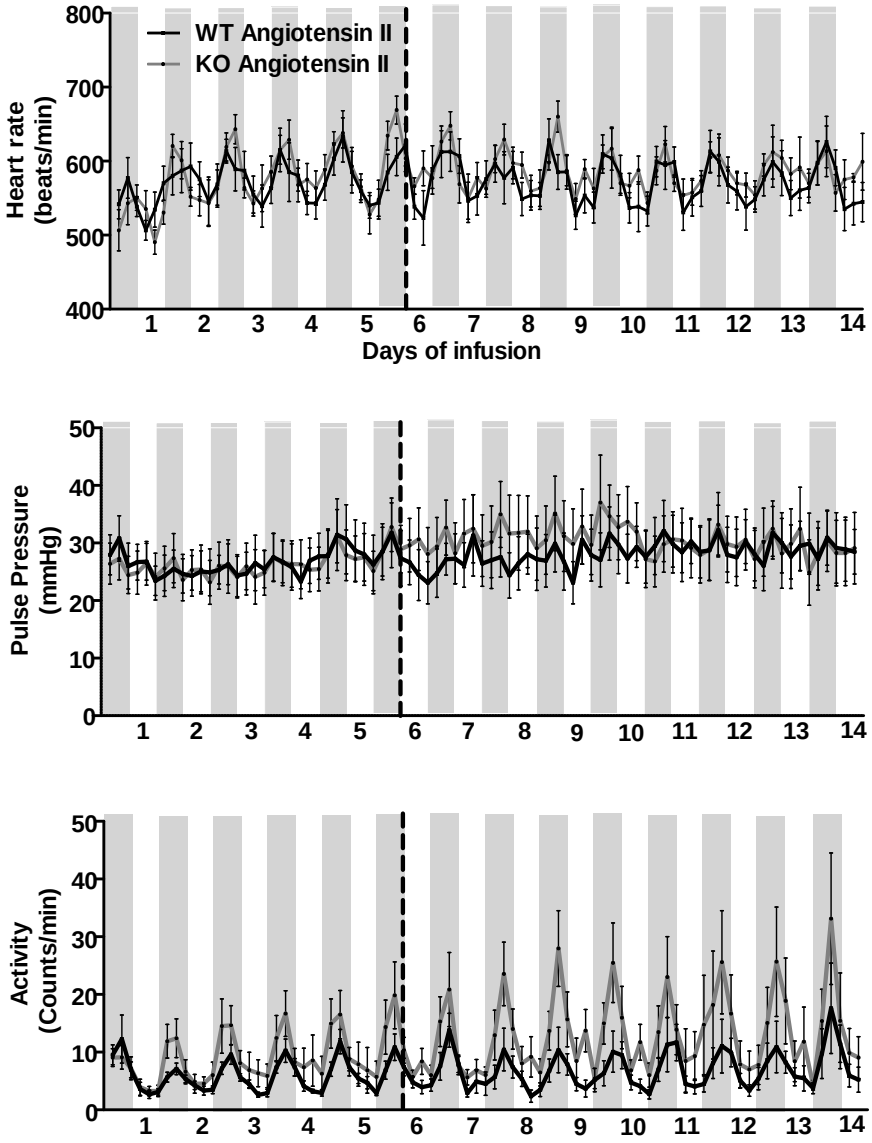

Figure 5.10 Heart Rate, Pulse Pressure And Activity Measurements From All Ang II Treated TRPA1 WT And KO Mice Entering The Protocol, Collected By Telemetry. Results show measurements taken every 15 minutes from the aortic arch during 14 day Ang II infusion (1.1mg/kg/day) expressed as 4 hour averages. Data includes mixed gender mice. Dark stripes indicate nocturnal period. Graph all mice entering the protocol, including those who died prematurely. Time of first death is shown as dashed line (WT loss 2x day 5, 1x day 10, KO loss 2x day 6). N=8-11. No significance seen in a two way ANOVA.

Measuring Hypertrophy In Hypertensive TRPA1 WT And KO Mice

Ang II in the brain is associated with increased sympathetic outflow and energy expenditure, along with appetite suppression (McKinley *et al.*, 2003). As body weight is frequently used as a ratio base in this study, it was important to determine the effect of the treatment protocol on body mass. This data is presented in figure 5.11. Figure 5.11 A shows absolute body weights are similar between TRPA1 WT and KO mice in all treatment groups, at the start and end of the treatment period. However, if this is examined as % of start weight, a clear trend for a decrease in body weight during Ang II treatment is seen in both genotypes. Control mice maintain a similar body weight to that at the start of the protocol (Figure 5.11 B). Although the decrease seen in Ang II treated groups is slight, averaging to less than a 5% body weight loss and not causing significant weight changes over the infusion period, this should be a consideration when analysing body weight ratio results.

As the rate of blood pressure increase and final blood pressure levels are similar in TRPA1 WT and KO mice, hypertrophy can be freely compared between genotypes without pressure considerations. Due to the non-significant trends for body weight changes during Ang II infusion, hypertrophy is measured as a ratio to body weight. This data is collected from paired mice which underwent blood pressure measurement by tail cuff plethysmography or telemetry to increase numbers. Heart mass was measured at or after necropsy as it has been suggested that Ang II induced hypertrophy is due to both myocyte hypertrophy and fibrosis (Schnee and Hsueh, 2000). This hypertrophy can contribute towards diastolic dysfunction and heart failure. Heart mass is shown in figure 5.12, expressed as a ratio to body weight, and also to tibia length. Both methods can be used to show hypertrophy, however the latter method is reported to be the more accurate ratio based on the slow change in bone size in healthy adults, contrasted with the relative flexibility of body weight. Here, similar trends are seen using both ratios, with Ang II treated animals having larger

heart mass than control animals. Significant differences are only seen between TRPA1 KO control and Ang II treated hearts using the ratio to body weight. The differences between Ang II treated TRPA1 WT and KO mice were investigated using t-test, showing significantly larger hearts in hypertensive TRPA1 KO mice than in hypertensive TRPA1 WT mice, using both measures of heart mass. Therefore, although Ang II causes an increase of mass in both WT and KO hearts, but this is significantly more in TRPA1 KO mice.

Heart morphology was also investigated *in vivo* using echocardiography. This is a more detailed measurement and allows investigation of hypertrophy localisation around the left ventricle. Figure 5.13 shows left ventricle mass compared to body weight, measured by echocardiography. As expected from previous figures, there are trends for increased left ventricle mass in Ang II treated animals. Hypertrophy is only significant in TRPA1 KO mice when all groups are compared with ANOVA. In line with previously presented data, trends in this graph also suggest that TRPA1 KO mice are more susceptible to cardiac hypertrophy. Echocardiography also allows measurement of left ventricular wall thicknesses in the working heart, expressed as a ratio to body weight. Measurements taken at the end of the infusion protocol are presented in figure 5.14. Changes seen in this graph show that the majority of left ventricle hypertrophy is derived from the septum and anterior wall, where there are non-significant increases in thickness compared to control animals.

Summary 2 – Hypertrophy In Ang II Treated TRPA1 WT And KO Mice.

- Body weight was not significantly altered by Ang II infusion, despite a trend for decreases in body mass in Ang II treated mice, which was not seen in control mice. This was not genotype dependent.
- Significant cardiac hypertrophy occurs in both TRPA1 WT and KO mice treated with Ang II. Several measures show TRPA1 KO mice have similar basal heart mass but KO mice develop significantly larger hearts than WT mice during Ang II induced hypertension.

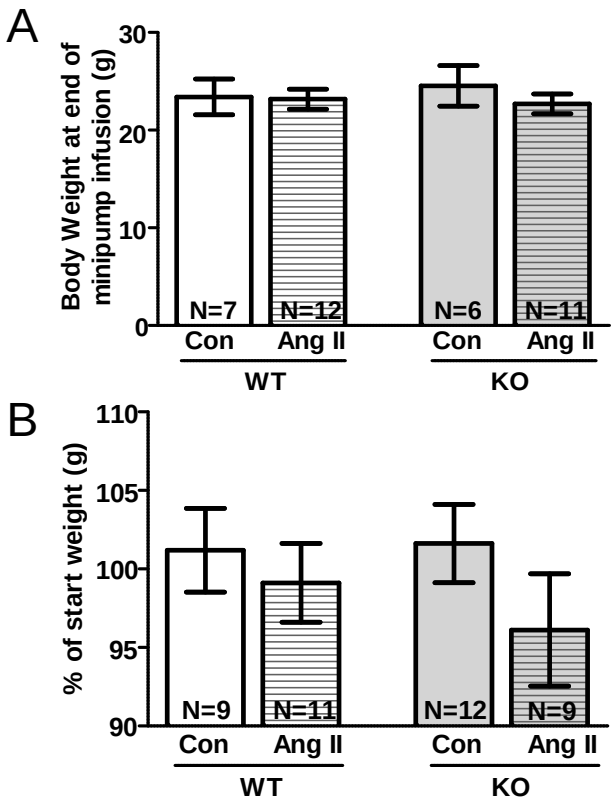

Figure 5.11 Body Weight Of TRPA1 WT And KO Mice Following 14 Day Ang II Infusion Or Control Operation. Results show body weight A. Measured after 14 days infusion (1.1mg/kg/day Ang II by osmotic minipump) or in operation control animals. B. Necropsy weight presented as a % of start weight. All graphs show mixed gender mice. No significance found in a one way ANOVA.

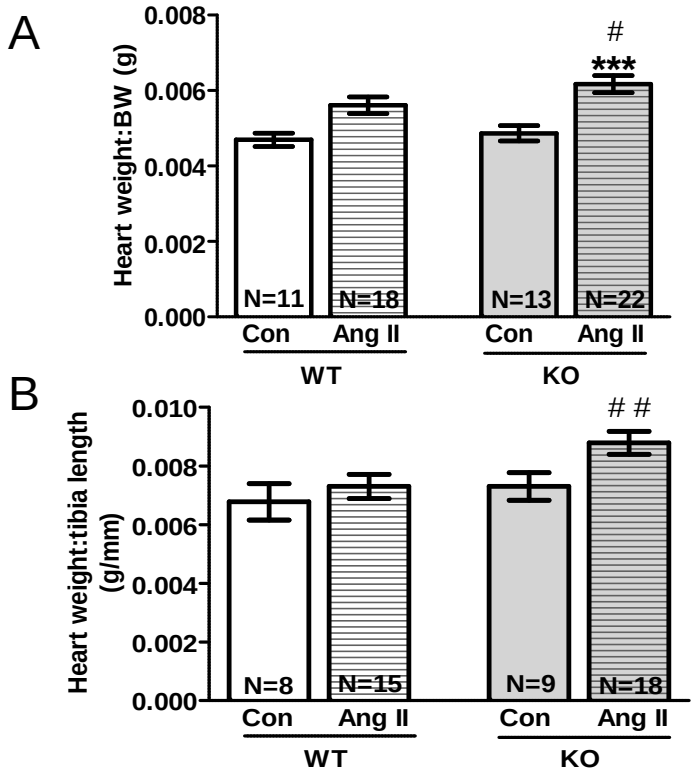

Figure 5.12 Heart Mass Measured At Necropsy Following Ang II Infusion For 14 Days Or Control Operation. Results show mixed gender mice terminated after 14 days treatment Ang II by osmotic minipump (1.1mg/kg/day), or after operation control. A. Shows heart weight as a ratio to BW. B. Shows heart weight as a ratio to tibia length. Statistics are from one way ANOVA with Bonferroni's post-test. ***$p<0.001$, compared to respective control operated animals, or from a one tailed, unpaired t-test comparing Ang II treated groups, #$p<0.05$, # # $p<0.01$.

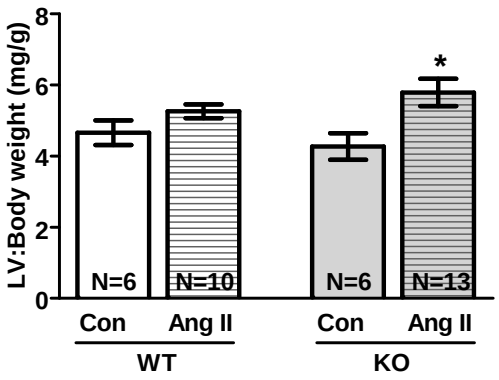

Figure 5.13 Heart Mass Measured By Echocardiography, Following 14 Days Ang II Infusion Or Control Operation. Results show A. Left ventricle mass as a ratio to body weight (BW). Graph shows mixed gender mice. Statistics are from a one way ANOVA with Bonferroni's post-test. *$p<0.05$ compared to control. One tailed, unpaired t-test between Ang II groups gives a value of $p=0.058$.

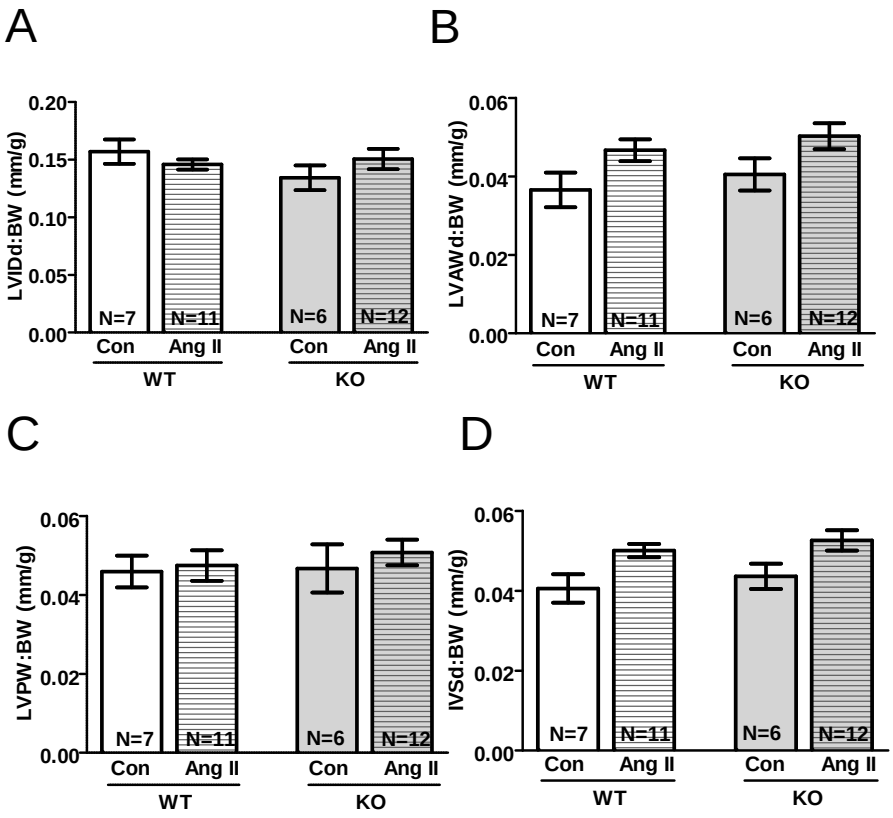

Figure 5.14 Heart morphology Measured By Echocardiography In Ang II Or Control Operated TRPA1 WT And KO Mice. Results show thicknesses measured after 14 days infusion of Ang II (1.1mg/kg/day by osmotic minipump), or in operation control mice. A. Left venticular internal diameter at diastole as a ratio to BW (LVIDd:BW). B. Left ventricular anterior wall thickness at diastole, as a ratio to BW (LVAWd:BW). C. Left ventricular posterior wall thickness at diastole, as a ratio to BW (LVPWd:BW) D. Interventricular septum thickness at diastole, as a ratio to BW (IVSd:BW). All graphs show mixed gender mice. No significant differences seen in a one way ANOVA.

Investigating The Inflammatory Endpoints Of Ang II Induced Hypertension In TRPA1 WT And KO Mice.

Measuring The Expression Of TRPA1 By RT qPCR And Comparing This With Expression Of TRPV1 And TRPC5, In Control And Hypertensive TRPA1 WT And KO Mice

In chapter 1, the genotype of the TRPA1 WT and KO mice was confirmed by endpoint PCR. Using RT qPCR, I have also determined the level of TRPA1 mRNA expression in a variety of tissues and investigated the influence of Ang II infusion. For all experiments, results are normalised against 3 housekeeping genes and a template free sample is also included to check for cross-contamination. The housekeeping genes are GAPDH, mPLA2 and actin. They have been chosen for their stable expression patterns in all treatment groups and are used as an index of mRNA expression for each sample. As described in chapter 2, their suitability for this purpose has been tested using the GeNorm software. Data presented in figure 5.15 shows TRPA1 expression levels in DRG, aorta, heart and mesenteric vessels. These tissues have been chosen as key areas of interest in the vasculature, which have the potential to be influenced by TRPA1 activity. The heart and aorta are of direct interest to hemodynamics and hypertrophy results, whilst the mesentery is of interest to link with my myography data in chapter 4. DRG's have been investigated as the main reported site of TRPA1 expression, where they mediate the majority of the receptors effects.

All WT tissues investigated expressed some TRPA1 mRNA, however no copies were found in TRPA1 KO tissues. Results shown in figure 5.15 indicate that low expression levels of TRPA1 mRNA are present in vascular tissues. I am not currently able to comment on the localisation of TRPA1 expression in this tissue, but this could potentially be a result to sensory neurone innervation. I am also unable to comment on the levels of translated TRPA1 protein. Western blots or immunohistochemistry would be needed to confirm expression, however the poor availability of selective

TRPA1 antibodies is an ongoing problem in the field. Ang II is known to activate many nuclear factors, inducing changes in mRNA expression (Mehta and Griendling, 2007). Data in figure 5.15 shows that Ang II infusion over 14 days significantly increases the level of TRPA1 mRNA transcription in the DRG, which also expresses high levels of TRPA1 basally. This data suggests that the main site of TRPA1 mRNA expression is the DRG, and that it is upregulated in Ang II induced hypertension.

TRPA1 is co-localised with TRPV1 in many locations, including in around 67% of TRPV1 expressing DRG neurones (Kobayashi *et al.*, 2005). It has also been suggested to have regulatory effects on TRPA1 activity and protein levels. Therefore, I have investigated the TRPV1 mRNA transcript levels in a variety of tissues, namely DRG, aorta and heart and mesenteric vessels (Figure 5.16). Unlike TRPA1, TRPV1 is found to be highly expressed in all tissues. This demonstrates that TRPA1 mRNA is expressed at far lower levels than TRPV1 in the vasculature. Therefore the effects of activating each population are likely to differ. In line with this, TRPV1 mRNA shows some evidence of non-significant upregulation in TRPA1 WT and KO aortas from Ang II treated mice. It is unknown if this is sensory neurone derived expression. Confirmation of this expression at the protein level and localisation studies such as immunohistochemistry, would be of additional value.

Due to the increases in physical activity seen in TRPA1 KO mice, I also conducted a preliminary study to investigate TRPA1 mRNA expression in different areas of the mouse brain, and if this was affected by Ang II induced hypertension. Several areas and systems in the brain have been shown to influence physical activity levels and behaviour phenotypes (Jordan *et al.*, 2008). Levels of TRPA1 expression were measured by RT qPCR in the medulla, cortex, and striatum, shown in figure 5.17. In WT mice, low levels of TRPA1 mRNA are found in all brain regions and this is unaffected by Ang II induced hypertension. A TRPA1 KO mouse shows no TRPA1 mRNA copies. These findings are in line with the expression of TRPA1 found in other tissues, suggesting TRPA1 is predominantly

expressed in the DRG and only sparsely in whole tissues. Small areas of the brain may express TRPA1 mRNA but be diluted by the inclusion of other brain areas, furthermore the nature of this expression is not clear as low level expression occurred in all brain areas. Low levels of expression were not related to poor RNA quality, as the same samples yielded high levels of TRPC5, another TRP channel expressed highly in the brain (Okada *et al.*, 1998). TRPC5 expression was also not altered during hypertension (5.17B).

Investigating The Levels Of Plasma CGRP In TRPA1 WT And KO Mice With Ang II Induced Hypertension.

Several studies have suggested that CGRP plays a compensatory role in hypertension. This has recently been reviewed by Smillie and Brain (2011), with some studies showing lower levels of plasma CGRP in hypertension, and others showing increased levels. My data also shows that neuronal TRPA1 mRNA expression is increased in Ang II infused TRPA1 WT mice, while results presented in chapter 4 show that TRPA1 mediated vasorelaxation occurs via CGRP. I have not found a difference in blood pressure between TRPA1 WT and KO mice either basally, or during Ang II infusion. However, increased TRPA1 expression levels in the DRG suggest it could have a role in hypertension, which may be masked by other factors. My original hypothesis was that TRPA1 would act to compensate against hypertension via the release of CGRP. Therefore I measured the plasma levels of α/βCGRP using ELISA. This will be referred to as CGRP collectively. As shown in figure 5.18, the results are in line with results from human essential hypertension patients, measured in a similar manner by Portaluppi *et al* (1992). No significant changes in plasma CGRP are seen between genotypes, or during experimental hypertension. However, there is a trend for decreased CGRP levels in hypertensive mice.

Summary 3 – Expression Of TRP Channel Receptors And Plasma CGRP Levels In Ang II Treated And Control TRPA1 WT And KO Mice.

- TRPA1 mRNA is not highly expressed at any level of the vasculature. This is demonstrated by comparing the findings of high TRPV1 expression in the vasculature and high TRPC5 expression in the brain, measured from the same samples. The responses of these other TRP channels are both largely unaffected by Ang II induced hypertension.
- TRPA1 mRNA is predominantly expressed in DRG neurones, and this expression significantly increases during Ang II infusion.
- Basal plasma CGRP levels are not affected by genotype and show a trend for reduction during Ang II induced hypertension. This suggests a lack of effect of TRPA1 activity on basal plasma CGRP and after 14 days Ang II infusion.

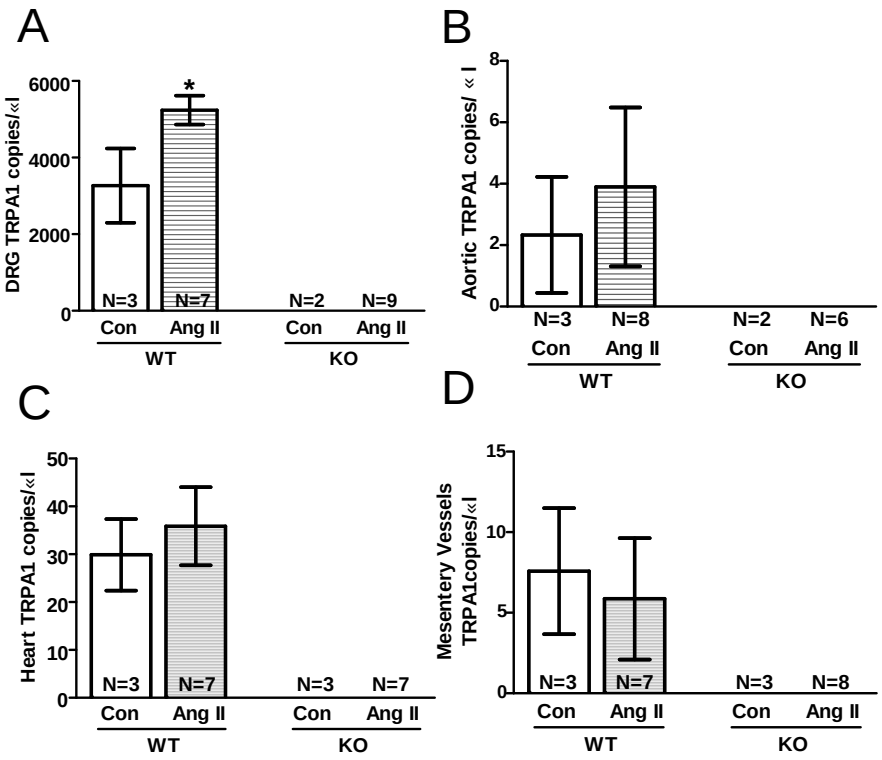

Figure 5.15 TRPA1 Gene Expression In TRPA1 WT And KO Mice After 14 Day Ang II Infusion Or Control Operation. Results show mRNA expression measured by RT qPCR after 14 days infusion of Ang II (1.1mg/kg/day by osmotic minipump), or operation control. A. DRG B. Aorta C. Heart D. Mesenteric vessels. All graphs show mixed gender mice. Statistics are from a one tailed t-test. *$p<0.05$ compared to control.

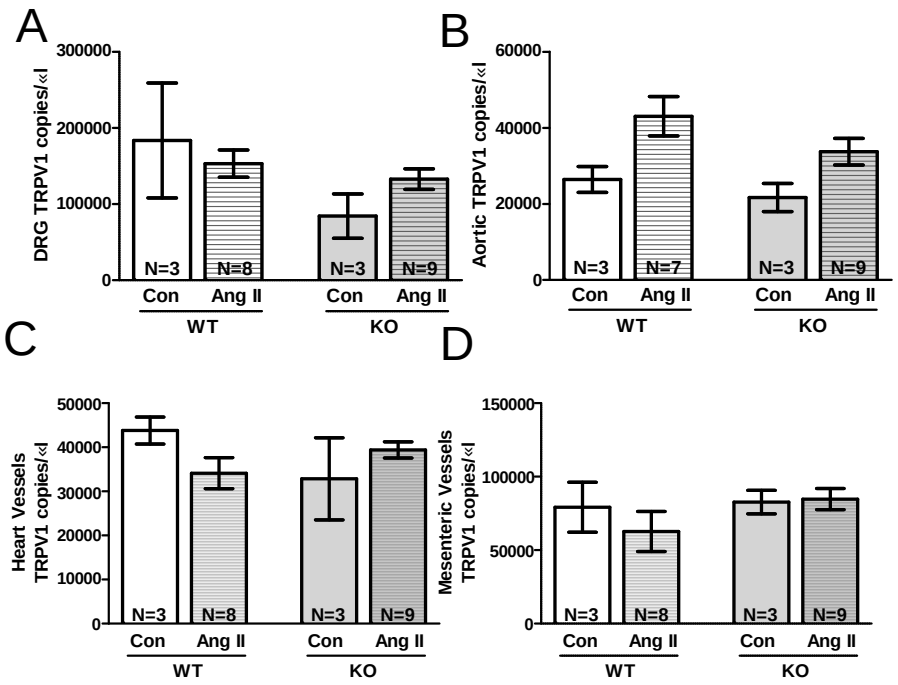

Figure 5.16 TRPV1 Gene Expression, Measured By RT qPCR, In 14 Day Ang II Or Control Treated TRPA1 WT And KO Mice. Results show mRNA expression measured by RT qPCR following 14 day Ang II infusion at 1.1mg/kg/day by osmotic minipump, or operation control. A. DRG. B. Aorta. C) Heart. D) Mesenteric Vessels. All graphs show mixed gender mice. No significance is seen using a one way ANOVA.

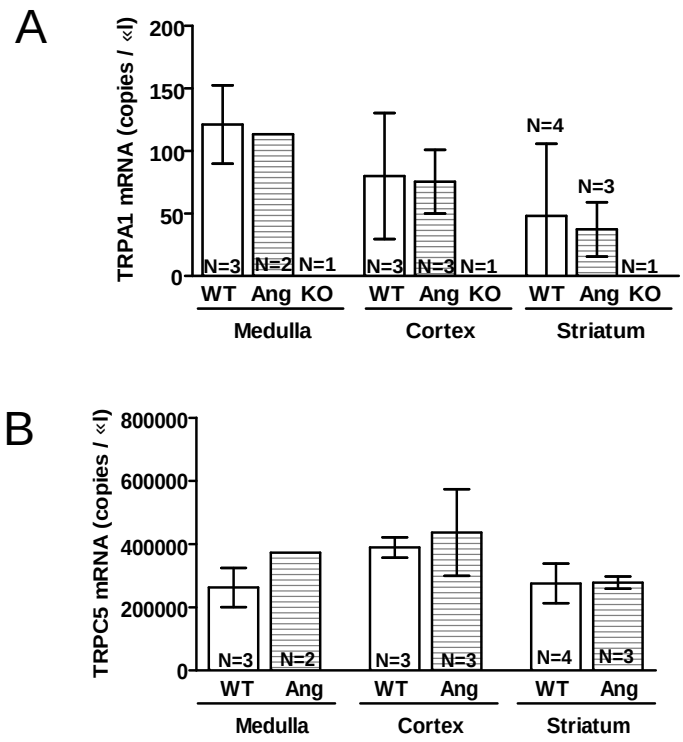

Figure 5.17 TRPA1 And TRPC5 Gene Expression In TRPA1 WT And KO Mice Following 14 Day Ang II Infusion Or Control Operation. Results show mRNA expression measured by RT qPCR from the medulla, cortex and striatum after 14 days infusion of Ang II (1.1mg/kg/day by osmotic minipump), or operation control. A) TRPA1 B) TRPC5 (not including TRPA1 KO). Graph shows mixed gender mice. No significant differences are seen using a one way ANOVA.

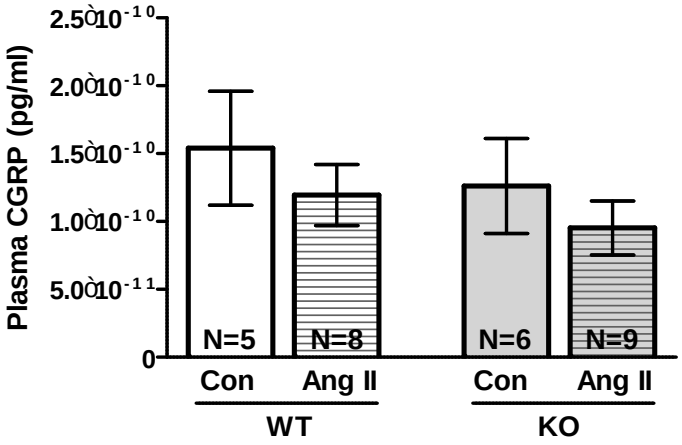

Figure 5.18 Plasma CGRP In TRPA1 WT And KO Mice Following 14 Day Ang II Infusion Or Control Operation. Results show plasma CGRP measured by ELISA from plasma samples collected after 14 days infusion of Ang II (1.1mg/kg/day by osmotic minipump), or operation control. Graph shows mixed gender mice. No significance seen using a one way ANOVA.

Measuring The Expression Of Inflammatory Biomarkers In Control And Hypertensive Mice, TRPA1 WT And KO Mice

Following the completion of 14 days Ang II infusion, tissues were collected for RT qPCR. The expression of pro and anti oxidant proteins and inflammatory mediators were measured. The mRNA expression levels of mediators were investigated in the heart and aorta, as these tissues showed significantly increased hypertensive hypertrophy in TRPA1 KO mice compared to WT mice, in the Ang II induced hypertension model.

Pro-Oxidative Markers

Figure 5.19 shows expression levels of NOX2 and NOX4 in the aorta and heart of control or Ang II treated TRPA1 WT and KO mice. These locations were chosen as there are direct links between Ang II activation of NOX and hypertrophy. TRPA1 WT and KO control mice display high copy numbers of NOX2 mRNA in the aorta and heart (5.19A and B), with a non-significant trend for decreased levels in KO mice. When analysed using unpaired t-test, Ang II induced hypertension significantly increases the levels of NOX2 mRNA expression in aortas of the TRPA1 KO mice, compared to that of the WT mice. In the heart there is a strong trend for increased NOX2 mRNA in both Ang II treated groups. Further N numbers will be needed to expand on the significance of these findings.

Both the aorta and heart show lower copy numbers of NOX4 (5.19C and D) than NOX2. Similar to that of NOX2, there is non significant trend for decreased expression of NOX4 in TRPA1 KO mice aortas, compared to those of WT mice. Using ANOVA analysis, NOX4 mRNA expression significantly increases in both WT and KO Ang II treated mouse hearts. This is of significantly smaller magnitude in TRPA1 WT mice when tested by t-test, following our interests in phenotype differences between TRPA1 WT and KO mice. In the aorta, NOX4 expression was not upregulated in TRPA1 WT mice during hypertension, but analysis by t-test shows significant upregulation in TRPA1 KO mice treated with Ang II, compared to their controls. However, a higher basal level of NOX4 mRNA

expression means that Ang II treated TRPA1 WT and KO aortas do not show significant differences. Together, differing regulation mechanisms of NOX isoforms expression is indicated in the heart and aorta.

Anti-Oxidative Markers

The expression studies on pro-oxidant genes suggest the increased hypertrophy in KO mice could be due to increased NOX expression and ROS levels. To avoid damaging oxidative stress levels, increased levels of ROS must be met by increased anti-oxidant defences, such as SOD and HO-1. Both the aorta and heart show high basal copy numbers of HO-1 and SOD1 mRNA (figure 5.20). These are not significantly different between genotypes. Ang II induced hypertension increases mRNA expression of HO-1 mRNA in both genotypes, however this seems more prominent in the aorta of TRPA1 KO hypertensive mice and the heart of TRPA1 WT hypertensive mice (figure 5.20A and B). This finding suggests differential regulation in each tissue. In a t-test, Ang II treated TRPA1 KO mice show significantly more HO-1 mRNA expression in the aorta, but significantly less in the heart, compared to Ang II treated WT mice.

SOD1 expression showed no significant differences in TRPA1 WT and KO control mice, however Ang II induced hypertension causes non-significant trends for an increase in SOD1 expression in hearts from both genotypes, and a decrease in expression in the aorta of TRPA1 KO mice. When Ang II treated groups are analysed by t-test, TRPA1 KO mice show a significantly decreased level of SOD1 mRNA in the aorta, but an increased expression level in the heart, compared to TRPA1 WT mice.

Summary 4 – Oxidative Markers In Ang II Induced Hypertensive Or Control TRPA1 WT And KO Mice

- NOX 4 expression significantly increases in the heart of both TRPA1 WT and KO mice during Ang II induced hypertension. Significantly more NOX2 and NOX4 mRNA are found in hypertensive TRPA1 KO mice, compared to that of hypertensive TRPA1 WT mice, in the heart and aorta of respectively. This suggests there may be increased ROS production in Ang II treated TRPA1 KO mouse vasculature.
- Anti-oxidative markers HO-1 and SOD1 show trends for upregulation in Ang II induced hypertension, except for SOD1 in the aorta. Ang II treated TRPA1 KO mice show significantly higher levels of HO-1 in the aorta but lower levels of SOD1 compared to Ang II treated TRPA1 WT mice. In the heart they also show significantly lower levels of HO-1 alongside higher SOD1 mRNA levels compared to Ang II treated TRPA1 WT mice. Therefore differential effects mean overall antioxidant status is unclear.
- Overall, data suggests that basal levels of oxidative stress would be similar in TRPA1 WT and KO mice, however during Ang II induced hypertension there may be increased oxidative stress in TRPA1 KO mouse heart and aortas.

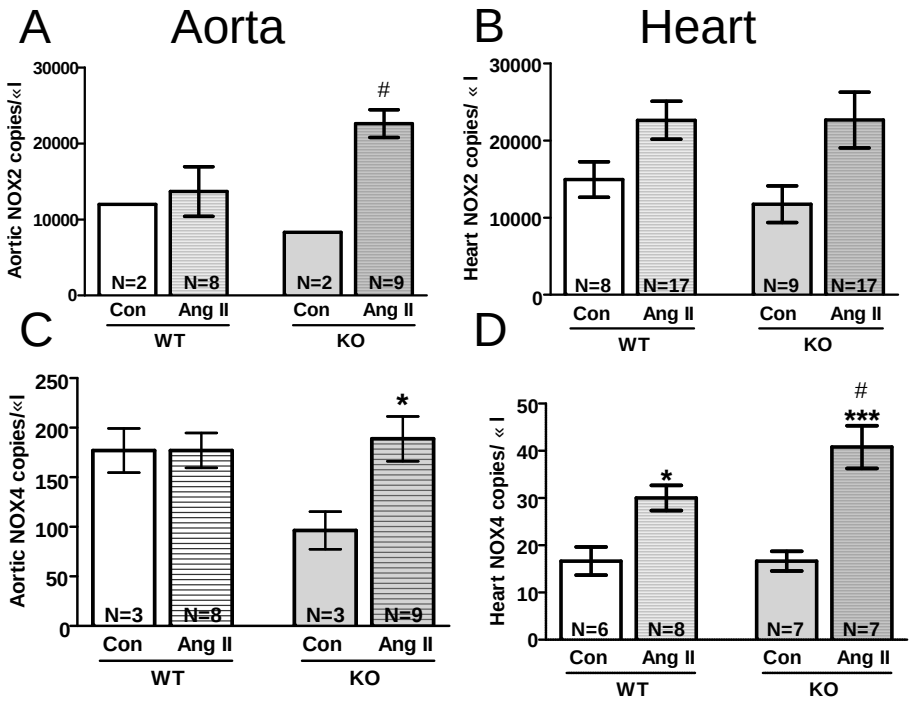

Figure 5.19 NOX2 And NOX4 Gene Expression Measured By RT qPCR From The Descending Aorta And Heart Of 14 day Ang II Treated Or Control TRPA1 WT And KO Mice. Results of mRNA expression measured by RT qPCR following 14 day infusion of Ang II (1.1mg/kg/day by osmotic minipump), or operation control. A/B. NADPH oxidase 2 (NOX2) in aorta and heart. C/D. NADPH oxidase 4 (NOX4) in aorta and heart. All graphs show mixed gender mice. Statistics were initially done are using one way ANOVA with Bonferroni's post test, but showed no significance except for that shown in D) *p<0.05, ***p<0.001, compared to respective control groups. Other graphs are statistically analysed using unpaired, one way t-test between two groups of special interest; *p<0.05 comparison to respective control, #p<0.05 comparison to WT Ang II treated group.

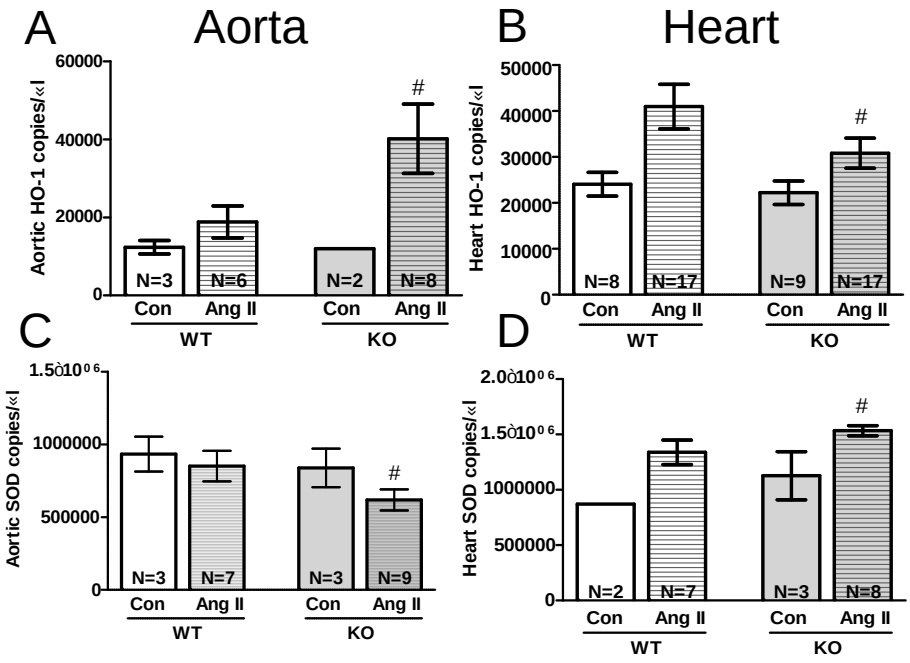

Figure 5.20 HO-1 And SOD1 Gene Expression Measured By RT qPCR From The Descending Aorta And Heart Of 14 Day Ang II Treated Or Control TRPA1 WT And KO Mice. Results show mRNA expression measured by RT qPCR following 14 days infusion of Ang II (1.1mg/kg/day by osmotic minipump), or operation control. A/B. Haemoxygenase-1 (HO-1) in aorta and heart. C/D. Intracellular superoxide dismutase (SOD1) in aorta and heart. All graphs show mixed gender mice. There is no significant differences using one way ANOVA with Bonferroni's post test. Statistics shown are from one way, unpaired t-tests comparing to Ang II treated WT group #$p<0.05$.

Inflammatory Biomarkers

Essential hypertension is an inflammatory disease associated with an increase in circulating chemokines and cytokines.

Figure 5.21, tissue expression of MCP-1 mRNA is measured from the aorta and heart. These locations have been chosen with respect to the pro-fibrotic nature of MCP-1 and the hypertrophy that was seen in the hypertensive mice. MCP-1 is highly expressed in TRPA1 WT and KO control mouse aortas and hearts. A slight trend for decreased levels of mRNA in TRPA1 KO mice is seen, but is not significant. Ang II induced hypertension induces non-significant increases in MCP-1 mRNA expression in the aorta and heart of TRPA1 WT mice, and in the Ang II treated TRPA1 KO heart. No trend for upregulation is seen in the TRPA1 KO aorta. As I am interested in differences between hypertensive TRPA1 WT and KO mice in particular, these two groups were analysed by t-test. This analysis shows significantly higher MCP-1 mRNA expression in Ang II treated TRPA1 WT aortas, compared to Ang II treated TRPA1 KO aortas. A similar, non-significant trend is seen in the heart. Therefore TRPA1 KO mice have blunted increase in MCP-1 expression in Ang II induced hypertension.

Figure 5.22A and B show the IL-6 mRNA expression in the aorta and heart of TRPA1 WT and KO mice. Figure 5.22C shows plasma protein levels. This data was analysed differently to that of previous expression data as it did not comply with a normal distribution, as tested by the Shapiro-Wilks test, thus is analysed with non-parametric tests. In control mice, basal levels of IL-6 mRNA expression and plasma protein are similar between TRPA1 WT and KO mice. In Ang II induced hypertension the levels of IL-6 expression and protein increase in both genotypes, but far more so in TRPA1 WT mice, showing significantly upregulated IL-6 mRNA in the heart and higher plasma protein levels. Data from the aorta follows an identical non-significant trend. Ang II treated TRPA1 KO mice show a blunted response, showing significantly less IL-6 mRNA in the heart and

IL-6 plasma protein levels, compared to Ang II treated TRPA1 WT mice. This data suggests that TRPA1 KO mice are unable to substantially increase their IL-6 production, or that they reacted differently to Ang II induced hypertension.

Plasma levels of KC, the murine analogue of IL-8, were also measured in this study. This will be referred to as mIL-8. mIL-8 is a cytokine associated with inflammatory cell infiltration and has been linked with cardiac fibrosis. Similar to that of IL-6, this data did not fit a normal distribution in the Shapiro-Wilks test, so is analysed with the Kruskall-Wallis test, with Dunn's post-test, a non-parametric form of ANOVA. In figure 5.23, plasma mIL-8 is shown to be similar in control TRPA1 WT and KO mice. Ang II induced hypertension increases expression in both genotypes, which was significant only in TRPA1 KO mice.

Summary 5 – Inflammatory Cytokines And Chemokines In Ang II Induced Hypertension Or Control Operated TRPA1 WT And KO Mice

- MCP-1 mRNA is highly expressed in the heart and aorta of TRPA1 WT and KO mice. There are non significant trends for slightly decreased basal levels in TRPA1 KO mice, and upregulation in both genotypes in hypertension. However, there is no upregulation in TRPA1 KO aortas, significantly differing from the response seen in TRPA1 WT aortas.
- IL-6 mRNA and protein expression is similar at basal levels in TRPA1 WT and KO mice, with significant upregulation during hypertension in TRPA1 WT mouse heart and plasma. This increase is significantly blunted in TRPA1 KO mouse heart and plasma.
- mIL-8 protein expression is similar between genotypes at baseline and upregulated in both TRPA1 WT and KO mice during hypertension. This was significant only for TRPA1 KO mice but did not show a strong genotype dependent effect.

- All of these inflammatory markers are associated with inflammatory cell infiltration and fibrotic remodelling. Although the overall impact of these findings is not clear.

Investigating The Ability Of Isolated Macrophages To Produce Inflammatory Cytokines

The expression studies shown previously suggest that TRPA1 KO mice may respond differently to Ang II induced hypertension. In particular, data suggests that oxidative stress may be increased in the aorta and heart of Ang II treated KO mice, but that they can also have reduced inflammatory cell infiltration and cytokine responses. Data in this study shows that upregulation of IL-6 and MCP-1 is blunted in TRPA1 KO mice. IL-8 and IL-6 are both typically produced by macrophages (Jovanovic *et al.*, 1998). When IL-8 is released in tissues, it causes accumulation of neutrophils into the area (Jorens *et al.*, 1992). In tissues, IL-6 induces expression of other pro-inflammatory markers such as MCP-1, a chemoattractant protein for macrophages (Tieu *et al.*, 2009). Therefore, all these molecules are interlinked and are important for the functioning of the innate immune system, but also induce inflammation that can precipitate cardiovascular disease. To further examine the role of macrophages in the production of cytokines measured in my hypertension model, I developed an experiment to measure cytokine production from isolated macrophages. Figure 5.24A and B shows data collected from a preliminary experiment, where macrophages are collected from the peritoneal cavity of CD1 mice following stimulation with 1% oysterglycogen to cause chemotaxis and increase retrieval numbers. These macrophages are plated and adhere to the base of culture dishes, where they are stimulated with Ang II for various lengths of time.

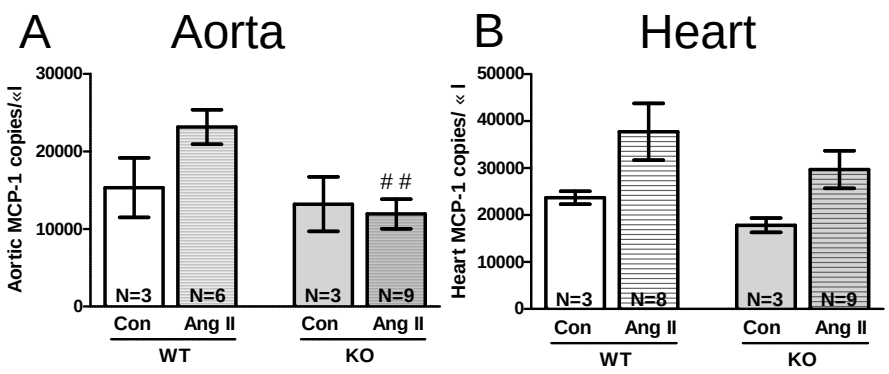

Figure 5.21 MCP-1 Gene Expression Measured By RT qPCR From The Descending Aorta And Heart Of 14 Day Ang II Treated Or Control TRPA1 WT And KO Mice. Results show mRNA expression measured by RT qPCR following 14 days infusion of Ang II (1.1mg/kg/day by osmotic minipump), or operation control. A) Aorta, B) Heart. All graphs show mixed gender mice. Statistics are one tailed, unpaired t-test comparing to WT Ang II treated group. # #p<0.01.

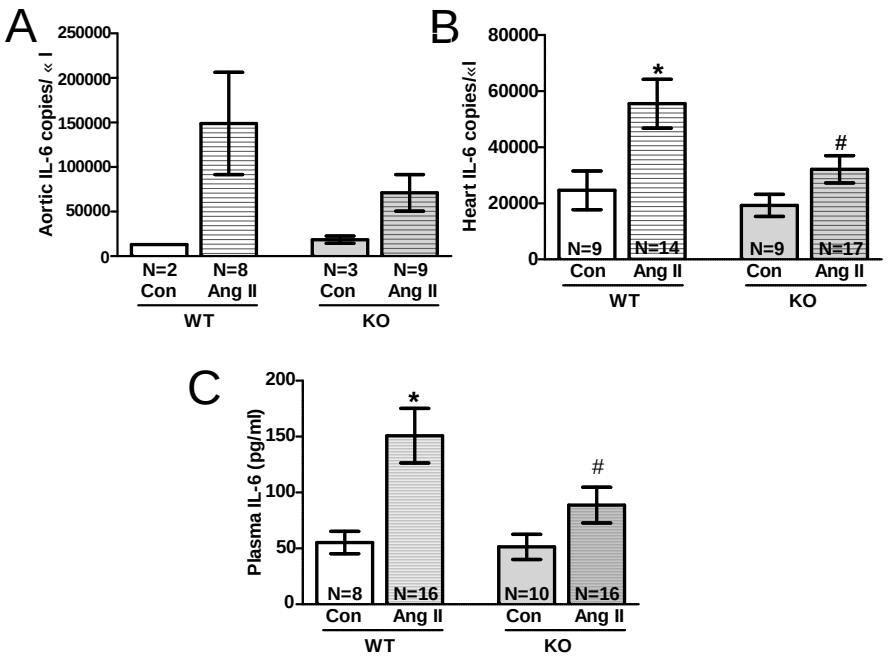

Figure 5.22 IL-6 Gene And Protein Expression In 14 Day Ang II Treated Or Control TRPA1 WT And KO Mice. Results show IL-6 mRNA expression in the A. descending aorta and B. Heart measured by RT qPCR after 14 days infusion of Ang II (1.1mg/kg/day by osmotic minipump), or operation control. C. Plasma IL-6 levels measured at the end of the 14 days infusion. All graphs show mixed gender mice. As not all groups show a normal distribution, statistics are from a Kruskal-wallis test with Dunn's post test, *$p<0.05$ compared to control. Following this, our specific groups of interest were compared with a Mann-whitney U test was used to compare Ang II treated groups, significance shown with #$p<0.05$.

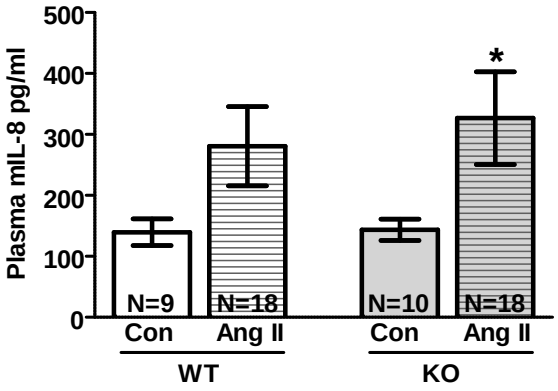

Figure 5.23 Changes In Plasma mIL-8 Levels In Ang II Treated Or Control TRPA1 WT And KO Mice. Results show mIL-8 plasma protein measured after 14 days infusion of Ang II infusion (1.1mg/kg/day by osmotic minipump), or operation control. Graph shows mixed gender mice. Statistics from Kruskal-Wallis test with Dunn's post-test due non-Gaussian distribution. *$p<0.05$ compared to control.

The supernatent is then analysed using an MSD multiplex ELISA, quantifying the amount of IL-6 and mIL-8 produced. Both IL-6 and mIL-8 are detectable 4 hours post Ang II stimulation, peaking at 12 hours. Levels decline towards 24 hours. This data shows that our experiment is functional, and that cytokine production can be effectively measured over 24 hours post stimulation. It also highlights the 12 hours time point as the peak of Ang II induced cytokine production.

This method was used to investigate the ability of macrophages from TRPA1 WT and KO mice to produce IL-6 and mIL-8 following Ang II stimulation. As shown in figure 5.25A and B. IL-6 production occurs later than expected from our preliminary experiments, peaking at the 24 hour time point. Although no significance was achieved within the data, trends in the graph indicate that macrophages from TRPA1 KO mice do not produce as much IL-6 as those from paired WT mice. However, the graph shows no effect of Ang II stimulation, suggesting that macrophages from these mice behave differently than those from CD1 mice, and the protocol may require further optimisation.

The same experiment was conducted to analyse mIL-8 production levels. In macrophages from TRPA1 WT mice there was no effect of Ang II stimulation, however, a small peak of mIL-8 is seen at 24 hours. In TRPA1 KO mice there seems to be some induction of mIL-8 production by Ang II, however the profile is unclear. Control macrophages from TRPA1 KO mice again show a small peak of mIL-8 production after 24 hours Ang II stimulation.

Therefore, our studies using isolated macrophages are currently at a preliminary stage, requiring further optimisation. However, loose interpretation of the existing data could indicate potential trends showing a reduction in IL-6 production from macrophages isolated from TRPA1 KO mice, in parallel with increased mIL-8 production.

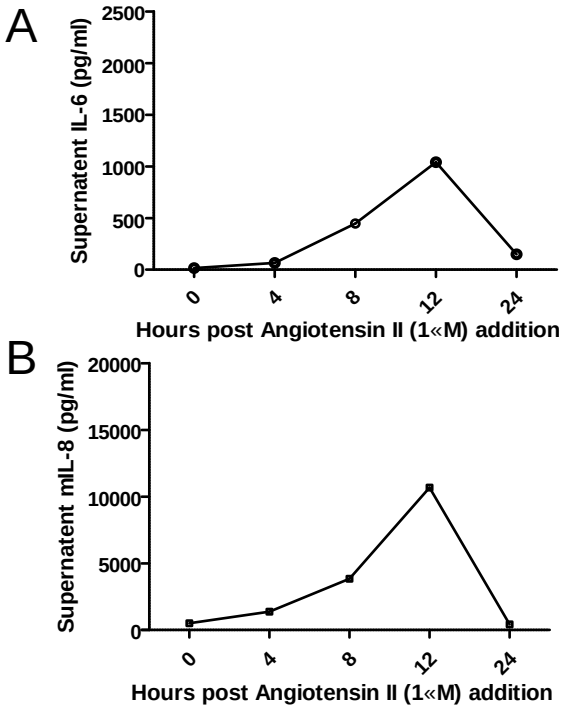

Figure 5.24 IL-6 And mIL-8 Production By Isolated CD1 Macrophages, Treated With Ang II. Results show cytokine protein concentration in the culture supernatent measured at various time points after addition of Ang II (1μM). A. IL-6. B. mIL8. All graphs show female mice, N=2.

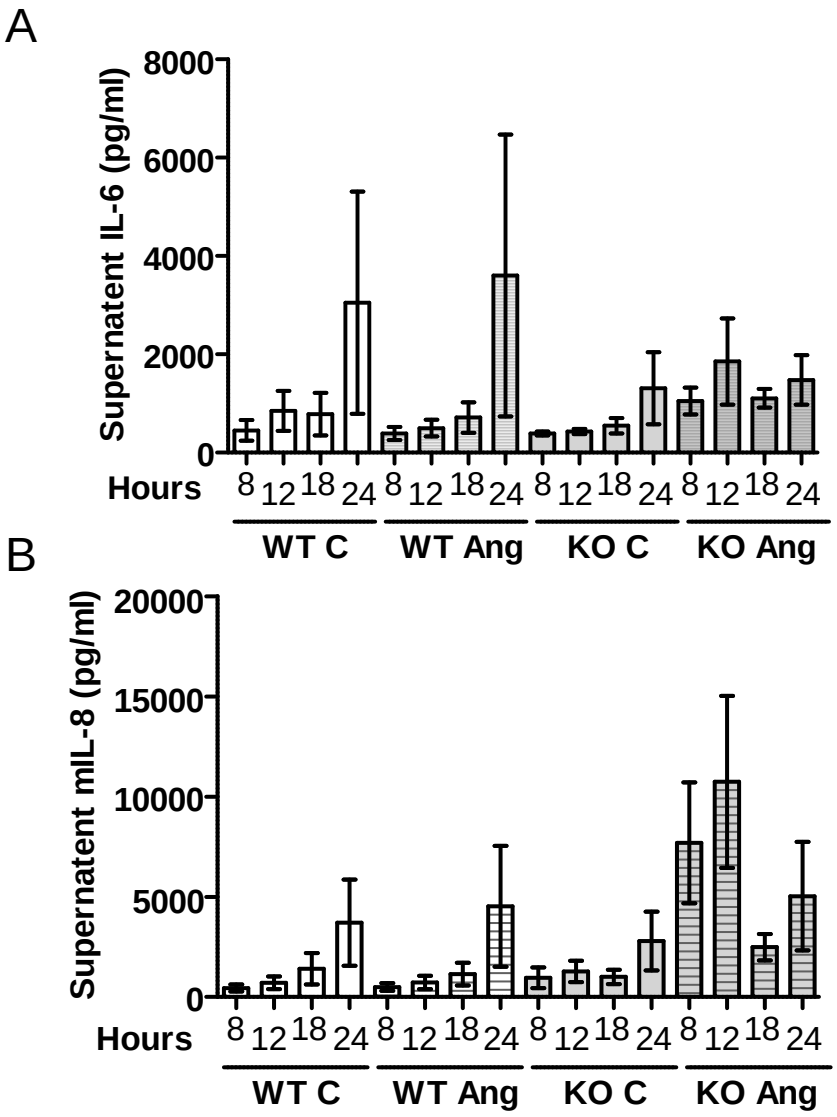

Figure 5.25 IL-6 And mIL-8 Production By Isolated TRPA1 WT And KO Macrophages, Treated With Ang II Or Vehicle. Results show cytokine protein concentration in the culture supernatent measured at various time points after addition of Ang II (1μM, (Ang)) or tissue culture medium (vehicle (C)). A. Shows IL-6. B. Shows mIL8. All graphs show female mice. N=3-4.

Discussion

In this chapter I have investigated the effect of Ang II induced hypertension in TRPA1 WT and KO mice. Similar trends in hypertension, hypertrophy and systemic inflammation are seen in both genotypes of mice, suggesting that TRPA1 has a limited role in the pathogenesis of this experimental disease. Data analysis has been hampered by poor statistical powering, likely due to low control group N values. Further studies should focus on confirmation of the findings by increasing control group numbers. Significant findings and differences between genotypes found in this chapter are summarised in table 5.1 and discussed below.

Hypertension; Using Tail Cuff Plethysmography And Telemetry To Characterise The Profile Of Ang II Induced Hypertension In TRPA1 WT And KO Mice.

At the beginning of this chapter I used TRPA1 WT and KO mice trained for blood pressure recordings to be taken by tail cuff plethysmography in a model of hypertension induced by Ang II infusion. As discussed in chapter 3, naive TRPA1 KO mice present with a hypotensive phenotype; the reason for which is unknown. In this chapter I present serial blood pressure recordings collected from control mice over a period of one month by tail cuff plethysmography (Figure 5.3). In this figure, a strong trend was shown for a lower mean blood pressure in TRPA1 KO mice, which reached significance on some occasions. Whilst demonstrating the stability of readings from the trained mice, it also suggests that the hypotensive phenotype is not consistent and frequently lost at intervals coinciding with weekends, when the animal facility is markedly quieter. This indicates that housing environment could be a potential source of blood pressure differences when measuring by tail cuff plethysmography and that these may be influencing our genotypes differently. This was not followed up with further investigation, but stress is known to be an important factor in readings gained from tail cuff plethysmography (Kramer and Kinter, 2003). To our knowledge, there is no current literature linking TRPA1 with stress.

	TRPA1 WT	TRPA1 KO
Hypertension	- Similar magnitude and associated hemodyamics - Possible trend for faster onset	- Similar magnitude and associated hemodyamics
Activity Levels	- Unaffected by hypertension	- Significantly increased nocturnal activity levels basally which increase during hypertension compared to WT comparable group, when measured by telemetry.
Hypertrophy		- Significant cardiac hypertrophy during hypertension -Significantly more cardiac hypertrophy in Ang II treated TRPA1 KO mice than WT Ang II treated mice.
TRP Channel expression	- TRPA1 largely in the DRG, upregulated in hypertension	- TRPV1 widely expressed and not effected by TRPA1 KO or hypertension
Plasma CGRP	- Similar between genotypes, trend for reduction in hypertension	- Similar between genotypes, trend for reduction in hypertension
Oxidative Stress	- Heart NOX4 significantly upregulated in hypertension. -Significantly more aortic SOD1 and heart HO-1 in hypertensive TRPA1 WT mice compared to KO equivalent.	- Aortic and heart NOX4 significantly upregulated in hypertension. -Significantly higher expression of aortic NOX2 and cardiac NOX4 in Ang II treated TRPA1 KO mice compared to WT equivalent. -Significantly more aortic HO-1 and heart SOD1 in hypertensive TRPA1 KO mice compared to WT equivalent.
Chemokines and Cytokines	- Cardiac expression and plasma levels of IL-6 significantly increased in hypertension	- Significantly blunted increase in aortic MCP-1, cardiac IL-6 mRNA expression and plasma IL-6 protein in Ang II treated KO mice compared to WT equivalent. - Significant increase in plasma IL-8 levels in hypertension

Table 5.1 Summary Of Significant Findings From Data In Chapter 5

There are also no described links between TRPA1 and emotional state, however it is not unfeasible that such a role exists, particularly in light of the activity data. In an attempt to learn more about this phenotype, a preliminary investigation into TRPA1 mRNA expression in the brain was conducted. However, the receptor was found to be poorly expressed (see figure 5.17). Story *et al* (2003) have previously failed to find TRPA1 RNA expression in the whole mouse and rat brain using northern blot analysis. However this method is less sensitive than the RT qPCR method used in this chapter. My results show that there are low levels of TRPA1 mRNA in the brain, suggesting that TRPA1 may be expressed in small nuclei, but extraction of mRNA from large areas of brain tissue may well dilute the signal. Further investigation will be needed to identify the location of TRPA1 expression in the brain.

Hypertension levels reached during Ang II infusion were of similar magnitude in TRPA1 WT and KO mice when measured by tail cuff plethysmography and telemetry. This data clearly shows that TRPA1 does not have a strong influence on the magnitude of hypertension in this model.

This study has produced several novel findings. Current literature and previously presented data has shown TRPA1 to be involved in local vasorelaxation processes, which have been proposed to influence blood vessel tone and blood pressure (Bodkin and Brain, 2010, Earley *et al.*, 2009). There is also some evidence that TRPA1 activation can alter the actions of the heart and systemic blood pressure (Pozsgai *et al.*, 2010). In chapter 4, the various mechanisms described for TRPA1 mediated vasoreactivity are discussed. Our TRPA1 KO mice were shown to lack a vasorelaxation pathway in mesenteric arteries, mediated by CGRP. This neuropeptide has suggested compensatory effects in experimental and essential hypertension, however the mechanism is unclear (See Smillie and Brain, 2011). Current data from our research group is demonstrating that CGRP deletion is detrimental in the Ang II induced hypertension model. These mice experience faster and more pronounced hypertension, along with increased hypertrophy and inflammatory markers (Smillie,

unpublished data). These traits are not seen strongly in the data presented here, using TRPA1 KO mice, which I further hypothesised would have blunted CGRP release in hypertension. However, this hypothesis is supported somewhat by results suggesting increased pathology and oxidative stress in hypertensive TRPA1 KO mice. The plasma protein concentrations of CGRP in our TRPA1 WT and KO, control and hypertensive mice were measured. No significant differences were observed between groups, despite the levels of expression and plasma content being within reasonable expected levels (see figure 5.18). Trends for a reduction in plasma CGRP during hypertension were also seen in both genotypes. This may reflect a downregulation of CGRP by pressor agents, a feature characteristic of established and severe hypertension (See Smillie and Brain, 2010). Lower doses of Ang II infusion, over a longer period may produce a longer hypertension development window where differences in CGRP levels may be apparent. The fast onset of hypertension in this model may be masking any subtle roles of TRPA1.

In the current model, differences in the onset time of Ang II induced hypertension were seen. However, these differed depending on the method of blood pressure measurement. Using tail cuff plethysmography, TRPA1 WT mice showed significantly higher blood pressure than their controls at an earlier time point, suggesting a quicker onset. Opposing trends are seen in telemetry data, however these are lost when data from mice who died prematurely is added. Together, this suggests that onset patterns are likely to be similar between genotypes and any non-significant differences seen in the data are due to animal to animal variability. Increasing N numbers would confirm this.

In hypertension measured by telemetry, the majority of pressure increase occurs within the first two days of infusion, with stable readings achieved after about 5 days. However, using the tail cuff method, blood pressure continued to increase over most of the 14 day Ang II infusion. As tail cuff measures blood pressure from a large peripheral artery, and telemetry measures central blood pressure, differences in vascular tone and pressure

wave deflection may be altering the appearance of measurable hypertension. Although correlations between central and peripheral blood pressure are strong, antihypertensive strategies are known to differentially influence each measurement. For example, beta-blockers reduce peripheral blood pressure more than central blood pressure (McEniery, 2009). Various studies have been done to show that central blood pressure is the best single measure for estimating cardiovascular event risks (Safar and Jankowski, 2009). However, detailed analysis of the pulse pressure wave at different anatomical sites can be valuable in assessing pathology (Nelson *et al.*, 2010). During Ang II induced hypertension there is vascular remodelling and peripheral vasoconstriction, which may act to alter pressure wave deflections and thus peripheral blood pressure measurements. Additionally, it is feasible that Ang II infusion induced hypertension may be resisted for longer in peripheral arteries, which have the capacity to dilate as systemic pressure increases. As both central blood pressure and peripheral blood pressure are important in hypertension, both are useful parameters to measure. Central blood pressure will better reflect the stresses made on the heart and large blood vessels, whereas peripheral blood pressure reflects the stress experienced by organs.

In addition to pressures, telemetry also allows collection of paired heart rate, pulse pressure and activity measurements. Apart from activity, which will be discussed later, no significant differences were observed between TRPA1 WT and KO mice in these parameters. Both WT and KO mice showed clear diurnal rhythms in their blood pressures and heart rate, in line with their activity levels, throughout the Ang II infusion period.

Activity; TRPA1 KO Mice Display A Hyperactivity Phenotype.

As shown in chapter 3, TRPA1 KO mice demonstrate a previously undescribed hyperactivity phenotype, measured using telemetry probes to quantify spontaneous activity counts and wheels to assess nocturnal exercise. In this chapter, the effect of Ang II induced hypertension on activity levels was examined. Data collected by telemetry shows that

nocturnal activity peaks in TRPA1 KO mice are gradually exacerbated over the 14 days of Ang II infusion, while TRPA1 WT mouse activity levels remain stable. The difference between TRPA1 WT and KO mice is significant when the total activity between day 8 and 14 is analysed. The reason for hyperactivity in TRPA1 KO mice is not clear, or is the nature of the motions being made. This finding is unexpected and deserves further study. Ang II has not shown direct modulation of activity levels, however exercise has been shown to reduce AT1 and NADPH expression, associated with decreases in endothelial dysfunction (Rush and Aultman, 2008). These features are unlikely to be present in my hypertension study as the mice included in this experiment did not have access to running wheels. Additionally, in my study Ang II and AT1 levels have not been measured, but TRPA1 KO mice seem to have high NADPH expression despite increased spontaneous activity. This data will be further discussed with that of basal activity levels in the general discussion.

Hypertrophy; TRPA1 KO Mice Show Significantly Exacerbated Hypertrophy In The Ang II Model Of Experimental Hypertension

TRPA1 WT and KO mice both experience hypertension and hypertrophy during Ang II infusion, in line with the expected outcome of this experimental model (Simon *et al.*, 1995). However, necropsy based and echocardiographical data show significantly increased hypertrophy of the heart in hypertensive TRPA1 KO mice, compared hypertensive to TRPA1 WT mice.

Hypertrophy can occur through many mechanisms, for example increased blood pressure or systemic inflammation. Shear stress and pressure can be a major initiator of inflammation and stress signalling in the cardiomyocyte, causing hypertrophy (Hayashi and Naiki, 2009). Hypertension was similar in TRPA1 WT and KO mice, and has undoubtedly contributed to myocyte hypertrophy, but is not responsible for the differences between TRPA1 WT and KO mice as blood pressures were similar. Further additions to this work would be to use slower onset or sub-pressor doses of Ang II, allowing more accurate dissection of blood

pressure and inflammatory changes. Sub-pressor doses, causing remodelling in the absence of hypertension, would allow more detailed investigations into the potential protective effects of TRPA1 in hypertrophy. Additionally, increasing N numbers to compensate for those animals lost during the procedure would improve the statistical power of this study, allowing trends to be better established as a starting point for further investigation.

Cytokine and chemokine production from myocytes can also increase inflammatory cell infiltration, perpetuating the inflammatory nature of the environment and encouraging fibrosis through the activation of fibroblasts (Kakkar and Lee, 2010). The details of this data will be discussed later in this chapter, however the main differences found in cytokine production were blunted increases in IL-6 and MCP-1 in TRPA1 KO mice. Literature suggests that these findings should have a protective effect against hypertrophy, which is not found in our data. Although these inflammatory mediators are not responsible for the differences in hypertrophy seen, Ang II induced hypertension is associated with a wide range of cytokines and chemokines which may well be influencing hypertrophy.

Oxidative stress and inflammation independent of those induced by increased blood pressure are more likely to be mediating these changes. I have investigated several markers of oxidative stress, showing increased levels of NOX isoforms in the heart of both TRPA1 WT and KO hypertensive mice and in the aorta of hypertensive TRPA1 KO mice. Significantly increased NOX2 mRNA expression in the aorta and NOX4 mRNA expression in the heart was seen in Ang II treated TRPA1 KO mice, compared to Ang II treated WT mice. This was met with varying degrees of SOD1 and HO-1 expression. In general, trends for increased pro-oxidant and anti-oxidant gene expression were seen in both genotypes of hypertensive mice. However, trends suggest there may be increased oxidative stress in hypertensive TRPA1 KO mice compared to WT mice, which could be inducing hypertrophy via activation of inflammatory and remodelling genes in myocytes or fibroblasts. Myocytes can move to a

more fibrotic phenotype, producing extracellular matrix components and remodelling enzymes (Sampson *et al.*, 2011). The levels of remodelling enzymes have not been measured in this study, but would be a valuable addition to the work.

Gene Expression Of TRP Receptors And CGRP; TRPA1 WT Mice Display An Upregulation Of TRPA1 During Ang II Induced Hypertension

TRPA1 has been demonstrated to be upregulated in diseases where sensory neurones are activated (Diogenes *et al.*, 2007) and in response to cytokines such as IL-1α (Hatano *et al*, 2012). I investigated the effects of Ang II infusion on the mRNA expression of TRPA1. Low copy numbers of TRPA1 mRNA were found in vascular tissues of all sizes, namely the mesenteric bed, aorta and heart. TRPA1 was expressed at higher levels in DRG, which additionally showed significant upregulation of TRPA1 during hypertension. This suggests that sensory neurones are active in the hypertension model, however their role is unclear.

In chapter 4, I demonstrate a role for TRPA1 in cinnamaldehyde induced relaxation of mesenteric arteries. The finding of low expression in this location therefore suggests either that relatively few copies are needed for a physiological effect, and/or that the expression seen in the mesenteric arteries may have represented presence of innervating sensory neurones. The same reverse transcribed cDNA pool was then used to investigate the levels of TRPV1 and several housekeeping genes, which showed higher copy numbers in all tissues, suggesting that the low TRPA1 expression accurately reflects the situation in the tissue and is not a result of poor cDNA template. It is also not due to poor primers, as no TRPA1 copies were found in TRPA1 KO animals and significant levels of TRPA1 were found in the DRG, which is likely to represent the main expression site of the receptor for consideration in this study.

Previous publications have suggested the activity and expression level of TRPA1 can influence that of TRPV1, and vice versa (See Introduction). In

this study, I observed high levels of TRPV1 mRNA expression in the DRG, aorta, heart and mesenteric vessels of TRPA1 WT and KO mice. This suggests that TRPV1 expression is not regulated by TRPA1 expression in our mouse strain. TRPV1 has been found in a number of non-neuronal tissues including vascular smooth muscle and endothelial cells (Bratz *et al.*, 2008, Kark *et al.*, 2008), thus some of this expression may be related to non-neuronally expressed TRPV1. The level of TRPV1 mRNA expression was increased in the aorta of both genotypes during experimental hypertension, but not in the other tissues studied. As upregulation of TRPA1 was not seen in the aorta, and TRPV1 was not upregulated on DRG, these results suggest that different expression regulation mechanisms may be operating for each of the receptors and show tissue specificity. This may be related to non-neuronal expression of TRPV1.

Upregulation of TRPA1 expression in DRG from hypertensive mice was not associated with an increased plasma level of CGRP (figure 5.17). This may be related to the inhibitory effect of Ang II on CGRP release (Kawasaki *et al.*, 1997). The detailed mechanisms that control the transcription of TRPA1 in DRG's have not been described but recent reports have demonstrated upregulation of TRPA1 by NFκB and HIF1α transcription factors activated by cytokines (Hatano *et al*, 2012). Studies also show that TRPA1 is upregulated in diseases where sensory neurones are activated (Diogenes *et al.*, 2007), leading to the suggestion that sensory neurones were active in our model. However the nature of their activity cannot be found from our data. These findings are in keeping with my hypothesis that sensory neurone expressed TRPA1 may be part of the protection mechanisms against hypertension onset. The model of hypertension used in this study appeared to be severe, with fast onset, potentially covering up a more subtle protection afforded by TRPA1 induced dilation mechanisms.

Inflammatory Biomarkers

Oxidative Stress

Pro-Oxidants; Hypertension Increases The Expression Of NOX Isoforms

Inducing the production of ROS is an important component of Ang II induced hypertension and vascular inflammation. There are strong correlations between the level of oxidative stress and the end organ damage associated with hypertension (Touyz, 2004), which propagates the progression of cardiovascular disease. In this study, changes in mRNA expression of NADPH oxidases, the main producers of Ang II induced ROS, were quantified. Although I did not measure the levels of tissue oxidative stress, it is known that Ang II can activate these enzymes to increase the level of ROS (Oudot *et al.*, 2003). It is also almost impossible to know the enzymatic and anatomical source of ROS, even where tissue levels are measured.

NOX2 is a form of NADPH oxidase. It predominantly produces extracellular superoxide that can go on to damage surrounding cells (Bedard and Krause, 2007). NOX2 is found on immune cells and the vasculature, heart and kidney, expressed within intracellular compartments and at the plasma membrane (Bedard and Krause, 2007). It is not found in vascular smooth muscle from large arteries (Wang *et al.*, 2007). NOX2 is commonly associated with the severity and damage of Ang II induced hypertension (Paravicini and Touyz, 2008). NOX2 KO mice have a lower basal blood pressure (Bandell *et al.*, 2007) and aortic NOX2 over-expression significantly worsens hypertension (Bandell *et al.*, 2007, Lassègue and Griendling, 2010). NOX2 is also implicated in hypertrophy, independently of hypertension and blood pressure control. Using the two kidney two clip (2K2C) model of hypertension, which causes overactivity of the RAS system, Wang *et al* (2007) show that AT1 activation upregulates NOX2 in the left ventricle of the heart, correlating with increased superoxide and cardiac hypertrophy. Similarly, Johar *et al* (2006) used NOX2 KO mice to show that Ang II activates NOX2 causing

fibrosis in the heart, building on a previous study by Bendall *et al* (2002), also using NOX2 KO mice to demonstrate NOX2 mediates cardiac hypertrophy. In light of these findings, I determined the gene expression of NOX2 in the aorta and heart, using RT qPCR.

In this chapter, control TRPA1 KO mice showed some non-significant trends for lower basal expression of NOX isoforms in the heart and aorta, compared to that of TRPA1 WT mice. This may mean that TRPA1 KO mice have a lower level of basal oxidative stress, which would be beneficial in terms of inflammatory diseases. After inducing hypertension, there was some evidence of NOX2 upregulation in the heart and aorta of TRPA1 KO mice and in the heart of TRPA1 WT mice. Upregulation of mRNA expression seemed to be strongest in the KO mice, where NOX2 expression is significantly higher in aortas from hypertensive KO mice compared to that of hypertensive WT mice. Aortic expression of NOX2 likely represents that of endothelial cells, infiltrated phagocytes and potentially fibroblasts. Several reviews show NOX2 upregulation in the aorta following Ang II infusion is associated with vascular hypertrophy, endothelial dysfunction and increased blood pressure (Lassegue and Clempus, 2003, Lassègue and Griendling, 2010). In this study, significantly upregulated NOX2 mRNA in TRPA1 KO mice was not associated with increased blood pressure but may be linked to the observed increase in cardiac hypertrophy.

The NOX4 isoform of NADPH oxidase also has strong links with hypertension. It is often found on intracellular membranes, is abundantly expressed in the kidneys, but also found in all vascular cells, fibroblasts and cardiomyocytes (Lassègue and Griendling, 2010). NOX4 differs from other isoforms in that it has been reported to predominantly produce H_2O_2 (Dikalov *et al.,* 2008), which is a vasodilator (Matoba and Shimokawa, 2003) and the major signalling ROS form, possibly accounting for its more favourable role in hypertension. The role of NOX4 in the vasculature is not well defined, as studies show it to be differentially regulated in endothelial cells by different stress stimuli, and to have both positive and

inhibitory influences on vascular smooth muscle growth (Lassègue and Griendling, 2010). Wang *et al* (2007) have shown AT1 dependent upregulation of NOX4 in the heart and aorta in rats undergoing 2K2C induced hypertension, associated with elevated blood pressure and cardiac remodelling. However, Ang II reduced NOX4 expression in cultured vascular smooth muscle cells in a study by Lassegue *et al* (2001), and Chabrashvili *et al* (2003) also show Ang II infusion *in vivo* causes AT1 dependent reduction of renal NOX4. NOX4 also has influences on Ang II pressor responses. Ray *et al* (2011) have shown endothelial NOX4 over-expressing mice to have a lower blood pressure, as a consequence of increased H_2O_2. A role for NOX4 in cardiac fibrosis has also been suggested, as it has been shown to correlate with TGF-β induced conversion of cardiomyocytes to myofibroblasts (Cucoranu *et al.*, 2005). Anilkumar *et al* (2008) found over-expression of NOX4 in HEK293 cells to substantially increase basal ROS level, leading to ERK and JNK signalling. Therefore, there appears to be location specific changes in Ang II regulation of NOX4 expression.

In this chapter, basal levels of NOX4 mRNA expression in the aorta and heart were lower than that of NOX2, with a trend for lower expression levels in the TRPA1 KO aorta compared to the WT aorta. NOX4 was significantly upregulated in the heart of both TRPA1 WT and KO hypertensive mice, and also in the aorta of TRPA1 KO mice, bringing it up to comparable levels with control and Ang II treated TRPA1 WT mice. Additionally, significantly higher levels of NOX4 mRNA expression were seen in hearts from hypertensive TRPA1 KO mice compared to hearts from hypertensive WT mice. The consequences of this are not clear, but are not linked to genotype specific changes in blood pressure. They may be linked to increased hypertrophy in KO Ang II treated mice.

Combined, these findings demonstrate that Ang II increases the expression of NADPH oxidases, which is likely to increase the production of ROS. These increases are frequently of significantly larger magnitude in TRPA1 KO mice, where if these changes are not balanced by an increase in anti-

oxidant mechanisms, increased levels of damaging oxidative stress will exist and may have pathological consequences.

Anti-oxidant defences; Hypertension Increases Anti-Oxidant Gene Expression

Evidence of the role of exogenous anti-oxidants in protecting against hypertension is conflicting. Several preliminary animal and patient studies have shown benefits of antioxidant supplements in essential hypertension, however large clinical studies have been disappointing (See Sedeek *et al* (2009), Paravicini and Touyz (2008) and Touyz and Briones (2011)). Despite this, effective endogenous anti-oxidant mechanisms are needed to counter Ang II induced ROS production if the creation of damaging levels of oxidative stress is to be avoided. In order to gauge the amount of oxidant defences mounted in our hypertensive model, the expression of some anti-oxidant enzymes were measured, namely HO-1 and intracellular SOD.

Intracellular SOD, or SOD1, is known to participate in redox signalling involved in inflammation, angiogenesis and vascular function. SOD is an antioxidant gene which converts superoxide to H_2O_2, in order for its degradation. Studies using extracellular SOD KO mice in Ang II induced hypertension have shown that it provides a protective mechanism in large arteries, reducing oxidative stress and blood pressure (Gongora *et al.*, 2006). This SOD isoform is heavily implicated in the control of vascular tone in a variety of vessel types, both due to its ability to reduce NO inactivation by superoxide, and to produce dilative H_2O_2 (Fukai and Ushio-Fukai, 2011). Similarly, intracellular SOD KO mice show increased myogenic tone in carotid artery rings, impaired endothelial dependent relaxations and augmented vasoconstrictor responses (Didion *et al.*, 2002). Wang *et al* (2002) have previously shown intracellular SOD expression to be increased by Ang II infusion in mice, lowering the superoxide levels. In my study, basal levels of intracellular SOD were similar in the aorta and showed a non significant trend for lower levels in the heart of TRPA1 WT

mice, compared to KO mice. Ang II induced hypertension caused some trends for upregulation in the hearts of both genotype, however this was stronger in the KO, where significantly higher levels were measured compared with hypertensive WT mouse hearts. Conversely, in the aorta, Ang II treated mouse aortas showed significantly less SOD1 mRNA expression than Ang II treated TRPA1 WT mouse aortas. These differences make the level of antioxidant defences in each tissue hard to conclude and suggest different regulation pathways occur in each tissue, with differing effects of TRPA1. This may depend on the predominant cell types present. These findings are consistent with some of our other results, showing increased expression of inflammatory molecules and anti-oxidant defence genes in hypertension.

HO-1 was also measured in the aorta and heart. HO-1 is an antioxidant mechanism induced by oxidative stress, thus can be used as both an indicator of ROS production and as a level of mounted anti-oxidant defence. The protective effects of HO-1 activity are multifold (Turkseven *et al.*, 2005). HO-1 breaks down heme to form bilirubin and carbon monoxide (CO). CO is a vasodilator in all vascular beds, inducing vascular smooth muscle relaxation via induction of cGMP and by stimulation of calcium activated potassium channels (Chen *et al.*, 2003). It also reduces the production of vasoconstrictor agents such as endothelin-1 (Morita and Kourembanas, 1995) and induces antioxidant defence genes (Peterson *et al.*, 2009). CO acts on vascular smooth muscle cells in a similar manner to NO; however, although it is more stable, it is 1000x less potent at relaxing vessels (Furchgott and Jothianandan, 1991). Bilirubin is a potent antioxidant, mopping up potentially harmful ROS that may mediate increases in blood pressure and end organ damage during hypertension. Following Ang II application, bilirubin has been shown to reduce migration and ROS production from monocytes, and oxidative stress damage to endothelial cells (Peterson *et al.*, 2009). It can also inhibit the action of neutrophil NOX2 (Kwak *et al.*, 1991). In endothelial cells, HO-1 acts to increase eNOS expression and decrease inflammatory gene expression, including cell adhesion molecules; an effect likely to be occurring via

bilirubin (Peterson *et al.*, 2009). However, i.p. administration of biliverdin, the precursor of bilirubin, does not alter blood pressure in rats (Johnson *et al.*, 1995). Together, these findings suggest that HO-1 is an important mediator in essential and experimental hypertension, providing a protective effect and opposing disease progression.

In this chapter, control mice showed similar levels of HO-1 mRNA expression, which was not affected by TRPA1 deletion. The induction of hypertension caused non-significant increases in HO-1 expression in both tissues. Similarly to SOD the magnitude of increase was tissue and genotype dependent. This produced significantly higher levels of HO-1 expression in the aorta, and significantly lower levels of HO-1 in the heart of TRPA1 KO mice treated with Ang II, compared to the Ang II treated TRPA1 WT group. This again makes interpretation of anti-oxidant defence levels difficult.

The combined analysis of SOD1 and HO-1 gene expression suggest anti-oxidant defences are increased during hypertension, as expected from the increase in pro-oxidant proteins. ROS can induce upregulation of both pro- and anti-inflammatory genes via a range of signalling pathways, such as NF-κB, MAPK, AP-1 etc (Fukai and Ushio-Fukai, 2011, Touyz and Briones, 2011). Potential links to TRPA1 activity also exist as ROS and their products are known to activate the receptor (Andersson *et al.*, 2008).

Cytokines And Chemokines

Cardiovascular diseases are pro-inflammatory in nature, and are associated with several inflammatory biomarkers. In this study, IL-6, mIL-8 and MCP-1 were selected as markers of inflammation, as they are linked to hypertrophy and inflammatory cell infiltration. Cytokines and chemokines are produced from cells activated by stress, via signalling pathways such as NF-κB. IL-6 and IL-8 are both typically produced by macrophages (Jovanovic *et al.*, 1998), whereas MCP-1 is produced by a range of cells, including those of the vasculature wall. The main function of IL-8 is to

attract neutrophils to a tissue site (Jorens *et al.*, 2009), whereas MCP-1 is used to traffic monocytes. Both of these chemokines are linked to cardiac remodelling (Collier *et al.*, 2011). IL-6 has more diverse functions, but in the context of hypertension it is linked to cardiac stress.

MCP-1

MCP-1 is a key chemokine expressed by vascular, renal and cardiac cells. It can be expressed by all vascular tissues, including endothelial cells, fibroblasts, vascular smooth muscle and cardiomyocytes (Niu and Kolattukudy, 2009). It has a role in the physiological trafficking of monocytes into tissues, where it is upregulated by inflammatory stimuli such as increased shear stress, oxidative stress and Ang II, under the control of NFκB (Zhuo, 2004). MCP-1 can be attached to the lumen wall by proteoglycans, or can be free in the tissue. Its primary function is as a chemotactic source for monocytes. MCP-1 is a potential biomarker for chronic inflammatory diseases, with plasma levels correlating with disease severity (Yao *et al.*, 2006). Treatment of isolated leukocytes with MCP-1 causes respiratory burst, expression of pro-inflammatory cytokines and upregulation of matrix metalloproteins (Niu and Kolattukudy, 2009). In the heart, MCP-1 expression is associated with fibrosis, remodelling and upregulation of stress response genes. Behr *et al* (2004), previously used Ang II infusion to induce experimental hypertension, showing a low dose of AT1 antagonist Eprosartan, which does not affect blood pressure, to reduce MCP-1 expression in the myocardium whilst also reducing macrophage infiltration, disease progression and mortality. This suggests that MCP-1 is important in Ang II induced inflammatory responses associated with organ damage. Furthermore, Kolattukudy *et al* (1998) have produced a mouse overexpressing MCP-1 specifically in the myocardium. This mouse strain presented with myocarditis, characterised by monocyte infiltration, remodelling and a decrease in contractile function. This also indicates that inflammatory cell migration may be an important step in initiating the pro-inflammatory conditions in the heart,

leading to harmful complications and cardiovascular disease progression in hypertension.

In this chapter, MCP-1 expression increased in hearts from both genotypes during hypertension, however this does not show statistical significance. In the aorta, increased expression only occurred in WT mice, created a significant difference between Ang II infused WT and KO mouse aortas. This suggests MCP-1 production in the aorta is blunted by TRPA1 KO. These findings were not consistent with the end points of my study, where TRPA1 KO display more cardiac hypertrophy. The reasons for this, and the role played by MCP-1 in my experimental model, are currently unclear. Further analysis could benefit from measurement of protein levels, as these do not necessarily follow on from mRNA expression patterns.

mIL-8

IL-8 has powerful chemoattractant properties for inflammatory cells. It has recently been correlated with hypertensive diastolic dysfunction, where cardiac fibrosis reduces heart function (Collier *et al.*, 2011). The mouse homolog of IL-8 is KC, which was measured in this study and will be referred to as mIL-8. In this chapter, mIL-8 plasma levels were similar in control TRPA1 WT and KO mice, and show similar magnitudes of increase following Ang II infusion, but only reaching significance in TRPA1 KO mice. The effect of Ang II stimulation of isolated macrophages was further investigated, where it appeared that macrophages from TRPA1 KO may produce more mIL-8 than those from WT mice. The data is potentially conflicting, however the isolated macrophage studies show the effects of acute application, which may differ from the effects of chronic stimulation. Therefore, in balance, mIL-8 is unlikely to be a mediator of increased hypertrophy in hypertensive TRPA1 KO mice. Studies of cell infiltration into heart and vessel samples would be of value to back up this data suggesting inflammatory cell infiltration.

IL-6

Lastly, I have measured the mRNA expression and plasma levels of IL-6. IL-6 is produced in large amounts from macrophages, but can also be produced by other cell types, notably fibroblasts, endothelial cells, vascular smooth muscle and exercising skeletal muscle. IL-6 has positive actions relating to exercise and the clearance of bacterial infection (See Fisman and Tenenbaum, 2010). IL-6 is rapidly produced and released by skeletal muscle during exercise, in an amount proportional to duration, intensity, muscle mass and endurance capacity. Its main effect is to increase insulin sensitivity, allowing more effective glucose uptake to exercised muscles (Fisman and Tenenbaum, 2010). IL-6 levels are positively correlated with all-cause mortality, often showing parallels with other biomarkers reflecting harmful processes (Fisman and Tenenbaum, 2010). IL-6 has been linked to hypertension, as a marker of severity and end organ damage. IL-6 is a plasma biomarker of diastolic dysfunction in asymptomatic hypertensive patients (Collier *et al.*, 2011). Previous studies have shown a strong association between IL-6 plasma levels and gene polymorphisms with systemic inflammation and risk of cardiovascular disease (Liu *et al.*, 2006, Aker *et al.*, 2009).

A recent study by Melendez *et al* (2010), where IL-6 is infused subcutaneously in normotensive rats, this cytokine caused myocardial fibrosis, hypertrophy and diastolic dysfunction, independently of blood pressure. IL-6 has been described as a dominant marker of myocardial cytokine activity in a model of spontaneously hypertensive rat heart failure (Haugen *et al.*, 2008). It is produced from isolated vascular smooth muscle cells upon stimulation with pro-inflammatory cytokines, such as IL-1, and during proliferation, but does not stimulate further direct effects on endothelial or smooth muscle cells (Loppnow and Libby, 1990). Therefore, the actions of IL-6 may be targeted on activation of accumulated inflammatory cells, which in turn produce more ROS and cytokines, causing myocardial hypertrophy and leading to heart failure in hypertension. IL-6 expression is known to be upregulated following Ang

II treatment and related to the expression of other chemokines, attracting inflammatory cells to the tissue (Manhiani *et al.*, 2007).

In this chapter, IL-6 expression and plasma levels were similar in TRPA1 WT and KO control mice. A similar level of IL-6 release was also seen from TRPA1 WT and KO isolated macrophages. Following experimental hypertension, IL-6 levels were significantly increased TRPA1 WT mice but less so in KO mice. IL-6 expression in hypertensive TRPA1 WT mouse hearts and plasma protein levels were both significantly increased compared to hypertensive TRPA1 KO mice. Similar non-significant trends were seen in IL-6 expression in the aorta. In isolated macrophages, changes in IL-6 production were unclear, potentially suggesting a lower capacity for production in TRPA1 KO mouse macrophages. However, these studies are acute rather than for chronic angiotensin stimulation and require further optimisation. Our findings are not consistent with those in the literature, suggesting that high IL-6 levels induce cardiac hypertrophy in WT mice, whereas KO mice should show some protection.

The findings of blunted MCP-1 and IL-6 increase during hypertension in TRPA1 KO mice are interesting. This indicates that TRPA1 KO mice have an anti-inflammatory pathway in operation, which is not at play in WT mice, blocking the rise in these cytokines associated with cell infiltration and cardiac fibrosis. This suggests TRPA1 expression may be pro-inflammatory and combines well with the literature and previous work from our lab, showing TRPA1 activation to cause inflammatory cell infiltration (Silva *et al.*, 2011, Bodkin *et al*, Unpublished data). However, our findings contrast with those from single cell cultures by Hatano *et al* (2012), who show TRPA1 activity in synoviocytes inhibits their production of IL-6 and IL-8. Furthermore, the effects of reduced IL-6 in our model are not as expected, as KO mice showed increased pathology. This suggests complex interactions I attempted a preliminary study of the capacity for Ang II to stimulate cytokine release from macrophages isolated from TRPA1 WT and KO mice, investigating whether the low levels of cytokine production are based around inherent changes to

macrophages. However, this protocol needs further work to provide clear conclusions.

Conclusion

In this chapter I have conducted a novel study investigating the effect of genetic TRPA1 deletion in a model of experimental hypertension, mediated by the infusion of Ang II. My original hypothesis was that TRPA1 KO mice would far worse in terms of hypertension, associated pathology and biomarkers. This would be due to a lack of dilative and anti-inflammatory mechanisms, mediated by CGRP, which would compensate for the onset of these disease characteristics. Results stemming from this study are complex, and summarised at the beginning of this discussion, but suggest that TRPA1 has only a mild influence on the pathogenesis involved in our model of Ang II induced hypertension. The magnitude and onset of hypertension was not significantly different in TRPA1 WT and KO mice, neither were heart rate measurements. Similar to data presented in chapter 3, KO mice showed a hyperactivity phenotype which will be discussed further in the general discussion. Hypertrophy, a pathological change in hypertension associated with diastolic function and heart failure, occurred significantly in the heart of both genotypes. However, data consistently showed more hypertrophy in Ang II treated TRPA1 KO mice compared to Ang II treated WT mice. Further analysis of biomarkers was used to associate this with potentially higher levels of hypertensive oxidative stress in TRPA1 KO mouse vasculature. Significant increases in pro-oxidative markers occurred in both genotypes of hypertensive mice, but of significantly larger magnitude in TRPA1 KO mice. This appeared not to be compensated for by consistently increased antioxidant markers. Levels of inflammatory chemokines and cytokines, which may mediate remodelling, were increased in both hypertensive mouse groups, however TRPA1 KO mice showed significantly blunted increases in MCP-1 and IL-6 production. This is surprising considering the suggested increase in pathology and is indicative that TRPA1 mediates some pro and anti-inflammatory effects.

A further important finding was made in terms of TRPA1 expression, where TRPA1 mRNA was found to be predominantly expressed on DRG neurones, where it was upregulated in Ang II induced hypertension. TRPA1 mRNA was found to be poorly expressed at all levels of the vasculature and brain, in contrast to TRPV1 and TRPC5 respectively. This finding supports our previous conclusions of a sensory neurone mediated effect of TRPA1 activation. However, TRPA1 KO or upregulation in the DRG during hypertension in WT mice, was not associated with changes in plasma CGRP levels. This disproves my hypothesis, at least for the hypertension model used and time points investigated. However, as detailed above, TRPA1 was seen to have some interesting modulatory responses in Ang II induced hypertension, which suggest both pro and anti-inflammatory actions exist for the receptor *in vivo*. These, along with the findings of similar blood pressure and hyperactivity in TRPA1 KO mice, are novel additions to the current knowledge of the TRPA1 role in pathophysiology.

Chapter 6 - General Discussion

My hypothesis was that TRPA1 is involved in the control of resistance vessel tone. *In vivo*, it contributes to the control of blood pressure by keeping peripheral resistance low and will resist the onset of hypertension by releasing neuropeptides when it is activated by elevated levels of endogenous agonists. Genetic deletion of TRPA1 will lead to a loss of this process, increasing basal blood pressure and resulting in susceptibility to hypertension, with increased vascular inflammation and worsened hypertensive endpoints.

Using the evidence presented in this thesis, I am now able to address the previously stated aims and comment on how the evidence collected fits with my hypothesis.

Aim 1

Investigate the basal cardiovascular phenotype of TRPA1 KO mice compared to matched WT mice. I wish to particularly focus on basal blood pressure control and will measure this in conscious animals by both tail cuff plethysmography and telemetry.

This study was novel, producing new information for the field. To achieve this aim, I characterised the basal cardiovascular phenotype of mixed gender TRPA1 WT and KO mice. The majority of data relating to this aim is presented in chapter 3. Measurements of basal blood pressure were collected by tail cuff plethysmography and telemetry on different sets of experimental animals. Tail cuff plethysmography measured peripheral blood pressure, whereas telemetry measured central blood pressure. Whilst TRPA1 KO mice were seen to show higher basal blood pressure using telemetry, a significant hypotensive phenotype was seen in TRPA1 KO mice measured by tail cuff. The reasons for these differences are discussed in chapter 3, but are likely to represent methodological differences, where

the contribution of stress and temperature were suggested to play a role. My conclusion from this data is that TRPA1 deletion does not influence basal blood pressure. Further measurements of heart size, heart rate and heart function showed no effect of TRPA1 deletion. Additionally, data presented in chapter 5 showed basal levels of plasma CGRP to be similar in TRPA1 WT and KO mice. Together, this data suggests that TRPA1 is either not involved in basal cardiovascular control, or that the effect of TRPA1 deletion has been compensated for in the KO mice. The outcome contrasts with my hypothesis, but adds valuable evidence to the field. Compensation could be further investigated using systemic administration of TRPA1 antagonists to WT mice. These are currently being developed for respiratory and inflammatory conditions. If my data is further substantiated, this supports the development of such antagonists for clinical use, as it suggests cardiovascular side effects may be few.

The most interesting and unexpected findings made in chapter 3 were related to activity levels. Similar findings have not been observed previously. In telemetered animals, TRPA1 KO mice showed increased nocturnal activity counts. I further investigated this phenotype using voluntary running wheels to measure exercise in the home cage of naïve mouse pairs. This again showed TRPA1 KO mice to participate in an increased amount of voluntary activity compared to WT mice. In addition to this, in chapter 5 TRPA1 was shown to be poorly expressed in grossly dissected brain segments, and the spontaneous activity levels of TRPA1 KO mice to be exacerbated during hypertension. This indicated that the hyperactivity phenotype could be peripherally mediated. Further discussion of this potentially novel hyperactivity phenotype will be given later.

Aim 2

Analyse the role of TRPA1 in the vasorelaxant response to cinnamaldehyde. I will use isolated mesenteric arteries in a wire myograph to study the nature of TRPA1 involvement in this process and attempt to dissect the contributing signalling.

Several groups, including ours, have previously shown that TRPA1 agonists can induce vasorelaxation of vessels from many vascular beds. This leads to an increase in blood flow *in vivo*. The studies of relevance have been summarised in table 1.1. However, despite a number of investigations, the dependence of this phenomenon on the TRPA1 receptor is poorly defined. Additionally, a range of mechanisms have been attributed. Therefore, I conducted a series of investigations into the mechanism of cinnamaldehyde induced vasorelaxation of murine mesenteric arteries. This agonist was chosen for its suitability for *in vivo* use, along with evidence of receptor selectivity and previously defined cardiovascular effects via TRPA1 (Pozsgai *et al.*, 2010). The mesenteric artery was selected as the tissue of interest as together they comprise a large component of total peripheral resistance, a major determinant of blood pressure.

In chapter 4, cinnamaldehyde was shown to cause concentration dependent vasorelaxation, in a partially TRPA1 dependent manner, occurring independently of the endothelium. These findings were made using TRPA1 WT and KO arteries, with and without functional endothelium. The *in vivo* relevance of this was demonstrated in our group by Aisah Aubdool; using Laser Doppler flowmetry, topically applied cinnamaldehyde was shown to cause an increase in ear blood flow which was significantly reduced by addition of a TRPA1 antagonist or in TRPA1 KO mice. In the myograph, isolated mesenteric artery vasorelaxation to cinnamaldehyde was found to be CGRP mediated, as it was significantly reduced in CGRP KO mice and after pre-treatment with a non-peptide CGRP receptor antagonist. Using elevated potassium to block

hyperpolarisation, I also showed hyperpolarisation to mediate the relaxation, but this was not occurring via the BK_{Ca} channel, as shown by a lack of effect of the antagonist paxilline. Together, this data suggests that TRPA1 is involved in a vasorelaxant mechanism via the release of CGRP which acts to hyperpolarise the vascular smooth muscle. The majority of TRPA1 expression was shown to be in DRG neurones, supporting a sensory neurone derived mechanism. Specifics of the data are discussed in chapter 4, where significant difficulties were encountered with the use of several antagonists and limited availability of TRPA1 WT mice lead to the use of CD1 WT mice for some pharmacological studies. Although the data is in no way conclusive, the findings from this chapter are in line with those proposed in my hypothesis, and suggest that this mechanism may occur *in vivo*. The relevance of this during normal physiology and pathophysiology are unknown, however data from chapters 3 and 5 suggest that it is not involved in the control of systemic blood pressure.

Aim 3

Study the onset and endpoints of experimental hypertension in TRPA1 WT and KO mice, investigating the potential roles of TRPA1. This will be done in terms of blood pressure, hypertrophy and endpoint inflammation measures in matched TRPA1 WT and KO mice treated with Ang II.

Despite findings showing no clear role for TRPA1 in the control of basal cardiovascular parameters, there are clear potential roles for the receptor, and its dilative response, in pathological settings. For example, CGRP KO mice used in our group do not differ in their basal blood pressure, but fair worse in an experimental model of hypertension similar to the one used here (Smillie *et al*, Unpublished data). As CGRP was shown to mediate cinnamaldehyde induced vasorelaxation, a similar effect may be seen in TRPA1 KO mice. This is in line with my hypothesis. Similarly, TRPV1 KO do not alter from WT mice in terms of basal blood pressure (Pacher *et al.*, 2004) but show susceptibility to hypertension models (Wang *et al.*, 2008, Yang *et al.*, 2010).

TRPA1 WT and KO mice were made hypertensive over 14 days using infusion of pressor doses of Ang II. Both genotypes showed significantly elevated blood pressure when measured by tail cuff plethysmography and telemetry. The onset profile was also similar. These findings are discussed in chapter 5 and disprove part of my hypothesis. They suggest that TRPA1 does not have a strong influence on blood pressure either basally or during the model of Ang II induced hypertension used in this study. The reason that TRPA1 does not have a protective role in hypertension, but that CGRP does, is interesting and deserves further study, particularly in light of my myography findings where CGRP is implicated in TRPA1 mediated vasorelaxation.

The endpoints of hypertension were analysed in this study, in terms of hypertrophy, and mRNA expression of TRP receptors, cytokines/chemokines and pro and anti-oxidant proteins, along with the plasma protein levels of cytokines and CGRP. Only mild differences were seen between TRPA1 WT and KO mice, suggesting that there is little influence of TRPA1 on the pathogenesis occurring in this model. However, some interesting findings were made. These are fully discussed in chapter 5, but include significantly increased cardiac hypertrophy in Ang II treated TRPA1 KO mice compared to Ang II treated TRPA1 WT mice. The reasons for this are unclear, but may relate to increased oxidative stress in hypertensive TRPA1 KO mice. This was suggested as both genotypes of mice show significant upregulation of pro-oxidative genes NOX2 and NOX4 during hypertension, but these were frequently of significantly larger magnitude in TRPA1 KO mice. Upregulation of anti-oxidative genes HO-1 and SOD1 were also seen, but were of similar magnitude between genotypes. Together, this data suggest a potential protective role for TRPA1 in remodelling and some aspects of inflammation, but further work will be needed to investigate these finding. Potentially, increased oxidative stress may be mediating excessive remodelling in hypertensive TRPA1 KO mice, perhaps via inflammatory cell infiltration.

TRPA1 KO mice showed significant upregulation of plasma mIL-8, an effect seen more mildly in WT mice. Measurement of other inflammatory markers, such as MCP-1 and IL-6, suggest that TRPA1 KO mice may be protected from some aspects of systemic inflammation. The levels of these markers are significantly higher in hypertensive WT mice than hypertensive KO mice. This effect was shown strongly for IL-6, where KO mice showed this trend consistently, through gene expression and plasma protein analysis. This suggests a pro-inflammatory mechanism occurs via TRPA1 in WT mice which may influence inflammation at multiple levels and could potentially influence cardiovascular disease progression.

Additional studies in this chapter showed that TRPA1 expression was low at all levels of the vasculature. Predominant expression was found in DRG neurones. This occurs in line with my hypothesis that the majority of TRPA1 activity occurs through sensory neurone activation and neuropeptide release. The levels of TRPV1, a related TRP channel, were not affected by genotype and are only non-significantly increased by Ang II treatment in the aorta. During hypertension, TRPA1 mRNA expression was significantly increased in the DRG of WT mice. This suggests that TRPA1 and sensory neurones may be playing a role in hypertension pathogenesis, although inflammation induced from non-neuronal TRPA1 cannot be dismissed (Nassini *et al*, 2012). As discussed in chapter 5, sensory neurones are thought to play a compensatory role in hypertension, but the role of TRPA1 activity may be mild and thus masked by the severity of acute hypertension in my model. The finding that TRPA1 is upregulated is of importance aside from the other data. It suggests involvement of DRG neurones in hypertension, particularly a role for TRPA1. My hypothesis was based on TRPA1 activation causing the release of CGRP, which would compensate for the introduction of Ang II as a pressor agent. To investigate this, CGRP plasma levels were measured from hypertensive mice, but showed no genotype or treatment dependent differences. Therefore TRPA1 may not be acting in this way. However, previous reviews of the literature have shown that CGRP levels can

become depleted in established hypertension (Smillie and Brain, 2011), and its release inhibited by Ang II (Kawasaki *et al.*, 1998), which may reflect the situation in our hypertension model as CGRP levels tended to be lower than those of control animals. Therefore, a protective role for TRPA1 and/or CGRP in this model may have been missed and deserves further study.

One of the most interesting findings of this thesis was of hyperactivity in TRPA1 KO mice. This has been previously discussed in the context of chapter 3, but was also shown in chapter 5, where Ang II induced hypertension exacerbated the hyperactivity phenotype. These findings are novel and of special interest, they will therefore be discussed for the remainder of this chapter.

TRPA1 Deletion Induces A Hyperactivity Phenotype

The data presented in this thesis demonstrates that TRPA1 KO mice are more active during basal conditions. Significant increases in spontaneous activity counts measured by telemetry were also mirrored when pairs of mice were allowed to voluntarily exercise in a running wheel placed in their cage. Here, TRPA1 KO mice ran further, and showed a significant preference for running at faster speeds than TRPA1 WT mice. The additional increase in running speed further indicates that there are potential physiological differences between the strains, allowing an increased capacity for exercise. Conversely, this may also support a psychological motivation for increased activity, where an increased feeling of reward allows more intensive exercise.

There are a number of mechanisms that may mediate spontaneous locomotion. The typical human disease associated with this trait is attention deficit hyperactivity disorder (ADHD). There are several mouse models used to investigate the causes of this condition, which largely focus genetic effects on activity mediators in the brain. One of these models is the spontaneously hypertensive rat (Meneses *et al.*, 2011), however the

causes of the ADHD are not thought to be related to blood pressure control or RAS.

The mechanisms controlling both spontaneous activity and voluntary exercise levels in mice are currently unclear. However, several lines of evidence suggest that activity levels are modulated by central pathways. This process can be modulated by a variety of neurotransmitters. Several transmitters are involved with the initiation of locomotion in mammals, including dopamine, glutamine, serotonin, noradrenaline, endocannabinoids and neuropeptides linked to appetite, see reviews by Jordan *et al* (2008) and Garland *et al* (2011). Within the brain, there are some areas particularly rich in specific neurotransmitters and are linked to motor activity control, however it is commonly thought that the end effect of modulation of any of these neurotransmitters will be alteration of dopamine neurotransmission, as the motivation behind increased activity of laboratory mice is commonly reward based (Garland *et al.*, 2011). It is also thought that activity levels may be linked to several personality traits and disposition, as exercise can drive neurogenesis in the hippocampus, an effect that has been linked to several neuropsychiatric diseases (Fuss and Gass, 2010, Thakker-Varia and Alder, 2009). Several animal ADHD models have been linked to changes in the neurotransmitter release in the striatum, cortex and medulla (Magara *et al.*, 2000, Wilson, 2000, Jordan *et al.*, 2008, Kamimura *et al.*, 2001).

Hyperactivity was correlated with deletion of TRPA1; however, there have been no previous reports of TRPA1 expression in the brain. A preliminary investigation of TRPA1 mRNA expression was conducted in grossly dissected striatum, cortex and medullas from TRPA1 WT and KO control mice, and Ang II treated WT mice. TRPA1 was poorly expressed in all areas of the WT brain and was not affected by Ang II infusion. As expected, KO mice expressed no detectable TRPA1 in any brain areas. As a positive control, I also measured the levels of several housekeeping genes and TRPC5, which is a TRP channel highly expressed in brain (figure 5.18). This suggests that TRPA1 may not be involved in a central

modulation of activity, unless via stimulation in the periphery, causing signalling to the brain. This is a possibility, via both afferent neurones and blood borne factors. To investigate this, I would need to measure the levels of neurotransmitters in specific nuclei related to activity. In line with these suggestions, I show TRPA1 mRNA to be upregulated on DRG neurones in WT mice undergoing experimental hypertension. On the other hand, expression studies were completed on grossly dissecting brain. This may mean that small areas of rich TRPA1 expression are diluted by the presence of other tissue, giving us low mRNA copy numbers per µl. Further investigation of this will demand isolation of these areas, but a single TRPA1 rich area is unlikely as low copy numbers were found throughout the brain.

Mood modulation is another possible determinant of spontaneous activity, with increased physical activity seen to be an effective anti-depressive therapy (Byrne and Byrne, 1993). Depression has been recently correlated with plasma IL-6 levels in male twins, where increased IL-6 was shown to be genetically linked to the risk of experiencing depressive symptoms (Su *et al.*, 2009). My data shows the hyperactivity phenotype in TRPA1 KO mice is not associated with a basal change in IL-6. In hypertensive mice, activity is further increased in KO mice, but the IL-6 level does not change. This pattern is not supported by publications showing that plasma IL-6 levels to be consistently and reliably linked to the levels of skeletal muscle activity (Febbraio and Pedersen, 2002, Fisman and Tenenbaum, 2010). However, these IL-6 peaks may have been absent in my data due to their transient nature, and that the mice in which IL-6 was measured did not have access to a wheel. Therefore the magnitude of exercise needed to induce this IL-6 peak may not have been reached. IL-6 has is also suggested to be responsible for the insulin sensitivity and anti-inflammatory effects of exercise (Febbraio and Pedersen, 2002), showing short term positive effects. Previous studies have shown that IL-6 KO mice have a lower capacity for exercise, due to poorer endurance, leading to inactivity induced obesity (Fäldt *et al.*, 2004). However, IL-6 is also produced by adipocytes (Hoch *et al.*, 2008) and moderate training in men

lowers plasma levels of IL-6 as receptor sensitivity increases (Thompson *et al.*, 2010), suggesting that inverse relationships with activity can also occur. I am not able to comment on the emotional status of the mice, yet several easily available tests could be done to investigate this. For example, defecation can be a good indicator of emotional stress (Gentsch *et al.*, 1981), and stress is a modulator of blood pressure.

IL-6 production can also be linked to the TRPA1 receptor, as patients with sulphur mustard poisoning show increased IL-6 levels, which correlate with severity (Attaran *et al.*, 2010). TRPA1 agonist's cinnamaldehyde and gingerol have both been shown to reduce spontaneous activity in animal model, albeit without mechanistic links to the TRPA1 receptor (Harada and Ozaki, 1972, Suekawa *et al.*, 1984). These studies link activity levels to TRPA1 receptor activity, but suggest opposing correlations to my data from TRPA1 KO mice. In contrast, use of the TRPA1 antagonist HC-300031 is not associated with changes in activity measured by the rotor-rod system (McNamara *et al.*, 2007). My findings may be related to some compensatory changes occurring following deletion of the receptor, or indicate that different pathways are involved in exercise associated pathways in these mice. It may also suggest that the hyperactive mice could be more sensitive to IL-6, or that their spontaneous movements are not of the right kind to elicit IL-6 release.

The effect of Ang II on activity levels in TRPA1 KO mice is also unexplained. During days 8-14, activity counts from telemetered and Ang II infused TRPA1 KO animals was significantly higher than those of the comparable WT group. This increase could have been due to Ang II infusion, exacerbating the hyperactivity phenotype. Both WT and KO hypertensive mice lost weight during the protocol, compared to control mice, however this could not be related to activity levels. Ang II infusion is associated with a loss of skeletal muscle mass in mice, which may be partially mediated by ROS produced from NOX2 (Semprun-Prieto *et al.*, 2011) or by increased protein degradation (Brink *et al.*, 2001). This is supported by my RT qPCR data, showing Ang II infused mice to express

higher levels of vascular NOX2 mRNA, correlating with their reduction in body weight. However there is no evidence this weight reduction is due to muscle loss as this would require further measurements to be taken. Ang II infusions themselves are unlikely to be affecting appetite, unless as a side effect of hypertensive pathology. Ang II positively correlates with leptin and body fat levels in obese patients (Saiki *et al.*, 2009) linking it to metabolic syndrome pathology. Ang II is also commonly associated with water retention, increasing blood volume and thus potentially body weight. In my mice, the cause of body weight reduction in hypertensive mice is unclear. It is most likely to be due to changes in appetite due to hypertensive morbidity and not the procedure itself, which was also undergone by control mice. These suggestions could be further examined by measuring food and water intake and using metabolic cages. Analysis of the data also did not exclude the conclusion that activity levels were reduced following surgery, and that the significant difference seen between hypertensive TRPA1 WT and KO mice is a reoccurrence of the hyperactivity phenotype seen at baseline. As previously discussed, there are currently limited known links between TRPA1 and activity levels.

To conclude, my findings demonstrate a hyperactivity phenotype in the TRPA1 KO mice, which may be exacerbated on Ang II infusion. However, the current evidence cannot link these changes to central pathways, mood, changes in body weight or IL-6 production, all factors are linked to initiation of, or involvement in, spontaneous exercise. Further investigations would need to analyse more specific measures of activity, such as specialist cages or open field tests. These would be required, along with learning tests, to fully determine if our TRPA1 KO mouse qualifies as a model of ADHD. If so, more detailed physiological tests would then be warranted to investigate the role of TRPA1.

Limitations

Based on results as a whole, several limitations of the present study and potential future directions have been highlighted;

1. Myography studies presented in chapter 4 show some shortfalls, which were discussed in the text and could be addressed in future studies. These include the lack of positive control for TRPA1 antagonists used, particularly HC-030031. Attempts were made to obtain this in other rodent tissues; namely the bronchi, cerebral and pulmonary arteries, however I was unable to demonstrate an inhibition of a cinnamaldehyde response in the wire myograph preparation despite established use of HC-030031 within our group to inhibit the *in vivo* actions of cinnamaldehyde. My study has focussed on cinnamaldehyde as a TRPA1 agonist, which showed consistent relaxation actions in all tissues studied and evidence of neuropeptide dependence in the mesentery and bronchi. Concentrations of TRPA1 antagonists used were in the range shown to have TRPA1 inhibitory activity in published studies, but were not effective in blocking the cinnamaldehyde responses in my preparations. Therefore, I cannot currently conclude if my data represents a TRPA1 independent neuropeptide release by cinnamaldehyde, or problems with antagonist activity *in vitro*.

   A similar lack of activity was seen with the CGRP receptor antagonist $CGRP_{8-37}$, where I was able block exogenous CGRP-induced vasorelaxation but not cinnamaldehyde-induced vasorelaxation. This suggested that cinnamaldehyde activity is CGRP independent; however this conclusion was challenged when another CGRP receptor antagonist was able to strongly inhibit the cinnamaldehyde response. Collectively, findings suggest that there may be difficulties with the use of some antagonists in the wire myograph preparation.

The investigation of pharmacological interventions would also ideally have been carried out in vessels from TRPA1 WT and KO mice; in particular, the use of BIBN and 30mM potassium treatments. A lack of activity in TRPA1 KO mice would imply a CGRP and hyperpolarisation is induced specifically in the TRPA1 dependent component of cinnamaldehyde induced vasorelaxation. However a particular concern with BIBN is its current lack of commercial availability, which limits our study.

Further limitations are associated with the use of mice from different strain backgrounds, which has been discussed in chapter 4. The cinnamaldehyde response demonstrated TRPA1 dependent and independent components using mesenteric arteries from TRPA1 WT and KO mice. On-going studies would ideally have been conducted in vessels from WT and KO mice, but was not feasible due to availability and the necessity to use genetically modified strains on a different mouse background. Contractile abilities were shown to be similar in CD1, C57/BL6 and mixed background TRPA1 WT mice, also demonstrating comparable EC_{50} values for cinnamaldehyde vasorelaxation. Although this does not rule out strain related mechanistic differences, I suggest that this does not represent a major factor in the response to cinnamaldehyde.

Finally, although the findings from the myography studies are not conclusive, they do provide some novel insight on the mechanism of cinnamaldehyde induced vasorelaxation in the mouse mesenteric artery, a tissue not previously investigated for TRPA1 activity. Further studies could consolidate this investigation around the TRPA1 dependent component, perhaps using more selective TRPA1 agonists, antagonists of candidate potassium channels or by direct measurement of smooth muscle membrane potential. There are additional considerations of how this mechanism may translate to the *in vivo* scenario, where central reflexes play a major role in controlling resistance artery tone. These challenges could be

approached by further use of Laser Doppler flowmetry and measurement of localised/systemic changes in blood pressure.

2. The Ang II induced hypertension model used in this study produced an acute and severe hypertension model. Characterised by a systolic blood pressure of >160mmHg and diastolic blood pressure >120mmHg after only a week of Ang II infusion. This was useful to us because it allowed the rapid development of pathology over the 14 days infusion, but the strength of the model may have masked some of the compensatory changes of interest to us. This includes changes in CGRP levels. In response to my hypothesis, my aim was to investigate potential compensatory mechanisms initiated by TRPA1 during hypertension. I have some evidence that sensory neurones, and potentially TRPA1, were active during the experimental period through upregulation of TRPA1 receptor expression on DRG. However, CGRP plasma levels were lower than in control mice for both hypertensive groups. Together, this suggests that any compensatory role for sensory neurones in my hypertension model occurred before the end of the experimental protocol.

   Future experiments may benefit from using a lower dose of pressor agent, possibly infused over a longer time. This would also allow groups of mice to be sacrificed at time points along the protocol, demonstrating how the pathology develops. This approach would be more likely to highlight a role for TRPA1 and neuropeptides in hypertension. Alternatively, other methods of hypertension could be used, for example L-NAME or high fat feeding models. However, these models have different pathologies.

3. The statistical outcomes of this study have suffered from underpowering. Initial power calculations were based on the numbers needed in similar studies which are both published and have been carried out within this laboratory, as the size of any

differences could not be predicted in such a novel study. The N numbers needed were expected to be around 5-8 for blood pressure studies, and were met in much of the study. During the experiment, several areas reduced available N numbers and increased variability around the mean. Individual animals were lost in each protocol, likely due to acute hypertensive events. Animals were also grouped into several batches due to availability of time and materials, meaning that each protocol was conducted on 2-3 separate occasions and an extra aspect of variability was introduced into the data. This was compounded by the grouping of tail cuff and telemetry measured mice for *ex vivo* analysis. As I frequently serially used tissue from each animal for several analyses, this then led to some problems with under powering and lack of statistical significance in places. This is disappointing as it does not allow me to confirm the findings mathematically. With more time, interesting findings seen in this thesis could be followed up with increased experimental numbers. Ideally this would then also allow proper splitting of the data by gender, which seems not to be a determinant in this study, but would be of value to establish conclusively.

4. The breadth of this study has highlighted several areas of interest for further investigation. The first is the novel findings of hyperactivity in TRPA1 KO mice. This is of interest for future studies where the mechanisms can be further investigated.

5. Despite findings showing a mild role for TRPA1 in cardiovascular regulation. Several potentially interesting findings were made that deserve further investigation. In particular, the significantly increased hypertrophy and oxidative stress, and blunted increase in IL-6 and MCP-1 in hypertensive TRPA1 KO mice, suggesting that TRPA1 may mediate both pro and anti-inflammatory mechanisms. During chapter 5, I detailed how investigations have continued to study the source of IL-6 in the Ang II induced hypertension model.

Further investigation of oxidative stress would particularly be useful as TRPA1 is reported to be activated by ROS (Bessac, 2008), therefore a lack of anti-oxidant defence induction in KO mice suggests that TRPA1 may be important in sensing oxidant levels *in vivo*. This study would benefit from measurement of tissue ROS levels in particular. Lastly, several markers of inflammation measured in chapter 5 suggested that TRPA1 may be involved in inflammatory cell infiltration. TRPA1 KO mice showed significantly blunted increases in MCP-1, in addition to IL-6. However, mIL-8 upregulation was significant in hypertensive TRPA1 KO mice, but not in TRPA1 WT mice. Previous studies from this group have shown TRPA1 activation cause inflammatory cell infiltration (Bodkin, Unpublished data). A TRPA1 mediated cell infiltration mechanism would fit well with data in this thesis, however the mechanism is unclear. Sun *et al* (2007) show that treatment with NK_1 antagonists reduces the expression of MCP-1 on leukocytes during acute pancreatitis, suggesting that SP is chemotactic for granulocytes in particular, occurring via MCP-1. TRPA1 KO may be associated with decreased SP release, thus explaining the decreased MCP-1 expression and IL-6 production, through a reduced cell accumulation. This hypothesis cannot be fully determined until cell accumulation is quantified by histology, but currently available aortic sections do not show striking differences in cell accumulation. Therefore the mechanism behind these differences is currently unknown, but of potential value for the development of anti-TRPA1 therapeutics. As TRPA1 antagonists are currently in development for airway disease, which is often cellular based, part of their anti-inflammatory effect may be derived from a reduction in cell accumulation. Further *in vivo* and *ex vivo* cell accumulation assays would be of value to support these conclusions.

Future Studies To Clarify Mechanisms Discussed In This Thesis

- Extension of myography studies using TRPA1 WT and KO mice with more selective TRPA1 agonists and channel specific antagonists.
- An *in vivo,* long term low dose pressor study, with increased N numbers to improve the power of the study.
- Investigation of the exercise capacity in TRPA1 WT and KO mice.
- Investigation of TRPA1 WT and KO mice in other inflammatory diseases areas, particularly those which show a major role for IL-6

Conclusion

This thesis has described my novel study, investigating the role of TRPA1 in cardiovascular regulation. Though the role of TRPA1 proved to be mild, there were some valuable findings which add to current knowledge in the field. Firstly, the finding that TRPA1 is poorly expressed in the vasculature, but is expressed at high levels in DRG and upregulated during hypertension. Secondly, that TRPA1 activation on mesenteric arteries leads to endothelial independent vasorelaxation, which shows a hyperpolarisation and CGRP component. Thirdly, that TRPA1 may potentially modulate the production of inflammatory mediators, in particular IL-6. Fourthly, that TRPA1 may be protective against heart hypertrophy. Finally, and maybe most importantly, that TRPA1 deletion causes a previously undescribed hyperactivity phenotype in mice.

Appendix

This appendix is to be used alongside chapter 4, containing representative myograph traces collected in LabChart software from the DMT wire myograph, as described in the methods section. These images are screenshots of the raw data, which is collected by direct reading of the mN scale at the appropriate point.

A

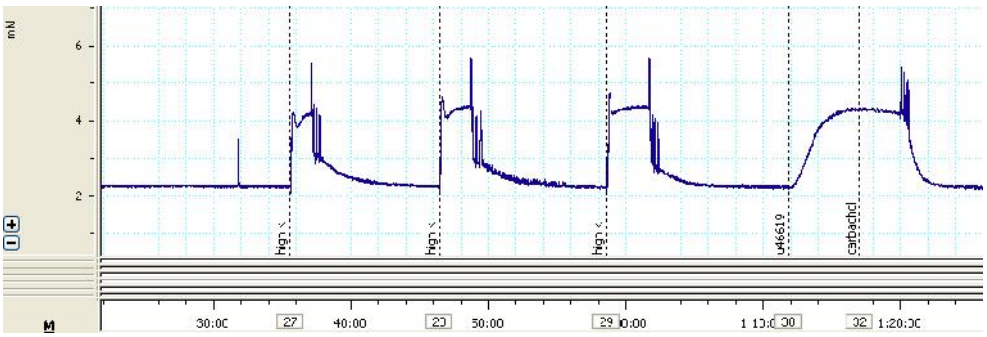

B

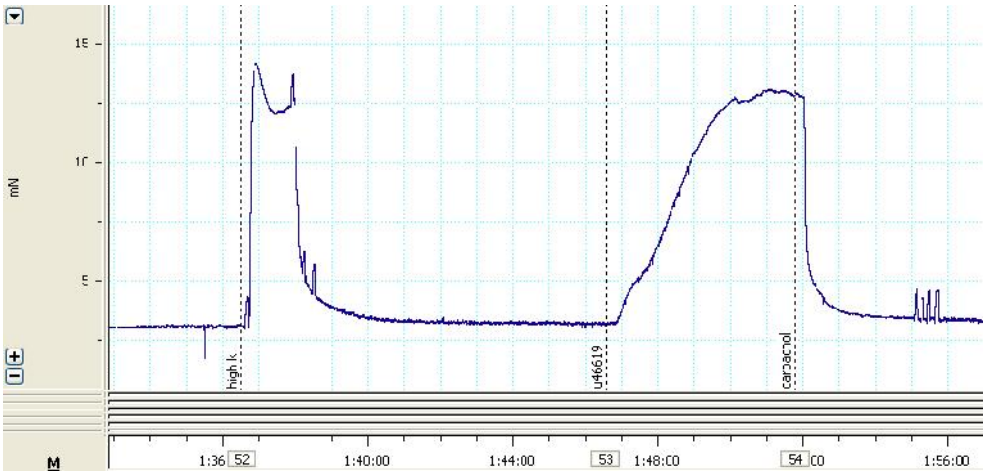

Appendix Figure 1: Representative Traces Of Responses To High K^+ And Assessment Of Endothelial Function Using Carbachol. Basal tone in mouse mesenteric arteries was set using a normalisation procedure (to 13.3kPa). Vessels were challenged with Krebs containing a depolarising level of K^+ (80mM) for two minutes, followed by 3 washouts with basic Krebs and a 5 minute rest. This is depicted in the first 3 peaks of panel A. Vessel were then pre-constricted using U46619 (10nM in 5µl water, 5 minutes) at a concentration used for all vessels and previously shown to approximate the EC_{70}, followed by an addition of Carbachol (10µM in 5µl water). Relaxation >60% at 2 minutes, is indicative of the vessels holding intact endothelium. The vessel shown in panel A is a mesenteric artery from a TRPA1 KO mouse. Panel B shows a more detailed trace with the 3rd 'High K+', U46619 and carbachol additions only, and is taken from a mesenteric artery from a TRPA1 WT mouse.

A **TRPA1 WT**

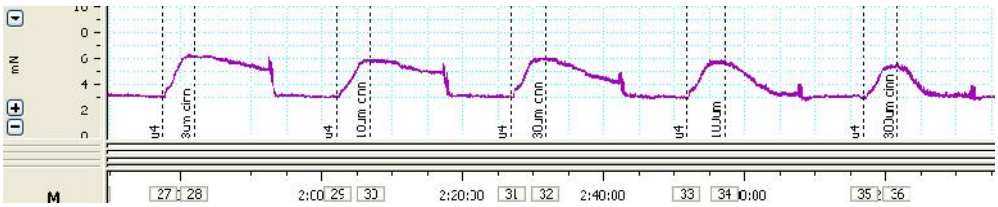

B **TRPA1 KO**

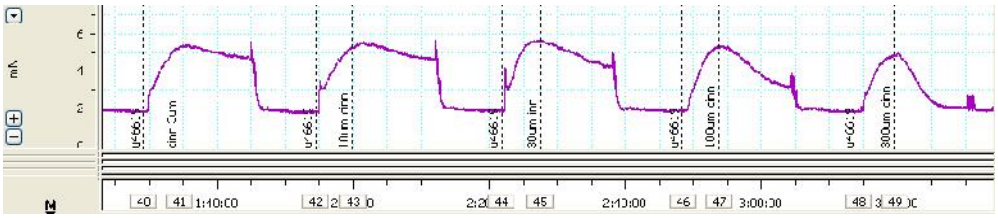

Appendix Figure 2; Representative Traces Showing The Effect Of Single Cinnamaldehyde Concentrations On TRPA1 WT And KO Mesenteric Arteries Without Functional Endothelium. TRPA1 WT (A) and KO (B) mesenteric arteries without endothelium were mounted on a wire myograph. Peaks show pre-constriction to U46619 (10nM in 5µl water, 5 minutes), followed by an addition of cinnamaldehyde in 5µl ethanol. Each consecutive peak shows effect of an incremental cinnamaldehyde concentration (3-300µM). % relaxation from pre-constriction is calculated 5 minutes after each cinnamaldehyde addition. This is followed by 3 wash-outs with basic Krebs and a 5 minute rest.

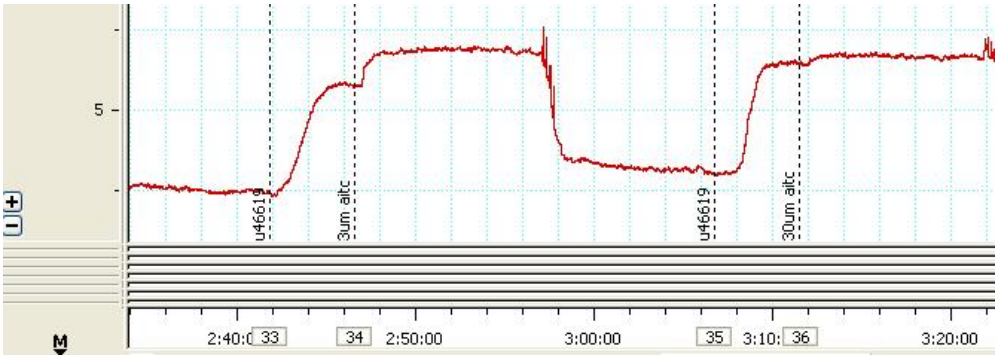

Appendix Figure 3: Representative Trace Of The Effect Of MO On A Mouse Mesenteric Artery. A TRPA1 WT mouse mesenteric artery without functional endothelium is pre-constricted to U46619 (10nM in 5µl water, 5 minutes), followed by addition of 3 or 30µM MO (AITC on the trace) in 5ul ethanol, for 10 minutes. This is followed by a 3 wash-outs with basic Krebs and a 10 minute rest. % relaxation from pre-constriction is calculated 10 minutes after each MO addition.

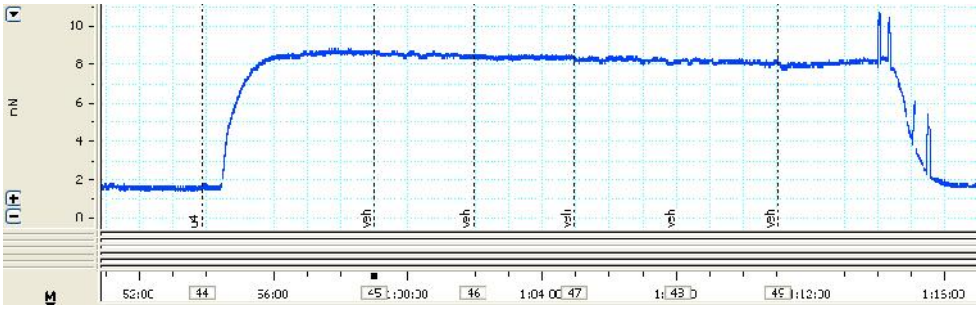

Appendix Figure 4: Representative Trace Of Cinnamaldehyde Vehicle Additions On U46619 Pre-constriction. A CD1 (TRPA1 WT) mesenteric artery with functional endothelium is pre-constricted with U46619 (10nM in 5ul water, 5 minutes). Additions of 1.5µl of ethanol are made every 3 minutes for 15 minutes, representing the vehicle of cinnamaldehyde. Final 5ml bath contains 7.5µl of ethanol. This is followed by 3 wash-outs with basic Krebs. % relaxation from pre-constriction is calculated 3 minutes after each vehicle addition.

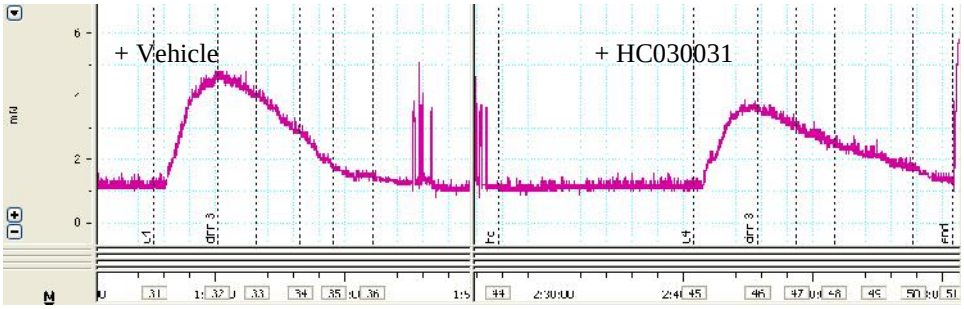

Appendix Figure 5; Representative Trace Showing The Effect Of HC-030031 Or Vehicle On The Concentration Dependant Relaxation To Cinnamaldehyde. A CD1 (TRPA1 WT) mouse mesenteric artery without functional endothelium is pre-treated for 15 minutes with either the TRPA1 antagonist HC030031 (30µM) or its vehicle (DMSO, 5µl) before pre-constriction with U46619 (10nM in 5µl water, 5 minutes). Cumulative concentrations of cinnamaldehyde are then added every 3 minutes (3-300µM, each in 1.5µl ethanol). The same vessel received vehicle first, followed by antagonist treatment. % relaxation from pre-constriction is calculated 3 minutes after each cinnamaldehyde addition.

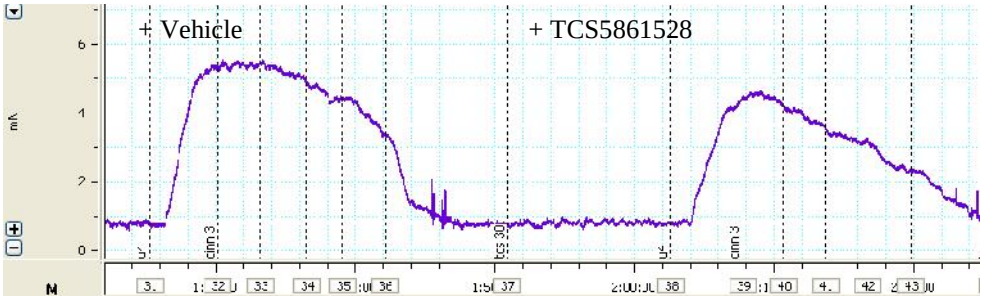

Appendix Figure 6; Representative Trace Showing The Effect Of TCS5861528 Or Vehicle On The Concentration Dependant Relaxation To Cinnamaldehyde. A CD1 (TRPA1 WT) mouse mesenteric artery without functional endothelium is pre-treated for 15 minutes with either the TRPA1 antagonist TCS5861528 (30µM) or its vehicle (DMSO, 5µl) before pre-constriction with U46619 (10nM in 5µl water, 5 minutes). Cumulative concentrations of cinnamaldehyde are then added every 3 minutes (3-300µM, each in 1.5µl ethanol). The same vessel received vehicle first, followed later by antagonist treatment. % relaxation from pre-constriction is calculated 3 minutes after each cinnamaldehyde addition.

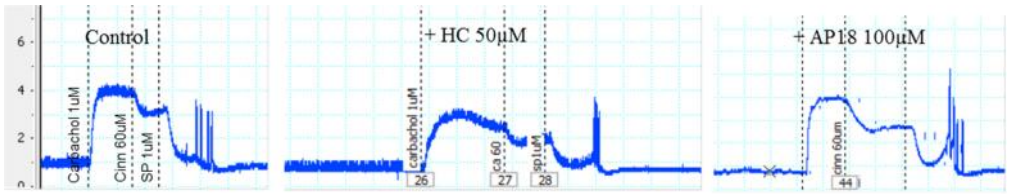

Appendix Figure 7; Representative Trace Showing The Effect Of TRPA1 Antagonists On Bronchial Ring Relaxation To Cinnamaldehyde and SP. Bronchial rings with functional epithelium, from CD1 (TRPA1 WT) mice, are pre-treated with HC-030031 (50µM in 0.05% DMSO/Krebs)**,** AP-18 (100µM in 0.1% DMSO/Krebs) or normal Krebs for 15 minutes before pre-constriction with carbachol (1µM in 5µl water, 3 minutes or to plateau). % relaxation from pre-constriction/cinnamaldehyde response is calculated 3 minutes after application of cinnamaldehyde (60µM in 10µl ethanol), then SP (1µM in 5µl 0.01% BSA/water). Between peaks there are 3 wash-outs with basic Krebs and a 20 minute rest period.

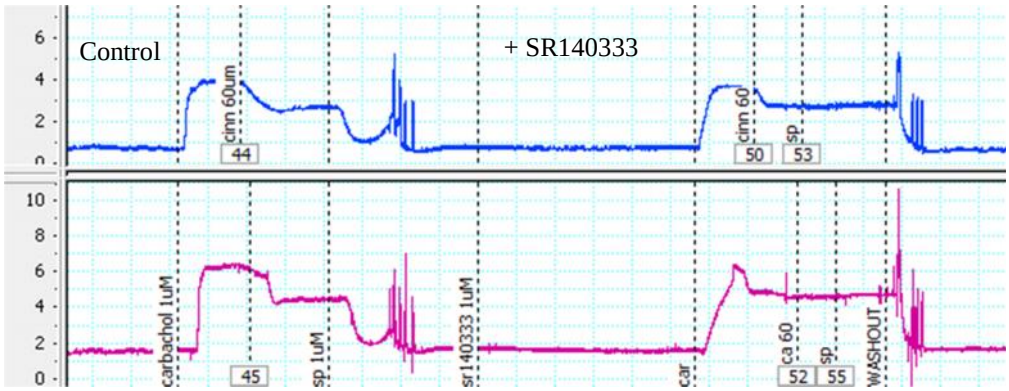

Appendix Figure 8; Representative Trace Showing The Effect Of NK_1 Antagonists On Bronchial Ring Relaxation To Cinnamaldehyde and SP. Bronchial rings with functional epithelium, from CD1 (TRPA1 WT) mice, are pre-treated with SR140333 (1µM in 5µl water) or normal Krebs for 15 minutes before pre-constriction with carbachol (1µM in 5µl water, 3 minutes or to plateau). % relaxation from pre-constriction/cinnamaldehyde response is then calculated 3 minutes after application of cinnamaldehyde (60µM in 10µl ethanol), then SP (1µM in 5µl 0.01% BSA/water). Between peaks there are 3 wash-outs with basic Krebs and a 20 minute rest period. Traces are from separate bronchi run in parallel.

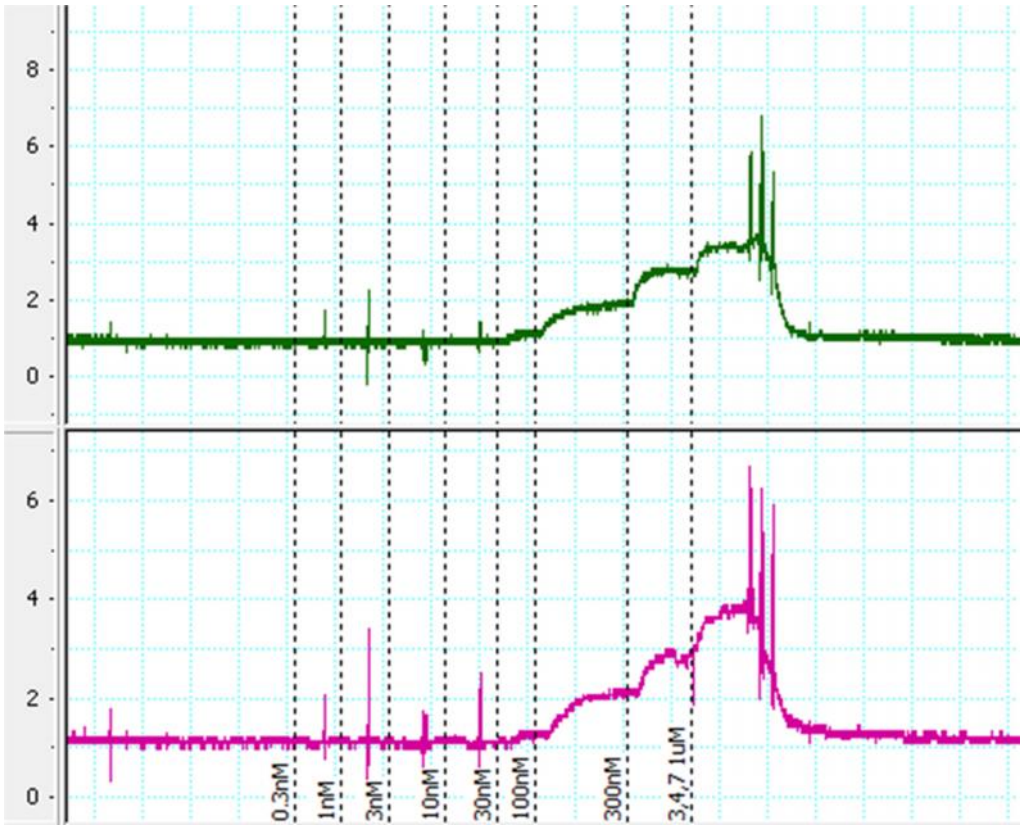

Appendix Figure 9; Representative Trace Showing The Contractile Effect Of U46619 On Rat Cerebral Arteries. Wistar rat cerebral arteries without functional endothelium were mounted in a wire myograph and tested for maximum contractile ability using three sets of 2 minute treatments with Krebs containing a depolarising concentration of potassium (80mM). Following a 10 minute rest, vessels were constricted with cumulative concentrations of U46619 (0.3nM-1µM in 1-5µl water), with additions every 2 minutes. Baseline tension was set using normalisation to a physiological tension (9kPa). Completion of the curve is followed by 3 wash-outs with basic Krebs. Traces are from separate bronchi run in parallel. % contraction from baseline is calculated 2 minutes after each addition.

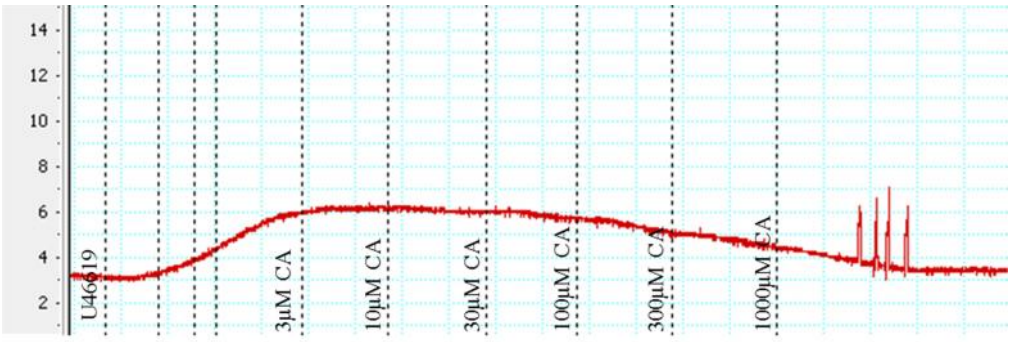

Appendix Figure 10; Representative Trace Showing The Concentration Dependent Vasorelaxation Of Rat Cerebral Arteries To Cinnamaldehyde. Wistar rat cerebral arteries with functional endothelium were mounted in a wire myograph and constricted with U46619 (30nM in 3µl water, 5 minutes) before addition of cumulative concentrations of cinnamaldehyde (3-1000µM in 1.5µl ethanol each addition, one every 2 minutes). % relaxation from pre-constriction is calculated 3 minutes after each addition.

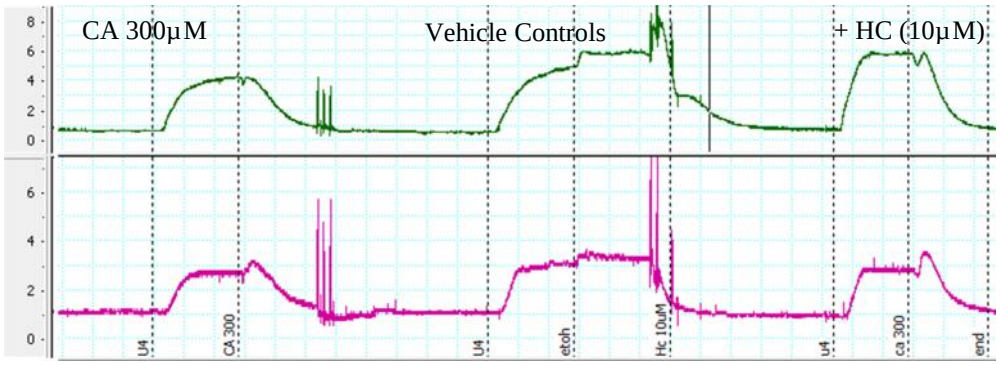

Appendix Figure 11; Representative Trace Showing The Vasorelaxation Of Rat Cerebral Arteries To Cinnamaldehyde With And Without Pre-Treatment With A TRPA1 Antagonist. Wistar rat cerebral arteries without functional endothelium were mounted in a wire myograph and pre-treated with HC-030031 (10µM), normal Krebs or vehicle (0.05% DMSO in Krebs) for 15 minutes before pre-constriction with U46619 (30nM in 3µl water, 5 minutes) and addition of cinnamaldehyde (300µM) or vehicle (5µl ethanol) for 5 minutes. This is followed by 3 wash-outs with Krebs and a 15 minute rest. 2 separate arteries are shown, conducted in parallel. % relaxation from pre-constriction is calculated 5 minutes after cinnamaldehyde addition.

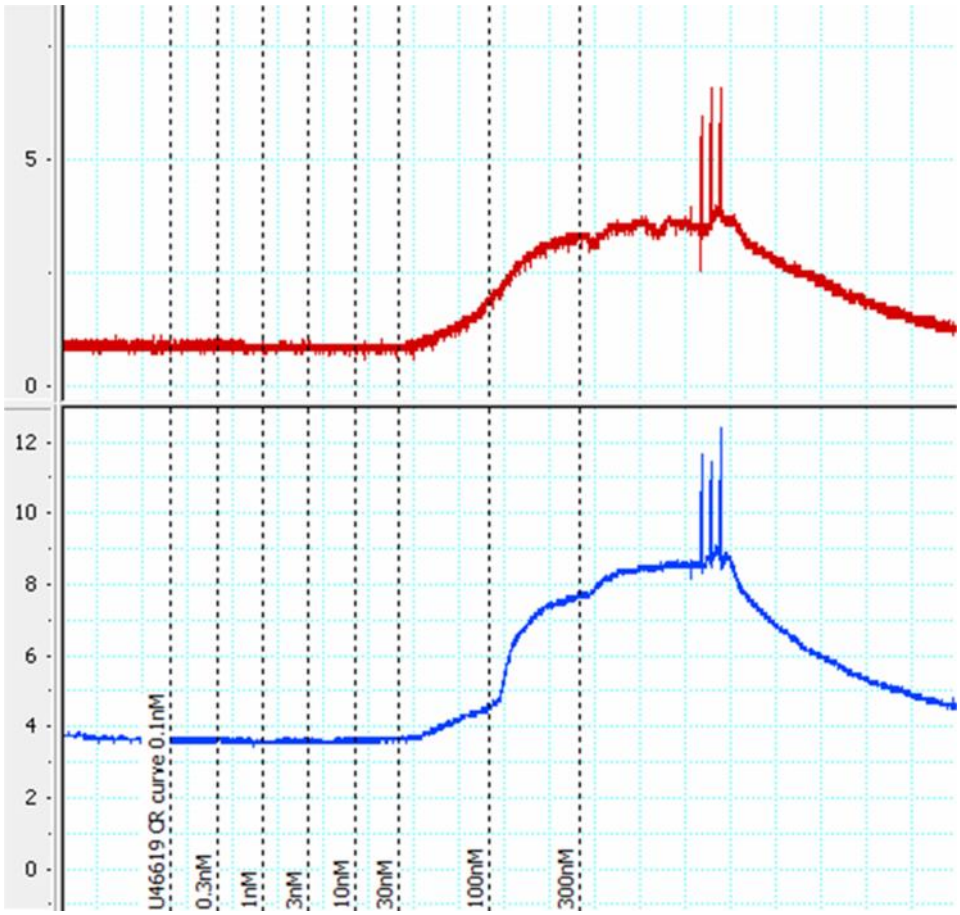

Appendix Figure 12; Representative Trace Showing The Contractile Effect Of U46619 On Rat Pulmonary Arteries. Wistar rat pulmonary arteries with functional endothelium were mounted in a wire myograph and tested for maximum contractile ability using three sets of 2 minutes treatments with Krebs containing a depolarising concentration of potassium (80mM). Following a 10 minute rest, vessels were constricted with cumulative concentrations of U46619 (0.1-300nM in 1-5µl water), with additions every 2 minutes. Baseline tension was set using normalisation to a physiological tension (2kPa). Completion of the curve is followed by 3 wash-outs with basic Krebs. % contraction from baseline is calculated 2 minutes after each addition. Traces are from separate vessels run in parallel

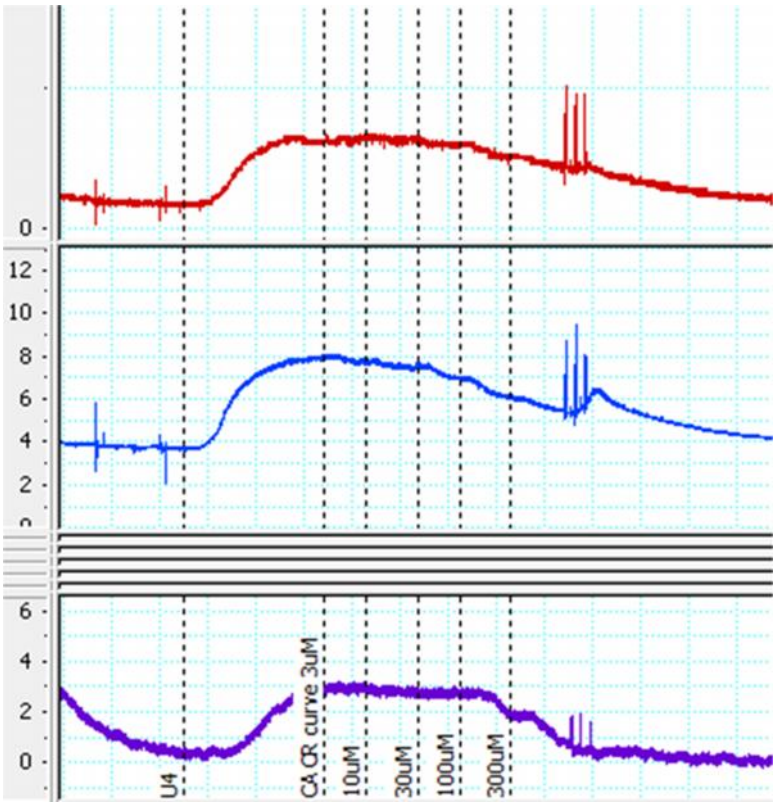

Appendix Figure 13; Representative Trace Showing The Concentration Dependent Vasorelaxation Of Rat Pulmonary Arteries To Cinnamaldehyde. Wistar rat pulmonary arteries with functional endothelium were mounted in a wire myograph and constricted with U46619 (100nM in 5µl water, 5 minutes) before addition of cumulative concentrations of cinnamaldehyde (3-300µM in 1.5µl ethanol each addition, every 2 minutes). This is followed by 3 wash-outs with basic Krebs. % relaxation from pre-constriction is calculated 3 minutes after each addition. Traces are from separate vessels run in parallel

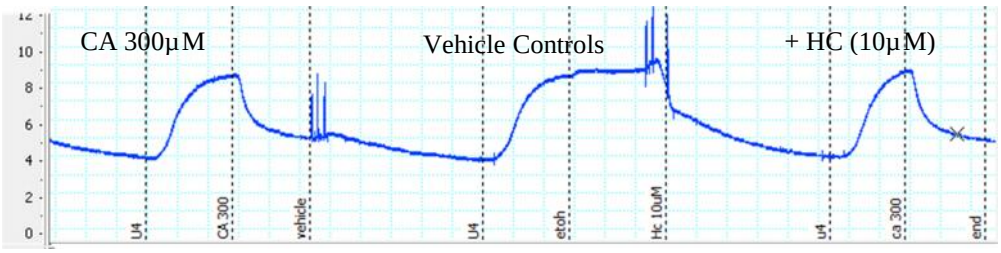

Appendix Figure 14; Representative Trace Showing The Vasorelaxation Of Rat Pulmonary Arteries To Cinnamaldehyde With And Without Pre-Treatment With A TRPA1 Antagonist. Wistar rat pulmonary arteries with functional endothelium were mounted in a wire myograph and pre-treated with HC-030031 (10µM), normal Krebs or vehicle (0.05% DMSO in Krebs) for 15 minutes before pre-constriction with U46619 (100nM in 5µl water, 5 minutes) and addition of cinnamaldehyde (300µM) or vehicle (5µl ethanol). This is followed by 3 wash-outs with basic Krebs and a 15 minute rest. % relaxation from pre-constriction is calculated 5 minutes after cinnamaldehyde addition.

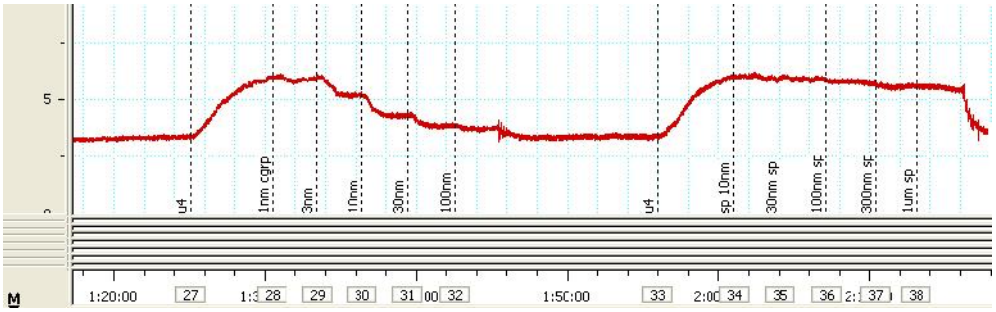

Appendix Figure 15; Representative Trace Showing The Effect Of CGRP And Substance P On Mesenteric Artery Tone. Mesenteric artery without functional endothelium from a CD1 (TRPA1 WT) mouse is mounted on a wire myograph and pre-constricted with U46619 (10nM, 5 minutes). This is followed by cumulative concentrations of αCGRP (1-100nM, in 1-5µl 0.01% BSA in water, left side of the panel) or SP (10-1000nM in 1-5µl 0.01% BSA in water, right side of the panel) every 3 minutes. % relaxation from pre-constriction is calculated 3 minutes after each addition.

A

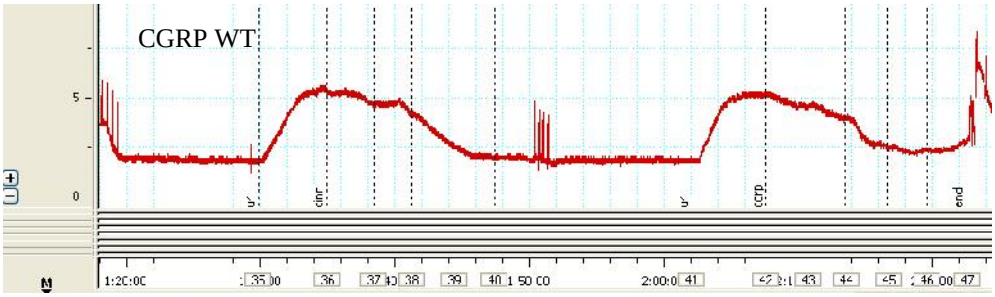

B

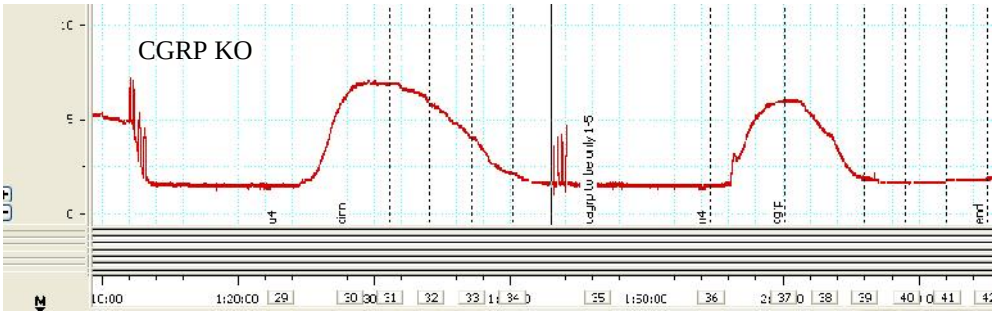

Appendix Figure 16; Representative Traces Showing Concentration Dependant Relaxation To Cinnamaldehyde And CGRP In CGRP WT And KO Mesenteric Arteries. Mesenteric arteries from CGRP WT (A) and KO (B) mice without functional endothelium are pre-constricted to U46619 (10nM, 5 minutes) before cumulative concentrations of cinnamaldehyde (3-300µM in 1.5ul ethanol per addition, left of the panel) or αCGRP (1-100nM in 1-5µl 0.01% BSA/water, right of the panel) are added every 3 minutes. % relaxation from pre-constriction is calculated 3 minutes after each addition. This is followed by 3 wash-outs with basic Krebs and a 10 minute rest.

A

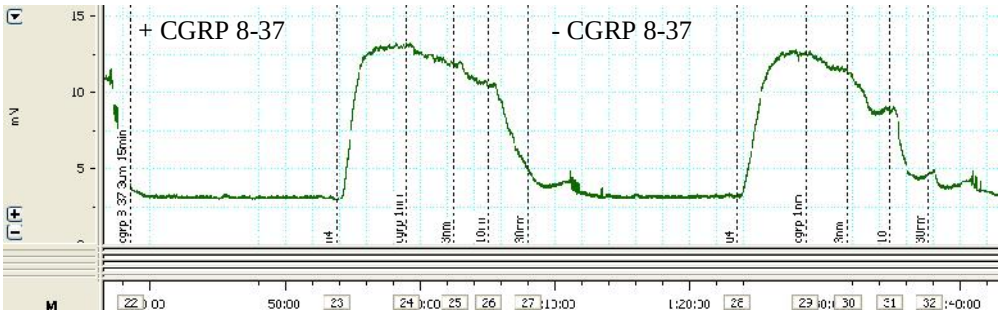

B

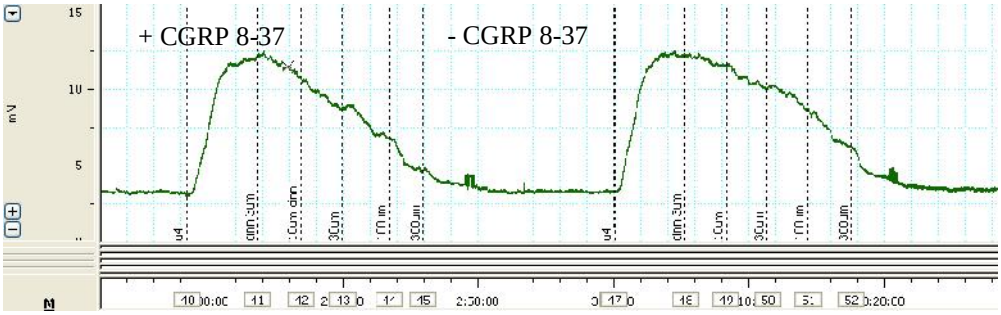

Appendix Figure 17; Representative Trace Showing The Effect Of CGRP 8-37 On Concentration Dependant Relaxation To CGRP And Cinnamaldehyde In A Mesenteric Artery. Mesenteric arteries without functional endothelium from a CD1 (TRPA1 WT) mouse are mounted on a wire myograph and pre-treated with the CGRP receptor antagonist CGRP 8-37 (3µM) or vehicle (10µl 0.01% BSA/water) for 15 minutes before pre-constriction with U46619 (10nM in 5µl water, 5 minutes) followed by cumulative concentrations of αCGRP (1-100nM in 1-5µl 0.01% BSA/water, panel A) or cinnamaldehyde are shown (3-300µM in 1.5µl ethanol, panel B). % relaxation from pre-constriction is calculated 3 minutes after each addition. Both A and B show the same vessel.

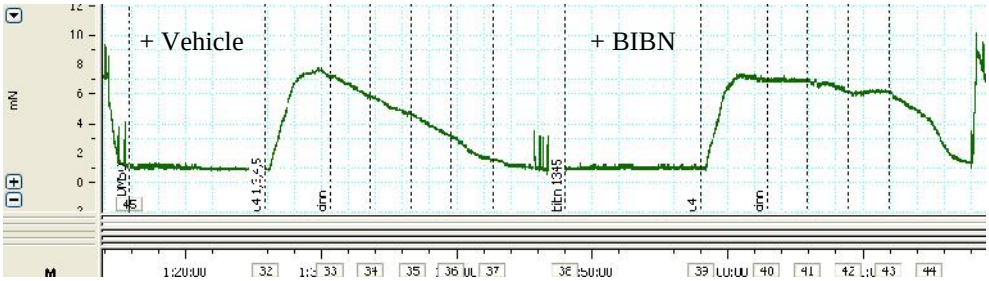

Appendix Figure 18; Representative Trace Showing The Effect Of BIBN 4096 BS Vehicle On Concentration Dependant Relaxation To Cinnamaldehyde. Mesenteric arteries without functional endothelium from a CD1 (TRPA1 WT) mouse are mounted on a wire myograph and pre-treated with the non-competitive CGRP antagonist BIBN 4096 (10µM) or vehicle (5µl DMSO) for 15 minutes before pre-constriction with U46619 (10nM in 5µl water, 5 minutes) and cumulative concentrations of cinnamaldehyde (3-300µM in 1.5ul ethanol per addition, every 3 minutes). % relaxation from pre-constriction is calculated 3 minutes after each addition.

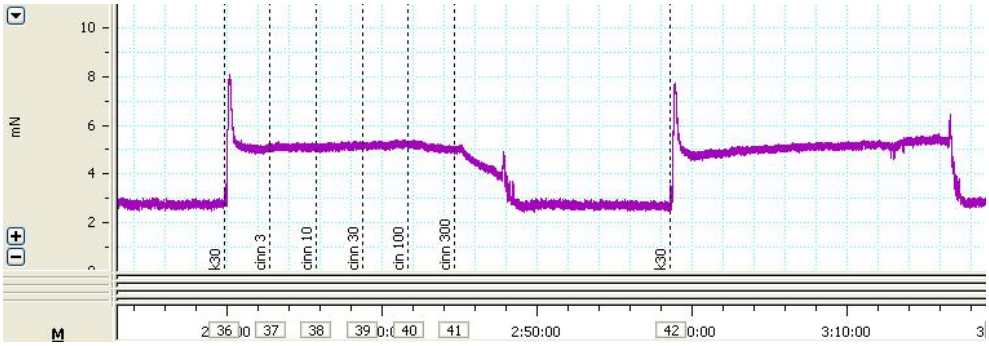

Appendix Figure 19; Representative Trace Showing The Effect Of Pre-constriction With 30mM K^+ On Concentration Dependant Relaxation To Cinnamaldehyde. Mesenteric arteries without functional endothelium from a CD1 (TRPA1 WT) mouse are mounted on a wire myograph and pre-constricted with a Krebs solution containing a slightly depolarising concentration of potassium which blocks hyperpolarisation of the tissue (30mM K^+). This is followed by cumulative concentrations of cinnamaldehyde (3-300µM in 1.5ul ethanol per addition, every 3 minutes, left of the panel) or without additions over a similar timecourse (right of the panel). This is followed by 3 wash-outs with basic Krebs and a 10 minute rest. % relaxation from pre-constriction is calculated 3 minutes after each addition or at the equivalent time-point.

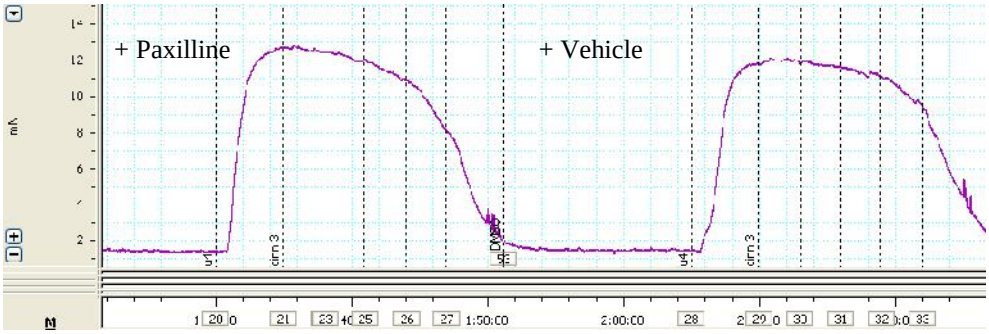

Appendix Figure 20; Representative Trace Showing The Effect Of Paxilline Or Vehicle On Concentration dependant Relaxation To Cinnamaldehyde. Mesenteric arteries without functional endothelium from a CD1 (TRPA1 WT) mouse are mounted on a wire myograph and pre-treated with the non-competitive BK_{Ca} channel antagonist paxilline (1µM) or vehicle (5µl DMSO) for 15 minutes before pre-constriction with U46619 (10nM in 5µl water, 5 minutes) and cumulative concentrations of cinnamaldehyde (3-300µM in 1.5ul ethanol per addition, every 3 minutes). % relaxation from pre-constriction is calculated 3 minutes after each addition.

References

Adlam, D., de Bono, J. P., Danson, E., Zhang, M., Casadei, B., Paterson, D. J. & Channon, K. M. 2011. Telemetric analysis of haemodynamic regulation during voluntary exercise training in mouse models. *Exp Physiol,* **8,** 8.

Ahluwalia, A. & Vallance, P. 1997. Evidence for Functional Responses to Sensory Nerve Stimulation of Rat Small Mesenteric Veins. *Journal of Pharmacology and Experimental Therapeutics,* **281,** 9-14.

Ajijola, O. A., Dong, C., Herderick, E. E., Ma, Q., Goldschmidt-Clermont, P. J. & Yan, Z. 2009. Voluntary running suppresses proinflammatory cytokines and bone marrow endothelial progenitor cell levels in apolipoprotein-E-deficient mice. *Antioxid Redox Signal,* **11,** 15-23.

Aker, S., Bantis, C., Reis, P., Kuhr, N., Schwandt, C., Grabensee, B., Heering, P. & Ivens, K. 2009. Influence of interleukin-6 G-174C gene polymorphism on coronary artery disease, cardiovascular complications and mortality in dialysis patients. *Nephrology Dialysis Transplantation,* **24,** 2847-2851.

Akopian, A. N., Ruparel, N. B., Jeske, N. A. & Hargreaves, K. M. 2007. Transient receptor potential TRPA1 channel desensitization in sensory neurons is agonist dependent and regulated by TRPV1-directed internalization. *The Journal of Physiology,* **583,** 175-193.

Anand, P., Murali, K. Y., Tandon, V., Murthy, P. S. & Chandra, R. 2010. Insulinotropic effect of cinnamaldehyde on transcriptional regulation of pyruvate kinase, phosphoenolpyruvate carboxykinase, and GLUT4 translocation in experimental diabetic rats. *Chem Biol Interact,* **186,** 72-81.

Anand, U., Otto, W. R., Facer, P., Zebda, N., Selmer, I., Gunthorpe, M. J., Chessell, I. P., Sinisi, M., Birch, R. & Anand, P. 2008. TRPA1 receptor localisation in the human peripheral nervous system and functional studies in cultured human and rat sensory neurons. *Neuroscience Letters,* **438,** 221-227.

Andersson, D. A., Gentry, C., Moss, S. & Bevan, S. 2008. Transient Receptor Potential A1 Is a Sensory Receptor for Multiple Products of Oxidative Stress. *J. Neurosci.,* **28,** 2485-2494.

Andersson, K.-E., Gratzke, C. & Hedlund, P. 2010. The role of the transient receptor potential (TRP) superfamily of cation-selective channels in the management of the overactive bladder. *BJU International,* **106,** 1114-1127.

Ando, K., Pegram, B. L. & Frohlich, E. D. 1990. Hemodynamic effects of calcitonin gene-related peptide in spontaneously hypertensive rats. *Am J Physiol,* **258,** R425-9.

Andrade, E. L., Ferreira, J., Andre, E. & Calixto, J. B. 2006. Contractile mechanisms coupled to TRPA1 receptor activation in rat urinary bladder. *Biochem Pharmacol,* **72,** 104-14.

Andrade, E. L., Forner, S., Bento, A. F., Leite, D. F. P., Dias, M. A., Leal, P. C., Koepp, J. & Calixto, J. B. 2011. TRPA1 receptor modulation attenuates bladder overactivity induced by spinal cord injury.

American Journal of Physiology - Renal Physiology, **300,** F1223-F1234.

Andrade, E. L., Luiz, A. P., Ferreira, J. & Calixto, J. B. 2008. Pronociceptive response elicited by TRPA1 receptor activation in mice. *Neuroscience,* **152,** 511-520.

Andrè, E., Campi, B., Materazzi, S., Trevisani, M., Amadesi, S., Massi, D., Creminon, C., Vaksman, N., Nassini, R., Civelli, M., Baraldi, P. G., Poole, D. P., Bunnett, N. W., Geppetti, P. & Patacchini, R. 2008 . Cigarette smoke-induced neurogenic inflammation is mediated by alpha,beta-unsaturated aldehydes and the TRPA1 receptor in rodents. *J Clin Invest.,* **118,** 2574-82.

Andre, E., Gatti, R., Trevisani, M., Preti, D., Baraldi, P. G., Patacchini, R. & Geppetti, P. 2009. Transient receptor potential ankyrin receptor 1 is a novel target for pro-tussive agents. *Br J Pharmacol,* **158,** 1621-8.

Anilkumar, N., Weber, R., Zhang, M., Brewer, A. & Shah, A. M. 2008. Nox4 and Nox2 NADPH Oxidases Mediate Distinct Cellular Redox Signaling Responses to Agonist Stimulation. *Arteriosclerosis, Thrombosis, and Vascular Biology,* **28,** 1347-1354.

Attaran, D., Lari, S. M., Towhidi, M., Marallu, H. G., Ayatollahi, H., Khajehdaluee, M., Ghanei, M. & Basiri, R. 2010. Interleukin-6 and airflow limitation in chemical warfare patients with chronic obstructive pulmonary disease. *Int J Chron Obstruct Pulmon Dis,* **5,** 335-40.

Bandell, M., Story, G., Hwang, S., Viswanath, V., Eid, S., Petrus, M., Earley, T. & Patapoutian, A. 2004. Noxious cold ion channel TRPA1 is activated by pungent compounds and bradykinin. *Neuron,* **41,** 849 - 857.

Banerjee, S. & Maulik, S. 2002. Effect of garlic on cardiovascular disorders: a review. *Nutrition Journal,* **1,** 4.

Bánvölgyi, A., Pozsgai, G., Brain, S. D., Helyes, Z. S., Szolcsányi, J., Ghosh, M., Melegh, B. & Pintér, E. 2004. Mustard oil induces a transient receptor potential vanilloid 1 receptor-independent neurogenic inflammation and a non-neurogenic cellular inflammatory component in mice. *Neuroscience.,* **125,** 449-59.

Baraldi, P. G., Preti, D., Materazzi, S. & Geppetti, P. 2010. Transient Receptor Potential Ankyrin 1 (TRPA1) Channel as Emerging Target for Novel Analgesics and Anti-Inflammatory Agents. *Journal of Medicinal Chemistry*.

Bassoli, A., Borgonovo, G., Caimi, S., Scaglioni, L., Morini, G., Moriello, A. S., Marzo, V. D. & Petrocellis, L. D. 2009. Taste-guided identification of high potency TRPA1 agonists from Perilla frutescens. *Bioorganic & Medicinal Chemistry,* **17,** 1636-1639.

Baumann, P. Q., Sobel, B. E., Tarikuz Zaman, A. K. M. & Schneider, D. J. 2008. Gender-Dependent Differences in Echocardiographic Characteristics of Murine Hearts. *Echocardiography,* **25,** 739-748.

Bautista, D. M., Jordt, S.E., Nikai, T., Tsuruda, P.R., Read, A.J., Poblete, J., Yamoah, E.N., Basbaum, A.I., Julius, D. 2006 TRPA1 mediates the inflammatory actions of environmental irritants and proalgesic agents. *Cell,* **124,** 1269-82.

Bautista, D. M., Movahed, P., Hinman, A., Axelsson, H.E., Sterner, O., Högestätt, E.D., Julius, D., Jordt, S.E., Zygmunt, P.M. 2005. Pungent products from garlic activate the sensory ion channel TRPA1. *PNAS,* **102,** 12248-12252.

Bedard, K. & Krause, K.-H. 2007. The NOX Family of ROS-Generating NADPH Oxidases: Physiology and Pathophysiology. *Physiological Reviews,* **87,** 245-313.

Behr, T. M., Willette, R. N., Coatney, R. W., Berova, M., Angermann, C. E., Anderson, K., Sackner-Bernstein, J. D. & Barone, F. C. 2004. Eprosartan improves cardiac performance, reduces cardiac hypertrophy and mortality and downregulates myocardial monocyte chemoattractant protein-1 and inflammation in hypertensive heart disease. *J Hypertens,* **22,** 583-92.

Bendall, J. K., Cave, A. C., Heymes, C., Gall, N. & Shah, A. M. 2002. Pivotal Role of a gp91phox-Containing NADPH Oxidase in Angiotensin II-Induced Cardiac Hypertrophy in Mice. *Circulation,* **105,** 293-296.

Bendall, J. K., Rinze, R., Adlam, D., Tatham, A. L., de Bono, J., Wilson, N., Volpi, E. & Channon, K. M. 2007. Endothelial Nox2 overexpression potentiates vascular oxidative stress and hemodynamic response to angiotensin II: studies in endothelial-targeted Nox2 transgenic mice. *Circ Res,* **100,** 1016-25.

Berthiaume, N., Hess, F., Chen, H., Regoli, D. & D'Orléans-Juste, P. 1997. Pharmacology of kinins in the arterial and venous mesenteric bed of normal and B2 knockout transgenic mice. *European Journal of Pharmacology,* **333,** 55-61.

Bessac, B. F., Sivula, M., von Hehn, C. A., Escalera, J., Cohn, L. & Jordt, S. E. 2008. TRPA1 is a major oxidant sensor in murine airway sensory neurons. *J Clin Invest,* **118,** 1899-910.

Bianchi B.R., Zhang X.F., Reilly R.M., Kym P.R., Yao B.B., Chen J., 2012, Species comparison and pharmacological characterization of human, monkey, rat, and mouse TRPA1 channels. *J Pharmacol Exp Ther*. **2**, 360-8.

Birrell, M. A., Belvisi, M. G., Grace, M., Sadofsky, L., Faruqi, S., Hele, D. J., Maher, S. A., Freund-Michel, V. & Morice, A. H. 2009. TRPA1 Agonists Evoke Coughing in Guinea Pig and Human Volunteers. *Am. J. Respir. Crit. Care Med.*, **180,** 1042-1047.

Bochkov, V. N. 2007 Inflammatory profile of oxidized phospholipids. *Thromb Haemost.* , **97,** 348-54.

Bodkin, J. V. & Brain, S. D. 2010. Transient receptor potential ankyrin 1: emerging pharmacology and indications for cardiovascular biology. *Acta Physiol (Oxf),* **15,** 1748-1716.

Bölcskei, K., Zsuzsanna, H., Szabó, A., Sándor, K., Elekes, K., Németh, J., Almási, R., Pintér, E., Pethő, G., Szolcsányi, J. 2005. Investigation of the role of TRPV1 receptors in acute and chronic nociceptive processes using gene-deficient mice. *Pain,* **117,** 368-376.

Brain, S. D. & Grant, A. D. 2004. Vascular Actions of Calcitonin Gene-Related Peptide and Adrenomedullin. *Physiol. Rev.*, **84,** 903-934.

Brain, S. D., Williams, T. J., Tippins, J. R., Morris, H. R. & MacIntyre, I. 1985. Calcitonin gene-related peptide is a potent vasodilator. *Nature. ,* **313,** 54-6.

Bratz, I. N., Dick, G. M., Tune, J. D., Edwards, J. M., Neeb, Z. P., Dincer, U. D. & Sturek, M. 2008. Impaired capsaicin-induced relaxation of coronary arteries in a porcine model of the metabolic syndrome. *American Journal of Physiology - Heart and Circulatory Physiology,* **294,** H2489-H2496.

Brink, M., Price, S. R., Chrast, J., Bailey, J. L., Anwar, A., Mitch, W. E. & Delafontaine, P. 2001. Angiotensin II induces skeletal muscle wasting through enhanced protein degradation and down-regulates autocrine insulin-like growth factor I. *Endocrinology,* **142,** 1489-96.

Brône, B., Peeters, P. J., Marrannes, R., Mercken, M., Nuydens, R., Meert, T. & Gijsen, H. J. M. 2008. Tear gasses CN, CR, and CS are potent activators of the human TRPA1 receptor. *Toxicology and Applied Pharmacology,* **231,** 150-156.

Bunag, R. & Riley, E. 1974. Simultaneous measurements in awake rats of drug-induced changes in carotid and tail-cuff systolic pressures. *Journal of applied physiology,* **36,** 621-624.

Bunag, R. D. 1973. Validation in awake rats of a tail-cuff method for measuring systolic pressure. *Journal of Applied Physiology,* **34,** 279-282.

Byrne, A. & Byrne, D. G. 1993. The effect of exercise on depression, anxiety and other mood states: A review. *Journal of Psychosomatic Research,* **37,** 565-574.

Byrne, J. A., Grieve, D. J., Bendall, J. K., Li, J. M., Gove, C., Lambeth, J. D., Cave, A. C. & Shah, A. M. 2003. Contrasting roles of NADPH oxidase isoforms in pressure-overload versus angiotensin II-induced cardiac hypertrophy. *Circ Res,* **93,** 802-5.

Caceres, A. I., Brackmann, M., Elia, M. D., Bessac, B. F., del Camino, D., D'Amours, M., Witek, J. S., Fanger, C. M., Chong, J. A., Hayward, N. J., Homer, R. J., Cohn, L., Huang, X., Moran, M. M. & Jordt, S.-E. 2009. A sensory neuronal ion channel essential for airway inflammation and hyperreactivity in asthma. *Proceedings of the National Academy of Sciences,* **106,** 9099-9104.

Cao D.S., Zhong L., Hsieh T.H., Abooj M., Bishnoi M., Hughes L., Premkumar L.S., 2012, Expression of transient receptor potential ankyrin 1 (TRPA1) and its role in insulin release from rat pancreatic beta cells. *PLoS One*. 7, e38005.

Cao, T., Pinter, E., Al-Rashed, S., Gerard, N., Hoult, J. R. & Brain, S. D. 2000. Neurokinin-1 Receptor Agonists Are Involved in Mediating Neutrophil Accumulation in the Inflamed, But Not Normal, Cutaneous Microvasculature: An *In vivo* Study Using Neurokinin-1 Receptor Knockout Mice. *J Immunol,* **164,** 5424-5429.

Capasso R., Aviello G., Romano B., Borrelli F., De Petrocellis L., Di Marzo V., Izzo A.A., 2012, Modulation of mouse gastrointestinal motility by allyl isothiocyanate, a constituent of cruciferous vegetables (Brassicaceae): evidence for TRPA1-independent effects. *Br J Pharmacol.* **165**, 1966-77.

Carretero, O. A. & Oparil, S. 2000. Essential Hypertension : Part I: Definition and Etiology. *Circulation,* **101,** 329-335.

Caspani, O. & Heppenstall, P. A. 2009. TRPA1 and Cold Transduction: An Unresolved Issue? *The Journal of General Physiology,* **133,** 245-249.

Caterina, M., Leffler A., Malmberg, A., Martin, W., Trafton, J., , Petersen-Zeitz, K., Koltzenburg, M., Basbaum, A. & Julius, D. 2000. Impaired Nociception and Pain Sensation in Mice Lacking the Capsaicin Receptor. *Science,* **288.,** 306-313.

Caterina, M. J. 2007. Transient receptor potential ion channels as participants in thermosensation and thermoregulation. *Am J Physiol Regul Integr Comp Physiol,* **292,** R64-76.

Caterina, M. J., Schumacher, M. A., Tominaga, M., Rosen, T. A., Levine, J. D. & Julius, D. 1997. The capsaicin receptor: a heat-activated ion channel in the pain pathway. *Nature,* **389,** 816-824.

Cavanaugh, E. J., Simkin, D. & Kim, D. 2008. Activation of transient receptor potential A1 channels by mustard oil, tetrahydrocannabinol and Ca2+ reveals different functional channel states. *Neuroscience,* **154,** 1467-1476.

Chabrashvili, T., Kitiyakara, C., Blau, J., Karber, A., Aslam, S., Welch, W. J. & Wilcox, C. S. 2003. Effects of ANG II type 1 and 2 receptors on oxidative stress, renal NADPH oxidase, and SOD expression. *Am J Physiol Regul Integr Comp Physiol,* **285,** R117-24.

Chao, L. K., Hua, K.-F., Hsu, H.-Y., Cheng, S.-S., Lin, I. F., Chen, C.-J., Chen, S.-T. & Chang, S.-T. 2008. Cinnamaldehyde inhibits pro-inflammatory cytokines secretion from monocytes/macrophages through suppression of intracellular signaling. *Food and Chemical Toxicology,* **46,** 220-231.

Charles, A. S., Baskaran, S. A., Murcott, C., Schreiber, D., Hoagland, T. & Venkitanarayanan, K. 2008. Reduction of Escherichia coli O157:H7 in cattle drinking-water by trans-cinnamaldehyde. *Foodborne Pathog Dis,* **5,** 763-71.

Chen J., Kym P.R., TRPA1: the species difference. 2009. *J Gen Physiol.* **133**, 623-5.

Chen, J., Kim, D., Bianchi, B., Cavanaugh, E., Faltynek, C., Kym, P. & Reilly, R. 2009a. Pore dilation occurs in TRPA1 but not in TRPM8 channels. *Molecular Pain,* **5,** 3.

Chen, J., Zhang, X.-F., Kort, M. E., Huth, J. R., Sun, C., Miesbauer, L. J., Cassar, S. C., Neelands, T., Scott, V. E., Moreland, R. B., Reilly, R. M., Hajduk, P. J., Kym, P. R., Hutchins, C. W. & Faltynek, C. R. 2008. Molecular Determinants of Species-Specific Activation or Blockade of TRPA1 Channels. *J. Neurosci.,* **28,** 5063-5071.

Chen, Y.-H., Yet, S.-F. & Perrella, M. A. 2003. Role of Heme Oxygenase-1 in the Regulation of Blood Pressure and Cardiac Function. *Exp. Biol. Med.,* **228,** 447-453.

Chen, Y., Ma, Y. & Ma, W. 2009b. Pharmacokinetics and bioavailability of cinnamic acid after oral administration of Ramulus Cinnamomi in rats. *Eur J Drug Metab Pharmacokinet,* **34,** 51-6.

Cheung, C., Hotchkiss, S. A. & Pease, C. K. 2003. Cinnamic compound metabolism in human skin and the role metabolism may play in determining relative sensitisation potency. *J Dermatol Sci,* **31,** 9-19.

Cocks T.M., King S.J., Angus J.A., 1990. Glibenclamide is a competitive antagonist of the thromboxane A2 receptor in dog coronary artery in vitro. *Br J Pharmacol.* **100**, 375-8.

Cohen, D. M. 2007. The transient receptor potential vanilloid-responsive 1 and 4 cation channels: role in neuronal osmosensing and renal physiology. *Current Opinion in Nephrology & Hypertension,* **16,** 451-8.

Collier, P., Watson, C. J., Voon, V., Phelan, D., Jan, A., Mak, G., Martos, R., Baugh, J. A., Ledwidge, M. T. & McDonald, K. M. 2011. Can emerging biomarkers of myocardial remodelling identify asymptomatic hypertensive patients at risk for diastolic dysfunction and diastolic heart failure? *European Journal of Heart Failure*.

Collin, M., Patel, N., Dugo, L., Thiemermann, C. 2004 Role of peroxisome proliferator-activated receptor-[gamma] in the protection afforded by 15-deoxy[DELTA]12,14 prostaglandin J2 against the multiple organ failure caused by endotoxin. *Critical Care Medicine,* **32,** 826-31.

Collins, K. A., Korcarz, C. E. & Lang, R. M. 2003. Use of echocardiography for the phenotypic assessment of genetically altered mice. *Physiological Genomics,* **13,** 227-239.

Corey, D. P., García-Añoveros, J., Holt, J.R., Kwan, K.Y., Lin, S.Y., Vollrath, M.A., Amalfitano, A., Cheung, E.L., Derfler, B.H., Duggan, A., Géléoc, G.S., Gray, P.A., Hoffman, M.P., Rehm, H.L., Tamasauskas, D., Zhang, D.S. 2004 TRPA1 is a candidate for the mechanosensitive transduction channel of vertebrate hair cells. *Nature,* **432,** 723-30.

Costa, S. K. P., Esquisatto, L. C. M., Camargo, E., Gambero, A., Brain, S. D., De Nucci, G. & Antunes, E. 2001. Comparative effect of Phoneutria nigriventer spider venom and capsaicin on the rat paw oedema. *Life Sciences,* **69,** 1573-1585.

Cruz-Orengo, L., Dhaka, A., Heuermann, R.J., Young, T.J., Montana, M.C., Cavanaugh, E.J., Kim, D., Story, G.M. 2008 Cutaneous nociception evoked by 15-delta PGJ2 via activation of ion channel TRPA1. *Mol Pain.,* **31,** 30.

Cucoranu, I., Clempus, R., Dikalova, A., Phelan, P. J., Ariyan, S., Dikalov, S. & Sorescu, D. 2005. NAD(P)H Oxidase 4 Mediates Transforming Growth Factor-β1–Induced Differentiation of Cardiac Fibroblasts Into Myofibroblasts. *Circulation Research,* **97,** 900-907.

Cvetkov, T. L., Huynh, K. W., Cohen, M. R. & Moiseenkova-Bell, V. Y. 2011. Molecular architecture and subunit organization of TRPA1 channel revealed by electron microscopy. *J Biol Chem,* **9,** 9.

da Costa, D. S. M., Meotti, F. C., Andrade, E. L., Leal, P. C., Motta, E. M. & Calixto, J. B. 2010. The involvement of the transient receptor potential A1 (TRPA1) in the maintenance of mechanical and cold hyperalgesia in persistent inflammation. *Pain,* **148,** 431-437.

Davis, J. B., Gray, J., Gunthorpe, M. J., Hatcher, J. P., Davey, P. T., Overend, P., Harries, M. H., Latcham, J., Clapham, C., Atkinson, K., Hughes, S. A., Rance, K., Grau, E., Harper, A. J., Pugh, P. L., Rogers, D. C., *et al.* 2000. Vanilloid receptor-1 is essential for inflammatory thermal hyperalgesia. *Nature,* **405,** 183-187.

DeFalco, J., Steiger, D., Gustafson, A., Emerling, D. E., Kelly, M. G. & Duncton, M. A. J. 2010. Oxime derivatives related to AP18: Agonists and antagonists of the TRPA1 receptor. *Bioorganic & Medicinal Chemistry Letters,* **20,** 276-279.

del Camino, D., Murphy, S., Heiry, M., Barrett, L. B., Earley, T. J., Cook, C. A., Petrus, M. J., Zhao, M., D'Amours, M., Deering, N., Brenner, G. J., Costigan, M., Hayward, N. J., Chong, J. A., Fanger, C. M., Woolf, C. J., *et al.* 2010. TRPA1 Contributes to Cold Hypersensitivity. *The Journal of Neuroscience,* **30,** 15165-15174.

Deng, P.-Y. & Li, Y.-J. 2005. Calcitonin gene-related peptide and hypertension. *Peptides,* **26,** 1676-85.

Didion, S. P., Ryan, M. J., Didion, L. A., Fegan, P. E., Sigmund, C. D. & Faraci, F. M. 2002. Increased Superoxide and Vascular Dysfunction in CuZnSOD-Deficient Mice. *Circulation Research*.

Dikalov, S. I., Dikalova, A. E., Bikineyeva, A. T., Schmidt, H. H., Harrison, D. G. & Griendling, K. K. 2008. Distinct roles of Nox1 and Nox4 in basal and angiotensin II-stimulated superoxide and hydrogen peroxide production. *Free Radic Biol Med,* **45,** 1340-51.

Diogenes, A., Akopian, A. N. & Hargreaves, K. M. 2007. NGF up-regulates TRPA1: implications for orofacial pain. *J Dent Res,* **86,** 550-5.

Doihara, H., Nozawa, K., Kawabata-Shoda, E., Kojima, R., Yokoyama, T. & Ito, H. 2009. TRPA1 agonists delay gastric emptying in rats through serotonergic pathways. *Naunyn-Schmiedeberg's Archives of Pharmacology,* **380,** 353-357.

Donnerer J., Yan Z., Lembeck F., 1988, Effects of clonidine and yohimbine on a C-fibre-evoked blood pressure reflex in the rat. *Br J Pharmacol*. **94**, 848-52.

Dong, Y., Shi, H. L., Shi, J. R. & Wu, D. Z. 2010. Transient receptor potential A1 is involved in cold-induced contraction in the isolated rat colon smooth muscle. *Sheng Li Xue Bao,* **62,** 349-56.

Dong, Y. L., Vegiraju, S., Chauhan, M., Gangula, P. R., Hankins, G. D., Goodrum, L. & Yallampalli, C. 2004. Involvement of calcitonin gene-related peptide in control of human fetoplacental vascular tone. *Am J Physiol Heart Circ Physiol,* **286,** H230-9.

Doods, H., Hallermayer, G., Wu, D., Entzeroth, M., Rudolf, K., Engel, W. & Eberlein, W. 2000. Pharmacological profile of BIBN4096BS, the first selective small molecule CGRP antagonist. *Br J Pharmacol,* **129,** 420-3.

Dorn, G. W. & Becker, M. W. 1993. Thromboxane A2 stimulated signal transduction in vascular smooth muscle. *Journal of Pharmacology and Experimental Therapeutics,* **265,** 447-456.

Dwivedi, C., Muller, L. A., Goetz-Parten, D. E., Kasperson, K. & Mistry, V. V. 2003. Chemopreventive effects of dietary mustard oil on colon tumor development. *Cancer Lett,* **196,** 29-34.

Earley, S. 2011. Endothelium-dependent cerebral artery dilation mediated by transient receptor potential and Ca(2+)-activated K(+) channels. *J Cardiovasc Pharmacol,* **57,** 148-53.

Earley, S., Gonzales, A. L. & Crnich, R. 2009. Endothelium-Dependent Cerebral Artery Dilation Mediated by TRPA1 and Ca2+-Activated K+ Channels. *Circ Res,* **104,** 987-994.

Earley, S., Gonzales, A. L. & Garcia, Z. I. 2010. A Dietary Agonist of TRPV3 Elicits Endothelium-Dependent Vasodilation. *Molecular Pharmacology*.

Edvinsson, L. & Goadsby, P. 1994. Neuropeptides in Migraine and Cluster Headache. *Cephalalgia,* **14,** 320-327.

Eid, S. R., Crown, E.D., Moore, E.L., Liang, H.A., Choong, K.C., Dima, S., Henze, D.A., Kane, S.A., Urban, M.O. 2008 HC-030031, a TRPA1 selective antagonist, attenuates inflammatory- and neuropathy-induced mechanical hypersensitivity. *Mol Pain.,* **27,** 48.

Eisele, J., Schaefer, I.-M., Randel Nyengaard, J., Post, H., Liebetanz, D., Brüel, A. & Mühlfeld, C. 2008. Effect of voluntary exercise on number and volume of cardiomyocytes and their mitochondria in the mouse left ventricle. *Basic Research in Cardiology,* **103,** 12-21.

El-Bassossy, H. M., Fahmy, A. & Badawy, D. 2011. Cinnamaldehyde protects from the hypertension associated with diabetes. *Food and Chemical Toxicology,* **In Press, Corrected Proof**.

El Karim, I. A., Linden, G. J., Curtis, T. M., About, I., McGahon, M. K., Irwin, C. R., Killough, S. A. & Lundy, F. T. 2011. Human Dental Pulp Fibroblasts Express the "Cold-sensing" Transient Receptor Potential Channels TRPA1 and TRPM8. *Journal of Endodontics,* **37,** 473-478.

Everaerts, W., Gees, M., Alpizar, Y. A., Farre, R., Leten, C., Apetrei, A., Dewachter, I., van Leuven, F., Vennekens, R., De Ridder, D., Nilius, B., Voets, T. & Talavera, K. 2011. The Capsaicin Receptor TRPV1 Is a Crucial Mediator of the Noxious Effects of Mustard Oil. *Current Biology,* **21,** 316-321.

Fäldt, J., Wernstedt, I., Fitzgerald, S. M., Wallenius, K., Bergström, G. & Jansson, J.-O. 2004. Reduced Exercise Endurance in Interleukin-6-Deficient Mice. *Endocrinology,* **145,** 2680-2686.

Febbraio, M. A. & Pedersen, B. K. 2002. Muscle-derived interleukin-6: mechanisms for activation and possible biological roles. *The FASEB Journal,* **16,** 1335-1347.

Feng, M., Whitesall, S., Zhang, Y., Beibel, M., Alecy, L. D. & DiPetrillo, K. 2008. Validation of Volume-Pressure Recording Tail-Cuff Blood Pressure Measurements. *Am J Hypertens,* **21,** 1288-1291.

Fernandes, E. S., Russell, F. A., Spina, D., McDougall, J. J., Graepel, R., Gentry, C., Staniland, A. A., Mountford, D. M., Keeble, J. E., Malcangio, M., Bevan, S. & Brain, S. D. 2011. A distinct role for transient receptor potential ankyrin 1, in addition to transient receptor potential vanilloid 1, in tumor necrosis factor alpha-induced inflammatory hyperalgesia and Freund's complete adjuvant-induced monarthritis. *Arthritis Rheum,* **63,** 819-29.

Fidone S.J., Sato A.A., 1969, study of chemoreceptor and baroreceptor A and C-fibres in the cat carotid nerve. *J Physiol***. 3**, 527-48.

Fisman, E. Z. & Tenenbaum, A. 2010. The ubiquitous interleukin-6: a time for reappraisal. *Cardiovasc Diabetol,* **9,** 62.

Fountain, S. J., Cheong, A., Flemming, R., Mair, L., Sivaprasadarao, A. & Beech, D. J. 2004. Functional up-regulation of KCNA gene family expression in murine mesenteric resistance artery smooth muscle. *J Physiol,* **556,** 29-42.

Franco-Cereceda, A., Gennari, C., Nami, R., Agnusdei, D., Pernow, J., Lundberg, J. & Fischer, J. 1987. Cardiovascular effects of calcitonin gene-related peptides I and II in man. *Circulation Research,* **60,** 393-397.

Franco-Cereceda, A. & Liska, J. 2000. Potential of Calcitonin Gene-Related Peptide in Coronary Heart Disease. *Pharmacology,* **60,** 1-8.

Fujimori, A., Saito, A., Kimura, S. & Goto, K. 1990. Release of calcitonin gene-related peptide (CGRP) from capsaicin-sensitive vasodilator nerves in the rat mesenteric artery. *Neurosci Lett,* **112,** 173-8.

Fujita, F., Uchida, K., Moriyama, T., Shima, A., Shibasaki, K., Inada, H., Sokabe, T., Tominaga, M. 2008 Intracellular alkalization causes pain sensation through activation of TRPA1 in mice. *J Clin Invest.,* **118,** 4049-57.

Fukai, T. & Ushio-Fukai, M. 2011. Superoxide Dismutases: Role in Redox Signaling, Vascular Function, and Diseases. *Antioxid Redox Signal,* **6,** 6.

Furchgott, R. F. & Jothianandan, D. 1991. Endothelium-dependent and -independent vasodilation involving cyclic GMP: relaxation induced by nitric oxide, carbon monoxide and light. *Blood Vessels,* **28,** 52-61.

Fuss, J. & Gass, P. 2010. Endocannabinoids and voluntary activity in mice: Runner's high and long-term consequences in emotional behaviors. *Experimental Neurology,* **224,** 103-105.

Gangula, P., Zhao, H., Supowit, S., Wimalawansa, S., Dipette, D., Westlund, K., Gagel, R. & Yallampalli, C. 2000. Increased Blood Pressure in a-Calcitonin Gene–Related Peptide/Calcitonin Gene knockout mice. *Hypertension,* **35,** 470-475.

Garland C.J., Yarova P.L., Jiménez-Altayó F., Dora K.A., 2011, Vascular hyperpolarization to β-adrenoceptor agonists evokes spreading dilatation in rat isolated mesenteric arteries. *Br J Pharmacol.* **164**, 913-21.

Garland, T., Schutz, H., Chappell, M. A., Keeney, B. K., Meek, T. H., Copes, L. E., Acosta, W., Drenowatz, C., Maciel, R. C., van Dijk, G., Kotz, C. M. & Eisenmann, J. C. 2011. The biological control of voluntary exercise, spontaneous physical activity and daily energy expenditure in relation to obesity: human and rodent perspectives. *Journal of Experimental Biology,* **214,** 206-229.

Gavras, I. & Gavras, H. 2002. Angiotensin II as a cardiovascular risk factor. *J Hum Hypertens,* **16 Suppl 2,** S2-6.

Gentsch, C., Lichtsteiner, M. & Feer, H. 1981. Locomotor activity, defecation score and corticosterone levels during an openfield exposure: A comparison among individually and group-housed rats, and genetically selected rat lines. *Physiology & Behavior,* **27,** 183-186.

Gomes, R. N., Castro-Faria-Neto, H. C., Bozza, P. T., Soares, M. B., Shoemaker, C. B., David, J. R. & Bozza, M. T. 2005. Calcitonin gene-related peptide inhibits local acute inflammation and protects mice against lethal endotoxemia. *Shock,* **24,** 590-4.

Gongora, M. C., Qin, Z., Laude, K., Kim, H. W., McCann, L., Folz, J. R., Dikalov, S., Fukai, T. & Harrison, D. G. 2006. Role of extracellular superoxide dismutase in hypertension. *Hypertension,* **48,** 473-81.

Gopalan, C., Krishnamurthi, D., Shenolikar, I. S. & Krishnamachari, K. A. 1974. Myocardial changes in monkeys fed mustard oil. *Nutr Metab,* **16,** 352-65.

Grace, M. S. & Belvisi, M. G. 2011. TRPA1 receptors in cough. *Pulm Pharmacol Ther,* **24,** 286-8.

Graepel, R., Fernandes, E. S., Aubdool, A. A., Andersson, D. A., Bevan, S. & Brain, S. D. 2011. 4-Oxo-2-nonenal (4-ONE): Evidence of Transient Receptor Potential Ankyrin 1-Dependent and -Independent Nociceptive and Vasoactive Responses *In vivo*. *Journal of Pharmacology and Experimental Therapeutics,* **337,** 117-124.

Grant, A. D., Pinter, E., Salmon, A.-M. L. & Brain, S. D. 2005. An examination of neurogenic mechanisms involved in mustard oil-induced inflammation in the mouse. *European Journal of Pharmacology,* **507,** 273-280.

Grant, A. D., Tam, C. W., Lazar, Z., Shih, M. K. & Brain, S. D. 2004. The calcitonin gene-related peptide (CGRP) receptor antagonist BIBN4096BS blocks CGRP and adrenomedullin vasoactive responses in the microvasculature. *Br J Pharmacol,* **142,** 1091-8.

Gratzke, C., Streng, T., Waldkirch, E., Sigl, K., Stief, C., Andersson, K.-E. & Hedlund, P. 2009. Transient Receptor Potential A1 (TRPA1) Activity in the Human Urethra--Evidence for a Functional Role for TRPA1 in the Outflow Region. *European Urology,* **55,** 696-704.

Grisk O., Rettig R.. 2004, Interactions between the sympathetic nervous system and the kidneys in arterial hypertension. *Cardiovasc Res.* **2**, 238-46.

Gunthorpe, M. J. & Szallasi, A. 2008. Peripheral TRPV1 receptors as targets for drug development: new molecules and mechanisms. *Curr Pharm Des,* **14,** 32-41.

Guyenet P.G., 2006, The sympathetic control of blood pressure. *Nat Rev Neurosci*. **7**, 335-46.

Harada, M., Hirayama, Y. & Yamazaki, R. 1982. Pharmacological studies on Chinese cinnamon. V. Catecholamine releasing effect of cinnamaldehyde in dogs. *J Pharmacobiodyn,* **5,** 539-46.

Harada, M. & Ozaki, Y. 1972. Pharmacological studies on Chinese cinnamon. I. Central effects of cinnamaldehyde. *Yakugaku Zasshi,* **92,** 135-40.

Harada, M. & Saito, A. 1978. Pharmacological studies on Chinese cinnamon IV. Effect of cinnamaldehyde on the isolated heart of guniea pigs and its catecholamine releasing effect from the adrenal gland of dogs. . *Journal of pharmacobio-dynamics,* **1,** 89-97.

Harada, M., Yano, S., Hirayama, Y. & Yamazaki, R. 1975. Pharmacological studies on Chinese cinammon. II. Effects of

cinnamaldehyde on the cardiovascular and digestive systems. *Chem Pharm Bull (Tokyo),* **23,** 941-7.

Hatano N., Itoh Y., Suzuki H., Muraki Y., Hayashi H., Onozaki K., Wood I.C., Beech D.J., Muraki K., 2012, HIF1α switches on TRPA1 gene expression via a hypoxia response element-like motif to modulate cytokine release. *J Biol Chem.* Jul 26. [Epub ahead of print]

Haugen, E., Scharin Täng, M., Isic, A., Andersson, B. & Fu, M. 2008. TNF[alpha] antagonist upregulates interleukin-6 in rats with hypertensive heart failure. *International Journal of Cardiology,* **130,** 64-68.

Hay, D. L. & Poyner, D. 2005. The preclinical pharmacology of BIBN4096BS, a CGRP antagonist. *Cardiovasc Drug Rev,* **23,** 31-42.

Hayashi, K. & Naiki, T. 2009. Adaptation and remodeling of vascular wall; biomechanical response to hypertension. *J Mech Behav Biomed Mater,* **2,** 3-19.

Hazari, M. S., Haykal-Coates, N., Winsett, D. W., Krantz, Q. T., King, C., Costa, D. L. & Farraj, A. K. 2011. TRPA1 and sympathetic activation contribute to increased risk of triggered cardiac arrhythmias in hypertensive rats exposed to diesel exhaust. *Environ Health Perspect,* **119,** 951-7.

Hikiji, A., Yamamoto, H., Sunakawa, M. & Suda, H. 2000. Increased blood flow and nerve firing in the cat canine tooth in response to stimulation of the second premolar pulp. *Archives of Oral Biology,* **45,** 53-61.

Hilgers, R. H. P., Todd, J. & Webb, R. C. 2006. Regional heterogeneity in acetylcholine-induced relaxation in rat vascular bed: role of calcium-activated K+ channels. *American Journal of Physiology - Heart and Circulatory Physiology,* **291,** H216-H222.

Hill, K. & Schaefer, M. 2009. Ultraviolet light and photosensitising agents activate TRPA1 via generation of oxidative stress. *Cell Calcium,* **45,** 155-64.

Hinman, A., Chuang, H.H., Bautista, D.M., Julius, D. 2006 TRP channel activation by reversible covalent modification. *Proc Natl Acad Sci U S A.*, **103,** 19564-8.

Hitomi, H., Kiyomoto, H., Nishiyama, A. 2007. Angiotensin II and oxidative stress. *Curr Opin Cardiol. ,* **22,** 311-5.

Hoch, M., Eberle, A. N., Peterli, R., Peters, T., Seboek, D., Keller, U., Muller, B. & Linscheid, P. 2008. LPS induces interleukin-6 and interleukin-8 but not tumor necrosis factor-alpha in human adipocytes. *Cytokine,* **41,** 29-37.

Holzer, P. 1998. Neurogenic vasodilatation and plasma leakage in the skin. *General Pharmacology: The Vascular System,* **30,** 5-11.

Huang, J., Wang, S., Luo, X., Xie, Y. & Shi, X. 2007. Cinnamaldehyde reduction of platelet aggregation and thrombosis in rodents. *Thrombosis Research,* **119,** 337-342.

Huang, J., Zhang, X. & McNaughton, P. A. 2006. Modulation of temperature-sensitive TRP channels. *Seminars in Cell & Developmental Biology,* **17,** 638-645.

Hughes J.M., Bund S.J., 2002, Arterial myogenic properties of the spontaneously hypertensive rat. *Exp Physiol*. **5**, 527-34.
Huxley, V. H. 2007. Sex and the cardiovascular system: the intriguing tale of how women and men regulate cardiovascular function differently. *Advances in Physiology Education,* **31,** 17-22.
Iggo, A., Steedman, W. M. & Fleetwood-Walker, S. 1985. Spinal processing: anatomy and physiology of spinal nociceptive mechanisms. *Philos Trans R Soc Lond B Biol Sci,* **308,** 235-52.
Immke, D. C., Gavva, N.R. 2006. The TRPV1 receptor and nociception. *Seminars in Cell & Developmental Biology,* **17,** 582-591.
Inoue, H., Asaka, T., Nagata, N. & Koshihara, Y. 1997. Mechanism of mustard oil-induced skin inflammation in mice. *European Journal of Pharmacology,* **333,** 231-240.
Inoue, R., Jensen, L. J., Shi, J., Morita, H., Nishida, M., Honda, A. & Ito, Y. 2006. Transient receptor potential channels in cardiovascular function and disease. *Circulation Research,* **99,** 119-131.
Inoue, R., Jian, Z. & Kawarabayashi, Y. 2009. Mechanosensitive TRP channels in cardiovascular pathophysiology. *Pharmacology & Therapeutics*, **123,** 371-85.
Iwasaki, Y., Tanabe, M., Kayama, Y., Abe, M., Kashio, M., Koizumi, K., Okumura, Y., Morimitsu, Y., Tominaga, M., Ozawa, Y. & Watanabe, T. 2009. Miogadial and miogatrial with [alpha],[beta]-unsaturated 1,4-dialdehyde moieties—Novel and potent TRPA1 agonists. *Life Sciences,* **85,** 60-9.
Iwasaki, Y., Tanabe, M., Kobata, K. & Watanabe, T. 2008. TRPA1 Agonists-Allyl Isothiocyanate and Cinnamaldehyde-Induce Adrenaline Secretion. *Bioscience, Biotechnology, and Biochemistry*, **72,** 2608-2614.
Jackson, S. M., Parhami, F., Xi, X.-P., Berliner, J. A., Hsueh, W. A., Law, R. E. & Demer, L. L. 1999. Peroxisome Proliferator–Activated Receptor Activators Target Human Endothelial Cells to Inhibit Leukocyte–Endothelial Cell Interaction. *Arterioscler Thromb Vasc Biol*, **19,** 2094-2104.
Jain, A. K., Vargas, R., Gotzkowsky, S. & McMahon, F. G. 1993. Can garlic reduce levels of serum lipids? a controlled clinical study. *The American Journal of Medicine*, **94,** 632-635.
Jaquemar, D., Schenker, T. & Trueb, B. 1999. An Ankyrin-like Protein with Transmembrane Domains Is Specifically Lost after Oncogenic Transformation of Human Fibroblasts. *J. Biol. Chem.*, **274,** 7325-7333.
Ji, G., Zhou, S. & Carlton, S. M. 2008. Intact A[delta]-fibers up-regulate transient receptor potential A1 and contribute to cold hypersensitivity in neuropathic rats. *Neuroscience,* **154,** 1054-1066.
Johar, S., Cave, A. C., Narayanapanicker, A., Grieve, D. J. & Shah, A. M. 2006. Aldosterone mediates angiotensin II-induced interstitial cardiac fibrosis via a Nox2-containing NADPH oxidase. *FASEB J,* **20,** 1546-8.
Johns D.G., Behm D.J., Walker D.J., Ao Z., Shapland E.M., Daniels D.A., Riddick M., Dowell S., Staton P.C., Green P., Shabon U., Bao W., Aiyar N., Yue T.L., Brown A.J., Morrison A.D., Douglas S.A.,

2007, The novel endocannabinoid receptor GPR55 is activated by atypical cannabinoids but does not mediate their vasodilator effects., *Br J Pharmacol*. **152**, 825-31.

Johnson, C. D., Melanaphy, D., Purse, A., Stokesberry, S. A., Dickson, P. & Zholos, A. V. 2009. Transient receptor potential melastatin 8 channel involvement in the regulation of vascular tone. *American Journal of Physiology - Heart and Circulatory Physiology,* **296,** H1868-H1877.

Johnson, R. A., Lavesa, M., Askari, B., Abraham, N. G. & Nasjletti, A. 1995. A heme oxygenase product, presumably carbon monoxide, mediates a vasodepressor function in rats. *Hypertension,* **25,** 166-9.

Jones R.O., Matsuda Y., Koyama S., Uematsu H., Fujita T., Shibamoto T., 1990, Reflex responses on blood pressure and renal nerve activity to local intra-arterial injection of capsaicin in anesthetized dogs. *Jpn J Physiol*. **40**, 491-502.

Jordan, L. M., Liu, J., Hedlund, P. B., Akay, T. & Pearson, K. G. 2008. Descending command systems for the initiation of locomotion in mammals. *Brain Research Reviews,* **57,** 183-191.

Jordt, S. E., Bautista, D.M., Chuang, H.H., McKemy, D.D., Zygmunt, P.M., Högestätt, E.D., Meng, I.D., Julius, D. 2004 Mustard oils and cannabinoids excite sensory nerve fibres through the TRP channel ANKTM1. *427,* **6971**.

Jorens, P. G., Richman-Eisenstat, J. B., Housset, B. P., Graf, P. D., Ueki, I. F., Olesch, J. & Nadel, J. A. 1992. Interleukin-8 induces neutrophil accumulation but not protease secretion in the canine trachea. *American Journal of Physiology - Lung Cellular and Molecular Physiology,* **263,** L708-L713.

Jovanovic, D. V., Di Battista, J. A., Martel-Pelletier, J., Jolicoeur, F. C., He, Y., Zhang, M., Mineau, F. & Pelletier, J.-P. 1998. IL-17 Stimulates the Production and Expression of Proinflammatory Cytokines, IL-ß and TNF-α, by Human Macrophages. *The Journal of Immunology,* **160,** 3513-3521.

Kakkar, R. & Lee, R. T. 2010. Intramyocardial Fibroblast Myocyte Communication. *Circulation Research,* **106,** 47-57.

Kamimura, E., Ueno, Y., Tanaka, S., Sawa, H., Yoshioka, M., Ueno, K. I., Inoue, T., Li, X., Koyama, T., Ishikawa, R. & Nagashima, K. 2001. New rat model for attention deficit hyperactive disorder (ADHD). *Comp Med,* **51,** 245-51.

Kamo, H., Honda, K., Kitagawa, J., Tsuboi, Y., Kondo, M., Taira, M., Yamashita, A., Katsuyama, N., Masuda, Y., Kato, T. & Iwata, K. 2008. Topical capsaicin application causes cold hypersensitivity in awake monkeys. *Journal of Oral Science,* **50,** 175-179.

Kannan M.S., Seip A.E., 1986, Neurogenic dilatation and constriction of rat superior mesenteric artery in vitro: mechanisms and mediators. *Can J Physiol Pharmacol*. **64**, 729-36.

Karashima, Y., Prenen, J., Talavera, K., Janssens, A., Voets, T. & Nilius, B. 2010. Agonist-Induced Changes in Ca2+ Permeation through the Nociceptor Cation Channel TRPA1. *Biophysical Journal,* **98,** 773-783.

Kardon M.B., Peterson D.F., Bishop V.S., 1975, Reflex heart rate control via specific aortic nerve afferents in the rabbit. *Circ Res*. **37**, 41-7

Kark, T., Bagi, Z., Lizanecz, E., Pasztor, E. T., Erdei, N., Czikora, A., Papp, Z., Edes, I., Porszasz, R. & Toth, A. 2008. Tissue-Specific Regulation of Microvascular Diameter: Opposite Functional Roles of Neuronal and Smooth Muscle Located Vanilloid Receptor-1. *Mol Pharmacol,* **73,** 1405-1412.

Katsouni, E., Sakkas, P., Zarros, A., Skandali, N. & Liapi, C. 2009. The involvement of substance P in the induction of aggressive behavior. *Peptides,* **30,** 1586-91.

Kawasaki, H., Takenaga, M., Araki, H., Futagami, K. & Gomita, Y. 1998. Angiotensin Inhibits Neurotransmission of Calcitonin Gene-Related Peptide-Containing Vasodilator Nerves in Mesenteric Artery of Spontaneously Hypertensive Rats. *Journal of Pharmacology and Experimental Therapeutics,* **284,** 508-515.

Keeble, J., Russell, F., Curtis, B., Starr, A., Pinter, E. & Brain, S. D. 2005. Involvement of transient receptor potential vanilloid 1 in the vascular and hyperalgesic components of joint inflammation. *Arthritis & Rheumatism,* **52,** 3248-3256.

Keeble, J. E., Bodkin, J. V., Liang, L., Wodarski, R., Davies, M., Fernandes, E. S., Coelho, C. d. F., Russell, F., Graepel, R., Muscara, M. N., Malcangio, M. & Brain, S. D. 2009. Hydrogen peroxide is a novel mediator of inflammatory hyperalgesia, acting via transient receptor potential vanilloid 1-dependent and independent mechanisms. *Pain,* **141,** 135-142.

Kerstein, P. C., del Camino, D., Moran, M.M., Stucky, C.L. 2009 Pharmacological blockade of TRPA1 inhibits mechanical firing in nociceptors. *Mol Pain.*, **21,** 19.

Kemp B.K., McPherson G.A., 1998 , Interspecies differences in thromboxane A2 receptors are distinguished by glibenclamide. *Eur J Pharmacol*. **354**, 173-8.

Kim, C. H., Zou, Y., Kim, D. H., Kim, N. D., Yu, B. P. & Chung, H. Y. 2006. Proteomic Analysis of Nitrated and 4-Hydroxy-2-Nonenal-Modified Serum Proteins During Aging. *J Gerontol A Biol Sci Med Sci,* **61,** 332-338.

Kobayashi, K., Fukuoka, T., Obata, K., Yamanaka, H., Dai, Y., Tokunaga, A. & Noguchi, K. 2005. Distinct expression of TRPM8, TRPA1, and TRPV1 mRNAs in rat primary afferent neurons with adelta/c-fibers and colocalization with trk receptors. *The Journal of Comparative Neurology,* **493,** 596-606.

Koizumi, K., Iwasaki, Y., Narukawa, M., Iitsuka, Y., Fukao, T., Seki, T., Ariga, T. & Watanabe, T. 2009. Diallyl sulfides in garlic activate both TRPA1 and TRPV1. *Biochemical and Biophysical Research Communications,* **382,** 545-548.

Kojima, R., Doihara, H., Nozawa, K., Kawabata-Shoda, E., Yokoyama, T. & Ito, H. 2009. Characterization of two models of drug-induced constipation in mice and evaluation of mustard oil in these models. *Pharmacology,* **84,** 227-33.

Kolattukudy, P. E., Quach, T., Bergese, S., Breckenridge, S., Hensley, J., Altschuld, R., Gordillo, G., Klenotic, S., Orosz, C. & Parker-

Thornburg, J. 1998. Myocarditis induced by targeted expression of the MCP-1 gene in murine cardiac muscle. *Am J Pathol,* **152,** 101-11.

Kondo, M., Oya-Ito, T., Kumagai, T., Osawa, T. & Uchida, K. 2001. Cyclopentenone Prostaglandins as Potential Inducers of Intracellular Oxidative Stress. *J. Biol. Chem.,* **276,** 12076-12083.

Kosugi, M., Nakatsuka, T., Fujita, T., Kuroda, Y. & Kumamoto, E. 2007. Activation of TRPA1 Channel Facilitates Excitatory Synaptic Transmission in Substantia Gelatinosa Neurons of the Adult Rat Spinal Cord. *J. Neurosci.,* **27,** 4443-4451.

Koteja, P., Garland, T., Jr., Sax, J. K., Swallow, J. G. & Carter, P. A. 1999. Behaviour of house mice artificially selected for high levels of voluntary wheel running. *Anim Behav,* **58,** 1307-1318.

Kramer, K., Kinter, L., Brockway, B. P., Voss, H. P., Remie, R. & Van Zutphen, B. L. 2001. The use of radiotelemetry in small laboratory animals: recent advances. *Contemp Top Lab Anim Sci,* **40,** 8-16.

Kramer, K. & Kinter, L. B. 2003. Evaluation and applications of radiotelemetry in small laboratory animals. *Physiological Genomics,* **13,** 197-205.

Kramer, K., Voss, H.-P., Grimbergen, J. A., Mills, P. A., Huetteman, D., Zwiers, L. & Brockway, B. 2000. Telemetric monitoring of blood pressure in freely moving mice: a preliminary study. *Lab Anim,* **34,** 272-280.

Krege, J. H., Hodgin, J. B., Hagaman, J. R. & Smithies, O. 1995. A Noninvasive Computerized Tail-Cuff System for Measuring Blood Pressure in Mice. *Hypertension,* **25,** 1111-1115.

Kremeyer, B., Lopera, F., Cox, J. J., Momin, A., Rugiero, F., Marsh, S., Woods, C. G., Jones, N. G., Paterson, K. J., Fricker, F. R., Villegas, A., Acosta, N., Pineda-Trujillo, N. G., Ramírez, J. D., Zea, J., Burley, M.-W., *et al.* 2010. A Gain-of-Function Mutation in TRPA1 Causes Familial Episodic Pain Syndrome. *Neuron,* **66,** 671-680.

Krueger D., Foerster M., Mueller K., Zeller F., Slotta-Huspenina J., Donovan J., Grundy D., Schemann M., 2012, Signaling mechanisms involved in the intestinal pro-secretory actions of hydrogen sulfide. *Neurogastroenterol Motil.* **22**, 1224-31, e319-20.

Krumins, S. A. & Broomfield, C. A. 1992. Evidence of NK1 and NK2 tachykinin receptors and their involvement in histamine release in a murine mast cell line. *Neuropeptides,* **21,** 65-72.

Ku, D. D., Abdel-Razek, T. T., Dai, J., Kim-Park, S., Fallon, M. B. & Abrams, G. A. 2002. Garlic And Its Active Metabolite Allicin Produce Endothelium- And Nitric Oxide-Dependent Relaxation In Rat Pulmonary Arteries. *Clinical and Experimental Pharmacology and Physiology,* **29,** 84-91.

Kunkler, P. E., Ballard, C. J., Oxford, G. S. & Hurley, J. H. 2011. TRPA1 receptors mediate environmental irritant-induced meningeal vasodilatation. *Pain,* **152,** 38-44.

Kwak, J. Y., Takeshige, K., Cheung, B. S. & Minakami, S. 1991. Bilirubin inhibits the activation of superoxide-producing NADPH oxidase in a neutrophil cell-free system. *Biochim Biophys Acta,* **1076,** 369-73.

Kwan, K. Y., Allchorne, A. J., Vollrath, M. A., Christensen, A. P., Zhang, D. S., Woolf, C. J. & Corey, D. P. 2006. TRPA1 contributes to cold, mechanical, and chemical nociception but is not essential for hair-cell transduction. *Neuron,* **50,** 277-289.

Kwan, K. Y. & Corey, D. P. 2009. Burning cold: involvement of TRPA1 in noxious cold sensation. *J Gen Physiol,* **133,** 251-6.

Kym, P. R., Kort, M. E. & Hutchins, C. W. 2009. Analgesic potential of TRPV1 antagonists. *Biochemical Pharmacology,* **78,** 211-216.

Lahoutte, T. 2007. Monitoring left ventricular function in small animals. *Journal of Nuclear Cardiology,* **14,** 371-379.

Lassegue, B. & Clempus, R. E. 2003. Vascular NAD(P)H oxidases: specific features, expression, and regulation. *Am J Physiol Regul Integr Comp Physiol,* **285,** R277-97.

Lassègue, B. & Griendling, K. K. 2010. NADPH Oxidases: Functions and Pathologies in the Vasculature. *Arteriosclerosis, Thrombosis, and Vascular Biology,* **30,** 653-661.

Lassègue, B., Sorescu, D., Szöcs, K., Yin, Q., Akers, M., Zhang, Y., Grant, S. L., Lambeth, J. D. & Griendling, K. K. 2001. Novel gp91phox Homologues in Vascular Smooth Muscle Cells : nox1 Mediates Angiotensin II–Induced Superoxide Formation and Redox-Sensitive Signaling Pathways. *Circulation Research,* **88,** 888-894.

Leinwand, L. A. 2003. Sex is a potent modifier of the cardiovascular system. *The Journal of Clinical Investigation,* **112,** 302-307.

Li, J. & Wang, D. H. 2005. Development of angiotensin II-induced hypertension: role of CGRP and its receptor. *J Hypertens,* **23,** 113-8.

Li, J., Zhao, H., Supowit, S. C., DiPette, D. J. & Wang, D. H. 2004. Activation of the renin-angiotensin system in alpha-calcitonin gene-related peptide/calcitonin gene knockout mice. *J Hypertens,* **22,** 1345-9.

Li, J. P. & Wang, D. H. 2008. Increased GFR and renal excretory function by activation of TRPV1 in the isolated perfused kidney. *Pharmacological Research,* **57,** 239-246.

Li, Y.-J. & Peng, J. 2002. The cardioprotection of calcitonin gene-related peptide-mediated preconditioning. *European Journal of Pharmacology,* **442,** 173-177.

Liang, L., Tam, C. W., Pozsgai, G., Siow, R., Clark, N., Keeble, J., Husmann, K., Born, W., Fischer, J. A., Poston, R., Shah, A. & Brain, S. D. 2009. Protection of angiotensin II-induced vascular hypertrophy in vascular smooth muscle-targeted receptor activity-modifying protein 2 transgenic mice. *Hypertension,* **54,** 1254-61.

Liao, B.-C., Hsieh, C.-W., Liu, Y.-C., Tzeng, T.-T., Sun, Y.-W. & Wung, B.-S. 2008. Cinnamaldehyde inhibits the tumor necrosis factor-[alpha]-induced expression of cell adhesion molecules in endothelial cells by suppressing NF-[kappa]B activation: Effects upon I[kappa]B and Nrf2. *Toxicology and Applied Pharmacology,* **229,** 161-171.

Lippe, I. T., Stabentheiner, A. & Holzer, P. 1993. Participation of nitric oxide in the mustard oil-induced neurogenic i inflammation of the rat paw skin. *European Journal of Pharmacology,* **232,** 113-120.

Liu, W., Liang, X., Gong, J., Yang, Z., Zhang, Y. H., Zhang, J. X. & Rao, Y. 2011. Social regulation of aggression by pheromonal activation of Or65a olfactory neurons in Drosophila. *Nat Neurosci,* **14,** 896-902.

Liu, Y., Berthier-Schaad, Y., Fallin, M. D., Fink, N. E., Tracy, R. P., Klag, M. J., Smith, M. W. & Coresh, J. 2006. IL-6 haplotypes, inflammation, and risk for cardiovascular disease in a multiethnic dialysis cohort. *J Am Soc Nephrol,* **17,** 863-70.

Loppnow, H. & Libby, P. 1990. Proliferating or interleukin 1-activated human vascular smooth muscle cells secrete copious interleukin 6. *The Journal of Clinical Investigation,* **85,** 731-738.

Lotti, T., Hautmann, G. & Panconesi, E. 1995. Neuropeptides in skin. *Journal of the American Academy of Dermatology,* **33,** 482-496.

Louis, S. M., Jamieson, A., Russell, N. J. & Dockray, G. J. 1989a. The role of substance P and calcitonin gene-related peptide in neurogenic plasma extravasation and vasodilatation in the rat. *Neuroscience,* **32,** 581-6.

Louis, S. M., Johnstone, D., Russell, N. J., Jamieson, A. & Dockray, G. J. 1989b. Antibodies to calcitonin-gene related peptide reduce inflammation induced by topical mustard oil but not that due to carrageenin in the rat. *Neurosci Lett,* **102,** 257-60.

Lu, J. T., Son, Y.-J., Lee, J., Jetton, T. L., Shiota, M., Moscoso, L., Niswender, K. D., Loewy, A. D., Magnuson, M. A., Sanes, J. R. & Emeson, R. B. 1999. Mice Lacking [alpha]-Calcitonin Gene-Related Peptide Exhibit Normal Cardiovascular Regulation and Neuromuscular Development. *Molecular and Cellular Neuroscience,* **14,** 99-120.

Macpherson, L., Dubin, A., Evans, M., Marr, F., Schultz, P., Cravatt, B. & Patapoutian, A. 2007a. Noxious compounds activate TRPA1 ion channels through covalent modification of cysteines. *Nature,* **445,** 541 - 545.

Macpherson, L. J., Hwang, S.W., Miyamoto, T., Dubin, A.E., Patapoutian, A., Story, G.M. 2006 More than cool: promiscuous relationships of menthol and other sensory compounds. *Mol Cell Neurosci.,* **32,** 335-43.

Macpherson, L. J., Xiao, B., Kwan, K. Y., Petrus, M. J., Dubin, A. E., Hwang, S., Cravatt, B., Corey, D. P. & Patapoutian, A. 2007b. An Ion Channel Essential for Sensing Chemical Damage. *J. Neurosci.,* **27,** 11412-11415.

Magara, F., Ricceri, L., Wolfer, D. P. & Lipp, H.-P. 2000. The acallosal mouse strain I/LnJ: a putative model of ADHD? *Neuroscience & Biobehavioral Reviews,* **24,** 45-50.

Maggi, C. A. 1995. The mammalian tachykinin receptors. *General Pharmacology: The Vascular System,* **26,** 911-944.

Mahoney, L. T. & Brody, M. J. 1978. A method for indirect recording of arterial pressure in the conscious cat. *Journal of Pharmacological Methods,* **1,** 61-66.

Manhiani, M. M., Quigley, J. E., Socha, M. J., Motamed, K. & Imig, J. D. 2007. IL6 suppression provides renal protection independent of

blood pressure in a murine model of salt-sensitive hypertension. *Kidney Blood Press Res,* **30,** 195-202.
Manzini S., 1992, Bronchodilatation by tachykinins and capsaicin in the mouse main bronchus. *Br J Pharmacol.* **105**, 968–972
Marmigère F, Ernfors P. 2007. Specification and connectivity of neuronal subtypes in the sensory lineage. *Nat Rev Neurosci.* **2**, 114-27.
Markowitz, K. 2010. Pretty painful: why does tooth bleaching hurt? *Med Hypotheses,* **74,** 835-40.
Materazzi, S., Nassini, R., Andrè, E., Campi, B., Amadesi, S., Trevisani, M., Bunnett, N.W., Patacchini, R., Geppetti, P.. 2008 Cox-dependent fatty acid metabolites cause pain through activation of the irritant receptor TRPA1. *Proc Natl Acad Sci U S A.* , **105,** 12045-50.
Matoba, T. & Shimokawa, H. 2003. Hydrogen peroxide is an endothelium-derived hyperpolarizing factor in animals and humans. *J Pharmacol Sci,* **92,** 1-6.
Mayeux, P. R., Agrawal, K. C., Tou, J. S. H., King, B. T., Lippton, H. L., Hyman, A. L., Kadowitz, P. J. & McNamara, D. B. 1988. The pharmacological effects of allicin, a constituent of garlic oil. *Inflammation Research,* **25,** 182-190.
McEniery, C. 2009. Antihypertensive drugs and central blood pressure. *Current Hypertension Reports,* **11,** 253-259.
McEwan J.R., Benjamin N., Larkin S., Fuller R.W., Dollery C.T., MacIntyre I., 1988, Vasodilatation by calcitonin gene-related peptide and by substance P: a comparison of their effects on resistance and capacitance vessels of human forearms. *Circulation.* **77**, 1072-80.
McGaraughty, S., Chu, K., Perner, R., DiDomenico, S., Kort, M. & Kym, P. 2010. TRPA1 modulation of spontaneous and mechanically evoked firing of spinal neurons in uninjured, osteoarthritic, and inflamed rats. *Molecular Pain,* **6,** 14.
McKinley, M. J., Albiston, A. L., Allen, A. M., Mathai, M. L., May, C. N., McAllen, R. M., Oldfield, B. J., Mendelsohn, F. A. & Chai, S. Y. 2003. The brain renin-angiotensin system: location and physiological roles. *Int J Biochem Cell Biol,* **35,** 901-18.
McLatchie, L. M., Fraser, N. J., Main, M. J., Wise, A., Brown, J., Thompson, N., Solari, R., Lee, M. G. & Foord, S. M. 1998. RAMPs regulate the transport and ligand specificity of the calcitonin-receptor-like receptor. *Nature,* **393,** 333-9.
McMahon, S. B. & Wood, J. N. 2006. Increasingly Irritable and Close to Tears: TRPA1 in Inflammatory Pain. *Cell,* **124,** 1123-1125.
McNamara, C. R., Mandel-Brehm, J., Bautista, D.M., Siemens, J., Deranian, K.L., Zhao, M., Hayward, N.J., Chong, J.A., Julius, D., Moran, M.M., Fanger, C.M. 2007. TRPA1 mediates formalin-induced pain. *PNAS,* **104,** 13525-13530.
Meens, M. J. P. M. T., Fazzi, G. E., van Zandvoort, M. A. & De Mey, J. G. R. 2009. Calcitonin Gene-Related Peptide Selectively Relaxes Contractile Responses to Endothelin-1 in Rat Mesenteric Resistance Arteries. *Journal of Pharmacology and Experimental Therapeutics,* **331,** 87-95.

Mehta, P. K. & Griendling, K. K. 2007. Angiotensin II cell signaling: physiological and pathological effects in the cardiovascular system. *American Journal of Physiology - Cell Physiology,* **292,** C82-C97.

Meléndez, G. C., McLarty, J. L., Levick, S. P., Du, Y., Janicki, J. S. & Brower, G. L. 2010. Interleukin 6 Mediates Myocardial Fibrosis, Concentric Hypertrophy, and Diastolic Dysfunction in Rats. *Hypertension,* **56,** 225-231.

Meneses, A., Perez-Garcia, G., Ponce-Lopez, T., Tellez, R., Gallegos-Cari, A. & Castillo, C. 2011. Spontaneously hypertensive rat (SHR) as an animal model for ADHD: a short overview. *Rev Neurosci,* **22,** 365-71.

Menozzi-Smarrito, C., Riera, C. E., Munari, C., Le Coutre, J., Robert, F. 2009. Synthesis and Evaluation of New Alkylamides Derived from α-Hydroxysanshool, the Pungent Molecule in Szechuan Pepper. *Journal of Agricultural and Food Chemistry,* **57,** 1982-1989.

Michel, M. C. 2008. Editorial comment on: distribution and function of the hydrogen sulfide-sensitive TRPA1 ion channel in rat urinary bladder. *Eur Urol.,* **53,** 399-400.

Mills, P. A., Huetteman, D. A., Brockway, B. P., Zwiers, L. M., Gelsema, A. J. M., Schwartz, R. S. & Kramer, K. 2000. A new method for measurement of blood pressure, heart rate, and activity in the mouse by radiotelemetry. *Journal of Applied Physiology,* **88,** 1537-1544.

Miyamoto, T., Dubin, A. E., Petrus, M. J. & Patapoutian, A. 2009. TRPV1 and TRPA1 mediate peripheral nitric oxide-induced nociception in mice. *PLoS ONE,* **4,** e7596.

Miyata N., Roman R.J., 2005, Role of 20-hydroxyeicosatetraenoic acid (20-HETE) in vascular system. *J Smooth Muscle Res*. **4**, 175-93

Monassier, L., Combe, R. & Fertak, L. E. 2006. Mouse models of hypertension. *Drug Discovery Today: Disease Models,* **3,** 273-281.

Moreira T.S., Takakura A.C., Damasceno R.S., Falquetto B., Totola L.T., Sobrinho C.R., Ragioto D.T., Zolezi F.P., 2011, Central chemoreceptors and neural mechanisms of cardiorespiratory control. *Braz J Med Biol Res.* **9**, 883-9.

Morita, T. & Kourembanas, S. 1995. Endothelial cell expression of vasoconstrictors and growth factors is regulated by smooth muscle cell-derived carbon monoxide. *J Clin Invest,* **96,** 2676-82.

Morris, R., Southam, E., Braid, D. J. & Garthwaite, J. 1992. Nitric oxide may act as a messenger between dorsal root ganglion neurones and their satellite cells. *Neurosci Lett,* **137,** 29-32.

Munns, C., AlQatari, M. & Koltzenburg, M. 2007. Many cold sensitive peripheral neurons of the mouse do not express TRPM8 or TRPA1. *Cell Calcium,* **41,** 331-342.

Mutoh T., Tsubone H., Nishimura R., Sasaki N., 1997, Cardiovascular reflex mechanisms by topical instillation of capsaicin and distilled water into the larynx in anesthetized dogs. *J Vet Med Sci*. **59**, 801-6.

Nagata, K., Duggan, A., Kumar, G. & Garcia-Anoveros, J. 2005. Nociceptor and hair cell transducer properties of TRPA1, a channel for pain and hearing. *J Neurosci,* **25,** 4052 - 61.

Nakashimo, Y., Takumida, M., Fukuiri, T., Anniko, M. & Hirakawa, K. 2010. Expression of transient receptor potential channel vanilloid (TRPV) 1–4, melastin (TRPM) 5 and 8, and ankyrin (TRPA1) in the normal and methimazole-treated mouse olfactory epithelium. *Acta Otolaryngol,* **130,** 1278-86.

Namer, B., Seifert, F., Handwerker, H. & Maihofner, C. 2005. TRPA1 and TRPM8 activation in humans: effects of cinnamaldehyde and menthol. *Neuroreport,* **16,** 955 - 999.

Nassenstein, C., Kwong, K., Taylor-Clark, T., Kollarik, M., MacGlashan, D. M., Braun, A. & Undem, B. J. 2008. Expression and function of the ion channel TRPA1 in vagal afferent nerves innervating mouse lungs. *The Journal of Physiology,* **586,** 1595-1604.

Nassini, R., Gees, M., Harrison, S., De Siena, G., Materazzi, S., Moretto, N., Failli, P., Preti, D., Marchetti, N., Cavazzini, A., Mancini, F., Pedretti, P., Nilius, B., Patacchini, R. & Geppetti, P. 2011. Oxaliplatin elicits mechanical and cold allodynia in rodents via TRPA1 receptor stimulation. *Pain,* **152,** 1621-31.

Nassini R., Pedretti P., Moretto N., Fusi C., Carnini C., Facchinetti F., Viscomi A.R., Pisano A.R., Stokesberry S., Brunmark C., Svitacheva N., McGarvey L., Patacchini R., Damholt A.B., Geppetti .P, Materazzi S., 2012, Transient receptor potential ankyrin 1 channel localized to non-neuronal airway cells promotes non-neurogenic inflammation. *PLoS One.* 7, e42454

Nelson, M. R., Stepanek, J., Cevette, M., Covalciuc, M., Hurst, R. T. & Tajik, A. J. 2010. Noninvasive measurement of central vascular pressures with arterial tonometry: clinical revival of the pulse pressure waveform? *Mayo Clin Proc,* **85,** 460-72.

Nelson, M. T., Huang, Y., Brayden, J. E., Hescheler, J. & Standen, N. B. 1990. Arterial dilations in response to calcitonin gene-related peptide involve activation of K+ channels. *Nature,* **344,** 770-3.

Nelson, R. J. & Chiavegatto, S. 2001. Molecular basis of aggression. *Trends in Neurosciences,* **24,** 713-719.

Neutra, M. R., O'Malley, L. J. & Specian, R. D. 1982. Regulation of intestinal goblet cell secretion. II. A survey of potential secretagogues. *Am J Physiol Gastrointest Liver Physiol,* **242,** G380-387.

Nicoletti, P., Trevisani, M., Manconi, M., Gatti, R., De Siena, G., Zagli, G., Benemei, S., Capone, J. A., Geppetti, P. & Pini, L. A. 2008. Ethanol causes neurogenic vasodilation by TRPV1 activation and CGRP release in the trigeminovascular system of the guinea pig. *Cephalalgia,* **28,** 9-17.

Niu, J. & Kolattukudy, P. E. 2009. Role of MCP-1 in cardiovascular disease: molecular mechanisms and clinical implications. *Clin Sci (Lond),* **117,** 95-109.

Obata, K., Katsura, H., Mizushima, T., Yamanaka, H., Kobayashi, K., Dai, Y., Fukuoka, T., Tokunaga, A., Tominaga, M., Noguchi, K. 2005 TRPA1 induced in sensory neurons contributes to cold hyperalgesia after inflammation and nerve injury. *J Clin Invest.,* **115,** 2393-401.

Ohta, T., Imagawa, T. & Ito, S. 2007. Novel agonistic action of mustard oil on recombinant and endogenous porcine transient receptor potential

V1 (pTRPV1) channels. *Biochemical Pharmacology,* **73,** 1646-1656.

Okada, T., Shimizu, S., Wakamori, M., Maeda, A., Kurosaki, T., Takada, N., Imoto, K. & Mori, Y. 1998. Molecular cloning and functional characterization of a novel receptor-activated TRP Ca2+ channel from mouse brain. *J Biol Chem,* **273,** 10279-87.

Okumura, Y., Narukawa, M., Iwasaki, Y., Ishikawa, A., Matsuda, H., Yoshikawa, M. & Watanabe, T. 2010. Activation of TRPV1 and TRPA1 by Black Pepper Components. *Bioscience, Biotechnology, and Biochemistry,* **74,** 1068-1072.

Oudot, A., Vergely, C., Ecarnot-Laubriet, A. & Rochette, L. 2003. Angiotensin II activates NADPH oxidase in isolated rat hearts subjected to ischaemia-reperfusion. *Eur J Pharmacol,* **462,** 145-54.

Pacher, P., Batkai, S. & Kunos, G. 2004. Haemodynamic profile and responsiveness to anandamide of TRPV1 receptor knock-out mice. *Journal of Physiology-London,* **558,** 647-657.

Palframan, R. T., Costa, S. K., Wilsoncroft, P., Antunes, E., de Nucci, G. & Brain, S. D. 1996 The effect of a tachykinin NK1 receptor antagonist, SR140333, on oedema formation induced in rat skin by venom from the Phoneutria nigriventer spider. *Br J Pharmacol.*, **118,** 295-8.

Parada, C. A., Tambeli, C.H., Cunha, F.Q., Ferreira, S.H. 2001 The major role of peripheral release of histamine and 5-hydroxytryptamine in formalin-induced nociception. *Neuroscience.,* **102,** 937-44.

Paravicini, T. M. & Touyz, R. M. 2008. NADPH Oxidases, Reactive Oxygen Species, and Hypertension. *Diabetes Care,* **31,** S170-S180.

Patil, M. J., Jeske, N. A. & Akopian, A. N. 2010. Transient receptor potential V1 regulates activation and modulation of transient receptor potential A1 by Ca2+. *Neuroscience,* **171,** 1109-1119.

Pecze, L., Pelsoczi, P., Kecskés, M., Winter, Z., Papp, A., Kaszás, K., Letoha, T., Vizler, C., Oláh, Z. 2009. Resiniferatoxin mediated ablation of TRPV1+ neurons removes TRPA1 as well. *Can J Neurol Sci. ,* **36,** 234-41.

Penuelas, A., Tashima, K., Tsuchiya, S., Matsumoto, K., Nakamura, T., Horie, S. & Yano, S. 2007. Contractile effect of TRPA1 receptor agonists in the isolated mouse intestine. *European Journal of Pharmacology,* **576,** 143-150.

Peterlin, Z., Chesler, A. & Firestein, S. 2007. A Painful Trp Can Be a Bonding Experience. *Neuron,* **53,** 635-638.

Peterson, S. J., Frishman, W. H. & Abraham, N. G. 2009. Targeting heme oxygenase: therapeutic implications for diseases of the cardiovascular system. *Cardiol Rev,* **17,** 99-111.

Petersson, J., Zygmunt, P. M., Brandt, L. & Hogestatt, E. D. 1995. Substance P-induced relaxation and hyperpolarization in human cerebral arteries. *Br J Pharmacol,* **115,** 889-94.

Petrus, M., Peier, A., Bandell, M., Hwang, S., Huynh, T., Olney, N., Jegla, T. & Patapoutian, A. 2007. A role of TRPA1 in mechanical hyperalgesia is revealed by pharmacological inhibition. *Molecular Pain,* **3,** 40.

Petruska, J. C. & Mendell, L. M. 2004. The many functions of nerve growth factor: multiple actions on nociceptors. *Neuroscience Letters,* **361,** 168-171.

Poli, G., Schaur, R. J., Siems, W. G., Leonarduzzi, G. 2008. 4-Hydroxynonenal: A membrane lipid oxidation product of medicinal interest. *Medicinal Research Reviews,* **28,** 569-631.

Portaluppi, F., Trasforini, G., Margutti, A., Vergnani, L., Ambrosio, M. R., Rossi, R., Bagni, B., Pansini, R. & degli Uberti, E. C. 1992. Circadian rhythm of calcitonin gene-related peptide in uncomplicated essential hypertension. *J Hypertens,* **10,** 1227-34.

Pozsgai, G., Bodkin, J. V., Graepel, R., Bevan, S., Andersson, D. A. & Brain, S. D. 2010. Evidence for the pathophysiological relevance of TRPA1 receptors in the cardiovascular system *in vivo*. *Cardiovascular Research,* **1:87(4),** 760-8.

Raemdonck, K., de Alba, J., Birrell, M. A., Grace, M., Maher, S. A., Irvin, C. G., Fozard, J. R., O'Byrne, P. M. & Belvisi, M. G. 2011. A role for sensory nerves in the late asthmatic response. *Thorax,* **13,** 13.

Ragino, I. I., Maliutina, S.K., Kashtanova, E.V., Ivanova, M.V., Voevoda, M.I., Nikitin, Iu.P. 2005. Oxidized low density lipoproteins and their association with some atherosclerosis risk factors in a population of Novosibirsk men. *Kardiologiia. ,* **45,** 39-44.

Rastogi, T., Reddy, K. S., Vaz, M., Spiegelman, D., Prabhakaran, D., Willett, W. C., Stampfer, M. J. & Ascherio, A. 2004. Diet and risk of ischemic heart disease in India. *Am J Clin Nutr,* **79,** 582-592.

Ray, R., Murdoch, C. E., Wang, M., Santos, C. X., Zhang, M., Alom-Ruiz, S., Anilkumar, N., Ouattara, A., Cave, A. C., Walker, S. J., Grieve, D. J., Charles, R. L., Eaton, P., Brewer, A. C. & Shah, A. M. 2011. Endothelial Nox4 NADPH oxidase enhances vasodilatation and reduces blood pressure *in vivo*. *Arterioscler Thromb Vasc Biol,* **31,** 1368-76.

Respress, J. L. & Wehrens, X. H. T. 2010. Transthoracic Echocardiography in Mice. *J Vis Exp,* e1738.

Rhodes, J. S., Gammie, S. C. & Garland, T. 2005. Neurobiology of Mice Selected for High Voluntary Wheel-running Activity. *Integrative and Comparative Biology,* **45,** 438-455.

Romana, L. K., Singh, S. & Ahuja, S. P. 1983. Effects of feeding mustard oil diets on the collagen biosynthesis in various tissues of male rats. *Z Ernahrungswiss,* **22,** 59-64.

Rosendorff, C. 1996. The Renin-Angiotensin System and Vascular Hypertrophy. *Journal of the American College of Cardiology,* **28,** 803-812.

Rothwell, P. 2011. Does Blood Pressure Variability Modulate Cardiovascular Risk? *Current Hypertension Reports,* **13,** 177-186.

Rottman, J. N., Ni, G. & Brown, M. 2007. Echocardiographic Evaluation of Ventricular Function in Mice. *Echocardiography,* **24,** 83-89.

Routledge, F. S., Campbell, T. S., McFetridge-Durdle, J. A. & Bacon, S. L. 2010. Improvements in heart rate variability with exercise therapy. *Can J Cardiol,* **26,** 303-12.

Rush, J. W. & Aultman, C. D. 2008. Vascular biology of angiotensin and the impact of physical activity. *Appl Physiol Nutr Metab,* **33,** 162-72.

Russell, F. A., Fernandes, E. S., Courade, J.-P., Keeble, J. E. & Brain, S. D. 2009. Tumour necrosis factor [alpha] mediates transient receptor potential vanilloid 1-dependent bilateral thermal hyperalgesia with distinct peripheral roles of interleukin-1[beta], protein kinase C and cyclooxygenase-2 signalling. *Pain,* **142,** 264-274.

Ryckmans, T., Aubdool, A. A., Bodkin, J. V., Cox, P., Brain, S. D., Dupont, T., Fairman, E., Hashizume, Y., Ishii, N., Kato, T., Kitching, L., Newman, J., Omoto, K., Rawson, D. & Strover, J. 2011. Design and pharmacological evaluation of PF-4840154, a non-electrophilic reference agonist of the TrpA1 channel. *Bioorg Med Chem Lett,* **21,** 4857-9.

Ryman, T., Brandt, L., Andersson, K. E. & Mellergard, P. 1989. Regional and species differences in vascular reactivity to extracellular potassium. *Acta Physiologica Scandinavica,* **136,** 151-159.

Saban R., Gerard N.P., Saban M.R., Nguyen N.B., DeBoer D.J., Wershil B.K.. 2002. Mast cells mediate substance P-induced bladder inflammation through an NK(1) receptor-independent mechanism. *Am J Physiol Renal Physiol.* **283**, F616-29.

Sabharwal, R., Zhang, Z., Lu, Y., Abboud, F. M., Russo, A. F. & Chapleau, M. W. 2010. Receptor Activity-Modifying Protein 1 Increases Baroreflex Sensitivity and Attenuates Angiotensin-Induced Hypertension. *Hypertension,* **55,** 627-635.

Safar, M. E. & Jankowski, P. 2009. Central blood pressure and hypertension: role in cardiovascular risk assessment. *Clin Sci (Lond),* **116,** 273-82.

Saiki, A., Ohira, M., Endo, K., Koide, N., Oyama, T., Murano, T., Watanabe, H., Miyashita, Y. & Shirai, K. 2009. Circulating angiotensin II is associated with body fat accumulation and insulin resistance in obese subjects with type 2 diabetes mellitus. *Metabolism,* **58,** 708-13.

Saha S., 2005, Role of the central nucleus of the amygdala in the control of blood pressure: descending pathways to medullary cardiovascular nuclei. *Clin Exp Pharmacol Physiol*. **5-6**, 450-6.

Salas, M. M., Hargreaves, K. M. & Akopian, A. N. 2009. TRPA1-mediated responses in trigeminal sensory neurons: interaction between TRPA1 and TRPV1. *European Journal of Neuroscience,* **29,** 1568-1578.

Salmon, A. M., Damaj, I., Sekine, S., Picciotto, M.R., Marubio, L., Changeux, J.P. 1999. Modulation of morphine analgesia in alphaCGRP mutant mice. *Neuroreport. ,* **10,** 849-54.

Sampson, N., Koziel, R., Zenzmaier, C., Bubendorf, L., Plas, E., Jansen-Durr, P. & Berger, P. 2011. ROS signaling by NOX4 drives fibroblast-to-myofibroblast differentiation in the diseased prostatic stroma. *Mol Endocrinol,* **25,** 503-15.

Saria, A. 1984. Substance P in sensory nerve fibres contributes to the development of oedema in the rat hind paw after thermal injury. *Br J Pharmacol. ,* **82,** 217-22.

Scher, J. U. & Pillinger, M. H. 2005. 15d-PGJ2: The anti-inflammatory prostaglandin? *Clinical Immunology,* **114,** 100-109.

Schnee, J. M. & Hsueh, W. A. 2000. Angiotensin II, adhesion, and cardiac fibrosis. *Cardiovascular Research,* **46,** 264-268.

Scotland, R. S., Chauhan, S., Davis, C., De Felipe, C., Hunt, S., Kabir, J., Kotsonis, P., Oh, U. & Ahluwalia, A. 2004. Vanilloid Receptor TRPV1, Sensory C-Fibers, and Vascular Autoregulation: A Novel Mechanism Involved in Myogenic Constriction. *Circ Res,* **95,** 1027-1034.

Seagard J.L., Hopp F.A., Drummond H.A., Van Wynsberghe D.M., 1993Selective contribution of two types of carotid sinus baroreceptors to the control of blood pressure. *Circ Res.* **72**, 1011-22.

Sedeek, M., Hebert, R. L., Kennedy, C. R., Burns, K. D. & Touyz, R. M. 2009. Molecular mechanisms of hypertension: role of Nox family NADPH oxidases. *Curr Opin Nephrol Hypertens,* **18,** 122-7.

Semprun-Prieto, L. C., Sukhanov, S., Yoshida, T., Rezk, B. M., Gonzalez-Villalobos, R. A., Vaughn, C., Michael Tabony, A. & Delafontaine, P. 2011. Angiotensin II induced catabolic effect and muscle atrophy are redox dependent. *Biochem Biophys Res Commun,* **409,** 217-21.

Sexton, A., McDonald, M., Cayla, C., Thiemermann, C. & Ahluwalia, A. 2007. 12-Lipoxygenase-derived eicosanoids protect against myocardial ischemia/reperfusion injury via activation of neuronal TRPV1. *FASEB J,* **21,** 2695-703.

Shepherd, J. T. 1987. Circulatory response to exercise in health. *Circulation,* **76,** VI3-10.

Simon, G., Abraham, G. & Cserep, G. 1995. Pressor and subpressor angiotensin II administration two experimental models of hypertension. *American Journal of Hypertension,* **8,** 645-650.

Singh, R. B., Niaz, A. M., Ghosh, S., Agarwal, P., Ahmad, S., Begum, R., Onouchi, Z. & Kummerow, F. A. 1995. Randomized, controlled trial of antioxidant vitamins and cardioprotective diet on hyperlipidemia, oxidative stress, and development of experimental atherosclerosis: the diet and antioxidant trial on atherosclerosis. *Cardiovasc Drugs Ther,* **9,** 763-71.

Sisignano M., Park C.K., Angioni C., Zhang D.D., von Hehn C., Cobos E.J., Ghasemlou N., Xu Z.Z., Kumaran V., Lu R., Grant A., Fischer M.J., Schmidtko A., Reeh P., Ji R.R., Woolf C.J., Geisslinger G., Scholich K., Brenneis C., 2012, 5,6-EET is released upon neuronal activity and induces mechanical pain hypersensitivity via TRPA1 on central afferent terminals. *J Neurosci.* **32**, 6364-72.

Smillie, S.-J. & Brain, S. D. 2011. Calcitonin gene-related peptide (CGRP) and its role in hypertension. *Neuropeptides,* **45,** 93-104.

Smith, M., Beacham, D., Ensor, E. & Koltzenburg, M. 2004. Cold-sensitive, menthol-insensitive neurons in the murine sympathetic nervous system. *Neuroreport.,* **15,** 1399-1403.

Smith, P. D., Brett, S. E., Luykenaar, K. D., Sandow, S. L., Marrelli, S. P., Vigmond, E. J. & Welsh, D. G. 2008. KIR channels function as electrical amplifiers in rat vascular smooth muscle. *J Physiol,* **586,** 1147-60.

Stadtman, E. R. 2001. Protein Oxidation in Aging and Age-Related Diseases. *Annals of the New York Academy of Sciences,* **928,** 22-38.

Starr, A., Graepel, R., Keeble, J., Schmidhuber, S., Clark, N., Grant, A., Shah, A.M., Brain, S.D. 2008 A reactive oxygen species-mediated component in neurogenic vasodilatation. *Cardiovasc Res.,* **78,** 139-47.

Staruschenko, A., Jeske, N. A. & Akopian, A. N. 2010. Contribution of TRPV1-TRPA1 Interaction to the Single Channel Properties of the TRPA1 Channel. *Journal of Biological Chemistry,* **285,** 15167-15177.

Steinhoff, M., Stander, S., Seeliger, S., Ansel, J. C., Schmelz, M. & Luger, T. 2003. Modern Aspects of Cutaneous Neurogenic Inflammation. *Arch Dermatol,* **139,** 1479-1488.

Story, G. M. & Gereau Iv, R. W. 2006. Numbing the Senses: Role of TRPA1 in Mechanical and Cold Sensation. *Neuron,* **50,** 177-180.

Story, G. M., Peier, A. M., Reeve, A. J., Eid, S. R., Mosbacher, J., Hricik, T. R., Earley, T. J., Hergarden, A. C., Andersson, D. A., Hwang, S. W., McIntyre, P., Jegla, T., Bevan, S. & Patapoutian, A. 2003. ANKTM1, a TRP-like Channel Expressed in Nociceptive Neurons, Is Activated by Cold Temperatures. *Cell,* **112,** 819-829.

Streng, T., Axelsson, H. E., Hedlund, P., Andersson, D. A., Jordt, S.-E., Bevan, S., Andersson, K.-E., Högestätt, E. D. & Zygmunt, P. M. 2008. Distribution and Function of the Hydrogen Sulfide-Sensitive TRPA1 Ion Channel in Rat Urinary Bladder. *European Urology,* **53,** 391-400.

Stypmann, J., Engelen, M., Epping, C., van Rijen, H., Milberg, P., Bruch, C., Breithardt, G., Tiemann, K. & Eckardt, L. 2006. Age and gender related reference values for transthoracic Doppler-echocardiography in the anesthetized CD1 mouse. *The International Journal of Cardiovascular Imaging (formerly Cardiac Imaging),* **22,** 353-362.

Su, S., Miller, A. H., Snieder, H., Bremner, J. D., Ritchie, J., Maisano, C., Jones, L., Murrah, N. V., Goldberg, J. & Vaccarino, V. 2009. Common Genetic Contributions to Depressive Symptoms and Inflammatory Markers in Middle-Aged Men: The Twins Heart Study. *Psychosomatic Medicine,* **71,** 152-158.

Subash Babu, P., Prabuseenivasan, S. & Ignacimuthu, S. 2007. Cinnamaldehyde--A potential antidiabetic agent. *Phytomedicine,* **14,** 15-22.

Suekawa, M., Ishige, A., Yuasa, K., Sudo, K., Aburada, M. & Hosoya, E. 1984. Pharmacological studies on ginger. I. Pharmacological actions of pungent constitutents, (6)-gingerol and (6)-shogaol. *J Pharmacobiodyn,* **7,** 836-48.

Sun, J. & Bhatia, M. 2007. Blockade of neurokinin-1 receptor attenuates CC and CXC chemokine production in experimental acute pancreatitis and associated lung injury. *American Journal of Physiology - Gastrointestinal and Liver Physiology,* **292,** G143-G153.

Sung, C.-P., Arleth, A. J., Aiyar, N., Bhatnagar, P. K., Lysko, P. G. & Feuerstein, G. 1992. CGRP stimulates the adhesion of leukocytes to vascular endothelial cells. *Peptides,* **13,** 429-434.

Swallow, J. G., Carter, P. A. & Garland, T., Jr. 1998. Artificial selection for increased wheel-running behavior in house mice. *Behav Genet,* **28,** 227-37.

Szallasi, A., Cortright, D. N., Blum, C. A., Eid, S. R. 2007. The vanilloid receptor TRPV1: 10 years from channel cloning to antagonist proof-of-concept. *Nature Reviews,* **6,** 357-373.

Szallasi, A., Cruz, F. & Geppetti, P. 2006. TRPV1: a therapeutic target for novel analgesic drugs? *Trends in Molecular Medicine,* **12,** 545-554.

Szarek J.L., Spurlock B., Gruetter C.A., Lemke S., 1998, Substance P and capsaicin release prostaglandin E2 from rat intrapulmonary bronchi. *Am J Physiol*. **275**, L1006-12.

Szolcsányi, J. 2004. Forty years in capsaicin research for sensory pharmacology and physiology. *Neuropeptides,* **38,** 377-384.

Takahashi, N., Mizuno, Y., Kozai, D., Yamamoto, S., Kiyonaka, S., Shibata, T., Uchida, K. & Mori, Y. 2008 Molecular characterization of TRPA1 channel activation by cysteine-reactive inflammatory mediators. *Channels (Austin),* **2,** 287-98.

Tam, C. W., Husmann, K., Clark, N. C., Clark, J. E., Lazar, Z., Ittner, L. M., Gotz, J., Douglas, G., Grant, A. D., Sugden, D., Poston, L., Poston, R., McFadzean, I., Marber, M. S., Fischer, J. A., Born, W., *et al.* 2006. Enhanced Vascular Responses to Adrenomedullin in Mice Overexpressing Receptor-Activity-Modifying Protein 2. *Circ Res,* **98,** 262-270.

Tammaro, P., Smith, A. L., Hutchings, S. R. & Smirnov, S. V. 2004. Pharmacological evidence for a key role of voltage-gated K+ channels in the function of rat aortic smooth muscle cells. *British Journal of Pharmacology,* **143,** 303-317.

Taylor-Clark, T. E., Ghatta, S., Bettner, W. & Undem, B. J. 2009. Nitrooleic Acid, an Endogenous Product of Nitrative Stress, Activates Nociceptive Sensory Nerves via the Direct Activation of TRPA1. *Mol Pharmacol,* **75,** 820-829.

Taylor-Clark, T. E., McAlexander, M. A., Nassenstein, C., Sheardown, S. A., Wilson, S., Thornton, J., Carr, M. J. & Undem, B. J. 2008a. Relative contributions of TRPA1 and TRPV1 channels in the activation of vagal bronchopulmonary C-fibres by the endogenous autacoid 4-oxononenal. *J Physiol,* **586,** 3447-3459.

Taylor-Clark T.E., Undem B.J., 2009, Ozone activates airway nerves via the selective stimulation of TRPA1 ion channels. *J Physiol.* **588**, 423-33.

Taylor-Clark, T. E., Undem, B. J., MacGlashan, D. W., Jr., Ghatta, S., Carr, M. J. & McAlexander, M. A. 2008b. Prostaglandin-Induced Activation of Nociceptive Neurons via Direct Interaction with Transient Receptor Potential A1 (TRPA1). *Mol Pharmacol,* **73,** 274-281.

Thakker-Varia, S. & Alder, J. 2009. Neuropeptides in depression: Role of VGF. *Behavioural Brain Research,* **197,** 262-278.

Thompson, D., Markovitch, D., Betts, J. A., Mazzatti, D., Turner, J. & Tyrrell, R. M. 2010. Time course of changes in inflammatory markers during a 6-mo exercise intervention in sedentary middle-aged men: a randomized-controlled trial. *Journal of Applied Physiology,* **108,** 769-779.

Tieu, B. C., Lee, C., Sun, H., LeJeune, W., Recinos, A., Ju, X., Spratt, H., Guo, D.-C., Milewicz, D., Tilton, R. G. & Brasier, A. R. 2009. An adventitial IL-6/MCP1 amplification loop accelerates macrophage-mediated vascular inflammation leading to aortic dissection in mice. *The Journal of Clinical Investigation,* **119,** 3637-3651.

Toh C.C., Lee T.S., Kiang A.K., 1955, The pharmacological actions of capsaicin and analogues. *Br J Pharmacol Chemother.* **10,** 175-82

Touyz, R. M. 2004. Reactive oxygen species, vascular oxidative stress, and redox signaling in hypertension: what is the clinical significance? *Hypertension,* **44,** 248-52.

Touyz, R. M. & Briones, A. M. 2011. Reactive oxygen species and vascular biology: implications in human hypertension. *Hypertens Res,* **34,** 5-14.

Trevisani, M., Siemens, J., Materazzi, S., Bautista, D., Nassini, R., Campi, B., Imamachi, N., Andre, E., Patacchini, R., Cottrell, G., Gatti, R., Basbaum, A., Bunnett, N., Julius, D. & Geppetti, P. 2007. 4-Hydroxynonenal, an endogenous aldehyde, causes pain and neurogenic inflammation through activation of the irritant receptor TRPA1. *Proc Natl Acad Sci USA,* **104,** 13519 - 13524.

Turgis, M., Han, J., Caillet, S. & Lacroix, M. 2009. Antimicrobial activity of mustard essential oil against Escherichia coli O157:H7 and Salmonella typhi. *Food Control,* **20,** 1073-1079.

Turkseven, S., Kruger, A., Mingone, C. J., Kaminski, P., Inaba, M., Rodella, L. F., Ikehara, S., Wolin, M. S. & Abraham, N. G. 2005. Antioxidant mechanism of heme oxygenase-1 involves an increase in superoxide dismutase and catalase in experimental diabetes. *American Journal of Physiology - Heart and Circulatory Physiology,* **289,** H701-H707.

Van Vliet, B. N., McGuire, J., Chafe, L., Leonard, A., Joshi, A. & Montani, J.-P. 2006. Phenotyping the level of blood pressure by telemetry in mice. *Clinical and Experimental Pharmacology and Physiology,* **33,** 1007-1015.

VanderEnde, D. S. & Morrow, J. D. 2001. Release of markedly increased quantities of prostaglandin D2 from the skin *in vivo* in humans after the application of cinnamic aldehyde. *Journal of the American Academy of Dermatology,* **45,** 62-67.

Vandesompele, J., De Preter, K., Pattyn, F., Poppe, B., Van Roy, N., De Paepe, A. & Speleman, F. 2002. Accurate normalization of real-time quantitative RT-PCR data by geometric averaging of multiple internal control genes. *Genome Biol,* **3,** RESEARCH0034.

Verheggen, R., Bumann, K. & Kaumann, A. J. 2002. BIBN4096BS is a potent competitive antagonist of the relaxant effects of alpha-CGRP on human temporal artery: comparison with CGRP(8-37). *Br J Pharmacol,* **136,** 120-6.

Wang, D. H. 2005. The vanilloid receptor and hypertension1. *Acta Pharmacologica Sinica,* **26,** 286-294.

Wang, D. H., Johns, D. G., Xu, S. & Cohen, R. A. 2002. Role of superoxide anion in regulating pressor and vascular hypertrophic response to angiotensin II. *American Journal of Physiology - Heart and Circulatory Physiology,* **282,** H1697-H1702.

Wang D.H., Li J., Qiu J., 1998, Salt-sensitive hypertension induced by sensory denervation: introduction of a new model. *Hypertension*. **32**, 649-53

Wang D.H., Wu W., Lookingland K.J.. 2001, Degeneration of capsaicin-sensitive sensory nerves leads to increased salt sensitivity through enhancement of sympathoexcitatory response. *Hypertension.* **37**, 440-3

Wang, L. H., Luo, M., Wang, Y., Galligan, J. J. & Wang, D. H. 2006. Impaired vasodilation in response to perivascular nerve stimulation in mesenteric arteries of TRPV1-null mutant mice. *J Hypertens,* **24,** 2399-408.

Wang, L. H. & Wang, D. H. 2005b. TRPV1 gene knockout impairs postischemic recovery in isolated perfused heart in mice. *Circulation,* **112,** 3617-3623.

Wang, P., Tang, F., Li, R., Zhang, H., Chen, S., Liu, P. & Huang, H. 2007. Contribution of different Nox homologues to cardiac remodeling in two-kidney two-clip renovascular hypertensive rats: Effect of valsartan. *Pharmacological Research,* **55,** 408-417.

Wang, S., Dai, Y., Fukuoka, T., Yamanaka, H., Kobayashi, K., Obata, K., Cui, X., Tominaga, M., Noguchi, K. 2008a Phospholipase C and protein kinase A mediate bradykinin sensitization of TRPA1: a molecular mechanism of inflammatory pain. *Brain.,* **131,** 1241-51.

Wang, Y., Babankova, D., Huang, J., Swain, G. M. & Wang, D. H. 2008b. Deletion of transient receptor potential vanilloid type 1 receptors exaggerates renal damage in deoxycorticosterone acetate-salt hypertension. *Hypertension,* **52,** 264-70.

Wang Y., Wang D.H., 2007, Increased depressor response to N-arachidonoyl-dopamine during high salt intake: role of the TRPV1 receptor. *J Hypertens*. **25**, 2426-33

Wang, Y. & Wang, D. H. 2009. Aggravated renal inflammatory responses in TRPV1 gene knockout mice subjected to DOCA-salt hypertension. *Am J Physiol Renal Physiol,* **297,** F1550-9.

Watkins, T. R., Lenz, P. H., Siderits, R., Struck, M. & Bierenbaum, M. L. 1995. Dietary mustard, rape seed oils and selenium exert distinct effects on serum Se, lipids, peroxidation products and platelet aggregability. *J Am Coll Nutr,* **14,** 176-83.

Watson, R. E., Supowit, S. C., Zhao, H., Katki, K. A. & Dipette, D. J. 2002. Role of sensory nervous system vasoactive peptides in hypertension. *Braz J Med Biol Res,* **35,** 1033-45.

Wei, H., Chapman, H., Saarnilehto, M., Kuokkanen, K., Koivisto, A. & Pertovaara, A. 2010. Roles of cutaneous versus spinal TRPA1 channels in mechanical hypersensitivity in the diabetic or mustard oil-treated non-diabetic rat. *Neuropharmacology,* **58,** 578-84.

Wei, H., Hamalainen, M. M., Saarnilehto, M. M. K., Ari . & Pertovaara, A. 2009. Attenuation of Mechanical Hypersensitivity by an Antagonist of the TRPA1 Ion Channel in Diabetic Animals. [Miscellaneous Article]. *Anesthesiology,* **111,** 147-154.

Weinhold, P., Gratzke, C., Streng, T., Stief, C., Andersson, K.-E. & Hedlund, P. 2010. TRPA1 Receptor Induced Relaxation of the Human Urethra Involves TRPV1 and Cannabinoid Receptor Mediated Signals, and Cyclooxygenase Activation. *The Journal of Urology,* **183,** 2070-2076.

Wetsel, W. C. 2011. Sensing hot and cold with TRP channels. *Int J Hyperthermia,* **27,** 388-98.

Whitesall, S. E., Hoff, J. B., Vollmer, A. P. & D'Alecy, L. G. 2004. Comparison of simultaneous measurement of mouse systolic arterial blood pressure by radiotelemetry and tail-cuff methods. *American Journal of Physiology - Heart and Circulatory Physiology,* **286,** H2408-H2415.

Wilson, M. C. 2000. Coloboma mouse mutant as an animal model of hyperkinesis and attention deficit hyperactivity disorder. *Neuroscience & Biobehavioral Reviews,* **24,** 51-57.

Wimalawansa, S. J. 1996. Calcitonin gene-related peptide and its receptors: molecular genetics, physiology, pathophysiology, and therapeutic potentials. *Endocr Rev,* **17,** 533-85.

Winter J., Bevan S., Campbell E.A., 1995, Capsaicin and pain mechanisms. *Br J Anaesth*. **2,** 157-68.

Winther, M. & Nielsen, P. V. 2006. Active packaging of cheese with allyl isothiocyanate, an alternative to modified atmosphere packaging. *J Food Prot,* **69,** 2430-5.

Wu, J., Bu, L., Gong, H., Jiang, G., Li, L., Ma, H., Zhou, N., Lin, L., Chen, Z., Ye, Y., Niu, Y., Sun, A., Ge, J. & Zou, Y. 2010. Effects of heart rate and anesthetic timing on high-resolution echocardiographic assessment under isoflurane anesthesia in mice. *J Ultrasound Med,* **29,** 1771-8.

Xue, Y. L., Shi, H. X., Murad, F. & Bian, K. 2011. Vasodilatory effects of cinnamaldehyde and its mechanism of action in the rat aorta. *Vasc Health Risk Manag,* **7,** 273-80.

Yanaga, A., Goto, H., Nakagawa, T., Hikiami, H., Shibahara, N. & Shimada, Y. 2006. Cinnamaldehyde Induces Endothelium-Dependent and -Independent Vasorelaxant Action on Isolated Rat Aorta. *Biological & Pharmaceutical Bulletin,* **29,** 2415-2418.

Yang, D., Luo, Z., Ma, S., Wong, W. T., Ma, L., Zhong, J., He, H., Zhao, Z., Cao, T., Yan, Z., Liu, D., Arendshorst, W. J., Huang, Y., Tepel, M. & Zhu, Z. 2010. Activation of TRPV1 by dietary capsaicin improves endothelium-dependent vasorelaxation and prevents hypertension. *Cell Metab,* **12,** 130-41.

Yao, T. C., Kuo, M. L., See, L. C., Ou, L. S., Lee, W. I., Chan, C. K. & Huang, J. L. 2006. RANTES and monocyte chemoattractant protein 1 as sensitive markers of disease activity in patients with juvenile rheumatoid arthritis: a six-year longitudinal study. *Arthritis Rheum,* **54,** 2585-93.

Yao, X. & Garland, C. J. 2005. Recent Developments in Vascular Endothelial Cell Transient Receptor Potential Channels. *Circ Res,* **97,** 853-863.

Yu S., Ouyang A., 2009, TRPA1 in bradykinin-induced mechanical hypersensitivity of vagal C fibers in guinea pig esophagus. *Am J Physiol Gastrointest Liver Physiol*. **296**, G255-65

Yuan, J. H., Dieter, M. P., Bucher, J. R. & Jameson, C. W. 1992. Toxicokinetics of cinnamaldehyde in F344 rats. *Food and Chemical Toxicology,* **30,** 997-1004.

Zalba, G., San Jose, G., Moreno, M. U., Fortuno, M. A., Fortuno, A., Beaumont, F. J. & Diez, J. 2001. Oxidative stress in arterial hypertension: role of NAD(P)H oxidase. *Hypertension*, **38,** 1395-9.

Zhang, X.-L., Mok, L.-P., Katz, E. J. & Gold, M. S. 2010. BKCa currents are enriched in a subpopulation of adult rat cutaneous nociceptive dorsal root ganglion neurons. *European Journal of Neuroscience,* **31,** 450-462.

Zhang, X. F., Chen, J., Faltynek, C.R., Moreland, R.B., Neelands, T.R. 2008. Transient receptor potential A1 mediates an osmotically activated ion channel. *European Journal of Neuroscience,* **27,** 605-611.

Zhang, Y., Oltman, C. L., Lu, T., Lee, H. C., Dellsperger, K. C. & VanRollins, M. 2001. EET homologs potently dilate coronary microvessels and activate BK(Ca) channels. *Am J Physiol Heart Circ Physiol,* **280,** H2430-40.

Zhong, B., Wang, D. H., Zhong, B. & Wang, D. H. 2007. TRPV1 gene knockout impairs preconditioning protection against myocardial injury in isolated perfused hearts in mice. *American Journal of Physiology - Heart & Circulatory Physiology,* **293,** H1791-8.

Zhuo, J. L. 2004. Monocyte chemoattractant protein-1: a key mediator of angiotensin II-induced target organ damage in hypertensive heart disease? *J Hypertens,* **22,** 451-4.

Zhou Y., Sun B., Li Q., Luo P., Dong L., Rong W., 2011. Sensitivity of bronchopulmonary receptors to cold and heat mediated by transient receptor potential cation channel subtypes in an ex vivo rat lung preparation. *Respir Physiol Neurobiol*. **177**, 327-32

Zsuzsanna, H., Szabó, A., Németh, J., Jakab, B., Pintér, E., Bánvölgyi, A., Kereskai, L., Kéri, G. & Szolcsányi, J. 2004. Antiinflammatory and analgesic effects of somatostatin released from capsaicin-sensitive sensory nerve terminals in a Freund's adjuvant-induced chronic arthritis model in the rat. *Arthritis & Rheumatism,* **50,** 1677-1685.